Application of agricultural wastes for removal of heavy metals from industrial wastewater by adsorption process

THESIS

SUBMITTED TO

BABASAHEB BHIMRAO AMBEDKAR UNIVERSITY

LUCKNOW

BABASAHEB
BHIMRAO
AMBEDKAR
UNIVERSITY

LUCKNOW

प्रज्ञा शील करुणा

ESTABLISHED 1996

FOR THE DEGREE OF

Doctor of Philosophy

IN

ENVIRONMENTAL SCIENCE

Submitted by

Poonam

Enrolment No. 505/11

Under the Supervision of

Dr. Narendra Kumar

DEPARTMENT OF ENVIRONMENTAL SCIENCE
SCHOOL FOR ENVIRONMENTAL SCIENCES
BABASAHEB BHIMRAO AMBEDKAR UNIVERSITY
(A Central University, NAAC Accredited 'A' Grade)
VIDYA VIHAR, RAEBARELI ROAD
LUCKNOW-226 025

2019

Dedicated to

my beloved PAPA

and MUMMY

CERTIFICATE

This is to certify that the thesis entitled **"Application of agricultural wastes for removal of heavy metals from industrial wastewater by adsorption process"** submitted by **Ms. POONAM** is an original research work and has not been previously submitted in part or full for the award of any other degree or diploma to this or any other university.

The thesis submitted to Babasaheb Bhimrao Ambedkar University, Lucknow satisfies all the requirements as stipulated in the *Doctor of Philosophy (Ph.D.) Regulations – 1999 as amended in 2008/2010/2013* and it is fit for submission and evaluation for the award of the degree of Doctor of Philosophy of the University.

Date: **Supervisor**

Head of Department

DECLARATION

This is to certify that the material embodies in the present Ph.D. work entitled **"Application of agricultural wastes for removal of heavy metals from industrial wastewater by adsorption process"** is original research work done in partial fulfillment of requirements for the award of the degree of Doctor of Philosophy under the supervision of Dr. Narendra Kumar, Assistant Professor, Department of Environmental Science, Babasaheb Bhimrao Ambedkar University (A Central University), Lucknow-226025, India. It has not been submitted in part or full for any other diploma or degree in any other University or institute. In this thesis, matter written, data presented and plagiarism, if any, is the sole responsibility of the student Ms. Poonam. If any allegations/query/question arises regarding the thesis, I, Ms. Poonam D/o Mr. Ram Harsh, will be solely responsible and answerable.

Date:

(Ms. Poonam)
D/o Mr. Ram Harsh
Department of Environmental Science,
Babasaheb Bhimrao Ambedkar University,
Lucknow, U. P., India.

ACKNOWLEDGEMENTS

Life is a journey where every individual with their own experiences lays milestones. This is a righteous opportunity to mention the name of those wonderful and caring persons who have shown me the right way to achieve the ultimate Milestone.

First of all, I would like to express my profound feeling of reverence and extend my heartfelt gratitude to ***Dr. Narendra Kumar****, my supervisor for his exemplary guidance and dynamic initiation, continuous encouragement, thoughtful discussions, and untiring supervision throughout the work helped me to develop the scientific expertise. His blessings, help and support given shall carry me a long way in the journey of life on which I am about to embark. He will always be remembered as the key factor that geared my career towards this path.*

I owe my sincere thanks the Head of Department, ***Prof. N. K. Arora*** *and the previous Head of the Department and present Dean* ***Prof. S.K. Dwivedi*** *for providing the necessary facilities in the department during my research tenure. I will always be grateful for their kind and helping attitude.*

I gratefully acknowledge and extend my heartfelt gratitude to all of faculty members ***Prof. D.P. Singh****,* ***Prof. R.P. Singh, Mr. N. K. S. More****,* ***Dr. Shikha****,* ***Dr. Venketash Dutta****,* ***Dr. Richa K. Tyagi*** *and* ***Dr. Jiwan Singh*** *for their valuable guidance and generous advice. I would also like to thank all teachers of the department for their help and support.*

Financial assistance provided from UGC (University Grants Commission) in the form of RGNF-JRF and SRF during the course of this study is kindly acknowledged.

I wish to thanks to the technical and administrative staff of the department especially Mr. ***A. K. Jain****, Mr.* ***Ranjeet Sharma****, Mr.* ***Aviral Kumar Dixit****, Mr.* ***Rakesh Kumar Shukla****, Mr.* ***Rahul Srivastav****, Mr.* ***Nagesh Tripathi****, Mr.* ***Abhishek Pandey****, Mr.* ***Vimal Kishore Singh*** *and* ***Mr. Yogendra Pratap Singh****. I would also like pay my*

gratefulness toward USIC and its staff Dr. ***Mukesh Kumar*** *and Mr.* ***Vijay Pratap Singh*** *for their support.*

. I would like to pay my gratitude to my seniors Dr. ***Shiv Shankar****, Dr.* ***Vertika Shukla****, Dr.* ***Vinayak V. Pathak****, Dr.* ***Rose P. Minj****, Dr.* ***Sanjeev Kumar*** *and Dr.* ***Mohammed Baqir*** *for their encouragement and help. I would also like to extend my sincere thanks to my colleagues and friends Mr.* ***Susheel Kumar,*** *Mr.* ***Dhananjay Kumar*** *and Ms.* ***Sangeeta Anand,*** *Mr.* ***Abhay Prakash Rawat****, Mrs.* ***Jyoti,*** *Ms.* ***Nikita Mundetia*** *for their unconditional assistance and encouragement.*

I would like to take this opportunity to pay my sincere and humble thankfulness to Mr. ***Mahesh Kumar*** *and Mr.* ***Shamshad Ahmad*** *for their unconditional support, help and motivation throughout this journey. I also want to thanks my sincere juniors* ***Arpna, Saroj, Suresh, Pradeep, Awdesh, Pradeep Kumar Majhi, Priyanka, Anjali, Neha, Pushpa, Lata, Kashifa, and Radheshyam*** *for their help and support.*

I would also like to share my humble gratefulness to my friends ***Abhishek, Ajay, Vijay****,* ***Sujata, Kanchan, Vidya*** *who always stood behind me, were always present and supported me. I would also like to thank my cousins from* ***Pushkar*** *family for their encouragement and appreciations that motivated me all the time.*

Lastly, I would like to dedicate the whole credit of my achievements so far to my ***parents*** *Mr.* ***Ram Harsh*** *and Mrs.* ***Gomti Devi****,* ***my grandmother*** *Mrs.* ***Shanti Devi****, elder sister Mrs.* ***Neelam,*** *brother-in-law Mr.* ***Jitendra Gautam*** *and sweet maternal nephew "****Ishivatav****" aka* ***"Parthava****" who were and are always there for me in all situations. It was their unshakable faith in me that has helped me to proceed further.*

Its great fortune that in vast universe, we worked on the omnipotent creature of the almighty God. To conclude, I would like to extend a warm thanks to everyone involved directly or indirectly, wished and helped me to reach the pinnacle of my life.

Place: Lucknow

Date: **POONAM**

PREFACE

Water pollution caused by toxic heavy metals originated from different industries is the most concern issue of environmental pollution in present scenario. Although, many conventional and non-conventional techniques have been developed for removal of heavy metals from industrial wastewaters, but theses have some difficulties related to their cost effectiveness, energy consumption, secondary pollutants etc. In this regard, biosorption has emerged as an innovative, eco-friendly, cost effective and probable alternative to prevalent conventional technologies for removal of toxic metal ions. The objective of present study was to treat industrial effluents of tannery and flashlight containing two very toxic heavy metals chromium (Cr) and lead (Pb), respectively by adsorption process. Biochar of commonly occurring fruit and industrial wastes *viz.* peels of sweet lemon (SLPB), lemon (LPB) & orange peel (OPB) and bagasse (BB) were for the process

The physicochemical characterizations of selected biosorbents were based on proximate and ultimate studies, CHNS, surface properties, SEM & EDX, FTIR and XRD eruditions. The Boehm titration was done to access important acid functional groups present in adsorbents which may aid in adsorption of Cr and Pb by different ion-exchange, complexion, addition and substitution chemical reactions. The alterations in surface morphology before and after adsorption were ascertained by SEM and EDX studies. The comparative study of all four adsorbents was based on optimization of different parameters *viz.* adsorbent dosage, contact time, pH, temperature and initial metal ion concentration. The optimized dose and contact time were found to be in range of 5.0 to 10 g L^{-1} and 160 to 180 minutes for Cr and 3.5 to 5.0 g L^{-1} and 140 to 180 minutes for Pb, respectively. The increasing order of removal efficiencies was BB<OBB<LPB<SLPB for all of the selected parameters. The maximum removal of Cr and Pb was found to be 95.47 and 97.42 %, at pH 3 and 5 and temperature of 65 and 55 ºC, respectively by SLPB. Further, effect of initial metal concentration on removal efficiencies of all selected adsorbents was lowest that may be due to dependence of this factor onto adsorbent dosage and contact time. Besides, the maximum removal of Cr and Pb from industrial wastewaters were attained by SLPB (97.82 & 97.11 %) followed by LPB (91.50 & 87.80 %), OPB (86.64 & 86.07%) and BB (74.23 & 75.38 %) at the end. The best results were obtained at

relatively less acidic pH (between 3-5). The most important parameter that affected the removal process was pH and the best-suited adsorbent was SLPB. Further, kinetics involved in adsorption of Cr and Pb present in tannery and flashlight wastewater, were studied following pseudo first and pseudo second order models. Further, due to their simplicity, Freundlich and Langmuir equations were used to describe the relationship between equilibrium metal biosorption q_e (mg L^{-1}) and final concentrations C_e (mg L^{-1}) at equilibrium. The interpretations of the isothermic model were also based on values of R^2. In addition to this, the monolayer adsorption capacity (q_{max}) of all adsorbents for the removal of Cr and Pb were also observed. The thermodynamic parameters (ΔG°, ΔH^{o} and ΔS^{o}) were also estimated to observe mode of processes at higher temperature. The desorption study was done to assess the reusability of adsorbents and possible extraction of metals with suitable eluants. The most important aspect of the study was the risk assessments of treated wastewaters. The phyto-toxicity experiments were conducted over some economic plants i.e. green moong, tomato and lady's finger. The bioaccumulation tendency of both metals with effect of treated wastewaters over growth parameters (root & shoot length, no. of root & leaves, fresh & dry weight) were also observed for selected plant species. The results were compared with limit prescribed by CPCB and WHO (0.1-0.2 mg kg^{-1} for Cr & 0.1 mg kg^{-1} for Pb). The results suggested that very less concentration of both heavy metals were observed in selected plants which may be considered as negligible. Further, development of fruits was found to be very low in comparison to control like that of growth parameters. This might be due to higher concentrations of salts present in treated wastewater, which may be removed by following various other eco-friendly techniques e.g. coagulation where alum is utilized as potential coagulant, electro dialysis that involve the application of electric field for removal of ionic contaminants etc. This might increase growth and development of plants as well as might reduce concentrations of heavy metals with combination of adsorption technique. Therefore, it may be concluded that irrigation of these plants with the biosorbent treated wastewaters will not cause any threat or risk to the lives of humans.

CONTENTS

LIST OF FIGURES

LIST OF TABLES

ABBREVIATIONS & SYMBOLS

α	Alpha
~	Approximately
°C	Degree Celsius
∆H°	Enthalpy
∆S°	Entropy
∆G°	Gibb's free energy
µ	Miu
-	Negative
%	Percentage
BB	Bagasse biochar
BC	Biochar
BOD	Biological Oxygen Demand
Bi	Bismuth
BIS	Bureau of Indian Standards
Ca	Calcium
C	Carbon
CO_2	Carbon dioxide
Cm	Centimeter
COD	Chemical Oxygen Demand
CMBC	Chemically modified biochar
CTA	Chemically treated adsorbent
Cl	Chloride
Conc.	Concentration
Cr	Chromium
DNA	Deoxyribonucleic acid
EC	Electrical Conductivity
FAO	The Food and Agriculture Organization of United States
H	Hydrogen
GC-MS	Gas Chromatography Mass Spectrophotometry
g	Gram
g L^{-1}	Gram per liter
HPLC	High Pressure Liquid Chromatography
HF	Hen feather
Hg	Mercury
HMs	Heavy metals
K	Potassium
kJ mol^{-1}	Kilo joule per mole
LPB	Lemon peel Biochar

Mg	Magnesium
mg L^{-1}	Milligram per liter
MB	Modified biochar
M	Molarity
ml	Mililitre
Mins	Minutes
MnP	Manganese peroxidase
N	Nitrogen
N	Normality
NA	Natural Adsorbent
nm	Nanometer
O	Oxygen
OD	Optical density
OPB	Orange peel biochar
Pb	Lead
ppm	Parts per million
Pt	Platinum
rpm	Revolution per minute
Si	Silicon
S	Sulfur
SLPB	Sweet lemon peel biochar
TDS	Total dissolved solids
TS	Total Solids
TSS	Total Suspended Solids
UV	Ultra violet
H_2O	Water
w/v	Weight over volume
WHO	World Health Organization
Zr	Zirconium

Chapter 1

Introduction

1. Introduction

Population of the developing countries like India is being increasing tremendously in last few decades. Increasing population pose several problems to the health of the environment such as unmanaged and blind consumption of the natural resources, pollution of the air, water and soil. Urbanization, industrialization, developmental and constructional activities have increased in passing years to fulfill needs of rapidly increasing population (Li et al. 2017). These activities have escalated the problem of contamination of the air, soil and aquatic environment systems. Among all natural resources, water is one of the most essential necessities of all living beings to sustain their lives as most of the civilizations have developed near water bodies. Living beings require water for drinking and is used for domestic, industrial and irrigation purposes. Furthermore, water is the most copious natural resources on the earth that is being contaminated continuously by the excessive and nonsensical usages by human beings (Kumar et al. 2015). This has caused a dangerous situation of scarcity and unavailability of save drinking water in many parts of the world including India. Thus, there emerges a need to save the water resources, treat & decontaminate surface water for sustainable development of present as well as of future generations.

1.1 Water profile on the earth

About 71% of the earth's surface is covered with water, 96.5% of which is found in oceans (saline in nature), 3.4% as groundwater (1.7%), in glaciers of Antarctica and Greenland (1.7%), a minor portion in other larger water forms, and 0.001% in air as vapors, clouds & rainfall (Gleick 1993). Merely 3% of total fraction of the earth's water is fresh water that contains 68.7% icecaps and glaciers and 30.1% in groundwater. Further, <0.3% of all freshwater is found to be present in rivers, lakes as surface water, and very lesser amount i.e. 0.003% freshwater is confined within biological systems and in the atmosphere (Fig. 1.1).

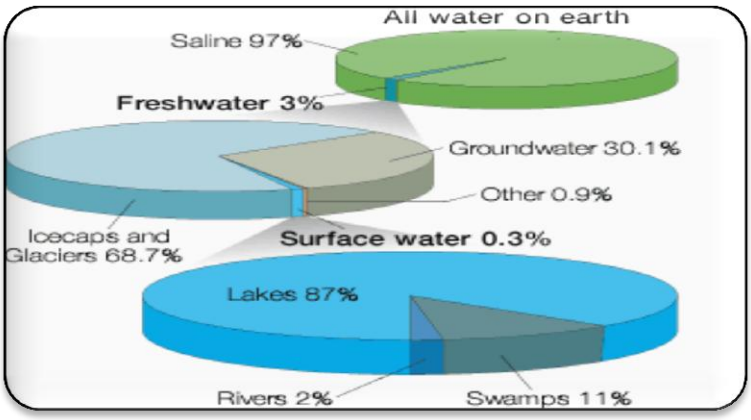

Figure 1.1 Water profile of the Earth (Source- SPC Water, Sanitation Program: Water Distribution)

1.2 Water Pollution

Hydrology, physiology, biology and chemistry of determine the quality of water. These factors not only influence the quality of water but may also cause water pollution if present in excess amount. Moreover, toxins and contaminants are being added to the aquatic system by various anthropogenic actions and also by some natural processes. Thus, water pollution may be defined as the variation in the physiochemical and biological properties of water that interfere in the color, taste and smell and threatens the health of living beings.

1.3 Sources and types of water pollution

Various point and non-point sources are responsible for rising up the complications of water contamination. Point sources included toxic chemicals present in effluents of factories, and industrial units and hazardous smokes released by automobiles. Whereas, pollution generated by agricultural, storm water runoff or rubbles carried into water bodies fall under non-point source. The most common sources of water pollution have been presented in Fig. 1.2 and details account of it have been given below -

i. **Industrial effluents**

Industries contribute to water pollution by disposing off treated/partially treated wastes directly into water bodies, releasing poisonous smokes that may intensify acid

rain and alteration in temperature of water. Further, disposal of wastes directly into aquatic systems and high temperature of effluents may reduce quantity of oxygen in water, resulting in deaths of aquatic fauna.

ii. **Agricultural run off**

Farmers normally apply different chemicals in the form of pesticides, insecticides, herbicides and fertilizers to enhance the growth and productivity. These nutrients and substances are soaked by soil which in filters into the ground water causing its pollution. During rain, these chemicals are added into run-off and flow into surface watercourses and pollute them.

iii. **Sewage and household wastes**

Sewage is commonly a cloudy, dilute, aqueous solution containing minerals and organic matter. Sewage, domestic wastes, households and food processing plants cause about 25% of total water pollution, which includes human excreta, soaps, detergents, metals, glass and garden rubbish.

iv. **Thermal and radioactive pollutants**

These pollutants include the wastes chiefly from atomic, nuclear and thermal power plants. The release of unutilized heat is highest in thermal power plants which adversely affect the aquatic environment. Apart from electric power plant, various industries with cooling requirement contribute in thermal loading. Whereas, large doses of radionuclides are also being added in water bodies by these thermal and nuclear power plants, nuclear tests, nuclear reactors, nuclear installation, operations of power, processing fission and fusion products etc. Extremely toxic radioactive elements e.g. thorium(Th), polonium(Po), radium (Ra), uranium(U), plutonium(Pu) etc. are produced from neutron bombardments of atomic fuel.

v. **Plastics**

Plastic is an unavoidable substance that is produced, used and greatly consumed all around the world on a large scale. About 400 years are required to degrade by natural

processes. Direct dumping of it into the water or on the road and land eventually contaminate the water body as it is washed away by the rain.

vi. **Pathogens**

Incompetently treated sewage discharges large amount of harmful pathogens especially sewage plants due to inadequately designed secondary treatment system. The common bacterial species used as bacterial indicator of water pollution are mainly coliform bacteria and others e.g. *Burkholderia pseudomallei*, *Giardia lamblia*, *Salmonella* sp., worms (helminthes), Novovirus, Hepatitis A. etc. that may cause various health related problems

vii. **Oil Leakage**

Oil stumbles from tankers and ships severely affect marine water quality as it forms a thick layer that chunks sunlight and suffocates the fishes and other aquatic animals leading to their death.

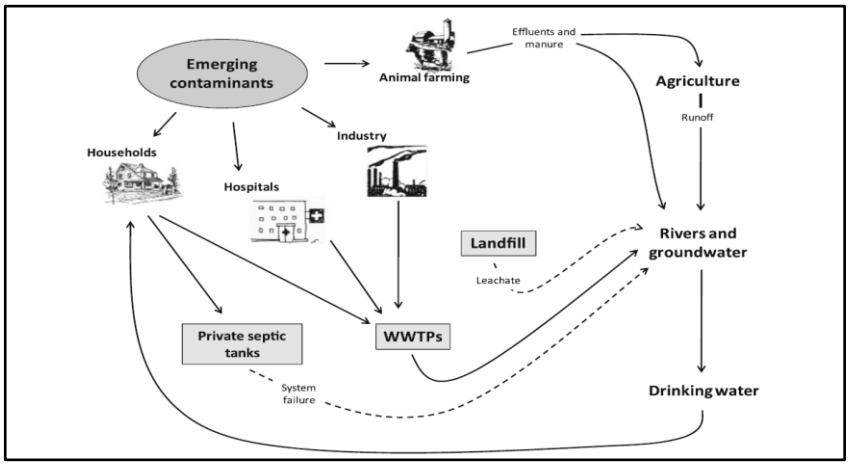

Figure 1.2 Probable sources and paths of emergent contaminants into the ambient environment (Source- Grassi et al. 2012)

1.3 Types of water pollution

It may be divided into ground water and surface water pollution depending upon the existence of water. Furthermore, it may also be categorized on the basis of pollutants e.g. physical, chemical and biological pollution of water.

1.3.1 Ground water pollution

It is defined as water occurring in inundated constituents below water table. Ground water pollution is usually irreversible and is very difficult to restore the original water quality after contamination. It is susceptible with contamination caused by domestic, industrial and agricultural wastes as well as run off from urban area etc.

1.3.2 Surface water pollution

Surface water is confined in rivers, lakes, soil profiles, atmospheric and biological systems. It comes in the direct contact with the atmosphere, streams, and surface drains. Therefore, there occurs a continuous exchange of dissolved and atmospheric gases, which may contaminate the water body. Main contaminants of surface water are compounds, which impart color, odor and turbidity, e.g. oil, grease, phenols, toxic metals and organics; toxic radionuclides; thermal effluents and chlorinated compounds (chloroform and chloramines) etc. Furthermore, same sources of ground water pollution are also responsible for surface water pollution.

1.3.3 Physical pollution of water

This kind of pollution causes fluctuations in water color, odor, taste, turbidity and current properties. Colloidal matter, fine suspended particles and soil, free chlorine, phenols, actinomycetes, hydrogen sulphite, ammonia, phenols, algae, fungi, bacteria and micro-organisms (protozoa, nematodes, bacteria etc.) are the main pollutants that alters the physical characteristics of water bodies.

1.3.4 Chemical pollution of water

It alters acidity, alkalinity, pH, oxygen content of the water body. Chemical pollution is caused by either inorganic & organic pollutants or by both. Organic pollutants may be biodegradable (proteins, fat , carbohydrates, sugar, starch, polymers from domestic wastes, slaughter houses, food processing, industrial wastes) or non–biodegradable (pesticides, fungicides, bactericides, herbicides, insecticides, nematocides etc.) whereas, inorganic pollutants of water consists of gases, toxic metals and compounds.

1.3.5 Biological pollution of water

Excretory products of warm blooded mammals including man, wild and domestic animals are main offenders of causing bacterial pollution. The main pollutants belong to coliform groups, fecal *streptococci* and miscellaneous organisms. It is also fetched by *bacteria, viruses, algae, diatoms* like protozoa, crustaceans, *and* plant *toxins.* Generally, control measures are not adopted to check these pathogenic contaminants.

1.4 Heavy Metal Pollution

Pollution of water resources with potentially toxic heavy metals e.g. arsenic, copper, lead, chromium, nickel, mercury etc. is a severe global problem (Zhang et al. 2014). Heavy metals (HMs) and other trace elements are vital for proper operation of biotic system and their shortage or excess may cause several ill effects on living beings. Heavy metals are highly toxic in nature, non-biodegradable, persistence and it's continuous deposition into the vicinity of receiving water body may contaminate food chain. Furthermore, it may get bio accumulated in the fatty living tissue causing threat to the lives if consumed for drinking and other purposes (Hernández-Montoya et al. 2013; Poonam and Kumar 2018). Therefore, it is essential to treat metal contaminated wastewater prior to discharge to the environmental systems mainly in aquatic bodies.

1.4.1 Definition

Heavy metal is a common collective term used to denote groups of metals and metalloids having atomic no between 63.5 to 200.6 and density greater than 5.0gm cm^{-3} (Thakur and Parmar 2013; Lakherwal 2014).

1.4.2 Sources of heavy metals

Natural and anthropogenic sources are responsible for the contamination of water bodies by HMs, however, in urban areas, activities like industrial and municipal effluent discharge without proper treatment, sewage disposal, mining, smelting processes etc. are making the situation more complex (Dirilgen et al. 2011). Discharge from the industries e.g. tanneries, electroplating, fertilizers, pesticides, batteries, refining ores, ore refineries, alloy industries, pigment, fuel, photographic material manufacturing explosive manufacturers, smelting of metalliferous, surface finishing aerospace, gasoline, radiator manufacturers etc. are mainly responsible for the HM contamination in the aquatic

system (Banerjee et al. 2012; Jadhav et al. 2015). Different sources and maximum permissible limits of the various heavy metals for the purpose of agricultural uses have been presented in Table 1.1.

Table 1.1 Probable sources of heavy metals in water

Heavy Metals	Probable Sources	References
Lead(Pb)	Painting, mining processes, automobiles, electroplating, detergents, chemical manufacturers, surfactants, preservatives etc.	Abas et al. (2013), Poonam et al. (2018)
Chromium(Cr)	Chrome plating, dyes, batteries, tanning and leather industries, textile industries, chemical industries etc.	Alluri et al. (2007); Poonam and Kumar (2018)
Mercury(Hg)	Chloro-alkali industries, chemical manufactures, pesticide factories, detergents, pharmaceuticals, alloy industries, oil refineries, fabric softeners, adhesives, drugs, fluorescent light tubes etc.	Alluri et al. (2007); Abas et al. (2013)
Cadmium(Cd)	Smelting, Cd-Ni batteries, phosphate fertilizers, mining activities, stabilizers, alloy industries, sludge etc.	Abas et al. (2013)
Copper(Cu)	Water pipes, electrical and metal plating industries, electroplating, metal finishing industries, photographic materials, pesticides, insecticides, copper jewelry, cooking pots etc.	Babel and Kurniawan (2003); Alluri et. al. (2007)
Nickel(Ni)	Battery manufacturing industries, pigments, explosives, papers, metal vending, fuel, effluent of silver refinery etc.	Alluri et. al. (2007); Babel and Kurniawan (2003)
Zinc(Zn)	Smelting, surface finishing industries, aerospace, galvanization, paints, fossil fuel consumption, pesticides manufacturers, polymer stabilizers etc.	Alluri et. al. (2007); Abas et al. (2013)
Arsenic (As)	Pesticides, fungicides, insecticides, metal smelters, car batteries, treated wood products, chemical weapons and pharmaceuticals etc.	Babel and Kurniawan (2003); Abas et al. (2013)

1.4.3 Heavy metal toxicity

In passing few decades, contamination of water by HMs has emerged as major environmental problem due to their toxicity and accumulative behavior. Selected of HMs are very vital to humans e.g. cobalt, copper, zinc etc., nevertheless larger magnitudes

may cause physiological illnesses. In contrast to other pollutants, HMs are not biodegradable and endure a global ecological cycle where main corridors are natural waters. An overview of toxicity of various HMs is presented in Table 1.2.

Table 1.2 Toxicity symptoms of various heavy metals

Heavy metals	**Toxicity**	**Health problems/Symptoms**	**References**
Lead(Pb)	Damage central nervous system (CNS), encephalopathy, kidney, liver and reproductive system, hyperactivity, vertigo, anorexia, respiration, digestion, cancer of lungs, bones etc.	Headache, nausea, vomiting, chest pain, dizziness, irritability, weakness of muscles, hallucination, thyroid dysfunction, fatigue, schizophrenic like behavior etc.	Alluri et. al. (2007); Vetriselvi and Santhi (2015); Bai et al. (2017)
Chromium (Cr)	Affects human physiology, skin diseases, respiratory problems, acute renal failure, alteration in genetic material, pulmonary fibrosis, carcinogenic etc.	Loss of appetite, irritation in skin, dizziness, vomiting, fever, weakened immune system, headache, diarrhea, nausea etc.	Alluri et. al. (2007); Sharma and Malaviya (2016)
Mercury(Hg)	Neurotoxin changes to CNS, cerebral palsy, tremors, impairment of pulmonary and kidney functions, gingivitis, hypertonia, rheumatoid arthritis, birth defects etc.	Nausea, termers, loss of vision, chest pain, vomiting, loss of hearing and vision, loss of appetite etc.	Babel and Kurniawan (2003); Alluri et al. (2007)
Cadmium(Cd)	Renal disorder, insomnia, inflammation & enlargement of liver, probable carcinogen etc.	Chest pain, whole body pain, weak digestion etc.	Fu and Wang (2011)
Copper(C u)	Wilson's disease, hypertension, schizophrenia, insomnia, autism, autism, stuttering, postpartum psychosis, heart problems, cystic fibrosis, convulsion or even death etc.	Vomiting, cramps, nausea, chest pain, loss of appetite, etc.	Alluri et al. (2007); Thakur and Parmar, (2013)
Nickel(Ni)	Carcinogenic, renal problems, gastro-intestinal distress, myocarditis, pulmonary fibrosis, skin dermatitis, damage to lungs & CNS, cancer of lungs, bones	Skin irritation, chest pain, vomiting, loss of appetite, improper digestion, rapid respiration, coughing,	Alluri et. al. (2007); Thakur and Parmar (2013)

	and nose etc.	chest pain, etc.	
Zinc(Zn)	Anemia, depression, lethargy, neurological problems, dermatitis etc.	Stomach cramps, skin irritation, nausea, higher thirst, diarrhea etc.	Thakur and Parmar (2013)
Arsenic (As)	Skin manifestations, visceral cancers, cardio-vascular diseases, damage to circulatory and nervous system, produces liver tumors, gastrointestinal problems, renal damage etc.	Nausea, vomiting, loss of appetite and vision, severe diarrhea, confusion, drowsiness, cramping muscles, hair loss, hypotension, night blindness and convulsion etc.	Alluri et. al. (2007); Ungureanu et al. (2015)

1.4.4 Regulatory guidelines on heavy metals

In Indian context, the regulatory guidelines for maximum limits of various toxic HMs into the nearby water bodies have been given by Central pollution Control Board (CPCB) under 'The Environmental Protection Rule (1986)'. The categorizations of maximum limits of HMs in the effluent discharge have been done on the basis of usage and quality of receiving water bodies. It is categorized into four categories i.e. inland surface water, public sewers, land for irrigation and marine coastal areas. The standards for various heavy metals have been summarized in the table 1.3.

Table 1.3 General standards for heavy metal concentration (mg L^{-1}) in wastewaters/effluents (CPCB 2013)

S.No.	Heavy metals	Inland surface water	Public Sewers	Land for irrigation	Marine coastal areas
1	**Lead (Pb)**	0.1	1.0	-	2.0
2	**Chromium (Cr)**	2.0	2.0	-	2.0
3	**Mercury (Hg)**	0.01	0.01	-	0.01
4	**Cadmium (Cd)**	2.0	1.0	-	2.0
5	**Copper (Cu)**	3.0	3.0	-	3.0
6	**Nickel (Ni)**	3.0	3.0	-	5.0
7	**Zinc (Zn)**	5.0	15.0	-	15.0
8	**Arsenic (As)**	0.2	0.2	0.2	0.2

1.4 Conventional and non-conventional techniques to remediate heavy metals from water

Over a few decades a number of conventional techniques have been identified by different scientists and researchers for elimination of HMs from different industrial effluents. These techniques include chemical precipitation, ion exchange, electrochemical removal, membrane filtration, chemical oxidation-reduction, reverse osmosis, ultra filtration, electro dialysis etc. (Banerjee et al. 2012). A brief account of these techniques have been described below-

1.4.1 Chemical precipitation process involves the addition of precipitating reagent in the wastewater. As precipitants are added, they attract the pollutants and transform it into the solid form, which is separated at the end, from the clean water following gravitational settling. Precipitation of metals and other impurities is accomplished by adding coagulants such as alum, lime, Fe salts and organic polymers.

1.4.2 Electrodialysis (ED), a membrane process, depends upon the power of electric field. Under the effects of electric fields, ions are transported through a semi permeable membrane, which is cation or anion selective. Generally, these membranes are made up of polyelectrolytes that in term are negatively charged. Thus, it rejects negative charged ions and permits positively charged ions to flow through.

1.4.3 Coagulation and flocculation followed by disinfection are an indispensable part of water treatment system (Ungureanu et al. 2015). Coagulation is a chemical process involving addition of coagulants or chemicals in water. The suspended materials are encouraged by coagulants to aggregate together to form a semisolid material called as "flocs". After this, flocculation process starts which is slow and mild mixing of water to boost up formation of flocs and grow to a size that can easily be settle out with the effect of gravity.

1.4.4 Ultrafiltration, as the name suggest, it is a filtration process, which occurs through membrane of pore size ranging from 0.1 to 0.001 micron. Its working involves different kinds of forces like pressure and concentration gradient. These forces enable the process to occur through a semi-permeable membrane. A semi-permeable membrane is a kind of biological membrane that works on the process of

diffusion and only allows the selective molecules or ions to pass through it. Thus, this process has the potential to remove different kinds of polluting agents with high molecular-weight, colloidal materials, organic and inorganic polymeric molecules. This process is utilized by different industries like chemical and pharmaceutical manufacturing industries, food and beverage processing industries and wastewater management plants for the purification and treatment of polluted water (Fu and Wang 2011).

1.4.5 Reverse osmosis, is a technique that uses semi-permeable membrane to remove suspended and larger particles from drinking water. This technique can also remove larger molecules, ions, and biological agents like bacteria from polluted water. It works on the principle of osmosis, which involve the movement of solvent from low concentration towards higher solute concentration through a membrane. This process is commonly applied for the purification of water from sea water for the removal of salt and other organic materials from wastewater, electroplating and metal finishing, pulp and paper industries, mining and petrochemical, textile, food processing industries, municipal wastewater, and polluted groundwater (Mohsen-Nia et al. 2007).

1.4.6 Nanofiltration is the transitional treatment technique between ultrafiltration and reverse osmosis. It is a promising technology for rejection of HM ions and other contaminants from wastewater. This technology takes advantage of ease in operation, consistency and moderately low energy consumption along with high competence for pollutant removal (Fu and Wang 2011).

1.4.7 Sorption is evolving as a probable substitute to the existing conventional technologies for removal and recovery of contaminants and metals from aqueous solutions. It is a physicochemical process that utilizes different dead or live biological substances for removal of HMs. It utilizes functional groups present inside or on the surface of biosorbents as binding sites for HM ions. It is further divided into two kinds i.e. absorption and adsorption. Absorption process involves the whole volume of the substance whereas, adsorption process utilizes only surface of the sorbent. Husks, peels, microbial biomass, agricultural and animals wastes have been used as efficient sorbents for treating water and wastewater (Ghaedi et al. 2010; Feng and Guo 2012; Poonam and Kumar 2018).

A comparative study of advantages and disadvantages of different convention techniques has been summarized in Table 1.4.

Table 1.4 Advantages and disadvantages different conventional technologies used for treatment of heavy metals from water and wastewater

S. No.	Mode	Methods	Advantages	Disadvantages
1	**Physical**	Electro-chemical methods	Metal selectivity; extraction of pure metals; chemical free operation; Potential treatment >2000 mg/dm^3	High capital cost; density and initial pH of the solution
2		Membrane filtration	Requirement of small place; high separation selectivity; work at low pressure; less production of solid waste; low chemical consumption	High operational cost of membrane fouling; high maintenance cost; low flow rate
3		Electro-dialysis	High separation selectivity	High operational cost and energy consumption
4	**Physicochemical**	Activated carbon	High efficiency (>99%); can remove most of the metals	Cost of activation of carbon; performance depends upon the kind of the adsorbate
5		Sorption	Cost efficient; minimization of sludge; regeneration of bio-sorbents; High efficiency; No additional nutrient requirement; metal recovery	Metal valance state cannot be altered
6		Photo-catalysis	By-products are less harmful; removal of metals and organic pollutants instantaneously	Limited application; operating time is longer
7	**C h**	Chemical	Inexpensive; simple operation;	Generation of huge

S. No.	Mode	Methods	Advantages	Disadvantages
		Precipitation	removal of most of the metals; nonmetal selective	amount of sludge and additional operating cost for sludge discard
8		Chemical Coagulation	Sludge settles down; dewatering	Costly; large ingesting of chemicals
9		Ion-exchange	High rejuvenation of materials; metal specific	High initial investment and maintenance cost

1.5 Adsorption process for treatment of heavy metals

Adsorption is identified as a very effective, efficient and economic technique for elimination of HMs from water and wastewater. Adsorption is a broad term, which includes removal of physicochemical and organic pollutants including HMs from the water resources through different organic, inorganic and biological substances. Whereas, the usage of organic and biological substances is called as 'biosorption', which is a subsidiary branch of adsorption processes.

1.5.1 Definition of 'Adsorption'

Adsorption is the adhesion of the molecules, ions or atoms of a liquid, soil or a gas to a surface by forming a film on the surface of the adsorbent. It a mass relocation procedure that comprises of gathering of ingredients at boundary of two phases i.e. at liquid-liquid, gas-liquid, gas-solid, or liquid-solid interface (Grassi et al. 2012). The term 'adsorption' was coined by a German Physicist **Heinrich Kaysen** in 1881.

1.5.2 Adsorbents and adsorbate

Adsorbents are the substances that are used as substrate to perform adsorption processes. Adsorbents may be activated charcoal (Arulkumar et al. 2012), agricultural wastes e.g. bagasse (Poonam et al. 2018), peels of orange (Feng et al. 2011; Bernard and Jimoh 2013), lemon (Rajoriya and Kaur 2014), sweet lemon (Poonam and Kumar 2018), tea waste (Thakur and Parmar 2013), water melon shell (Banerjee et al. 2012), leaves of palm (Alfa et al. 2012), industrial wastes like saw dust (Malwade et al.

2016), biological wastes like *Bacillus licheniformis* biomass (Upadhyay et al. 2017) or chemicals like zinc ferrite ($ZnFe_2O_4$) (Adeogun et al. 2017) etc. Whereas, adsorbate is the medium used to be treated by adsorbents e.g. water and wastewater, soil. The adsorptive performance of an adsorbent is strongly reliant on chemical structure of the adsorbate (Ungureanu et al. 2015).

1.5.3 Kinds of adsorbents

Usually adsorbents are divided into two broader categories i.e. natural and synthesized adsorbents (Fig. 1.3).

a. **Naturally occurring-** This include various living and non-living substance that occur naturally e.g. microorganisms, algae, fungi, agricultural wastes.
b. **Synthesized products-** This include various adsorbents obtained form from various industrial, domestic processes e.g. tea, paper & pulp, fertilizer wastes modified chemicals, activated carbons, biopolymers e.g. chitosan etc.

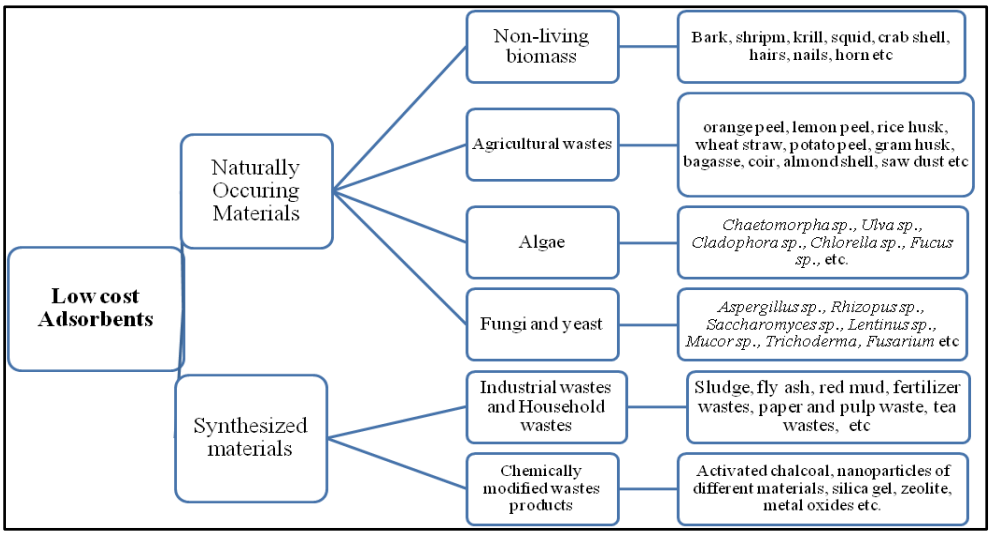

Figure 1.3 Classification of low cost adsorbents

1.6 Treatment of industrial wastewater by adsorption processes

With the dawn of civilization, industrial development has exceeded rapidly in the past few decades. It has added a huge amount of different pollutants including HMs into the receiving water bodies. In developing countries like India, tannery and battery manufacturing industries are very common and significantly contribute towards the

economy of the country. These industries generate a huge amount of colored, fowl smelling concentrated effluents. These effluents not only pollute the water bodies but also the ambient air and create toxicological and aesthetical problems (Anandkumar and Mandal 2011).

Currently, Indian leather Industry possesses 6th position all over the world in the leather production and is among the top ten foreign exchange recipients for the country (Sharma and Malaviya 2016). There are more than three thousand tanneries spread all over India specially located in Tamil Nadu, West Bengal, Uttar Pradesh, Andhra Pradesh, Bihar, Gujarat, and Maharashtra of which about 80% of tanneries come under small-scale zone (Bharagava and Mishra 2018). Moreover, as estimation, about 0.8 million tons chrome tanned leather wastes are generated per year globally (Yan et al. 2016). Therefore, tannery industry is known as one of the highest water polluting industries. It utilizes animal hides and skins that are transformed by use of water, chemicals and mechanical process. Normally, chrome-tanning technique is applied for leather manufacturing as it produces leather with the supreme performance at a reasonable price (Mohammed and Sahu 2015). About 60% of the tanneries use chromium tanning 32 times greater than vegetable and other tanning methods (Ouaissa et al. 2012). The effluents contain tons of organic substances, inorganic salts e.g. enzymes, sodium sulphide, lime, ammonium salts, sulphuric acidazo dyes, phenols, p-Cresol, dichloro-benzoic acid, phthalates, polychlorinated biphenyls, pesticides, sulphonated oils etc. (Goutam et al. 2017; Vilardi et al. 2018). These chemical are supposed to increase the TDS, TSS BOD, COD, pH, conductivity, high levels of Cr in the effluent (Ahmed et al. 2011; Bhatti et al. 2017;Kuppusamy et al. 2017). The main problematic part of the discharge of tannery effluent is with the amount of Cr, which is described as one of the most toxic element posing adverse effect on the health of living beings. Likewise, battery or flashlight manufacturing industry is also one of the eldest industries of India and uses large quantities of water. It also produces dense, fowl smelling hazardous effluent with heavy loads of inorganic pollutants and HMs e.g. Pb, Cu, Cd & Ni (Vergili et al. 2017). The highest concentration of Pb have been reported in the battery manufacturing industrial effluents as salts of lead are used on a larger scale to produce batteries as these have the characteristics of resistance to corrosion. The special reversible reaction between

lead oxides, lead sulfates and lead di oxides with sulphuric acid is used in production, negative and positive drying operations (Bahadir et al. 2007).

Industries discharge their effluent into the nearby water bodies without any or improper treatment (Poonam and Kumar 2018). Normally, farmers utilize water of these receiving water bodies for irrigation purpose that contains different pollutants with HMs including Cr and Pb. These HMs may contaminate the food chain and get bio-accumulated in the fatty and living tissue posing threat to the lives. Therefore, in order to prevent negative impacts of these HMs, it became essential to treat the effluent before discharge into receiving water bodies. Conventionally, physicochemical and biological processes such as flocculation, oxidation, sedimentation, filtration, activated sludge, bioremediation etc. are used to treat the wastewater generated by these industries (Ayoub et al. 2011; Martino et al. 2013; Mansoorian et al. 2014; Ahmed et al. 2016; Ravulapalli and Kunta 2018). However, adsorption process is preferred over these methods due to its affinity, selectivity toward HMs and other contaminants, possible regeneration of the metals and being economic as well as ecofriendly (Piccin et al. 2012; Fabbricino et al. 2013; Yan et al. 2016; Dinh et al. 2017; Mella et al. 2017). The present work was aimed to remove heavy metals present in industrial wastewater by application of different adsorbents in an ecofriendly and cost effective manner. More precisely, following specific objectives were drawn for this study –

1. Estimation of physicochemical properties and heavy metals present in the industrial wastewater.
2. Removal of heavy metals from wastewater using various combinations of agricultural wastes.
3. Optimization of control techniques for the removal of heavy metals from the wastewater using agricultural wastes.
4. Risk assessment of heavy metals to the environment.

Chapter 2

Review of Literatures

2. Review of Literature

Water is the most vital natural resources on the surface of the earth and one of the most essential needs of human beings. However, access to safe drinking water is very narrow especially in third world countries. Statistics shows water borne diseases cause about 90% of all deaths of children under five years old in developing nations. Here, resistance of children to infections is also very low (WHO 2015). Water pollution caused by organic and inorganic compounds, heavy metal is a foremost worry for environmental protection and human health (Kurniawan et al. 2011). Inorganic pollutants includes chlorides, phosphates, nitrates, sodium ions, potassium ions, carbonates and bicarbonates, heavy metals (HMs) like As, Cd, Pb, Ni, Fe, Cr, Hg, Co etc. Whereas organic pollutants comprise of pesticides, fertilizers, hydrocarbons, plastics, biphenyls, cleansers, oils, drugs, proteins and carbohydrates.

Toxic heavy metals contamination of water is a worldwide problem initiated by natural or manmade sources, primarily, wastewaters generated by metal plating, paints and pigments, ceramic and glass industries. According to the US Environmental Protection Agency (USEPA), HMs represent a serious problem for human health because they are non-biodegradable and tend to accumulate in living organisms causing several diseases in humans (Argun and Dursum 2008). Further, exposure to elevated levels of HMs causes various adverse effects not only to humans but all other living beings present in or near the vicinity of water by food chain. The excess of HMs may result in ill effects e.g. impairing mental and neurological function, kidney and liver malfunctioning etc. (Alluri et al. 2007; Song et al. 2011; Vetriselvi and Santhi 2015). In alive creatures, HM ions can bind to nucleic acids, proteins, and small metabolites that may end in altered or lost biological utilities of cells with losing homeostatic regulation, finally ensuing lethal health problems (Liu et al. 2009). Therefore, it is essential to abolish such lethal HMs before discharging it into the aquatic ecosystem (Singanan et al. 2013).

Various physicochemical conventional and non- conventional treatment techniques are used now days by the researchers to restore the quality of aquatic system and remove HMs such as ion exchange (Khan and Paquiza 2011), reverse osmosis and nanofiltration (Liu et al. 2008; Ungureanu et al. 2015), precipitation (Gharabaghi et al. 2011), and other physicochemical processes including electrochemical methods, coagulation & flocculation (Fu and Wang 2011; Ungureanu

et al. 2015). However, these methods are associated with noteworthy drawbacks, *e.g.* chemical and energy necessities, unsafe sludge generation, low efficacy for HM concentration below 100 mg L^{-1} and high cost at larger scale (Banerjee et al. 2012). Among these treatment techniques, adsorption is usually favored for exclusion of HM ions due to its high competence, easy handling, accessibility to raw materials and low cost (Salam et al. 2011; Kim et al. 2013; Poonam et al. 2018). Adsorption is an efficient method for the removal of low concentrations of toxic metal ions from aqueous solutions. In this context, biosorption has emerged as an auspicious technique, with many benefits as (1) high efficiency even with low metal concentrations, (2) low cost, (3) no additional nutrients requirements, (4) easy operation, (5) possible metal recovery, and (6) deprived of harmful effects on the environment (Manzoor et al. 2013; Poonam and Kumar 2018).

Low cost biosorbents are normally agricultural, animal, industrial and household wastes e.g. bark, stem, leaves, roots, flowers, husk, skin, bran, stone, tea waste, sawdust, paper wastes etc. (Banerjee et al. 2012; Nguyen et al. 2013). These are mainly composed of polymers like cellulose, hemi-cellulose and lignin that have large amount of surface functional groups (Basu et al. 2017; Shehzad et al. 2018). Some of the main functional groups present in biosorbents are carboxylic, phenolic, alcoholic, carbonyl, phenolic, amino groups etc. (Liang et al. 2010; Guiza 2017). These groups have the affinity towards inorganic ions and organic groups to form complexes or chelates. The process involves the substitution of H^+ for HM ions present in medium or contribution of an electron pair to form complexes with HM ions in solutions (Sarker et al. 2017). These biosorbents can be adapted for better efficiency and manifold reuses to improve their applicability at industrial scale (Poonam et al. 2018). Many researchers have reported adsorption as an effective and ecofriendly method for the removal of low concentrations of HM ions from aqueous solutions (Kim et al. 2013; Nguyen et al. 2013; Lakherwal 2014; Anastopoulos et al. 2016; Basu et al. 2017).

Numerous aspects are affect adsorption of HMs comprising kind of adsorbent, chemistry of HMs and environmental conditions. In this context, definite mechanism of biosorption is not completely implicated, however several mechanisms have been anticipated. Chief mechanisms of biosorption comprise of chemisorption, complexation, diffusion and ion exchange etc. For instances, Taha et al. (2011) reported removal of Pb(II), Cd(II) and Zn(II) using potato peel by ion-exchange

mechanism. They found the high adsorption capacity of potato peels to active functional groups such as carboxylic, phenolic and hydroxyl groups. Similarly, Netzahuatl-Muñoz et al. (2012) examined ion exchange and electrostatic interaction mechanisms for removal of Cr(III) and Cr(VI) by *Cupressus lusitanica* bark. They explained that principal mechanisms involved in biosorption of Cr(III) biosorption in four steps: (1) Cr(VI) complexes formation, (2) reduction of Cr(VI) to Cr(III), (3) formation of carboxyl groups and (4) interaction of Cr(III) with carboxyl groups to form Cr(III) carboxylate complexes. Through FTIR, SEM, EDX methods, Witek-Krowiak et al. (2013) exposed the prevailing mechanisms for biosorption of Cr(III) and Cu(II) onto soybean meal waste include (1) ion exchange, (2) chelation by carboxyl and hydroxyl groups, and (3) precipitation. It was reported that hydroxyl, carboxyl, phosphate, hydroxyl, amino and thio groups played major role in binding with the contaminants present in ionic form on biosorbent's cell walls (Witek-Krowiak et al. 2013). These functional groups may alter their hydrogen ions for metals or other hydrophilic groups or donate an electron pair for complex formation with HM ions (Kumar et al. 2011). Lasheen et al. (2012) specified participation of carboxylic groups in Pb adsorption by chemically modified orange peel. Whereas, Feng et al. (2011) reported that carboxyl and hydroxyl groups were involved in biosorption of metal ions by grafted polymerization-modified orange peel. Likewise, fluoride was removed from water by Zr–Mn composite material prepared via co-precipitation method (Tomar et al. 2013). A by-product of pyrolysis process, was successfully used as an alternative low-cost adsorbent for exclusion of Ni(II)and Co(II) ions from aqueous solution by Kılıc et al. (2013).

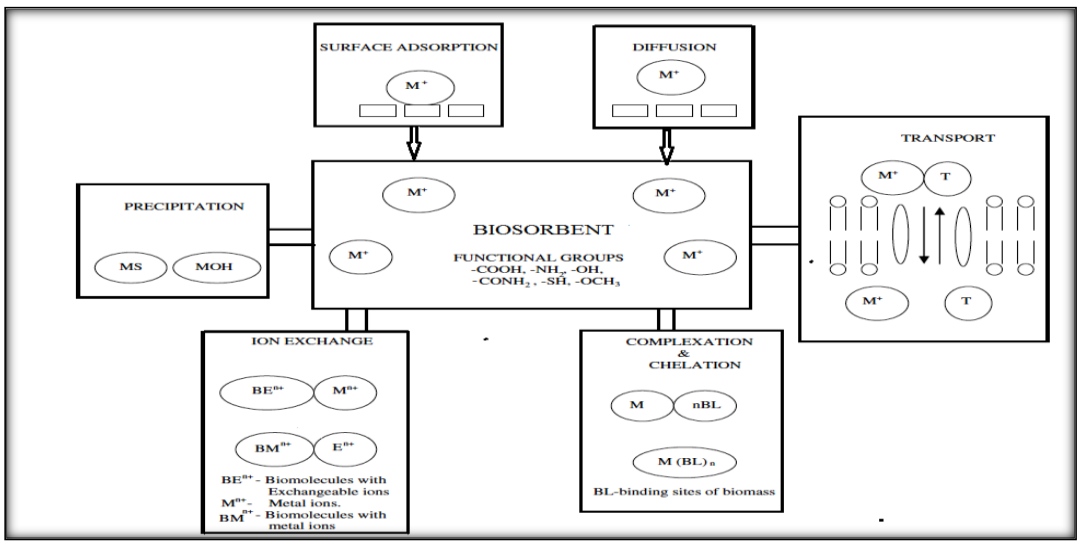

Figure 2.1 Possible mechanism of adsorption (Source- Sud et al. 2008)

In addition to this, various factors are also responsible for successful adsorption of HMs from water and wastewater. The details of these factors have been given below-

1. **pH** of the solution is an important factor that governs adsorption of HMs. The hydrogen ions effectively increase or decrease adsorption of metal ions present in the solution as H^+ ion compete with the cations or the ions of the solution. Thus, pH values affect surface charge of bio-sorbents and ionization of HMs and competition of these with co-existing ions of the solution (Park et al. 2010; Nguyen et al 2013). At lower pH, there will be positive charge on the surface of the adsorbent, thus there will be more competition for the cations. Thus, adsorption of metals with the positive charge will be low and of the negative charge will be comparatively higher. Rajoriya and Kaur (2014), reported increase in Zn uptake with increasing pH till the equilibrium was attained by using lemon and banana peel as adsorbent. The maximum removal of Zn by lemon and banana peel was 87.5% and 90.5% respectively at pH 4. In the same way, Li et al. (2013) and Božić et al. (2013), also reported the same pattern of increased removal percentage with increasing pH, for Cu, Cr^{3+} and Cu, Ni, Zn by using root powder of *Eicchornia crassipes* and beech saw dust, respectively. But, study of removal of Cr^{6+} by Li et al. (2008) through beads of powder of *Rhizopus cohnii* and Fe_3O_4 coated with alginate and polyvinyl alcohol did not supports this assumption, as they reported that at pH 1, almost all hexavalent Cr in the solution was removed. Fathima et al. (2015) also reported increased removal percentage of Cr^{3+}ions with increasing pH up to 4 by using fungal biomass (*Termitomyces clypeatus*) as adsorbent.
2. **Specific surface area** is described as total available area on the surface of biosorbents for adsorption (Naeem et al. 2007). Adsorption is a phenomenon that is very dependent upon specific surface area of particular adsorbent. Tomar et al. (2013) reported that specific surface area of nano-adsorbent Zr–Mn before and after F adsorption was found to be 234.973and 247.280 m^2 g^{-1}, respectively. Results clearly indicate that large surface area of the adsorbent facilitated process and after adsorption, surface areas increased accordingly. Ahmady-Asbchin et al. (2008) reported low surface area of *Ficus serratus* for

the removal of Cu which is increased by the water immersion thus enlargement of the surface area increased adsorption capacity.

3. **Particle size** is directly related to surface area of adsorbent as finer will be particle of adsorbent, larger the surface area and higher will be the probability of the adsorption of HMs on the surface. Tomar et al. (2013), Ahmady-Asbchin et al. (2008), Bernard and Jimoh (2013) etc. had reported that finer particles of the different adsorbent had higher efficiency to remove heavy metals from the solutions.
4. **Nature of adsorbent** can be described as the structure, physicochemical properties, solubility and the porosity of the adsorbent. An adsorbent with compact structure, high porosity and lower solubility in the solvent will be having a tendency to adsorb higher amount of the metals and other organic and inorganic contaminants (El-Sheikh et al. 2004).
5. **Effect of temperature on** biosorption of HMs has been analyzed by various researchers. Some of them have reported that adsorption is an exothermic process while others have reported it to be an endothermic process (Kılıç et al. 2013; Reddy et al. 2014; Elabbas et al. 2016; Khan et al. 2017; Lin et al. 2017). Temperature of the solution affects solubility of HMs, inorganic and organic contaminants, diffusion rate of the metals, damages the active binding sites and thus, the adsorption rate also (Park et al. 2010). Rajoriya and Kaur (2014) reported exothermic adsorption with decreased removal i.e. from 82.68 to 71.76% and 86.8 to 76.4% of Zn by using lemon and banana peel as adsorbent, with increase in the temperature from 30 to 50^0C by lemon peel and banana peel, respectively. Likewise, Fathima et al. (2015) also reported maximum removal efficiency (21.79 mg g^{-1}) of fungal biomass (*Termitomyces clypeatus*) for Cr^{3+} ions with minimum temperature ie 30^0C, when experiments were carried out among temperature range of 30, 40, 50, 60 and 70^0C. However, Buasri et al. (2012) reported opposite trend as they found increase in biosorption of Zn with an increase in the temperature up to 70^0C i.e. endothermic adsorption. It was explained as activation of metal ions at coordinating sites of minerals, available for biosorption amplified with higher temperature. Likewise, Kılıç et al. (2013) also reported higher rate of adsorption of Ni and Co by using bio-char of by-product of almond shell pyrolysis with increasing temperature. Authors explained it as increased

adsorption rate may be recognized as upsurge in no. of active surface sites accessible for adsorption at higher temperatures.

6. **Dosage** of adsorbents has been considered an important factor to influence adsorption of HMs by different researchers (Kılıç et al. 2013; Fathima et al. 2015; Chen et al. 2018). They have reported that as dosages of adsorbent have been increased, adsorption rates have also been found to increase until the equilibrium is reached. This may be described on basis of increase in surface area, adsorbent particles adjacent to metal ions or ratio of adsorbent particles available to metal ions (Guiza 2017; Temesgen et al. 2018). Bernard and Jimoh (2013) found increase in adsorption of Pb, Fe, Cu and Zn with increasing dosage of activated carbon of orange peel until equilibrium point. Pb attained maximum removal at lower dosage with 100% removal; Fe and Zn were removed by 70.06% and 32.53% with the dose of 1g and Cu 61.29% with the dose of 0.8g. Furthermore, Kılıç et al. (2013) also reported increased percentage of adsorption with increasing adsorbent dosage for Ni and Co, by using biochar of by-product of almond shell pyrolysis, till saturation point. They reported optimum adsorbent dose 7 and 4 g L^{-1} for Ni and Co, respectively. Likewise, Thakur and Parmar (2013) also reported increase in removal percentage of Ni, Cu and Zn with dose range 0.2 to 1gm/100ml of solution, by using tea waste as adsorbent. The maximum adsorption percentage was 91% for Ni at dose of 4 g L^{-1}, 84% for Cu and 91% for Zn at 6 g L^{-1}, respectively. Fathima et al. (2015) also reported increasing removal percentage of Cr^{3+} ions from fungal biomass (*Termitomyces clypeatus*) with increasing adsorption dosages upto the equilibrium point. The maximum removal of Cr^{3+} was found to be 92.40% at adsorbent dose of 5 g L^{-1}.
7. **Contact time** is also important factor as it affects the adsorption rate of HMs by different adsorbents. Most of the researchers have reported that initially, the rate of adsorption has been found to be rapid as there are numerous vacant active sites. It provides energy to bring HM ions from majority of solution to the accessible sites by reducing resistance of mass transfer between bulk phase and adsorbent (Rajoriya and Kaur 2014). However, after attaining the equilibrium, the rate of adsorption decreases because of saturation of available sites. Salam et al. (2011) studied consequences of contact time on exclusion of Cu and Zn by peanut husk, fly ash and natural zeolite. They found that the rate

of metal uptake was as high as 60% for Cu^{2+} and 62% for Zn^{2+}, when natural zeolite was used as adsorbent, in first 30 min and at equilibrium, 97.5% Cu^{2+} and 90% Zn^{2+}were removed from the aqueous solution. Further, Bernard and Jimoh (2013) studied effect of contact time on adsorption of Pb, Fe, Cu and Zn from wastewater of electroplating industry by activated carbon of orange peel. They reported removal rate of all of the HMs increased with increasing contact time till equilibrium point, which was 60 minutes for Pb(100%), Cu(51.47%) and Zn(20.12%) and 40 minutes for Fe(56.63%). Likewise, Thakur and Parmar (2013) and Tomar et al. (2013) and Rajoriya and Kaur (2014) have also reported same findings for different HMs. Tomar et al. (2013) also reported increased removal of F ion with increased contact time upto 145min by using Zr-Mn composite materials. Kılıç et al. (2013) studied effect of contact time (30-240 min) on removal of Ni and Co by using bio-char of by-product of almond shell pyrolysis. They also reported increased amount of adsorption for both of the metal until 150min after that the adsorption sites were found to be saturated and removal remained constant after that. Rajoriya and Kaur (2014) reported increased removal of Zn by lemon and banana peel with equilibrium time of 260 min for both.

8. **Initial metal ion concentration** enforces the transport of HM ions from solution to the surface of adsorbents (Taha et al. 2011). In common, it has been found that the rate of the adsorption increased as initial metal ion concentration increased. Busari et al. (2012) studied the biosorption of Zn on corn cob and reported that biosorption of Zn increased with upsurge in metal ion concentration up to 750 ppm, beyond that no significant biosorption was observed. According to authors this pattern of biosorption was because of the involvement of the energetically less favorable sites. Tomar et al. (2013) also found the same result of increased removal percentage of F^- ions with increase in initial metal ion concentration. Kılıç et al. (2013) also reported increased adsorption amount as initial concentration of Ni and Co were gradually increased within the range of 50-200 mg/L by using bio-char of by-product of almond shell pyrolysis. But, Salam et al. (2011) reported that removal of Cu and Zn reduced with increase in initial metal ions concentration, using peanut husk, fly ash and natural zeolite as adsorbents. According to the authors, the adsorption sites were saturated as the initial metal ion concentration increased. They reported that maximum removal of Cu and Zn was 91% and 96%

respectively, at concentration 10mg/l using natural zeolite. Similarly, the study of removal of Cu from solution by using water melon shells as adsorbent done by Banerjee et al. (2013) also reported decrease in removal percentage as the initial ion concentration was increased. Further, Rajoriya and Kaur (2014) also reported decrease in percentage removal of Zn as concentration of Zn increased from 50-300 mg/L, when lemon and banana peel were used as adsorbents. The results were explained on the basis of diffusion of metal ion by intraparticle diffusion to adsorbent surface and at higher metal ion concentration to adsorbent proportion, higher energy sites used to saturate and process start on lower energy sites.

9. **Selectivity of the adsorbents** is an important parameter as different organic materials are used as bio-adsorbents, which have different preferences for different metals to adsorb. Taha et al. (2011) reported that potato peel had higher efficiency to remove Pb in comparison to Cd and Zn. Likewise, Alfa et al. (2012) reported higher removal of Cu than Pb by frond and leave samples of dump palm. Similarly, Bernard and Jimoh (2013) reported higher removal of Pb by orange peel than Fe, Cu and Zn at different parameters like pH, contact time and adsorbent dosages. These studies indicated that some organic materials have higher selectivity towards different heavy metals, which highly depends upon the active sites and adsorbing groups present in adsorbents.

Adsorption Modeling

A no. of mathematical impressions, isotherms, kinetics, thermodynamic studies and desorption mechanisms have been given by different scientists and researcher to support and describe the hypothesis of adsorption as function of pressure (if gas) or concentration (if liquid) at constant temperature (Anastopoulos and Kyzas 2014). A brief aspect of these are given below-

Adsorption Isotherms

These models are mostly used to describe the maximum amount of heavy metals (adsorbate) adsorbed by certain adsorbent and the mode of interaction taking place between them (Bharathi and Ramesh 2013).

1. Langmuir Isotherm- In 1916, Irving Langmuir proposed an adsorption model to explain the variation of the adsorption with respect to the pressure. This model is used to define the single-layer adsorption, where molecules are adsorbed at fixed number of well-defined, homogeneously distributed all over the surface of adsorbent (Langmuir 1918).

Assumptions of Langmuir isotherms are as following-

i) There is the availability of fixed no. of vacant or adsorption sites on surface of solid.

ii) The shape and the size of adsorption sites on surface of the adsorbents are equal.

iii) All of the adsorption sites can adsorb maximum one gaseous molecule and in this process, a constant amount of heat energy is released.

iv) There exists a dynamic equilibrium between adsorbed gaseous molecules and free gaseous molecules-

$$A\ g\ +\ B\ S \underset{K_d}{\overset{K_a}{\rightleftharpoons}} AB$$

where, K_a is equilibrium constant for forward reaction and K_d is equilibrium constant for backward direction.

v) Adsorption is always monolayer or unilayer and reversible, when there is no interaction between molecules adsorbed on active site and neighboring site (Ruthven 1984; Febrianto et al. 2009).

The mathematical equation of Langmuir isotherms (non-linear form) have been given below-

$$\mathbf{q_e} = \mathbf{q_{max}} \frac{\mathbf{bC_e}}{\mathbf{1 + bC_1}}$$

Whereas, Langmuir isotherms linear form is as following-

$$\frac{\mathbf{C_e}}{\mathbf{q_e}} = \frac{\mathbf{1}}{\mathbf{q_m}} \mathbf{C_e} + \frac{\mathbf{1}}{\mathbf{b_L\, q_m}}$$

Where, q_e= equilibrium metal adsorption capacity of the adsorbent (mg g^{-1}), Ce (mg L^{-1}) = equilibrium solute concentration in the solution; b = Langmuir constant of maximum sorption monolayer capacity and bonding energy of the adsorption, q_m =

saturated monolayer adsorption capacity (mg g^{-1}), b_L= constant related to energy of sorption and equilibrium (L mg^{-1})

2. Freundlich Isotherm - On contrary with Langmuir's isotherm, this isotherm interprets the adsorption on heterogeneous surfaces and there is also no compulsion of the formation of a monolayer. In 1909, Herbert Freundlich gave this expression to describe the isothermal disparity of adsorption of gas molecules adsorbed by unit mass of solid adsorbent with pressure. It describes an empirical relation between concentrations of solute on surface of an adsorbent to concentration of solute in the liquid with which it is in contact with (Freundlich 1906).

This isotherm works on the assumption that when adsorbate concentration increases, the concentration of the adsorbate on adsorbent surface also increases, but the adsorption energy exponentially decreases, when the adsorption process is completed (Faust and Aly 1987).

The mathematical expression of Freundlich isotherm (non-linear form) is given below-

$$q_e = K_f \frac{1}{n}$$

Whereas, the linear form of Freundlich isotherm is s following-

$$\text{In } q_e = \text{In}K_f + \frac{1}{n} \text{ In } C_e$$

where, K_f = coefficient of adsorption equilibrium; 1/n = heterogeneity factor

3 BET Isotherm- This hypothesis works on the condition, where there is an adsorption on multilayer system i.e. some of the adsorbent molecules are adsorbed on already adsorbed molecules, forming a multilayer. This condition is contrary to the Langmuir isotherm's single layer system. To overcome with this kind of situation, in 1938 Stephen Brunauer, Paul Emmett, and Edward Teller discovered a model isotherm that consider these kinds of possibilities into account. On the name of all of the three scientists, their theory was called as BET theory, after initials in names of the scientists. This theory take into account that gaseous molecules behave ideally and each adsorbed molecule may provide a site for the adsorption of the molecule in the layer above it, thus producing a multiple layer system. The mathematical impression of their theory is as following-

$$\frac{\mathbf{x}}{\mathbf{v}\ \mathbf{1}-\mathbf{x}} = \frac{\mathbf{i}}{\mathbf{v_{mon}C}} + \frac{\mathbf{x(C-1)}}{\mathbf{v_{mon}C}}$$

where, x= pressure divide by the vapor pressure for the adsorbate at particular temperature, v= STP volume of the adsorbed adsorbent, v_{mon}= STP volume of the amount of adsorbate required to form a monolayer, and, c = equilibrium constant b (used in Langmuir isotherm) multiplied by the vapor pressure of the adsorbent (Source- Derivation of the BET and Langmuir Isotherms 2011).

4. Kisliuk Isotherm- Sometime there may be such kind of interaction where, a gaseous molecule is adsorbed on the surface of a solid from a significant interaction between a other gas molecules in the gaseous phase. On such kind of situation, Langmuir isotherm fails to be applied, as it considers no interaction between the adsorbing molecules. Such effect was studied by Paul Kisliuk in 1957, where he used nitrogen and tungsten as adsorbate and adsorbent respectively (Kisliuk 1957). He found that there was an increase in the probability of adsorption around molecules present on surface of the substrate. To compensate for this increased probability of adsorption, Kisliuk discovered precursor state theory, that defines that molecules would enter a precursor state at interface between solid adsorbent and adsorbate in the gaseous phase. The precursor state decides the probability of adsorption will depend upon the proximity of the adsorbate to other adsorbate molecule that has already been adsorbed. The mathematical expression for the Kisliuk isotherm is given by-

$$\boldsymbol{k_E = \frac{S_E}{k_E S_D}}$$

where, S_D= adsorption rate constant, k_E= sticking coefficient

5. Redlich-Peterson Isotherm- This isotherm is a hybrid form of Langmuir and Freundlich isotherm and it does not follow ideal monolayer adsorption (Wasewar 2010). It supports Freundlich model at higher concentration and Langmuir equation at lower concentration limit. The numerator is from the Langmuir isotherm and denominator has an exponential function (Redlich and Peterson 1959).This equation can be utilized in either homogenous system or heterogeneous system and can be described as follows-

$$q_e = \frac{K_R C_e}{1 + a_R C_e^{\beta}}$$

where, K_R and a_R= Redlich-Peterson isotherm constants (L mg^{-1}), q_e= equilibrium metal adsorption capacity of the adsorbent (mg g^{-1}), Ce= equilibrium concentration of adsorbate (mg L^{-1}), β = exponent (lie between 1 and 0).

When β = 1

$$q_e = \frac{K_R C_e}{1 + a_R C_e}$$

6. Temkin Isotherm- This isotherm is explains the condition of on account of the adsorbing material and the adsorbate interactions. This equation does not involve the concentration factor and the model undertakes that (i) heat of adsorption of all molecules in the layer decreases linearly rather than logarithmic with coverage due to adsorbate-adsorbate interaction and (ii) adsorption is characterized by an uniform dispersal of binding energies, up to some maximum binding energy (Temkin and Pyzhev 1940; Aharoni and Ungarish 1977). Temkin isotherm is represented by following equation:

$$q_e = \frac{RT}{b} \ln K_T C_e$$

where, K_T = equilibrium binding constant (L mg^{-1}), R = universal gas constant (8.314J mol^{-1} K^{-1}), T = Temperature at 298 K, K_T = Temkin isotherm equilibrium binding constant (L g^{-1}), b = Temkin isotherm constant

7. Dubinin-Radushkevich-This is an empirical isotherm equation. It is used, extensively, for the estimation of the nature of the biosorption process by the help of Gaussian energy distribution onto the heterogeneous surface of bio-sorbents (Dubinin and Radushkevich 1947). The equation is represented as following-

$$q_e = q_m e^{-B\pounds^2}$$

$$\pounds = RT \ln \left(1 + \frac{1}{C_e}\right)$$

where, q_m= the maximum biosorption capacity of the bio-sorbent (mg g^{-1}), B = constant related to free energy of biosorption {mol^2 $(kJ^{-2})^{-1}$}, £ = Polanyi potential

8. Sips model- This model is derived from the combination of Langmuir and Freundlich models (Deniz and Karabulut 2017). This model is more competent as compared to others to describe the biosorption equilibrium (Sips 1948). The equation is represent as-

$$\mathbf{q_e} = \frac{\mathbf{q_m}(\mathbf{K_s}\,\mathbf{C_e})^{\mathbf{1}\ \mathbf{n_S}}}{\mathbf{1} + (\mathbf{K_s}\,\mathbf{C_e})^{\mathbf{1}\ \mathbf{n_S}}}$$

where, K_s = Sips equilibrium constants (mg^{-1} L), n_S (-)= Sips model exponent

Kinetic models

Adsorption kinetics is a significant parameter to define basic characteristics of an effective adsorbent (Wang et al. 2012). These studies are conducted to find the optimum condition for full-scale adsorption process (Anastopoulos and Kyzas 2014). It describes the mechanisms involved that controls the sorbate interaction at the solid–solution interface at different time. Kinetic modeling reveals the adsorption mechanism and the rate controlling factors involved in the process. The rate of the adsorption process depends upon the mass transport and chemical reaction process (Kyzas and Matis 2014; Anastopoulos et al. 2016). There is several kinetic models e.g. pseudo-first order, pseudo-second order, Weber-Moris and Elovich are available. Among these pseudo first and second order kinetic models are commonly used (Table 2.1). In the present work, pseudo-first and second order reactions were employed to obtain the adsorption mechanisms involved in Cr and Pb elimination procedures by various biochars (Lagergren et al. 1898; Ho et al. 2000).

Pseudo-first kinetic model (Eq 1) is given as-

$$In\ \ q_1 - q_t\ \ = In\, q_1 - k_1 t \qquad (1)$$

where, q_1 and q_t are quantites of heavy metals (mg g^{-1}) absorbed at equilibrium time t, respectively, and k_1 is first-order rate constant (min^{-1}).

According to Mckay and Ho (1999), pseudo-second order kinetic model (Eq 2) is expressed as-

$$\frac{t}{q_t} = \frac{1}{k_2 q_2^2} + \frac{1}{q_2} t \quad (2)$$

$$\frac{1}{q_t} = \frac{1}{K_2 q_2 t} + \frac{1}{q_2} \quad (3)$$

Eq.(3), modified Ritchie's-second order kinetic model, is applied for calculation of initial sorption rate, h(mg $g^{-1}min^{-1}$) (Eq. 4).

$$h = K_2 q_2^2 \quad (4)$$

where, q_2 is the maximum adsorption capacity (mg g^{-1}) for pseudo-second-order adsorption, K_2 is equilibrium rate constant for pseudo-second-order adsorption (g mg^{-1} min^{-1}) and h is initial sorption rate (mg g^{-1} min^{-1}).

Thermodynamic models

It is a measure of adsorption spontaneity, the nature of adsorbents and adsorbate at equilibrium conditions (Anastopoulos and Kyzas 2014). It also explores the temperature range for favorable adsorption. The important thermodynamic parameters are change in Gibbs energy (ΔG°), adsorption enthalpy (ΔH°) and entropy (ΔS°). The expression of Gibbs free energy is given as-

$$\Delta G^{\circ} = -RT \ln K_L^a \quad (5)$$

where, ΔG^{o} = Gibbs free energy change (kJ mol^{-1}); R= universal gas constant; T= absolute temperature at 298K. The distribution coefficient K_L (L mol^{-1}) of isothermic fit is calculated by the following relationship-

$$K_L = \frac{Ce_{ads}}{Ce_{aq}}$$

The Van't Hoff equation for calculating enthalpy (ΔH°) and entropy (ΔS°) is given by-

$$\ln (K_L) = -\frac{\Delta H^{\circ}}{RT} + \frac{\Delta S^{\circ}}{R} \text{ and,}$$

$$\ln\left(\frac{Q_e}{C_e}\right) = -\frac{\Delta H^{\circ}}{RT} + \frac{\Delta S^{\circ}}{R}$$

where, Entropy change = K_L (L mol^{-1}) from Langmuir model; Q_e = metal ions adsorbed at concentration (mg L^{-1}); C_e = residual ion concentration in solution (mg L^{-1}); ΔH^o = enthalpy change (kJ mol^{-1}) and ΔS^o = entropy change (kJ mol^{-1})

The Clasius Clapeyron is given by-

$$\Delta H^0 = \frac{RT_1T_2}{T_2 - T_1} - \frac{In\ Ce_{ads}}{InCe_{aq}}$$

where, Ce_{ads} is the equilibrium concentration of HMs on the adsorbent (mg g^{-1}) and Ce_{aq} is the equilibrium concentration of HMs in the aqueous solution (mg L^{-1}). The values of ΔH^o and ΔS^o were calculated from the slope and intercept of Van't Hoff plot between ln $(\frac{Q_e}{C_e})$ versus 1/T. Further, the mathematical formulas are represented in Table 2.1 through which adsorption data at different temperatures are calculated.

Table 2.1 The mathematical impressions of important kinetic and thermodynamic models

Expression	Equation	Plots	Parameters	References
		KINETICS		
Pseudo first order kinetic (Non-linear)	$q_t = q_e(1 - \exp^{-k_1 t})$	-		
Pseudo first order kinetic (Linear)	$\ln\ q_e - q_t = \ln q_e - k_1 t$	ln (q_e-q_t) vs t	q_t (mg g^{-1}) = amount adsorbed at time t (min); k1 (min^{-1}) = pseudo first order rate constant;	Blanchard et al. (1984); Lagergren (1898); Ho and Mckay (1999); Anastopoulos et al. (2016)
Pseudo second order kinetic (Non-linear)	$q_t = \frac{k_2\, q_e{}^2 t}{1 + k_2 q_e t}$	-	k_2 (g mg^{-1} min) = pseudo second order rate constant	
Pseudo second order kinetic (Linear)	$\frac{t}{q_t} = \frac{1}{k_2\, q_e{}^2 t} + \frac{1}{q_e} t$	t/q_t vs t		

THERMODYNAMICS				
Gibbs	$\Delta G^{\circ} = -RT \ln b_1^a$	-	Gibbs free energy change; R= universal gas constant; T= Temperature at 298K	
Van't Hoff	$\ln (b_L) = -\frac{\Delta H^{\circ}}{RT} + \frac{\Delta S^{\circ}}{R}$ $\ln (\frac{Q_e}{C_e}) = -\frac{\Delta H^{\circ}}{RT} + \frac{\Delta S^{\circ}}{R}$	$\ln (b_L)$ vs $\frac{1}{T}$ $\ln (\frac{Q_e}{C_e})$ vs $\frac{1}{T}$	Entropy change; b_L (L/mol) from Langmuir model; Q_e metal ions adsorbed at concentration (mg/L); C_e residual ion concentration in solution (mg/L); K = $Q_m X b_L$ calculated from Langmuir constants	Anastopoulos and Kyzas (2014); Anastopoulos et al. (2016)
Clasius Clapeyron	$\Delta H^{\circ} = \frac{RT_1T_2}{T_2-T_1} - \frac{In\ C_{e1}}{InC_{e2}}$	-	Enthalpy change	

Desorption process

Although most of the naturally occurring agricultural wastes have the potential to adsorb heavy metals from aqueous medium, but the ability of adsorbents to be regenerated is a crucial factor to access its reusability. An ideal adsorbent should have better desorbing power together with higher adsorption capability to enhance the efficiency of the process (Peng et al. 2017). To regenerate bio-sorbents, desorption process is used which is the simple process of removing adsorbed metals from adsorbents. The most common practical method for desorption of HMs from biomass is leaching with dilute acid (Kariuki et al. 2017). Some of the adsorbents can be efficiently desorbed to reuse it as adsorbent but some of these may lose their natural structure after desorption process. Thus, these cannot be reused efficiently for further treatment of wastes water (Ngulube et al. 2017). Generally, desorption process is carried out to rejuvenate and regenerate precious metals and to reuse adsorbent for minimizing the loads of wastes/sludge in the environment. Different researchers and scientists have reported various eluants for the purpose of desorption of heavy metals. Reddy et al. 2014 reported 0.1M NaOH showed highest desorption capacity ie 98.7%

within 30 minutes for Cr^{3+} ions from watermelon rind as compared to 0.1M HCl and water as eluting agents. In the beginning, rate of desorption is comparatively higher due to escaping of gas phase molecules from the adsorbent surface towards liquid medium i.e. eluants (Hassan et al. 2015). Basu et al. (2017) have used 0.1M HCl, H_2SO_4, HNO_3, Na_2CO_3 and EDTA (ethylene diamine tetra acetic acid) as eluants for desorption of Pb adsorbed onto cucumber biomass. The desorption percentage of Pb was about 97% for 0.1 M HCl in comparison to other four eluants. They performed adsorption-desorption cycle for five times to reach to the results. Petrović et al. (2017) desorbed zinc and copper on raw corn silk by three different solutions: 0.1 mol L^{-1} HNO_3, deionized water at pH 2.0 and deionized water at pH 4.0. Maximum desorption efficiency was 92.80% for Cu in deionized water at pH 2.0 and 99.0% for Zn in 0.1 mol L^{-1} HNO_3. Other eluants ie 0.1 mol L^{-1} HNO_3 and deionized water at pH 4.0 desorbed 92.96% and 5.36% Cu, respectively; 91.60 and 2.52% for Zn by deionized water at pH 2.0 and deionized water at pH 4.0, respectively in three cycles. Further, it was also reported that desorption efficiencies of both metals were lower than 6.0% at pH 4.0 and almost all adsorbed metals were recovered in acidic solutions. The reason may be formation of coordination complexes between metal ions and active functional groups. In the same way, Altun and Pehlivan (2012) desorbed Cr(VI) ions on walnut shells modified with citric acid by 0.5M HCl. They reported 20-25% desorption of Cr^{6+} ions in the acidic medium by three cycles, which was comparatively low than the study made by Petrović et al. (2017) in the acidic medium for Cu and Zn ions. The pattern of desorption of metals in acidic eluants were also followed by Kariuki et al. (2017). They regenerated 70% Cu and 50% Pb by 0.1 M HCl and about 25% Cu and ~15% Pb by 0.1M EDTA from roger mushroom biomass. Li et al. (2013), Velazquez-Jimenez et al. (2013), Suksabye and Thiravetyan (2012), Basu et al. (2017) and Poonam et al. (2018) reported the same pattern of desorption of different heavy metals in acidic medium but Reddy et al. (2014) reported about 98.7% desorption of Cr^{3+} by NaCl from water melon rind. Thus, in most of the cases maximum desorption were reported by acidic eluants in comparison to bases, salts and deionized water.

Heavy metals are one of the most troublesome pollutants in respect to their toxicity, bioaccumulation properties and as precursor of many bio-chemical reactions in the environment. Although, many conventional and non-conventional techniques

have been developed for removal and treatment of the contaminated waste water, but none of them have proved to be the best one in all the aspects (like cost effectiveness, energy consumption, secondary pollutants etc.). In present scenario, biosorption is emerging as an innovative, eco-friendly, cost effective and possible substitute to current conventional technologies for elimination and/or retrieval of contaminants and metal ions from aqueous medium. The selection of appropriate adsorbent is one of the most crucial aspects of this technology. Among different biosorbents available, naturally occurring agricultural wastes with excess carbon substances have shown excellent potential for adsorption of heavy metals as well as dyes and different organic substances (volatile organic carbons, persistent organic pollutants etc.). Furthermore, most of the heavy metals and pollutants adsorbed can also be recycled and reused by the process of desorption.

Almost all of the naturally occurring biowastes show excellent heavy metal adsorption ability at suitable conditions and/or with appropriate modifications. Different functional groups associated adsorbents and their surface are and smaller pore size facilitate the adsorption process. The adsorption conditions such as temperature and pH of medium also influences adsorption process.

In the present study, potential of naturally occurring bio-wastes i.e. peels of sweet lemon, lemon, orange and bagasse were used to treat wastewater of tannery and flashlight manufacturing industries containing Cr and Pb. Different parameters, which influence the adsorption process like adsorbent dosage, contact time, pH, temperature and initial metal ion concentration, related isotherms, kinetics & thermodynamics, desorption potential were also studied.

In the present study, potential of naturally occurring bio-wastes i.e. peels of sweet lemon, lemon, orange and bagasse were used to treat wastewater of tannery and flashlight manufacturing industries containing Cr and Pb. Different parameters, which influence adsorption processes like adsorbent dosage, contact time, pH, temperature and initial metal ion concentration, related isotherms, kinetics & thermodynamics, desorption potential were also studied.

Chapter 3

Material and Methods

3. Material and Methods

3.1 Site Selection

Two sampling sites have been identified for the collection of industrial effluent, as follows-

1. **Common Effluent Treatment Plant, Banther, Unnao, U. P.-** It is located at 26º33’36’’N & 80º30’48”E and is a effluent treatment plant for the raw effluents coming out from different leather manufacturing industries of Unnao, Utter Pradesh.
2. **Eveready Industries India Ltd., Mill Road, Aishbagh Park, Lucknow, U. P**.- It is located at 26º50’22”N & 80º53’33”E and is a battery manufacturing industry engaged in manufacturing different kinds of batteries for cars, inverters, torches etc.

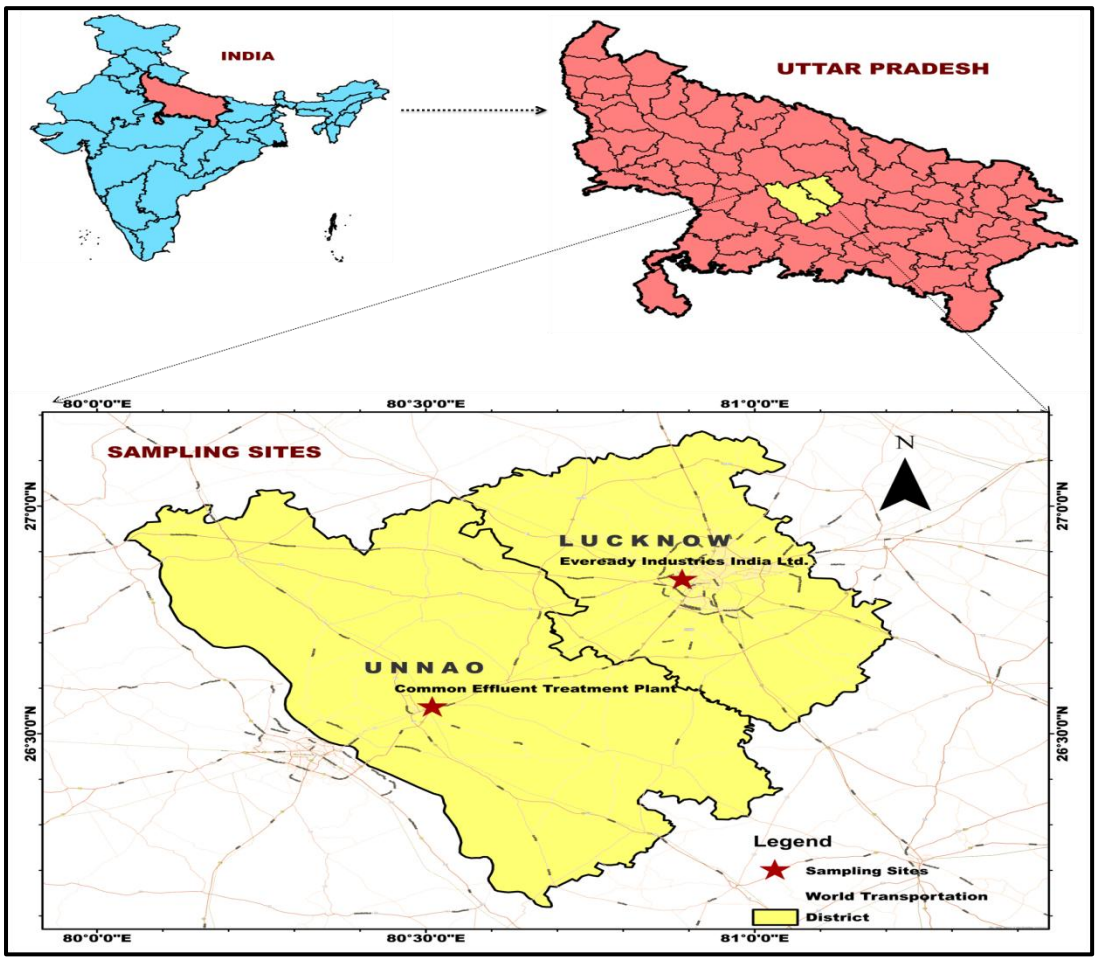

Figure 3.1 Description of sampling site for collection of wastewaters from Unnao and Lucknow, situated in Uttar Pradesh, India

3.2 Sample collection

The samples of wastewaters were collected from outlet both of the selected industries in plastic gallons of 10 litres during winters of January 2014, 2015 and 2016 to reduce the impact of microbial activity on physicochemical characteristics of wastewaters and for avoiding the maximum standard errors.

Figure 3.2 Sampling of wastewaters from tannery (a) and battery manufacturing (b) industries

3.3 Chemicals- The chemical reagents utilized in present study were of analytical reagent (AR) grade from E. Merck, Darmstadt, Germany.

Protocols- The wastewater samples were analyzed physico-chemically by using methods of APHA (2005) and Maiti (2004).

3.4 Analysis of the Samples

The analytical methods and instruments used for the physicochemical analysis of wastewater have been summarized in Table 3.1.

Table 3.1 Methods and instruments used in physicochemical analysis of wastewater

S.No.	Parameter	Method	Instrument/Equipment
1	**Total suspended solids**	Filtration and Weighing	Weighing Machine
2	**Total dissolved solids**	Filtration and Weighing	
3	**Total solids**	Filtration and Weighing	
4	**pH value**	Electrometric Method	pH meter
5	**Electrical Conductivity**	Instrumental Method	Conductivity meter
6	**BOD**	Titrimetric Method	-
7	**COD**	Open Reflux Method	-
8	**Alkalinity**	Titrimetric Method	-
9	**Total Hardness**	Titrimetric Method	-
10	**Chloride (Cl)**	Titrimetric Method	-
11	**Total phosphorus (P)**	Digestion in Kjeldhal method	Spectrophotometer
12	**Nitrogen-nitrate ($N\text{-}NO_3^-$)**	By Cataldo et al (1975) Method	Spectrophotometer
13	**Sulphate**	Turbidimetric Method	Spectrophotometer
14	**Cations(Na, K & Mg, Ca)**	Standard Calibration Method	Ion Chromatograph
15	**Anions (PO_4^{3-})**		
16	**Chromium (Cr)**	Open Digestion (nitric acid & perchloric acid in 5:1)	Atomic absorption spectroscope
17	**Lead (Pb)**		

3.5 Adsorbent preparation

Sweet lemon, lemon & orange peels and bagasse were gathered from juice stalls of Rajnikhand, Lucknow. Then all of these were brought to the laboratory and washed it carefully firstly with tap water and after that with deionized water for removing dust and unwanted objects. Lastly, all of them were air dried for 2-3 weeks to eliminate moisture content. Then, were subjected to pyrolysis at temperature of about 400±10ºC

for all of the peels and 300±10ºC for bagasse wit time duration of about 3.5 and 2.5 hours, respectively. Afterward, overnight cooling, biochars were washed thoroughly with deionized water to eliminate undesirable ash contents. Subsequently biochars were dehydrated in oven and stored in desiccated conditions in airtight dishes.

3.6 Characterization of the adsorbent

Following instruments and their techniques were used for characterization of selected adsorbents-

3.6.1 Atomic Adsorption Spectrometer (AAS): The concentrations of HMs were determined by AAS of VARIAN AA240FS.

3.6.2 Fourier Transform Infrared Spectroscopy (FT-IR): The functional groups involved in adsorption of HMs were determined by NicoletTM6700-FT-IR.

3.6.3 Scanning Electron Microscope (SEM): Alteration in surface morphology was examined by JSM-6490LV-SEM micrographs, manufactured by JEOL, Japan.

3.6.4 Energy-dispersive X-ray Analysis (EDX): Elemental compositions of biochars were analyzed by JSM-6490LV-EDX designed by JEOL, Japan.

3.6.5 Brunauer–Emmett–Teller (BET): Quanta Chrome Nova-1000- BET surface analyzer (under liquid N_2 temperature) was used to determine the surface area and pore size of biochars. Further, porosity and textural properties were studied by adsorption-desorption studies. Pore diameter and volume was evaluated Barrett-Joyner-Halenda (BJH) method and newly generated micropore volume was measured by de Boer t-method (Venkatesha et al. 2016).

3.6.6 X-ray diffraction (XRD): XRD was used to observe the structural integrity of SLPB. Step scanning at $2\theta = 0.0200$ /sec from 30 to 800 on PANalytical X' Pert PRO MPD X-ray diffraction was applied for data recording, with monochromatized Cu K α radiation ($\lambda = 0.15406$).

3.6.7 CHNS: The elemental configuration (C, H, N, S and O %) were analyzed by CHNS analyzer (model no. Flash EA112 Series, manufactured by Thermo Finnigan, Italy).

3.7 Quantitative evaluation of surface acidic functional groups on the adsorbent

Boehm titration method was used to detect acidic functional groups on surface of biochars (Boehm et al. 1964; Boehm 2002; Oickle et al. 2010). In the process 50 ml of 0.05 M $NaHCO_3$, Na_2CO_3 and NaOH bases were used in which 0.5 g of adsorbent was added. Likewise, samples along with blank were shaken for 24 hrs at 120 rpm and filtered to remove extra particles. Thereafter, 20 ml of filtrate from each one was titrated with 0.05 M HCl to neutralize base completely, and then back titration was done by blank solution with 0.05 M NaOH with phenolphthalein indicator to determine end point of the process at room temperature (25±3 ºC). All of the solutions were made up of millipore water. The difference between molar NaOH and Na_2CO_3 was anticipated to be the phenolic group content as described by Oickle (2010), Kurniawan et al. (2011) and Abdelhafez and Li (2016).

Following steps were used to calculate different surface acidic groups-

1. Calculation of surface acidic groups amount (A_x)

$$A_x = \frac{V_{bx} - V_x \ . M_{HCl}. 2.5}{m_x} mol\ g^{-1}$$

where, m_x = mass of biochar (gm), V_{bx} = volume (ml) of HCl utilized for titration of blank, V_x= volume (ml) used for sample titration of respective bases solution after biochar addition, M_{HCl} = molarity of HCl concentration in moles L^{-1}, 2.5 is a coefficient for decrease of titration sample volume in comparison to reaction sample volume (50ml/20ml), 2. Calculation of the amount of different kind of surface groups

a. Amount of phenolic groups, $A_{ph} = A_3 – A_2 – A_1$
b. Amount of carboxylic groups, $Aca = A_1$
c. Amount of carboxylic from lactones hydrolysis groups $A_{la} = A_2 – A_1$

where A_1, A_2 and A_3 are amount of surface acidic groups for $NaHCO_3$, Na_2CO_3 and NaOH, respectively.

3.8 Biochar Yield

5 g of agricultural wastes were subjected to production of biochar. The calculation of yield of biochar was done by following formula (Sadaka et al. 2014; Qiao et al. 2017)-

$$Yield_{biochar}(\%) = \frac{m_{biochar}}{m_{raw}} X\ 100$$

where, $m_{biochar}$ = mass of biochar (g), m_{raw} = mass of raw agricultural wastes (g)

3.9 Moisture and Ash Content

Moisture content: It was determined by drying up of 1 g of samples for 24 hrs in an oven at temperature of 100±5°C until constant weight was gained. Moisture content was calculated as-

$$\text{Moisture content}(\%) = \frac{W_i - W_f}{W_i} \times 100$$

where, w_i = initial weight of adsorbent (g), w_f= final weight of adsorbent after drying (g)

Ash content: 1gm of samples were taken into a porcelain crucible and placed in the muffle furnace at 500±5 °C for 5 hours. Afterwards, it was cooled down in a desiccator for 15-20 minutes. Finally, ash content was calculated as-

$$\text{Ash content}(\%) = \frac{W_2 - W_0}{W_1 - W_0} \times 100$$

where, W_0 = weight of empty crucible (g), W_1 = weight of crucible (g) + weight of adsorbent (g), W_2 = weight of crucible (g) + weight of ashed sample (g) (Basu et al. 2017; Poonam and Kumar 2018).

3.10 Experimental set-up

The experiments were performed altering adsorbent dosage from 1.0 to 10 g L^{-1} with difference of 0.5 g, for 100 ml in 250 ml Erlenmeyer flasks at 120 rpm with time duration of 10, 20 to 200 minutes at time intervals of 20 minutes. The pH was maintained from 2 to 6 by 0.1 N NaOH and 0.1 N HCl. The temperature ranges used in the experiments were 25, 35, 45, 55, 65 and 75 ºC which was maintained in orbital shaker (Uni-Tech Sales-1.21 A).The initial metal ion concentration ranged as 5, 10, 20, 40 and 80 ma L^{-1}. Analytical reagent (AR) grade stock solutions of 1000 mg L^{-1} of Cr and Pb were used in the experiments for preparing working and standard solutions.

3.11 Analytical Method

The amounts of HMs adsorbed were calculated by following mass balance relationship-

$$q_e = \frac{C_0 - C_e}{w} \times v$$

and, percent removal at equilibrium (q_e) was calculated as-

$$\text{Removal } (\%) = \frac{(C_0 - C_e)}{C_e} \times 100$$

where, C_0 and C_e (mg L^{-1}) are concentrations of metal ions at initial stage and equilibrium, respectively. v is volume of wastewaters in ml and w is weight of adsorbent in grams (g).

3.12 Adsorption rate kinetics

In the present study, pseudo-first and second order reactions were utilized to describe the adsorption mechanisms involve in Cr and Pb removal processes by different biochars following Lagergren et al. (1898) and Ho et al. (2000).

3.13 Adsorption isotherm studies

The data of experimental uptake (q_e) were verified by isothermic models (Langmuir and Freundlich) and separation factor (R_L) at room temperature (25±3ºC). Freundlich isotherm assumes the usage of heterogeneous surface and infinite surface coverage for adsorption of HMs. Whereas, Langmuir isotherm undertakes complete adsorption of heavy metals with monolayer coverage on homogenous adsorbent surface without any interaction between adsorbed ions. The adsorbent possess uniform adsorption sites with identical energy levels and at equilibrium the speed of molecules adsorption will be equal to their escape velocity from the adsorbent's surface (Langmuir 1916).

Furthermore, likelihood of Langmuir isotherm was proved by a dimensionless constant viz. separation factor or equilibrium parameter separation factor (R_L) (Hall et al. 1966; Weber and Chakraborti 1974). The expression of R_L is given as following-

$$R_L = \frac{1}{1 + K_L C_0}$$

where, C_0 is initial metal concentration. The value of R_L between 0 and 1present favorable adsorption and higher than 1 shows unfavorable adsorption.

3.14 Thermodynamic Studies

Thermodynamic studies measure adsorption spontaneity, nature of adsorbents and adsorbate at equilibrium. It also explores temperature range for favorable adsorption. The important thermodynamic parameters are change in Gibbs energy (ΔG^o), adsorption enthalpy (ΔH^o) and entropy (ΔS°) which were calculated by following Van't Hoff and Clasius Clapeyron equations (Anastopoulos and Kyzas 2014).

3.15 Desorption study

0.1 M HCl, HNO_3 and H_2SO_4, and NaOH were utilized as eluants. 1 g of metal encumbered adsorbent was added in 100 ml of eluants and incubated for 180 minutes at room temperature (25±3ºC) with rotatory speed of 150 rpm. Finally, HMs containing eluants were analyzed in AAS for analyzing the concentration of HMs (mg L^{-1}).

3.16 Seed germination test

The certified seeds of economic plants i.e. vegetables (lady's finger, sponge gourd, bottle gourd, pumpkin, bitter gourd), legumes and oil yielding seeds (green moong, tomato and rapeseed) and fruit (tomato) were obtained from Kisan Seeds Limited, Lucknow. The viability of the seeds was more than 90%. The viable seeds were surface sterilized in 0.1% $HgCl_2$ for five minutes for disinfection. Then seeds were washed thoroughly by distilled water for 2-3 times. After that 10 seeds of each were taken into petri dishes (100 mm) covered with double layered filter paper (Whatman no. 1) (Kumar et al. 2009; Asfaw et al. 2012). The seeds were wetted with the treated wastewaters and control was taken as tap water. The treated wastewater were diluted 50% by tap water as seeds used to wrought in highly polluted industrial wastewaters, if used without dilution. The experiments were performed in dark at 25± 3ºC for 3 days and germination percentage of all the seeds was determined for every 24 hrs. All of the experiments were performed in triplicates to avoid standard error and deviation. The germination percentage was calculated following Asfaw et al. (2012)-

$$Seed\ gemination\ \ \% \ = \frac{No.of\ seeds\ germiated}{No.of\ seeds\ sown} \times 100$$

3.17 Pot experiments and growth parameters

The pot experiments were conducted in the Research Field Station of Department of Environmental Science, BBA University, Lucknow (26°46'5.77"N and 80°55'38.92"E). Lady's finger (*Abelmoschus esculentus)*, tomato (*Solanum lycopersicum)* and green moong (*Vigna radiate)* were selected on the basis of seed germination percentage for pot experiments. Fifteen seeds of each plant were sown in 12 inch diameter earthen pots containing 8 kg soil which were placed under the net house conditions. The pots were irrigated with SLPB, LPB, OPB and BB treated wastewaters of tannery and flashlight industries. The control was taken as the tap water and irrigation was given equally to each pot. The randomly samples of all the three plants were uprooted at interval of 15, 30, 60, 90 and 120 days and were analyzed for growth parameters *e.g.* root length (cm), no. of roots, shoot length (c), no. of leaves, fresh weight (g), dry weight (g) and buds or fruits as well as concentration of Cr and Pb (mg g^{-1}) into the vegetative parts of the plants. The root and shoot length were measured by measuring ruler and fresh weight and dry weight by electric pan balance. Dry weight was taken after keeping plant samples into hot air oven at 80 ºC for 24 hours. Further, the concentration of HMs into the plant samples were analyzed after digestion of 1 g of dried plant parts on hot plate with 3:1 ratio of HNO_3 and $HClO_4$. After digestion, the samples were filtered and stored into tested tubes after making up with 0.1 N HNO_3. The stored samples were analyzed in AAS for observing the concentration (mg g^{-1}) of Cr and Pb into the plants.

Figure 3.3 Experimental setups for evaluation of risk assessment by different selected plants

Chapter 4
Results and Discussion

4. Results and Discussion

4.1 Estimation of physicochemical properties and heavy metals present in the industrial wastewater

The first objective of the study was to estimate concentration of heavy metals present in the industrial wastewaters. Industrial wastewaters were collected from tannery and flashlight manufacturing industries. The physicochemical characteristics of both wastewaters have been discussed below-

4.1.1 Physicochemical properties of tannery and flashlight wastewater

The tannery and flashlight wastewater were characterized based on its physicochemical properties, which have been summarized in Table 4.1. The examined parameters were compared with limits as prescribed by CPCB (2013) for irrigation on land, and Inland Surface Water-Bangladesh Standard (ISW-BDS, 1997) for surface water (Chowdhury et al. 2013).

4.1.1.1 Temperature

It is an important factor that affects all chemical and biological processes of water (Bhatia et al. 2018). The temperature of both wastewaters ranged between 18.533-32.60 $^{\circ}$C. The variation found among the temperatures was due to season and time of the sampling as tannery waste water were collected in the starting of winters (November, 2015) and flashlight were in the end of winters (March, 2016).

4.1.1.2 pH

pH is described as the hydrogen ion activity caused by the carbonates, bicarbonates and CO_2 of water (Kumar et al. 2015). It influences the ionic activity that affects the chemical reactions taking place in water (Poonam et al. 2018). pH of the collected tannery and flashlight wastewater was found to be 8.667 and 4.703 respectively. Similar observations were reported by Ayoub et al. (2011), Kumar et al. (2012), Islam et al. (2014), Shegani (2014), Goutam et al. (2017) and Bharagava and Mishra (2018) for tannery wastewater. They have also reported the range of pH as 6.45-9.04, 7.58, 2.8 to 12.50, 8.7 to 10.8, 8.2 and 8.49 respectively, in wastewater generated by

various tanning processes and referred the wastewater to unsuitable for direct irrigation to the nearby water bodies. The result of present study for flashlight wastewater was in agreement with Dermentzis et al. (2012); Vajihabanu et al. (2015) and Korrapati et al. (2017) reporting acidic pH as 2.96, 5.4 and 2.34, respectively.

4.1.1.3 Electrical Conductivity (EC)

It measures the ability of water to conduct electricity, which is influenced by different impurities, salts, chemicals present in wastewater (Agbalagba et al. 2011; Akpomie and Dawodua 2015). It depends upon the chelation belongings of aquatic systems and may cause an inequality in metal accessibility for aquatic fauna and flora (Akan et al., 2007). EC of tannery and flashlight wastewater was found to be 16.393 and 24.167 mS cm^{-1}. Such a high conductivity may be caused by different acidification and neutralization reaction during the industrial processes (Pintor et al. 2014). Regulatory agencies like BIS have not given any limit for EC, but ISI-2000/ISW-BDS has given the limit as 0.028 mS m^{-1}. The results were found to be beyond the limits of ISI an ISW-BDS. The observed results were supported by previous studies of Mandal et al. (2010), Baccar et al. (2013), Chowdhury et al. (2013), Swathi et al. (2014), Goutam et al. (2017) and Bharagava and Sandhya (2018) for tannery wastewater. They have also reported the same findings with 20, 14.71, 18.65, 13.24, 11.65 and 4.16 mS cm^{-1}, respectively for tannery wastewater. Whereas, Vergili et al. (2017) reported EC of flashlight industry as 7.83 $mScm^{-1}$ supporting results of preset study.

4.1.1.4 Dissolved Oxygen (DO)

The amount of oxygen dissolved per liter of water is referred as DO. It is an important parameter to judge the quality of the water as well also for different aquatic animals for sustaining their lives. As both wastewaters were too much polluted with different kinds of organic and inorganic pollutants, the DO was not available in any of them. Verma et al. (2008) have recommended that the low DO (≤ 4 ppm) of untreated effluents were the consequence of high organic contamination.

4.1.1.5 Biological Oxygen Demand (BOD)

The amount of oxygen required by different microbes for degradation of organic materials present in the wastewater is known as BOD. It is an indicator of organic

pollutants in the water body (Bhatia et al. 2018). The concentration of BOD in both wastewaters were found to be 3742.798 and 2968.02 mg L^{-1}, respectively, which is very outrageous in comparison to the recommended limits given CPCB (100 mg L^{-1}), ISI (30 mg L^{-1}) and ISW-BDS (250 mg L^{-1}). The reasons behind such a trend are the higher amounts of different organic materials, cleaning and preserving materials used in the processes. The results are in agreement with Chowdhury et al. (2013) and Islam et al (2014), who have reported BOD in various tannery effluents in the range of 600-7500 and 3980 mg L^{-1} in different tanning processes.

4.1.1.6 Chemical oxygen demand (COD)

COD is the measurement of oxygen required by the reactions to oxidize organic matters present in the wastewater. The levels of COD for both wastewater was 23780.0 and 12500.50, respectively, which exceeded the recommended limits given by CPCB (250 mg L^{-1}), ISI (400 mg L^{-1}) and ISW-BDS (250 mg L^{-1}). Such higher concentrations of COD represent noxious conditions and presence of resistant organic impurities (Bhatiya et al. 2018). These higher concentrations of COD in both wastewaters may be due to organic substances used to manufacture the leather and battery, respectively. These results for tannery wastewater were in agreement with Chowdhury et al. (2013), Islam et al. (2014), Shegani (2014) and Zhao et al. (2017a) who have reported COD ranges from 1550 to 18600; 47.2 to 2560, 920 and 14540 mg L^{-1}, respectively, in the wastewater of various practices applied during leather production.

4.1.1.7 Solids

Different semi-solid, solid inorganic salts, organic matter and dissolved gases found to be mixed up, dissolved or suspended in the wastewater for example sand, sediments, carbonates and bicarbonates etc. These are further divided into total dissolved solids (TDS), total suspended soils (TSS) and total solids (TS). The concentrations of TDS, TSS and TS in both wastewater were 13330.00 and 1455.333; 4388.667 and 757.333; and, 16405.333 and 2217.667 mg L^{-1}, respectively. The concentration of all solids in tannery wastewater was very high as compared to the recommended limits prescribed by CPCB, ISW-BDS. The reason for such an elevated concentration of solids may be the usage of excess amount of tanning agent,

preservatives and other chemicals. Whereas, the concentration of TDS for flashlight wastewater fell under the limits of CPCB (2100 mg L^{-1}), ISI and ISW-BDS (2100 mg L^{-1}) but the TSS exceeded the limits of CPCB (200 mg L^{-1}) ISI and ISW-BDS (100 mg L^{-1}). Overall, TS for flashlight also surpassed the limits as given by ISI and ISW-BDS (2200 mg L^{-1}). Results of the present study are in agreement with Islam et al. (2014) reporting ranges of TDS and TSS in different tanning wastewater as 9000-45000, 5800 to 49500 and 1500 to 9500 mg L^{-1}, respectively. They have reported that high concentrations of solids may be attributed to incomplete processing's of skin and hides in leather production causing turbidity in the receiving water body, demises in the photosynthetic activity and congestion of gills in aquatic animals. Higher values of TDS high TDS value may cause osmotic stress and interrupts the osmoregulatory functions (Bharagava and Mishra (2018). The results were also in good agreement with Kumar et al. (2012), Chowdhury et al. (2013) and Shegani (2014), and Bharagava and Mishra (2018). Kumar et al. (2012) have reported TDS, TSS and TS in tannery wastewater as 7681.20, 1873.12 and 9557.32 mg L^{-1} respectively. Chowdhury et al. (2013) have also reported the same pattern for TDS and TSS for tannery wastewater as 6800 and 14,000 mg L^{-1}, respectively. Whereas, Shegani (2014) has reported TDS and TSS as 1670 to 32269, 33 to 14174.0 mg L^{-1}, respectively. Goutam et al. (2017) observed 4064 and 2216 mg L^{-1} of TDS and TSS in tannery wastewater. Bharagava and Mishra (2018) reported 11,028, 3491.3 and 194 mg L^{-1} of TS, TDS and TSS in tannery wastewater, supporting the present study.

4.1.1.8 Alkalinity

Alkalinity measures the ability of water to nullify the effects of acids without any change in the pH. It was found to be 1260.00 and 400.00 mg L^{-1} for tannery and flashlight wastewater, respectively. The main causes for such high values may be hydroxides, carbonates and bicarbonates present in the wastewater (Kumar et al. 2015). None of the regulatory agencies (e.g. IS, WHO, BIS, FAO etc.) except CPCB (2013) has yet prescribed any limit for this parameter in water or wastewater, yet. CPCB (2013) has given the maximum limit as 500 mg $L^{-}1$, which was followed by flashlight wastewater. The results were found to be in agreement with Islam et al. (2014) and Shegani (2014) who have also reported alkalinity in the range of 654.26, 2500-17500 and 100- 380 mg L^{-1}, respectively, for wastewater generated from

different processes of tannery industry. Soaking, liming and unhairing, deliming & bating processes may be responsible for such results.

4.1.1.9 Chloride (Cl^-)

Chloride is an important parameter, which helps in balancing the acid-base reactions of the biological system. Cl^- concentration for both wastewater was 1626.15 and 140.41, respectively. The excess concentration of Cl^- in tannery wastewater may be due to usage of chloride preservatives (NaCl and $ZnCl_2$) for flesh and skin (FAO 2018). The results fell under CPCB (1000 mg L^{-1}) whereas, tannery wastewater never followed any recommended guideline. The results were supported by previous studies of Islam et al. (2014), Shegani (2014) and Zhao et al. (2017a), illustrating the range of Cl^- for wastewater generated from different processes occurring during leather production as 19250 to 23500 mg $L^{-1,}$ 177.25 to 30205.0 and 792.0 mg L^{-1}, respectively. The reason behind such higher concentrations of Cl^- may be soaking and pickling processes.

4.1.1.10 Sulphate (SO_4^{2-})

The main source of sulphate is natural from the oxidation of sulphite ores, gypsum and anhydrite (Prakash and Somashekar 2006). It is an important factor for analysis of wastewater as excess of this may cause catharsis, dehydration and gastro-intestinal irritation to human beings. The concentration of sulphate in both wastewaters was found to be 114.333and 43.757 mg L^{-1}, respectively. The results followed the limits prescribed by ISI and ISW-BDS and CPCB (1000 mg L^{-1}). The reason behind this may be the presence or absence of sulphate ores in the water body or secondary chemicals containing sodium sulphate (UNIDO, 2011). The result was supported by the previous studies of Kumar et al. (2012) who have reported the level of SO_4^{2-} in tannery wastewater as 86.30 mg L^{-1}. Chowdhury et al. (2013), Swathi et al. (2014) and Zhao et al. (2017a), have also given the range of SO_4^{2-} as 3.7 to 2586.4, 135.19, 733.0 mg L^{-1} in wastewater generated from various proceedings of the leather production. Previous study of Dermentzis et al. (2012) and Mansoorian et al. (2014) 5.0 and 280 mg L^{-1} of SO_4^{2-} indicating its presence in the battery manufacturing industry likewise the results of present study.

4.1.1.11 Total Phosphorus (TP)

This is an essential plant nutrient, which is used in the form of fertilizers for intensifying the crop growth and development. These practices pollute the nearby water bodies due to run off from agricultural fields. The concentration of TP in the tannery and flashlight wastewater were 4.53 and 67.50 mg L^{-1}, respectively. However, Zhao et al. (2017a) reported a much higher concentration of TP i.e. 349 mg Gallic acid equivalent L^{-1} in tannery wastewater. Whereas, Ayoub et al. (2011) supported the results of present study by finding TP concentration in tannery effluent in the range of 12.5 to 41.2 mg L^{-1}.

4.1.1.12 Nitrate (NO_3^-)

It is also an essential plant nutrient and very common pollutant of water bodies. The main source of its pollution is the agricultural practices where nitrogen fertilizers are used extensively for enhancing the productivity. Its elevated levels in drinking water may cause methemoglobinemia in infants and even stomach cancer in adults (Kumar et al. 2015). The concentration of NO_3^- in tannery wastewater was 88.06 mg L^{-1}, whereas, in flashlight wastewater, it was not detected. The results were very much higher than the prescribed guidelines of CPCB (10 mg L^{-1}) and IS (20 mg L^{-1}). The source of NO_3^- in tannery wastewater may be proteins and nitrogen complexes existing in animal hides and skins, used for the leather production (Ahmed et al. 2012; Poonam et al. 2018). Previous study done by Shegani (2014) and Goutam et al. (2017) supported the results by reporting NO_3^- range from 1 to 70 and 14.05 mg L^{-1}, supporting present study for tannery wastewater. However, Zhao et al. (2017a) reported a much higher concentration of NO_3^- i.e. 300.0 mg L^{-1} in tannery wastewater.

4.1.1.13 Total Hardness

The capacity of water to produce lather with soap is measured traditionally by total harness of the water. It reflects the occurrence of multivalent cations derived from salts of carbonates, bicarbonates and fluorides of calcium, magnesium, nitrate, strontium, iron etc. (WHO, 2011; Kumar et al. 2012). It was found to be 925.24 and 621.0 mg L^{-1}, for tannery and flashlight wastewater, respectively. These results, also,

did not follow the prescribed guidelines of WHO (100 mg L^{-1}) and IS (300 mg L^{-1}). Although the higher concentrations of hardness may cause urolithiasis but moderate concentration may also be beneficial in some cases as it prevents the corrosion of iron pipes, epidemiological and clinical incidence of atherosclerosis is also prevented (Abdellah et al. 2013). The results for tannery wastewater were supported by the previous study of Kumar et al. (2012) who reported it to be 455.04 mg L^{-1}.

4.1.1.14 Cations

Sodium (Na^+), potassium (K^+), magnesium (Mg^{2+}) and calcium (Ca^{2+}) have been analyzed in both wastewater. These cations and their salts are crucial for some of the important parameter of water/wastewater e.g. EC, hardness, alkalinity etc. Na^+ content in tannery and flashlight wastewater was 698.98 and 50.96, respectively.

Na^+ and K^+ are essential element for living beings and is often present in water in the form of salts of it e.g. sodium sulphate, sodium carbonate, sodium chloride, potassium permanganate and potassium chloride. These cations maintain the normal osmotic pressure in cells (WHO, 2003; WHO, 2009). Na^+ content in tannery and battery wastewater was 698.98 and 50.960 mg L^{-1}, respectively. In addition, concentration of K^+ in both wastewaters was 294.50 and 11.65 mg L^{-1}, respectively. Ahmed et al. (2011) and Chowdhury et al. (2013) have also reported similar findings for high Na^+ content in tannery wastewater. Whereas, Kumar et al. (2011) have illustrated low Na^+ content in the tannery wastewater. Ahmed et al. (2011) also support present study for K^+ content in tannery wastewater.

Mg^{2+} and Ca^{2+} are primary ions, existing in many sedimentary rocks (limestone and chalk), and vital mineral constituents of food. Salts of these cations are the main cause of hardness of the water (WHO, 2009a; WHO, 2011). The concentration of both cations in tannery wastewater was 207.77 and 8.94 mg L^{-1}, respectively. The concentration of Ca^{2+} in flashlight wastewater was 229.83 and 12.65 mg L^{-1}, respectively. Tannery wastewater exceeded the limit of CPCB specified for Mg^{2+} and Ca^{2+}, whereas, flashlight wastewater followed the same guidelines. Ahmed et al. (2011), Kumar et al (2011) and Chowdhury et al. (2013) have also reported similar findings for high Ca^{2+} content in tannery wastewater. Dermentzis et al. (2012)

illustrated similar findings for battery (flashlight) wastewater. Vajihabanu et al. (2015) also reported low Ca^{2+} and Mg^{2+} content in battery wastewater.

4.1.1.15 Heavy Metals (HMs)

Health of flora and fauna has been adversely influenced by the higher concentrations of toxic heavy metals. The concentrations of Cr and Pb were 3.84 and 2.39 mg L^{-1}, respectively. Results also exceeded the limits recommended by BIS for public sewer as 2.0 and 1.0 mg L^{-1} for Cr and Pb, respectively. The higher concentration of Cr and Pb may cause different serious health related problems and affect the nervous and reproductive system, kidney, liver, brain and bony tissues (Suksabye and Thiravetyan 2012; Poonam et al. 2018).

Studies of Kumar et al. (2012) and Swathi et al (2014) have supported present study, as the results were almost similar for concentration of Cr in the wastewater of tannery as 4.67 and 3.34 mg L^{-1}. Previous study of Bahadir et al. (2007), Mansoorian et al. (2014), Korrapati et al. (2017) and Vergili et al. (2017) have also reported the concentration of Pb in the battery wastewater as 3.09, 9.0, 1.21 and 4.5 mg L^{-1}. They have indicated that the release of such wastewater will pollute the water body with adversely affecting the health of the aquatic organisms.

Table 4.1 Physicochemical properties of Tannery and Flashlight wastewaters

S No	Parameters	Tannery (Average± S.D.)	Flashlight (Average± S.D.)	CPCB (2013)	(ISI-2000 /ISW-BDS)
1	Temperature	18.53 ± 0.06	32.6±0.30	40	-
2	pH	8.67±0.15	4.70±0.17	5.5-9.0	6-9
3	Electrical conductivity	16.39 ±0.31	24.17±0.75	-	0.029
4	Dissolved oxygen	nd	nd	-	4–6
5	Biological oxygen demand	3742.80±179.99	2968.02±29.20	100	30/250
6	Chemical oxygen demand	23780.0±1680.83	12500.50±165.75	250	250/400
7	Total dissolved solids	13330.0±69.54	1455.33±6.43	2100	2100
8	Total suspended solids	4388.67 ±84.67	757.33±74.72	200	100
9	Total solids	16405.33±204.47	2217.67±4.03	2300	2200
10	Alkalinity	1260.000±125.284	400.00±2.646	500	
11	Chloride	1626.153±155.668	140.413±1.86	1000	
12	Sulphate	1149.33±34.79	43.757±3.17	1000	1000
13	Total Phosphorus	4.53±0.24	67.50±1.40	-	-
14	Nitrate	88.06±1.68	nd	20	-
15	Total hardness	925.24 ±11.56	621.0±263.24	200-600	-
16	Na^+	698.98±61.83	50.96±0.54	-	-
17	K^+	294.50±8.501	11.65±1.27	-	-
18	Mg^{2+}	207.77±11.11	8.94±2.19	30-100	-
20	Ca^{2+}	229.83±7.65	12.65±0.39	75-200	200
21	Chromium (Cr)	3.84±0.12	nd	2.0	-
22	Lead (Pb)	nd	2.39±0.03	1.0	-

Data are presented as mean of five replicates ± S.D. (i.e. n = 5), parameters are expressed in mg L^{-1} except for pH, temperature ($^{\circ}C$) and EC (mS cm^{-1}); nd = not detected; CPCB = Central Pollution Control Board (2013); ISI-2000=Indian Standard Institute–2000, ISW-BDS=Inland Surface Water-Bangladesh Standard (Chowdhury et al. 2013)

4.2. Removal of heavy metals from water using various combinations of agricultural wastes/by-products

In the present study, adsorption techniques were used for the removal of HMs from tannery and flashlight manufacturing industry wastewater. The details of main physicochemical characteristics of the adsorbents used in the study and various combinations of the parameters affecting the adsorption processes have been given below-

4.2.1 Screening of the adsorbent

The adsorbent selected were peels of sweet lemon (*Citrus limetta*), peels of lemon (*Citrus limon*), peels of orange (*Citrus sinensis*) and bagasse. Among various adsorbents used by other researchers, these four were selected mainly due to- i) Ease in availability, ii) Low cost, iii) Environmental friendly, iv) Don't require chemical for preparation of biochar, and iv) Abundance of biopolymers with different surface binding groups. All of these wastes were easily available in the local fruit markets, juice shops and juice industries (Santos et al. 2015; Poonam et al. 2018). After juice extraction, these very promising lignocellulosic feedstock (are of no usage and create problem of their disposal which otherwise, may cause environmental pollution (Kelly-Vargas et al. 2012; Tahir et al. 2016). The usage of these agricultural wastes not only abate the environmental pollution, but also, is easily available and cost efficient to be used as bio-sorbent for HMs (Bhatnagar et al 2010; Shakoor and Nasar 2016). These substances are also rich in biopolymers like cellulose, pectin, hemicellulose, lignin etc. These components possess a no. of functional groups e.g. carboxyl, hydroxyl, amino, carbonyl, phosphate etc. which act as binding sites for HMs (Liang et al. 2010; Ning-chuan and Xue-yi 2012; Basu et al. 2017; Shehzad et al. 2018). Sugarcane bagasse is mainly composed of about 50% cellulose, 30% hemicelluloses and 25% lignin polymers and fat and waxes, ash, silica etc. in trace amounts, which also possesses different active functional groups facilitating the adsorption practices (Homagai et al. 2010; da Silva et al. 2013; Rocha et al. 2015; Martins et al. 2017). Primary and secondary hydroxyl groups are the main components among different other unique functional groups of bagasse, which play major role binding the HMs (Ramos et al. 2015; Sarker et al. 2017). Further, adsorption capacity, surface area, dry weight and carbon content were also brought into consideration before selecting these as adsorbent for treating the heavy metals present into tannery and flashlight manufacturing industry wastewater.

The adsorbents were utilized in the form of biochar; a carbonaceous, fine-grained, black, solid residue produced by thermal treatment/decomposition of plant or animal biomass, industrial wastages etc. These are rich in carbon content in limited condition of O_2 at relatively low temperature (from 300 to 1000 °C) and is normally resistant to bio-chemical decay (Lehmann and Joseph 2015; Shin 2017). The main advantage of biochar lies in its large surface area, high porosity, structural diversity, roughness heterogeneity and high adsorption capacity (Mary et al. 2016; Zhao et al. 2017). The International Biochar Initiative (IBI) states ‘‘biochar is a solid material obtained from the carbonization of biomass’’. The carbonization process produces much more heteroatoms than activated carbon. These heteroatoms with different functional groups present in biochar, aid in the adsorption of HMs on their surfaces (Yu et al. 2015; Štefelová et al. 2017). Present study was supported by previous studies of Pan et al. (2013); Karim et al. (2015); Park et al. (2015); Ahmadi et al. (2016); Shin et al. (2017) and Mehmood et al. (2017) etc. for successfully treating water and wastewater for Cr and Pb removal with the application of biochar of agricultural wastes. Mohan et al. (2011) used oak wood and oak bark for successful removal of Cr^{6+} from water, whereas, Pan et al. (2013) applied biochars of peanut, soybean, canola and rice straws for removal of Cr^{3+} and Karim et al. (2015) used banana peduncle biochar for removal of Cr^{6+} from aqueous solution. Park et al. (2015) utilized sesame straw biochar for removal of Pb^{2+}, Cr^{3+} and other heavy metals, Wang et al. (2015) used biochar of pinewood for Pb^{2+} removal and Abdelhafez and Li (2016) employed sugarcane bagasse biochar and orange peel biochar for Pb^{2+} removal. In addition to this, Ahmadi et al. (2016) applied dew melon peel biochar for removal of Cr^{6+} from industrial wastewater, Shin et al. (2017) utilized *Hizikia fusiformis* biochar for Pb^{2+} and other heavy metals from aqueous solution and Mehmood et al. (2017) applied rice straw based biochar for treating Pb^{2+} with other heavy metals.

Further, converting the agricultural wastes into biochar also enhances the surface area, which may be verified by results of physicochemical studies discussed in next section 4.2.2.

4.2.2 Physicochemical characterization of adsorbents

All the four adsorbents *viz.* SLPB, LPB, OPB and BB, were characterized on the basis of their physicochemical properties. The proximate and ultimate studies of all the four adsorbent are given in Table 4.2. The “ultimate analysis” signifies the charred

biomass composition in weight (%) of C, H and O in addition to S and N (if any). While, the "proximate analysis" contributes towards biochar yield, volatile, ash and moisture contents (Mohan et al. 2011). Elemental C, H and nitrogen (N) of all the charred agricultural wastes were analyzed by combustion. O was determined by difference. C/H ratio, C/N ration, BET surface area, pore volume and pore diameters were also determined.

Table 4.2 Physicochemical characteristics of different adsorbents

S.no.	Characteristics	Sweet lemon peel biochar	Lemon peel biochar	Orange peel biochar	Bagasse biochar
1	**Moisture content (%)**	0.44±0.01	0.20±0.01	0.93±0.019	1.97± 0.01
2	**Ash content (%)**	2.80±0.66	6.63±0.03	5.70±0.034	7.34± 0.03
3	**pH**	8.73±0.21	8.20±0.30	6.83±0.35	9.27±0.21
4	**C %**[c]	46.72±0.27	45.19±1.48	41.15±0.78	38.15±0.53
5	**H %** [c]	7.43±0.20	7.08±0.18	6.70±0.31	6.08±0.04
6	**N %** [c]	5.22±0.19	2.57±0.13	3.16±0.45	4.56±0.29
7	**S %** [c]	0.16±0.02	0.004±0.00	0.17±0.01	0.27±0.01
8	**O %**[c *]	50.94±0.22	45.16±1.73	48.82±1.12	40.47±0.64
9	**H/C ratio** [c]	0.16±0.004	0.16±0.00	0.16±0.00	0.16±0.00
10	**C/N ratio** [c]	9.48±0.22	18.64±0.29	6.48±0.35	8.76±0.00
11	**Yield $_{biochar}$ %**	86.67±1.62	84.47±2.12	79.20±1.83	73.33±3.16
12	**Pore Volume (cc g^{-1})**	0.05±0.00	0.04±0.01	0.03±0.00	0.04±0.00
13	**Pore Diameter (nm)**	1.61±0.05	2.15±0.01	2.37±0.05	1.58±0.02
14	**Surface area (m^2 g^{-1})**	30.62±0.45	24.89±0.52	15.21±0.40	12.63±0.30
15	**Tot. surface acidic groups (mol $g^{-1)}$**	7.38±0.02	7.48±0.02	7.41±0.08	7.03±0.05
16	**Carboxylic groups(mol g^{-1})**	5.30±0.25	4.93±0.12	4.48±0.08	5.15±0.08
17	**Lactonic groups (mol g^{-1})**	0.51±0.09	1.90±0.13	2.11±0.14	1.28±0.21
18	**Phenolic groups (mol g^{-1})**	1.57±0.32	0.66±0.04	0.812±0.09	0.60±0.11

[a] Data are represented as dry weight %; [b] Data are retrieved from BET study; [c] Data are retrieved from CHNS analyzer; [c]* Determined by difference

4.2.2.1 Moisture content

The moisture content of SLPB, LPB, OPB and BB was found to be low with average values of 0.44, 0.20, 0.93 and 1.97 % respectively. The order of moisture content was LPB<SLPB<OPB<BB. Higher moisture content may block the pores of the surface by attaching to it, which may result in decrease in the approachability of the HMs towards biochar. In addition to this, the accessibility and availability of the binding sites may also be affected. This may also decrease the durability and life span of the biochar (Lam et al. 2017). Thus, low moisture content favored the adsorption of HMs in present study. The results were found to be closer to earlier studies of Mohan et al. (2011); Vithanage et al. (2015); Ahmadi et al. (2016); Kołodyńska et al. (2017) and Zhao et al. (2017). The detailed values for these studies have been represented in Table 4.3

4.2.2.2 Ash content

The moisture content of SLPB, LPB, OPB and BB was found to be relatively low with average values of 2.80, 6.63, 5.70 and 7.34 %, respectively. The ash content were found to be order of SLPB< OPB< LPB<BB. Low ash content supported the adsorption of HMs by preventing the formation of unwanted by-products of catalytic reactions caused by inorganic minerals present in the ash (Mahamad et al. 2015; Lam et al. 2017). The reason for lower values may be the maximum elimination of O_2 in bio charring of the waste biomasses (Poonam et al. 2018). The results were found to be closely related to the earlier studies of Mohan et al. (2011); Fernandez et al. (2014); Van Vinch et al. (2015); Ahmadi et al. (2016); Kołodyńska et al. (2017); Lam et al. (2017); Štefelová et al. (2017) and Zhao et al. (2017). The results of these studies have been given in Table 4.3

4.2.2.3 CHNS

The amount of total carbon(C), the total hydrogen(H), nitrogen(N), sulfur(S) and oxygen present in the SLPB, LPB, OPB and BB have been shown in Table 4.2 The average C content in four of the selected adsorbents was moderate, comprising 46.72, 45.19, 41.15 and 38.15 % respectively. The average O content was comparatively high, occupying 50.94, 45.16, 48.82 and 40.47 % of average compositions of biochar. Further, average H content was 7.43, 7.08, 6.70 and 6.08 %, respectively, which may

be due to breakdown of weaker bonds in biochar configuration and exclusion of water, hydrocarbons, H_2, CO and CO_2 during pyrolysis (Ahmad et al. 2014). Further, average N and S content were 5.22, 2.57, 3.16, 4.56 and 0.16, 0.004, 0.17 and 0.27 %, respectively. The average C/H ratio was 6.58, 6.30, 12.73 and 6.31, whereas, C/N ratio was 9.48, 18.64, 6.49 and 8.76, respectively, for all of the four adsorbents. According to Yu et al. (2015), lower H/C ratios with C implies that biochar contain small amounts of organic remainders from the original plant, such as cellulose, lignin, but also have high carbonization. Moreover, Cely et al. (2014) have explained that H/C ratio of all of the four adsorbent was ≤0.3 with moderate C content, which point out the highly condensed aromatic ring system, whereas, molar H/C ratio of ≥0.7 suggested non-condensed structures of biochar. Although the difference among four was very little for H/C ratio, it was lowest for LPB followed by SLPB, BB and OPB suggesting the higher degree of carbonization occurred in LPB followed by the formerly said order (Chun et al. 2004; Vithanage et al. 2015). Further, all of the four biochar showed comparatively higher N and C/N ratio and comparatively lesser C% (Table 4.2) may be due to incomplete charring with remaining decomposed organic matter. This might be the reason for difference in specific surface area of all four biochar as examined by BET analysis described in next section 4.2.2.4 (Poonam et al. 2018). Furthermore, higher values of H and O percentage indicate accessibility of binding sites responsible for successful adsorption of Cr and Pb (Table 4.2). A very little concentration of N and S in all of the four adsorbents were also recorded as shown in Table 4.2. This was confirmed by the presence of some nitrogen and sulfur containing compounds/groups as discussed in upcoming section under 4.2.2.8. In brief, among all four adsorbents SLPB and LPB showed higher C and H content with lower H/C ratio which suggest it to be more efficient adsorbents than OPB and LPB which possessed comparatively lesser C and H content with higher H/C ratio. The comparison of previous studies with different biochars to present study has been summarized in Table 4.3. From there, we can figure out that the results of present study were in good agreement with Roberts et al. (2015), Vithanage et al. (2015), Yu et al (2015), Kołodyńska et al. (2017), Lam et al. (2017), Batista et al. (2018) etc.

4.2.2.4 Biochar yield

The biochar yield ($Yield_{biochar}$) from natural agricultural wastes has been presented in Table 4.2. Sweet lemon peel assimilated maximum biochar yield of 86.67 % followed

by lemon peel (84.47%), orange peel (79.20%) and bagasse (73.33%). The yield of biochar depends mainly upon the composition of waste biomass (cellulose or holocellulose, lignin, ash and extractives) used for the generation of biochar, temperature and time taken in pyrolysis processes (Novotny et al. 2015). SLPB, LPB and OPB were produced at 400±10ºC for 3 and half hours whereas, BB was produced at 300±10 ºC for 2.5 hours. It has been reported by many researchers that higher lignin and cellulose content gives higher biochar yield (Gani and Naruse 2007; Lee et al. 2013). In brief, higher temperature of pyrolysis generates higher carbon and ash content, carbon stability and biochar aromaticity, porosity, and specific surface area, but lowers the volatile content and yield of biochar (Wu et al., 2012; Zhao et al., 2013). The results of present study were in good agreement with Roberts et al. (2015) who have described the biochar yield of different seaweeds (*Saccharina, Undaria, Sargassum, Gracilaria, Kappaphycus* and *Eucheuma*) in the range of 49.0-61.8% and explained that seaweed yields more biochar than ligno-cellulosic biomass during pyrolysis regardless of species or location. Ahmadi et al. (2016) and Lam et al. (2016) observed 45.2 and 87% biochar yield from dew melon peel and orange peel, respectively; Štefelova et al. (2017) reported 28% biochar yield from beech and spruce sawdust. Whereas, Fernandez et al. (2016), Mohan et al. (2011) and Park et al. (2015) reported only 33, 20 and 22.6 % biochar yield from orange peel, oak wood and sesame straw, respectively, probably due to short pyrolysis time (Table 4.3).

4.2.2.5 Surface properties

The whole phenomenon of 'adsorption' depends upon the most important characteristic i.e. the 'surface area' and other properties like pore volume and pore size. Methods of Brunauer et al. (1938) were applied to determine these surface properties using BET analyzer. The surface areas of SLPB, LPB, OPB and BB with average values was as 30.62, 24.89, 15.21 and 12.63 m^2 g^{-1} and average pore volume was 0.05, 0.04, 0.03 and 0.04 cc g^{-1} and average pore diameter was 1.61, 2.15, 2.37 and 1.58, respectively. The values of pore diameter indicated that it might also participate in adsorption processes which dominant in all of the four biochars (Mohan et al. 2012). The order of surface area was BB<OPB<LPB<SLPB, pore volume was OPB<LPB<BB<SLPB, and, pore diameter was BB<SLPB<LPB<OPB (Fig 4.1). Relatively low value of BB surface area and pore diameter was may be because of

incomplete charring of the adsorbent, lesser carbonization and macro or meso porosity (Qiao et al. 2017; Poonam et al. 2018). The average pore size and pore volume were relatively high as compared to the studies of Ahmadi et al. (2016) and comparatively low than Shin et al. (2017) and Fernandez et al. (2014). However, the results of present study were supported by Mohan et al. (2011); Van Vinch et al. (2015); Yu et al. (2015); Lam et al. (2015) and Hu et al. (2018). The details of these previous studies have been mentioned in Table 4.3 In addition to this SEM studies may also confirm the results of surface properties which have been discussed in next section 4.2.2.5.

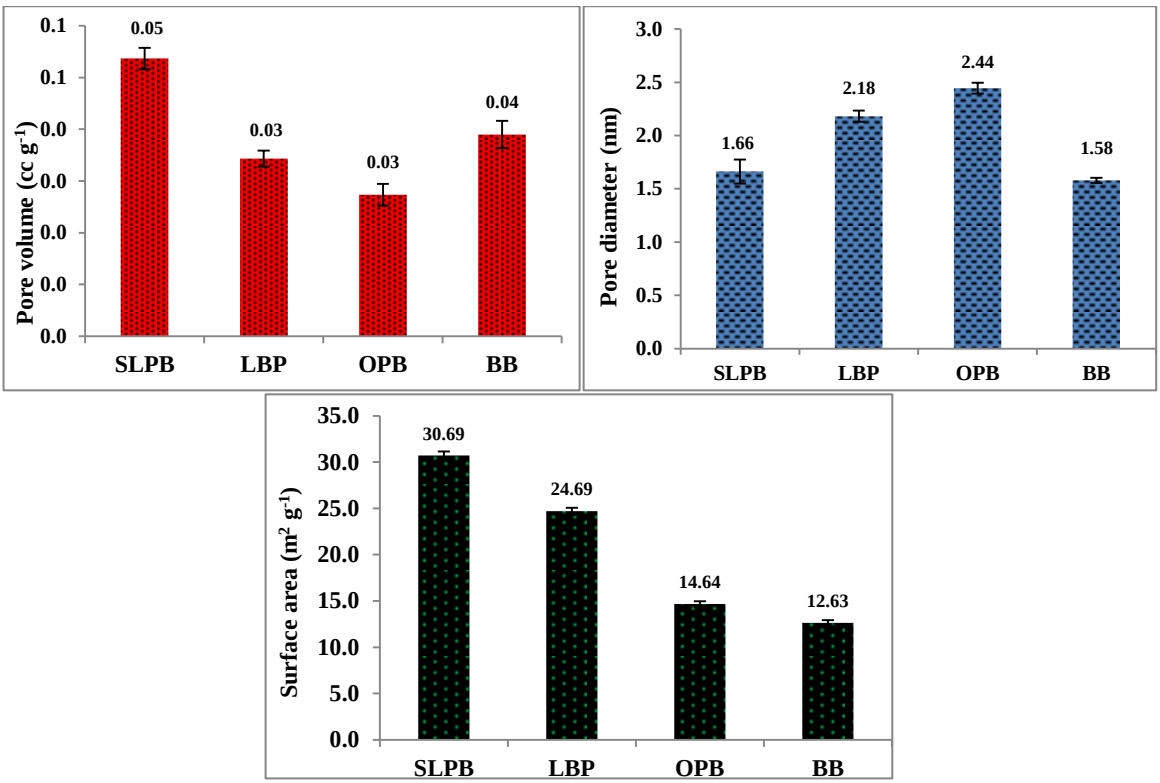

Figure 4.1 Surface properties (pore volume, pore size and pore diameter) of all the four adsorbents; bar representing ± S.D.

Table 4.3 Comparison of ultimate and proximate characteristics of biochars prepared by different waste biomasses

Sn	Adsorbent	Nature	Moisture Content	Ash Content	C	H	O[a]	N	S	Pore Volume	Pore Diameter	Surface area	Reference
1	Oak wood and	BC	3.17	2.92	82.83	2.70	8.05	0.31	0.02	0.41	-	2.73	Mohan et al. (2011)
	oak bark		1.56	11.09	71.25	2.63	12.99	0.46	0.02	1.06	-	1.88	
2	Marigold (*Tagetes* spp.)	BioC	5.30	32.50	65.55	-	-	-	-	-	-	178	Singanan and Peters (2013)
3	Orange peel	AC	-	3.4	82.5	2.5	14.1	0.9	0.0	1.2	4.3	1090	Fernandez et al. (2014)
4	Rice husk,	BC	-	-	40.4	0.28	2.69	0.22	-	-	-	295.57	Jindo et al. (2014)
	Rice straw	BC	-	-	29.17	0.25	3.71	0.25	-	-	-	256.96	
5	Sesame straw	BC	-	-	72.6	2.1	21.7	2.9	0.42	0.041	-	289.2	Park et al. (2015)
6	Orange peel	BC	-	7.8	62.1	3.6	30.9	2.4	0.8	-	-	-	Santos et al. (2015)
7	Eucalyptus sawdust	BC	-	-	45.48	6.33	45.34	0.12	-	0.0003	7.45	1.57	Sun et al. (2015)
8	Pine Cone	BC	3.12	2.13	67.88	3.89	22.07	0.55	<0.01	0.016	-	6.60	Van Vinh et al. (2015)
	Pine cone (Zn-loaded)	CMBC	3.08	2.14	71.21	3.03	20.43	0.51	<0.01	0.028	-	11.54	
9	Tea waste	BC	1.57	12.84	73.63	1.71	7.67	3.39	-	0.02	1.75	342.22	Vithanage et al. (2015)
	Rice husk	BC	3.42	39.24	47.71	1.29	7.69	0.65	-	0.05	5.29	377.00	
10	Pine wood	BC	-	4.02	85.68	2.13	11.19	0.33	-	0.003	-	209.6	Wang et al. (2015)
11	Corn straw	BC	-	10.17	85.26	1.75	5.16	-	-	-	-	60.97	Yu et al. (2015)
	Manganese oxide-modified biochar	CMBC	-	12.60	73.00	0.33	10.90	-	-	-	-	3.18	
12	Dew lemon peel	BC	2.1	14.23	83.2	3.12	13.47	0.2	nd	0.0013	0.71	196	Ahmadi et al. (2016)
13	Sugarcane bagasse	BC	-	12.21	74.02	2.61	2.37	1.00	-	0.045[b]	65.008	92.30	Abdelhafez and Li (2016)
	and Orange peel	BC	-	11.17	88.83	3.60	28.09	2.13	-	0.0001[b]	28773.7	0.21	

14	Biochar	BC	3.95	59.42	29.12	0.82	-	0.82	-	0.075	-	115.5	Kołodyńska et al. (2017)
15	Pea pod,	BC	7.0	3.50	3.32	4.75	53.30	2.40	0.23	-	-	-	Mary et al. (2016)
	Cauliflower leaves	BC	9.0	18.86	31.80	3.2	59.40	4.01	1.59	-	-	-	
	Orange peel	BC	13.0	5.50	3.20	4.83	52.90	1.56	0.27	-	-	-	
16	Orange peel,	NA	11.3	3.0	42.5	6.0	51.0	0.5	0	-	-	-	Lam et al. 2017
	Biochar and	BC	6.0	9.0	73.7	4.3	21.0	1.0	0	0.0075	65	20.8	
	Activated Carbon	AC	5.0	3.2	84.0	1.1	14.0	0.9	0	0.60	23	1350	
17	Seaweed (*Hizikia fusiformis*)	BC	-	-	-	-	-	-	-	0.036	2.851	50.24	Shin (2017)
18	Spruce sawdust	BC		1.7	49.1	6.2	30.7	-	-	0.32	-	910	Štefelová et al. (2017)
	Beech sawdust	BC		0.9	48.9	6.1	30.9	-	-	0.27	-	794	
19	Giant reed (*Arundo donax* L.)	BC	3.23	6.85	87.19	0.40	10.40	1.47	0.54	-	-	-	Zhao et al. (2017)
20	Corncobs and	BC	-	-	85.12	-	10.47	0.6	3.81	0.1197		11.813	Hu et al. (2018)
	Corncobs (Na_2S modified)	CMBC	-	-	83.28	-	1073	0.52	4.6	0.2340		195.643	
21	Orange peel and	BC	-	-	58.0	5.0	35.0	2.0	0.0	9.4×10^{-8}	-	186.0	Batista et al. (2018)
	sugarcane bagasse	BC	-	-	59.0	4.0	37.0	1.0	0.0	8.7×10^{-8} $m^3\ g^{-1}$		159.0	
22	**Bagasse (Present study)**	BC	1.968	7.337	38.153	6.076	50.94	4.557	0.272	0.039	1.579	12.628	Poonam et al. (2018)

*All the physicochemical properties have been expressed in % except for C/H ratio, C/N ratio, Pore Volume (cc g^{-1}), Pore Diameter (nm) and Surface area ($m^2\ g^{-1}$);

**AC-activated Carbon; BC-Biochar; CMBC-Chemically modified biochar; CTA-Chemically treated adsorbent; MB-Modified biochar; NA-Natural adsorbent; nd-not detected; BioC-Bio-Carbon

[a] Calculated by difference; [b] $m^3\ t^{-1}$

4.2.2.6 SEM and EDX analysis

SEM is used to witness the alterations arisen in the surface morphology by comparing the SEM micrographs before and after adsorption of metals (Basu et al. 2017). The surface structures of all the four waste biomasses, their biochar, before and after treatment, have been represented in Fig 4.2, 4.3, 4.4, 4.5. The agricultural bio-wastes in their natural form possessed flattened, walls smooth and homogenous surface (Fig 4.2–4.5a). Temperature treatments for biochar production not only increased the surface area but also, altered the surface structures and converted it into amorphous, uniformly porous and heterogeneous surfaces holding irregular cavities and pore of different shape and size as visible from Fig 4.2-4.5 (b) (Lam et al. 2017; Zhao et al. 2017). These cavities may be caused by the loss of water and volatiles from fresh biomass with remaining non-volatile components transformed into biochar (Uçar et al. 2015). In addition to this, the changes also occurred in the shape and size of the asymmetrical particles present on the surfaces of the adsorbents, some residues of cell wall, conducts and vessels could be seen (Fernandez et al. 2014). After adsorption of respective HMs (Cr and Pb) from wastewater (tannery and flashlight), the irregular cavities became filled with some white, crystalline structure which may be caused by the formation of different complexes of the respective metals. The results of present study were found to be in good agreement with previous studies of Baig et al. (2014), Fernandez et al. (2014), Abdelhafez and Li (2016), Mary et al. (2016), Guiza (2017), Lam et al. (2017) and Zhoa et al (2017) for adsorption of HMs and dyes bybiochar of different agricultural wastes.

The EDX analysis of all four adsorbents (SLPB, LPB, OPB and BB) confirmed adsorption of HMs as well as observations of SEM micrographs. Changes in the EDX peaks as natural agricultural waste material and as biochar before adsorption and after adsorption of HMs can be clearly anticipated by EDX spectrums presented in Fig 4.2, 4.3, 4.4 & 4.5b. Initially, the peaks of SLP, LP, OP and B showed the existence of some common elements such as C, O and Ca. Change in elemental composition was observed during conversion of former's natural wastes into biochar. Most of the time, biochars of selected materials retained peaks of C, O, Ca etc. as major elements. The reason behind this may be the removal of the basic material of natural adsorbents (lignin, cellulose, volatiles etc.) during thermal strokes. Further, SLPB, LPB and BB also showed the presence of Pt and Zr, and, the peaks of SLPB also had Bi, K and Mg. After, adsorption of Cr and Pb (20ppm), respective peaks in the spectrum of all of the four adsorbents appeared which supported successful adsorption of both HMs. When considering the

SLPB spectrums, peaks of Bi, Mg and Zr disappeared whereas peaks of Cr appeared during Cr adsorption. In addition to this, during Pb, removal peaks of Mg disappeared and Pb appeared which confirmed the successful adsorption of both HMs by SLPB. Similarly, EDX spectra adsorption of Cr and Pb by LPB represented disappearance of Si by Cr and Pb peaks by respective adsorption processes. In the same way, peaks of K and Si of OPB were replaced by the peaks of Cr and Pb after completion of the adsorption of Cr and Pb from respective aqueous solutions. Likewise, peaks of Cr and Pb replaced the peaks of O and Ca after accomplishment of the adsorption process in BB. Further, the appearances of some other peaks like Na, Pt, Zr, Si etc. may be due to their presence in chemicals used for the EDX analysis processes. All these reallocations of the peaks of metals with peaks of same oxidation numbers suggested that ion-exchange mechanism might be involved in the HMs adsorption processes (Uçar et al. 2015). At last, the EDX spectrums of treated wastewater i.e. tannery and flashlight also showed the presence of respective HMs (Cr and Pb) with the existence of other elements like Na, K, Cl, Mg, Bi, Zr, Pt etc. These extra elements were found to be present in both wastewaters as reported in physicochemical studies. Thus, the results of EDX suggested that both HMs present in wastewaters as well as the extra polluting elements may also be eliminated successfully by applying selected adsorbents. The results were found to be in agreement with Uçar et al. (2015), Mary et al. (2016), Kołodyńska et al. (2017), Basu et al. (2017), Poonam et al. (2018) etc.

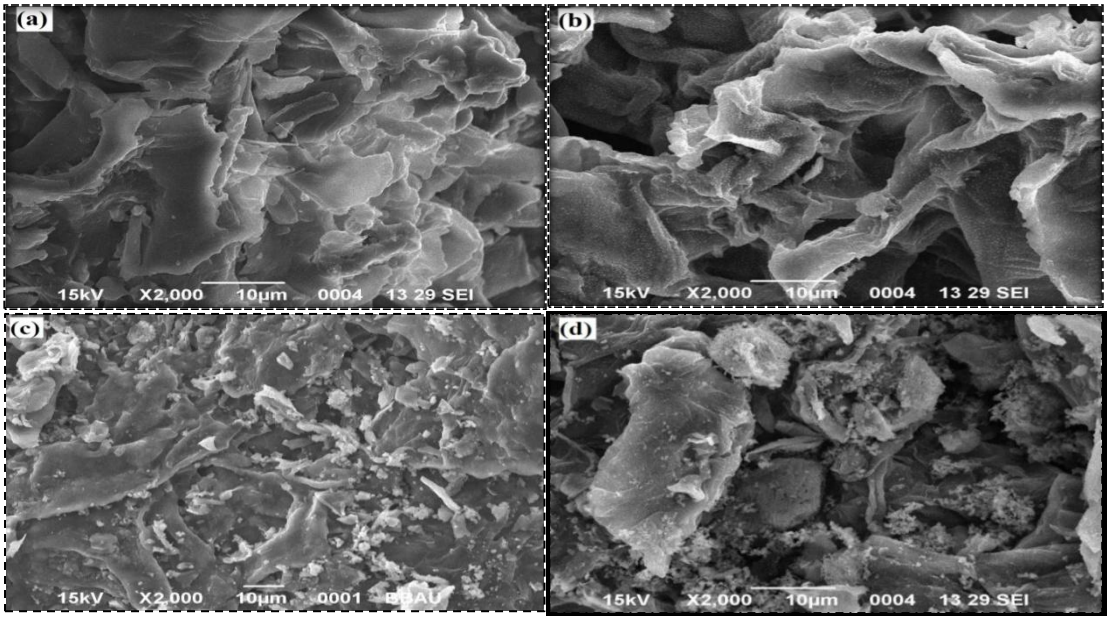

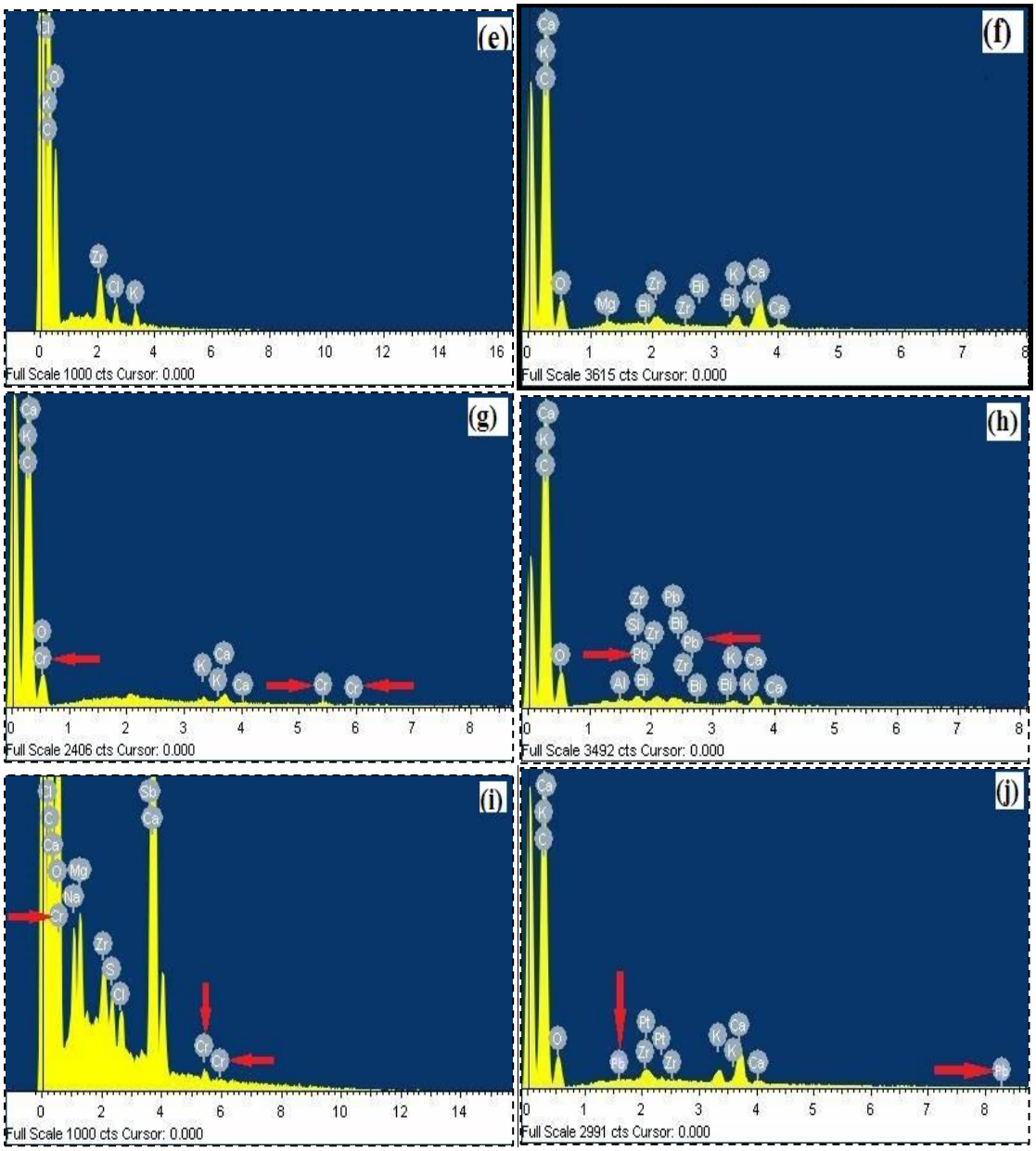

Figure 4.2 SEM micrographs of sweet lemon (*Citrus limetta*) peel (a), its biochar (b), after treatment of tannery (c) and flashlight (d) wastewater; EDX spectrum of sweet lemon (*Citrus limetta*) peel (e), its biochar (f), Cr(g), Pb (h), after treatment of tannery (i) and flashlight (j) wastewater

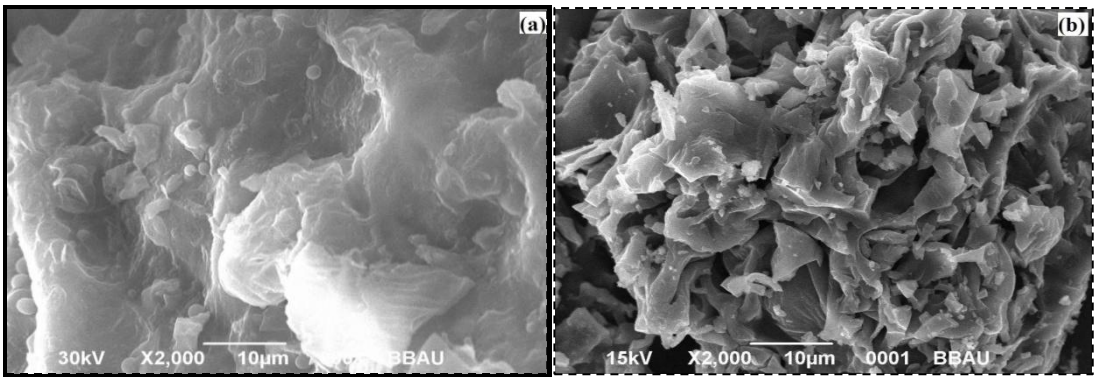

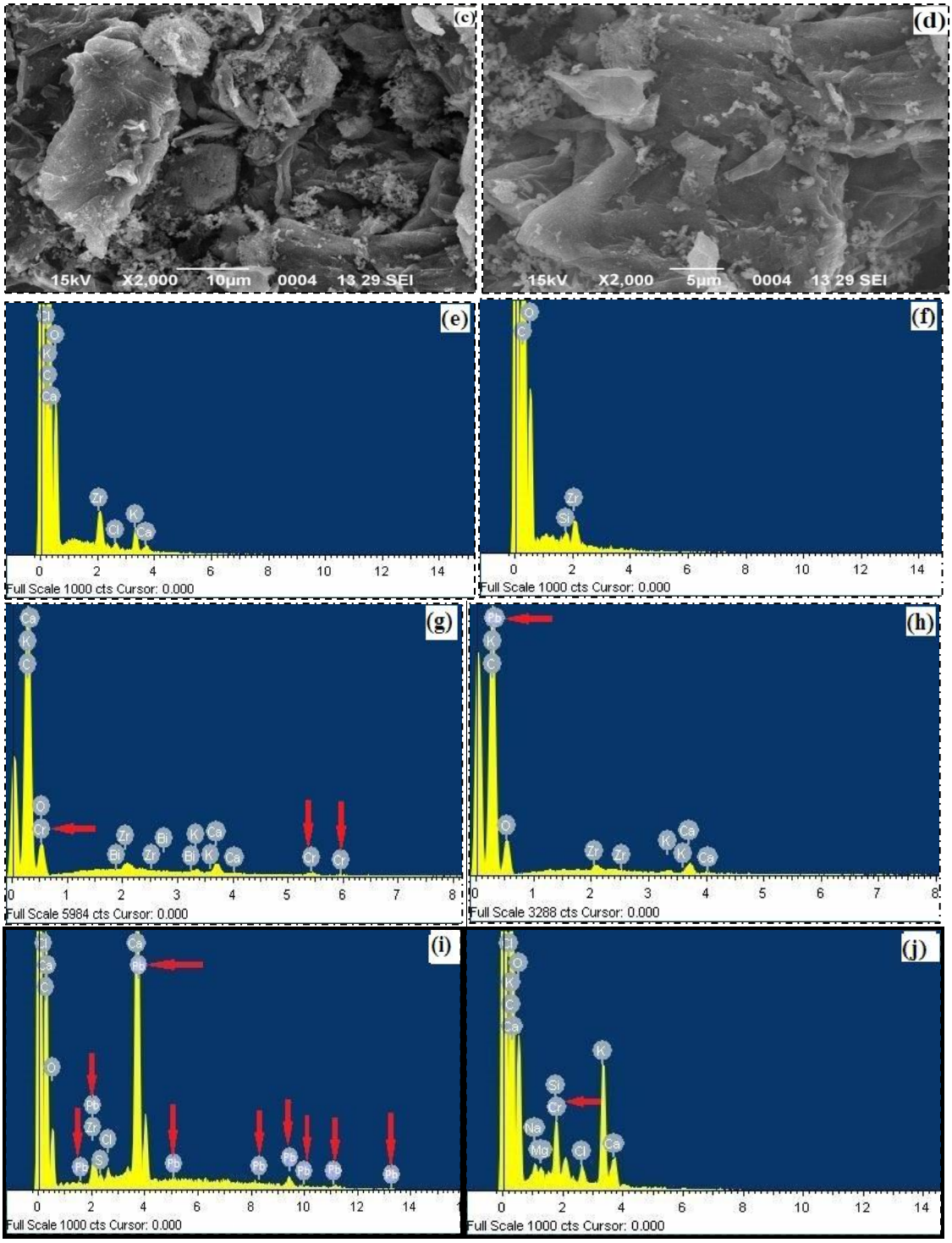

Figure 4.3 SEM micrographs of lemon (*Citrus limon*) peel (a), its biochar (b), after treatment of tannery (c) and flashlight (d) wastewater; EDX spectrum of lemon (*Citrus limon*) peel (e), its biochar (f), Cr(g), Pb (h), after treatment of flashlight (i) and tannery (j) wastewater

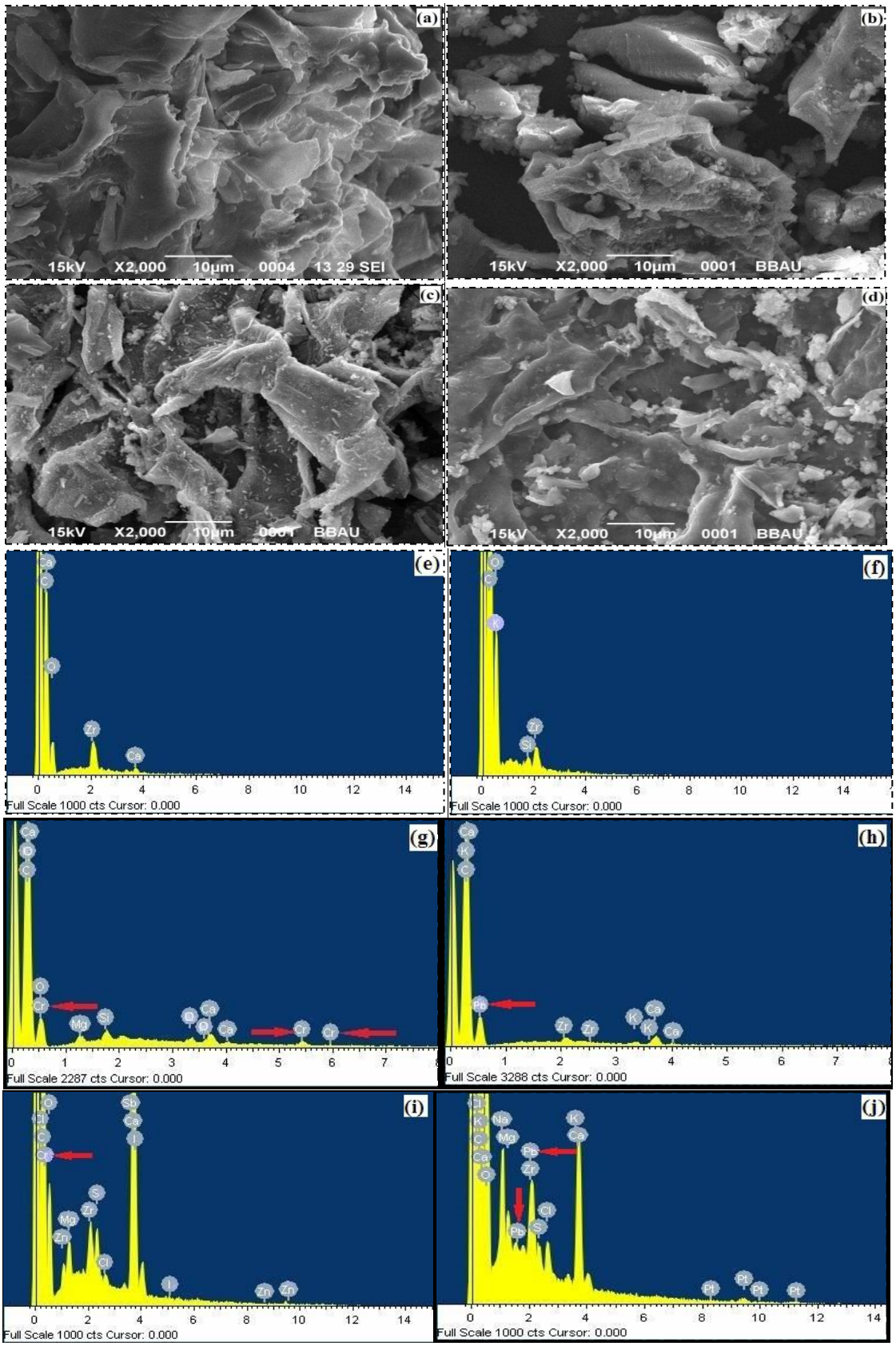

Figure 4.4 SEM micrographs of orange (*Citrus sinensis*) peel (a), its biochar (b), after treatment of tannery (c) and flashlight (d) wastewater; EDX spectrum of orange (*Citrus sinensis*) peel (e), its biochar (f), Cr (g), Pb (h), after treatment of tannery (i) and flashlight (j) wastewater

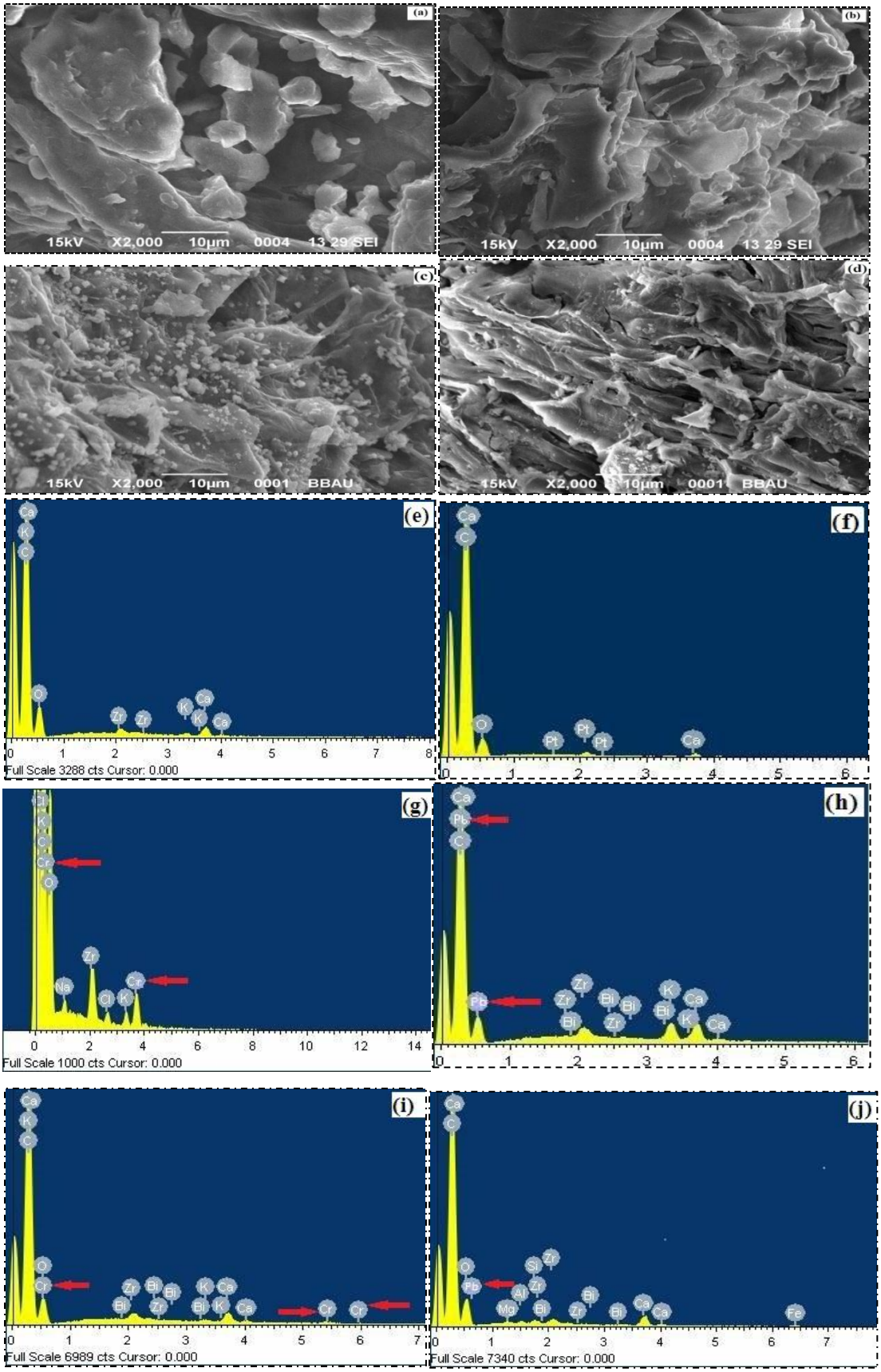

Figure 4.5 SEM micrographs of bagasse (a), its biochar (b), after treatment of tannery (c) and flashlight (d) wastewater; EDX spectrum of BB (e), its biochar (f), Cr(g), Pb (h), after treatment of tannery (i) and flashlight (j) wastewater

4.2.2.7 Surface acidic functional groups

The concentration of surface acidic groups in all of the four adsorbents was measured by Boehm titration method (Boehm 1994) and has been presented in Fig 4.6. The total concentration of these groups in SLPB, LPB, OPB and BB was 7.38, 7.48, 7.41 and 7.03 mol g^{-1}, respectively (Table 4.4). The concentration of carboxylic acidic groups in all of the adsorbents was maximum with average values of 5.30, 4.93, 4.48 and 5.15 mol g^{-1}, respectively. The concentration of lactonic and phenolic groups in the selected adsorbents was 0.51, 1.90, 2.11, 1.28 and 1.57, 0.66, 0.82, 0.60 mol g^{-1}, respectively.

Among these, carboxylic acid group occupied an average of 71.80, 65.84, 60.52 and 73.23 % in SLPB, LPB, OPB and BB, respectively. Except SLPB, all the remaining three adsorbents possessed lactonic groups in higher concentration than phenolic groups. The average concentration of lactonic groups in SLPB, LPB, OPB and BB was 9.57, 38.63, 47.05 and 24.96 %, respectively. Whereas, the average concentration of phenolic groups present in SLPB, LPB, OPB and BB was 21.31, 8.76, 11.03 and 8.55 %, respectively. The results of the Boehm titration for surface acidic groups concluded that all of the adsorbents had the important acid functional groups i.e. carboxylic groups, phenolic groups, lactonic (esters) groups that aid in the adsorption of HMs by different ion-exchange, complexion, addition and substitution chemical reactions. The obtained results are also supported by FTIR analysis described in next section.

The results of the present study was in agreement with Abdelhafez and Li (2016) who had also observed the majority of carboxylic acid surface function groups in sugarcane bagasse and orange peel biochar. Uçar et al. (2015) have also reported the similar results for majority of carboxylic acidic functional groups than phenolic and lactonic groups. Further, Han et al. (2013) had described the effect of pyrolysis temperature on surface acidic groups of switchgrass, hardwood and softwood. They found that carboxylic groups in the three types of biochars were reduced by fast pyrolysis than slow pyrolysis, the phenolic groups were found to be elevated and lactonic group showed no effect of pyrolysis conditions.

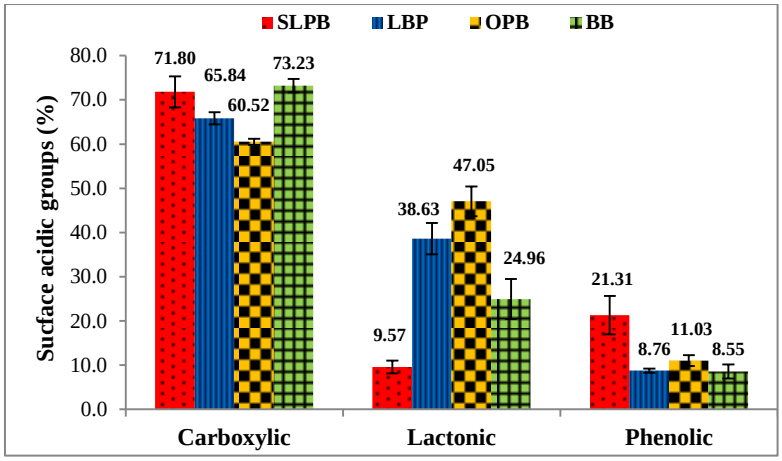

Figure 4.6 Surface acidic groups concentration (mol g^{-1}) present in SLPB, LPB, OPB and BB; bar represents ±S.D

4.2.2.8 FTIR

In order to explore the chemical structure and major surface functionalities groups present in the selected adsorbents (biochars), FTIR analysis was carried out (Solum et al. 1995; Gomez-Serrano et al. 1996; Hassan et al. 2014). These functional groups and chemical bonds present in them are one of the most important factors, which affect the adsorption of HMs. The spectra of the all of the four selected adsorbents, its biochar, HMs (Cr and Pb) loaded biochar and biochar after treating the tannery and flashlight wastewater have been presented in Fig 4.7-4.10 and were identified following the interpretations of Lambert et al. (1987).

Sweet lemon peel possessed broadest peak at 3409.8 cm^{-1} due to presence of OH groups may be in the form of moisture or phenolic or alcoholic groups (Gupta et al. 2011; Huang et al. 2012; Kim et al. 2013; Baig et al. 2014). Other major peaks at 2931.3, 1629.5, 1416.4, 1102.8 and 1064.0 cm^{-1} were, due to presence of OH in carboxylic acids, C=O of ketonic and ester groups, C-N in primary amides, C=S in thiocarbonyl groups and Si-O-Si in siloxane, respectively (Wang and Chen 2015; Abdelhafez and Li 2016; Basu et al. 2017). The minor peaks at 1740.7 and 1331.4 cm^{-1} were the representatives of C=O lactones, aldehydes, aromatic nitro compounds and sulfones, respectively. After thermal treatment during biochar production, the major peak responsible for OH groups due to moisture disappeared and a new peak at 3416.5 cm^{-1} appeared (Samsuri et al. 2013). This peak was existent owing to presence of NH_2 groups in the form of amines and amides offered by N-H stretch (Santos et al.

2015; Shin 2017). The other major peaks that appeared in SLPB were at 1568.4 and 1419.8 cm^{-1} due to NO_2 in aliphatic nitro compounds and CH_3 in aliphatic compounds, COOH in carboxylic acids (Lim et al. 2009; Baig et al. 2014) (Fig 4.7a). These OH, COOH and NO_2 groups were of the interest for successful adsorption of HMs present in solutions and wastewater. Now, when SLPB was subjected to Cr and Pb adsorption from synthetic solution of known concentration (20 ppm), shift in the position of peaks were observed. The major peaks in SLPB were shifted to 1618.2, 1445.8, 1365.1 and 1206.3 cm^{-1} after Cr adsorption. Conversion of carboxylic acids into phenolic groups, ketonic groups, formation of COO^- groups salts, C-O-C ethers with C=C stretching and C-C-N bending were evident from the appearance of these peaks (Basu et al. 2017). These transformations were evidence of formation, deformation and stretching of different bonds through ion exchange, addition or dissociation chemical reactions (Kim et al. 2015; Poonam et al. 2018). In the same way, the major peak of SLPB was shifted from 3416.5 to a minor peak at 3418.2 cm^{-1} after Pb adsorption (Fig 4.7b). The other major peak at 1568.4 and 1419.8 cm^{-1} were shifted to 1369.6 and 1318.5 cm^{-1}, respectively (Trakal et al. 2016). This shift may be because of the conversion of NO_2 in aromatic compounds to NO_2 in aliphatic compounds by symmetrical stretching of NO_2. On the other hand, when SLPB was added to tannery wastewater, the major peak was recorded at 3438.0, 1629.7 and 1441.6 cm^{-1}. These peaks were the result of the reallocation of major peaks of SLPB at 3416.5, 1568.4 and 1419.8 cm^{-1}, indicating involvement of esters, lactones, CH_3 deformation, C-N stretching and carboxylic acids in adsorption of Cr from the wastewater (Momcilovic et al. 2011; Basu et al. 2017; Shin 2017). The carboxylic acids might be converted to ketonic groups whereas, CH_3 deformation produced some aliphatic compounds of it, NO_2 in aliphatic nitro compounds were converted into primary amines and amides by NO_2 anti-symmetrical stretch. The disappearance of other weak peaks might be evident of exhaustion of the adsorbent for further association or dissociation reactions. Moreover, SLPB treated with flashlight wastewater showed the major peaks at 3415.7 cm^{-1} corresponding to the presence of moisture or OH groups in the form of alcohols or phenols by stretching of O-H bond (Fig 4.7c). Other major peaks were recorded at 1564.2, 1427.0, 1118.6 and 1045.2 cm^{-1}, which were the indicatives of the presence of COO^- groups in carboxylic acid salts, OH in carboxylic acids, C-O-C in in aliphatic ethers C-NH_2 in primary aliphatic amines Si-O-Si in silaxanes, S=O in alkyl sulfoxides, P-OH in organo-phosphorus

compounds (Basu et al. 2017; Shin 2017; Zhao et al. 2017; Hu et al. 2018). These groups might be created from different stretching and deformation of different bonds present in the esters, lactones, amines, amides and carboxylic acids.

Lemon peel also possessed a broad and strong peak at 3408.5 cm^{-1} that symbolize the existence of NH_2 in aromatic amines, primary amines and amides due to N-H stretch found in proteins (Yu et al. 2015). Other major peaks were at 1626.1 and 1066.4 cm^{-1} which represented ketonic groups by C=O stretch, C=C stretch of vinyl ethers, NH_2 deformation in primary amines, and C-N stretch in primary aliphatic amines, Si-O-Si in siloxanes, SO_3H in sulfonic acids, respectively (Jindo et al. 2014; Yorgun and Yıldız 2015). The weak peaks at 2928.1, 1733.0, 1414.7, 1321.8, 1242.9 and 1101.1 cm^{-1} validating the presence of $–CH_3$ and CH_2 in aliphatic compounds, C=O in lactones, OH in carboxylic acids, COO^- groups in carboxylic acids, NO_2 in nitro aromatic compounds, Ar-O in ethers, C-C-N in amines, C-O-C in ethers, respectively (Santos et al. 2015; Van Vinh et al. 2015; Abdelhafez and Li 2016). After conversion into biochar, some very minute peaks appeared at 3907.2 to 3730.2 cm^{-1}, which might be due to moisture content. The major peaks at 3404.4, 2923.1, 1629.1, 1426.8 and 1373.2 cm^{-1} corresponded to same groups as that of lemon peel except for 1058.7 cm^{-1} that represented OH groups in primary and cyclic alcohols and SO_3H in sulfonic acids (Baig et al. 2014). Weak peaks at 1266.8 and 1160.1 cm^{-1} showed the presence of $Si-CH_3$ in silanes and lactones, and C-OH in alcohols and SO_2 in sulfones, respectively (Basu et al. 2017; Hu et al. 2018). This implied that very little change in functional groups occurred during biochar production in comparison to SLPB. Now, when LPB was used to treat Cr and Pb present in solution of known concentration (20 ppm), the broad peak of LPB disappeared (Fig 4.8a). Cr treated LPB showed the presence of major peaks at 1614.2, 1366.1 and 1224.2 cm^{-1} resultants of shift in the peaks after adsorption. These peaks represented N-H deformation in primary amides, NH_3 deformation in amino acids, C=O stretch in ketones and C=C stretching in vinyl ethers, COO^- groups in carboxylic acids salts and NO_2 in aromatic nitro compounds, C-N in aromatic amines, C-O-C in ethers, lactones and sulfonic acids (Devi and Saroha 2014; Qiao et al. 2017; Zhao et al. 2017). Whereas, Pb treated LPB represented major peaks at 1608.1 and 1209.5 cm^{-1} indicating towards the existence of NH_2 deformation in primary amines and C=O stretching in ketones, and C-C-N bending in amines, C-O-C anti-symmetrical stretch in lactones and P=O stretch in

phosphorus oxy acids (Santos et al. 2015) (Fig 4.8b). Such stretch and deformations were evident of action and reactions of different chemical reactions after adsorption of HMs. Finally, when LPB was used for treating tannery wastewater a very minute shift in the position of strong peaks from 3404.4 to 3444.3 cm^{-1} and 1629.1 to 1632.0 cm^{-1} was recorded. These shift brought no change in the functional groups. However, other minor peaks at 1413.4 and 1223.5 cm^{-1} showed the presence of OH groups carboxylic acids, C-N stretch in primary amides and C-O-C in ester and lactones as well as in aromatic amines (Santos et al. 2015; Abdelhafez and Li 2016; Kołodyńska et al. 2017). Disappearance of other minor and major peaks from LPB after treating tannery wastewater and flashlight wastewater was evidence of transformation of functional groups by different addition, substitution, complexation reactions after adsorption of HMs. In the same way, LPB after treating flashlight wastewater, stronger peaks at 3404.4, 2923.1 and 1426.8 cm^{-1} were shifted a little at 3415.4, 2908.7 and 1431.2 cm^{-1}, respectively, which brought no change in the composition of functional groups (Baig et al. 2014; Yu et al. 2015; Zhao et al. 2017). Nevertheless, changes in the position of peak at 1629.1 and 1160.1 cm^{-1} were recorded which took the position at 1569.7 and 1023.5 cm^{-1}. These changes indicated that breaking of old bond in ketone and primary amides, and alcohols for the formation of new groups and bonds in carboxylic acids and aliphatic nitro compounds, and cyclic alcohols after adsorption of Pb (Fig 4.8c).

The orange peels possessed broad and strongest peaks at 3412.9 cm^{-1} corresponded to OH groups in alcohols and phenols, N-H stretching in aromatic amines, primary amines and amides (Tan et al. 2008; Luo et al. 2012). Other major peaks were present at 2936.1, 1632.4, 1104.5 and 1066.0 cm^{-1}, representing C-H anti-symmetrical and symmetrical stretching in aliphatic compounds of CH_3 and CH_2, C=O stretching in ketones and NH_2 deformation in primary amides, C-O-C stretch in ethers, C-O stretch in C-OH alcohols and C-N stretching in primary aliphatic amines, respectively (Santos et al. 2015; Van Vinh et al. 2015; Yu et al. 2015; Abdelhafez and Li 2016). The minor peaks at 1737.2, 1369.0 and 1262.4 cm^{-1} were the indicatives of C=O stretching on anhydrides, aldehydes and lactones, COO^- groups in carboxylic acids and N^+-O^- in pyridine, C-O-C anti-symmetrical stretch in esters and lactones (Han et al. 2013). Temperature treatment given during biochar production gave two broader peaks at 3384.2 and 1439.2 cm^{-1}(Lammers et al. 2009)(Fig 4.9a). These peaks

were the representatives of alcoholic and carboxylic groups and CH_3 anti-symmetrical deformations, respectively. The other major peaks at 2967.9 cm^{-1} for CH_3 anti-symmetrical and symmetrical stretching, 1569.8 cm^{-1} for COO^- in carboxylic acids and C=C stretching, 1162.4 cm^{-1} for C-O stretch in alcoholic groups and 1046.0 cm^{-1} for S=O in sulfoxides were recorded (Keiluweit et al. 2010; Seredych and Bandosz 2011; Hu et al. 2018). Major changes in the peaks positions were observed when OPB was subjected to adsorb Cr and Pb from solutions of known concentrations (20 ppm each). Only three strong peaks were recorded for Cr adsorption at 3405.4, 1606.2 and 1194.3 cm^{-1} which were the indicatives of NH_2 groups present in aromatic amines, primary and secondary amides, ketonic groups with C=O stretching and OH groups in alcohols (Pan et al. 2013; Santos et al. 2015). The absence of other major and minor peaks might be because of unavailability of other functional groups due to exhaustion the OPB after Cr adsorption. Likewise, changes and shift in the peaks of OPB were also recorded after Pb adsorption. The position of broadest peak was altered and it was recorded at 1614.3 cm^{-1}, which indicated presence of C=O groups in ketones, C=C in vinyl ethers, NH_3^+ in amino acids. Other major peaks were recorded at 1367.4 and 1225.3 cm^{-1} which were the indication of presence of COO^- groups in carboxylic acid salts, SO_2 in sulfonyl chlorides, and C-O-C in esters and lactones and C-N in aromatic amines, respectively (Özçimen and Ersoy-Meriçboyu, 2010; Hu et al. 2018) (Fig 4.9b). At the end, tannery and flashlight wastewater were treated with LPB, which showed shift in positions and disappearances of some major bands (Fig 4.9c). Tannery wastewater treated OPB showed minute shift in the position of strongest bond from 3384.4 to 3412.9 cm^{-1}, without affecting the functional groups. Whereas, minor bands at 2967.9, 1569.8, 1439.2 cm^{-1} shifted to 2925.8, 1578.2 and 1414.8 cm^{-1}, respectively. These alterations confirm the conversion of amides into amines due to N-H stretch, aliphatic compounds containing CH_3 and CH_2 groups into aldehyde groups due to C-H bending, and CH_3 in aliphatic compounds into carboxylic acids due to O-H bending, respectively (Devi and Saroha 2014;Yu et al. 2015). In the same way, when flashlight wastewater was treated with LPB, the broadest and sharp peaks at 3384.4 and 1439.2 cm^{-1} only changed its position to 3415.4 and 1427.4 cm^{-1}, respectively, which did not affect the functional groups (Fig 4.9d). But, other sharp peaks appeared at 1569.6, 1427.4, 1164.2 and 1054.7 cm^{-1} corresponded to COO- and OH groups in carboxylic acids, CH_3 in aliphatic compounds, COH in alcohol, C-O-C in ethers and CNH_2 in primary aliphatic amines, respectively same as that of OPB

(Zhang et al. 2007; Lu et al. 2012; Baig et al. 2014; Santos et al. 2015; Trakal et al. 2016). The reason behind the presence of same functional groups may be the affinity of the HMs to that places which did not come under the range of the IR spectra.

The spectra of the bagasse, its biochar (Fig 4.10a) Cr loaded BB, Pb loaded (Fig 4.10b), BB after treating tannery wastewater and BB after treating flashlight (Fig 4.10c) wastewater are presented Fig 4.10. The broad and strongest peak at 3352.9 and 1055.1 cm^{-1} indicated the presence of OH in alcohol and phenols by –OH stretching andSO_3 in sulfonic acids, CH-OH in cyclic alcohols, S=O in alkyl sulfoxides and P-O-C stretching in organo phosphorus compounds, respectively (Lu et al. 2012; Pan et al. 2013). Other major peaks were recorded at 2896.0, 1634.0, 1427.0, 1372.7, 1249.6, 1162.4 and 1113.0 cm^{-1} corresponding to $–CH_3$ and CH_2 in aliphatic compounds, C=O and NH_2 in amides due to C=O stretch and NH_2 deformation, OH in carboxylic acids, NO_2 in aromatic nitro compounds, Ar-O in aryl ethers due to C-O stretch, SO_2 in sulfones, C-O-C in aliphatic ethers and organo phosphorus compounds with S=O in alkyl sulfoxides, respectively (Pakula et al. 2007; Abdelhafez and Li 2016). After biochar production, the major peaks were vanished excluding –CH stretching at 2925.3 cm^{-1}, C=O stretch in ketones signified by minor peak at 1711.0 cm^{-1}, C=C stretch in alkenes and C=O stretch in secondary amides presented by a loud peak at 1631 cm^{-1}. Other minute peaks at 1364.4 and 1249.6 cm^{-1} showed the presence of NO_2 groups in aliphatic nitro compounds and Ar-O groups in alkyl ethers. After, adsorption of Cr and Pb from solutions of known conc. (20 ppm), shift in the position of peaks and disappearance of some minor peaks were observed (Fig 4.10a). After Cr adsorption, the sharp peaks were not shifted, but the minor peak at 1711.0 and 1364.4 cm^{-1} were shifted to 1631.2 and 1440.5 cm^{-1}, respectively, which symbolized the alteration of functional groups after adsorption of HMs (Trakal et al. 2016). The C=O in ketones and C=C groups in alkenes were transformed into C=O in primary amides and CH_3 in aliphatic compounds and OH in carboxylic acids, which indicated that breaking and formation of chemical bonds took place (Yao et al. 2011; Baig et al. 2014; Kołodyńska et al. 2017). In the same way, after the adsorption of Pb, the strong peaks were moved to 1618.1 and 1431.7 cm^{-1} representing C=O stretching and C-N stretch in primary amides and C-H and CH_2 deformations, respectively (Fig 4.10b). Likewise, BB after treating tannery and flashlight wastewater, the spectra represented emergence and disappearance of some minor peaks (Fig 4.10c). Very minute changes

in the position of broad and sharp peaks occurred, which symbolized the presence of same functional groups as that of BB after treating both wastewaters. Disappearance of minor peaks at 1711.0 cm^{-1} indicated merging of C=O groups of ketones into some other functional groups after tannery wastewater treatment. Further, emergence of a minor peak at 2856.2 cm^{-1} symbolized the presence CH_3 and CH_2 groups of aliphatic compounds after adsorption of Cr. Similarly, disappearance of peaks at 2925.3, 1711.0 and 1249.6 cm^{-1} indicated their involvement in the production of some other functional groups such as aliphatic, phenolic and ketonic compounds after flashlight wastewater treatment by BB (Wang et al. 2013; Qiao et al. 2017). Moreover, shift in the position of peak from 1364.4 to 1441.6 cm^{-1} was observed which symbolized the substitution of functional groups of NO_2 in aliphatic nitro groups with NO symmetrical stretch or COO^- group in carboxylic acid salts or SO_2 in sulfonic chloride compounds to CH_3 in aliphatic compounds with deformation of bond among C and H atoms (Baig et al. 2014;Abdel-Fattah et al. 2015). These phenomenons of alteration of peak positions, appearance and disappearance of major and minor peaks after adsorption of HMs suggested the involvement of different chemical reactions like addition, substitution, ion-exchange etc. in the process.

FTIR spectroscopy illustrated that all of the four adsorbents were found to be rich in the array of different functional and chemical groups which might have aided in the sequestration of HMs. The strong peaks between 3846.8 and 3352.9 cm^{-1} which may be ascribed to -OH stretching vibrations of cellulose, pectin and lignin (Guo et al. 2008; Chia et al. 2012; Reddy et al. 2014; Kołodyńska et al. 2017). The higher carbon content as well as the organic matter marked the stretching of the chemical bonds (Abdelhafez and Li 2016). Further, shift in the position of peaks among biochars before and after adsorption of HMs proposes that the process might be smoothed by chemisorption ensuing in binding of HMs by the nucleophilic functional groups (Poonam et al. 2018). The loss of some of the functional groups from biochars after adsorption, implied that these groups were consumed in the uptake of the respective HMs (Lima et al. 2016). The alteration of secondary amide into primary amide and -CH to C=C were marked of creation and detachment of bonds through ion exchange or other specific mechanisms (Kim et al. 2015). This phenomenon favored the adsorption of HMs onto the surfaces of all the selected adsorbents. It may also be established that the breakdown of cellulose, hemicellulose, lignin and polysaccharides

components present in the adsorbents point towards the breaking and reshuffle of stronger bonds of carboxyl groups and evolution of NO groups (Srinivasan and Ganguly 1991; Coates 2000; Wang et al. 2013; Mendez et al. 2014; Qiao et al. 2017). It addition to this, involvement of P, S and N were evident from the different related groups present in all of the four adsorbents in the form of sulfonic groups, amides, organo-phosphorus compounds etc. (Basu et al. 2017). According to Machado et al. (2011), phenolic, carboxylic and alkyl groups also played important role in adsorption of HMs as they have oxygen containing functional groups providing adsorption sites. Moreover, results of EDX analysis and surface acidic groups explained earlier in above sections 4.2.2.6 and 4.2.2.7 respectively supported the FTIR analysis for particular adsorbents. Further, previous studies of Van Vinh et al. (2015), Yu et al. (2015), Abdelhafez and Li (2016), Ahmadi et al. (2016), Kołodyńska et al. (2017), Mary et al. (2016), Trakal et al. (2016), Qiao et al. (2017), Shin (2017), Hu et al. (2018) etc. supported the finding of present study.

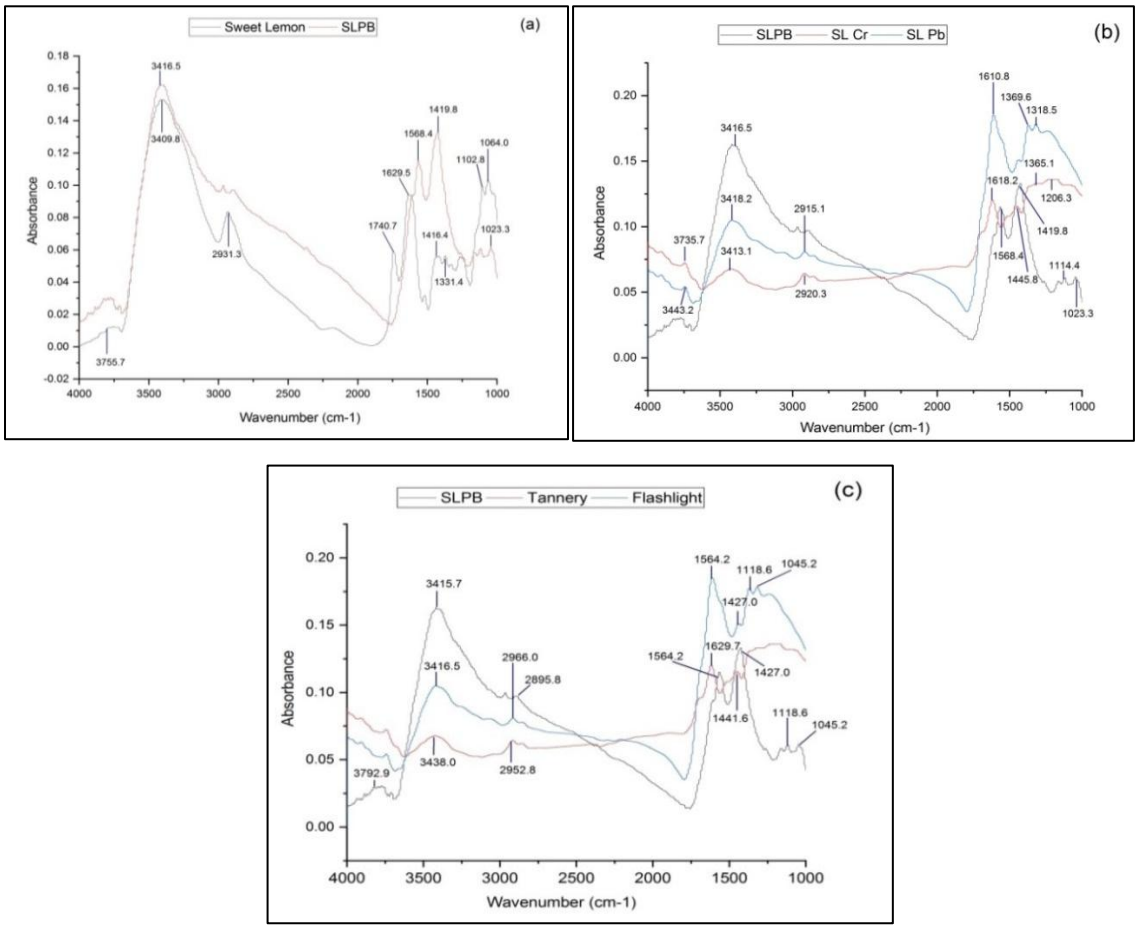

Figure 4.7 FTIR spectra of sweet lemon peel and its biochar (a), SLPB after adsorption of Cr and Pb (b), SLPB after treatment of tannery and flashlight wastewaters (c)

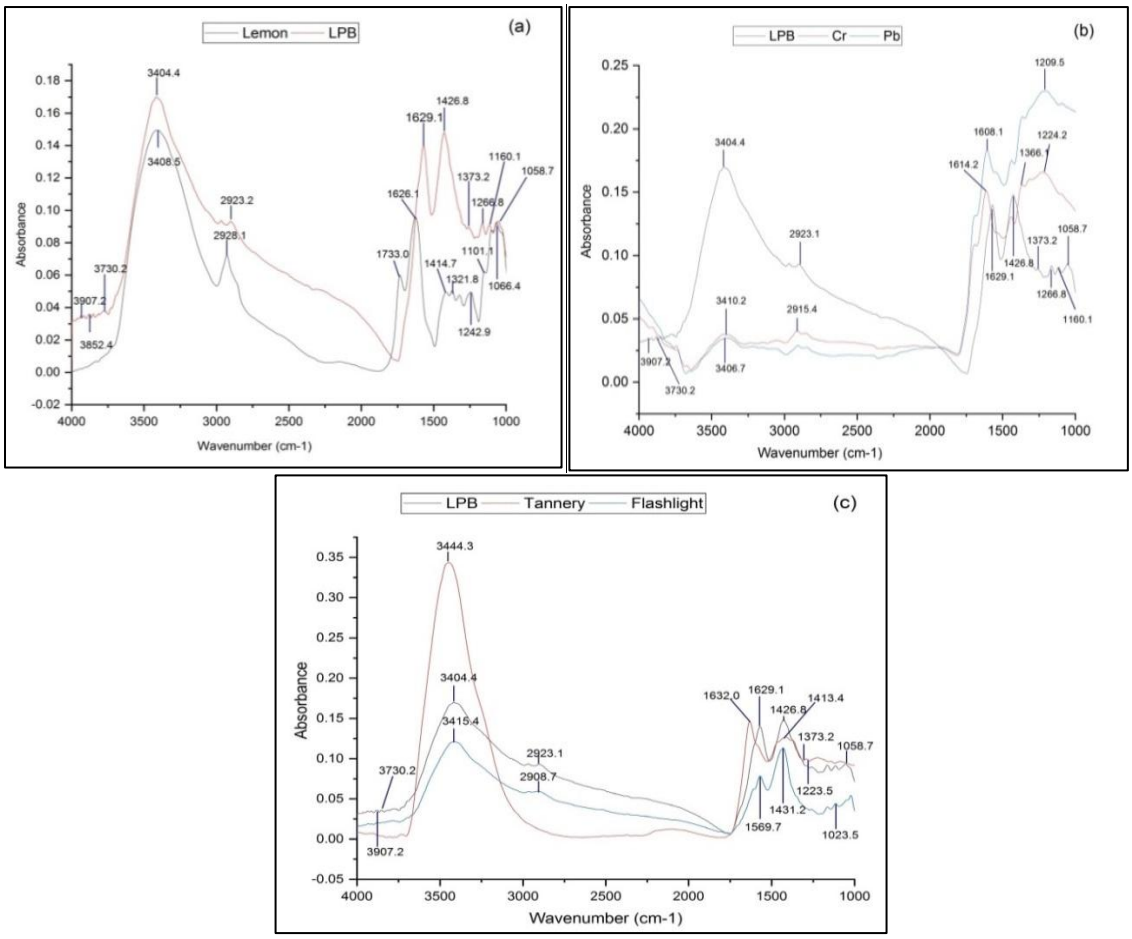

Figure 4.8 FTIR spectra of lemon peel and its biochar (a), LPB after adsorption of Cr and Pb (b), LPB after treatment of tannery and flashlight wastewaters (c)

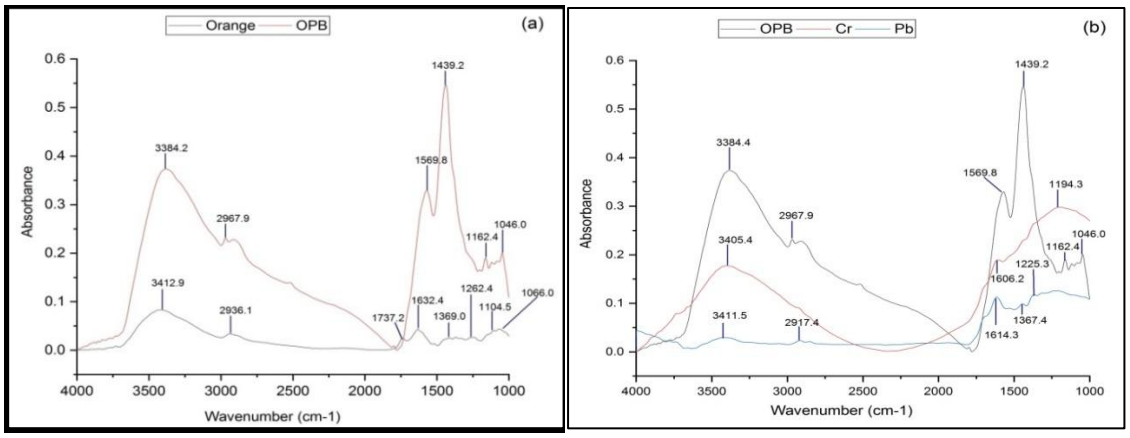

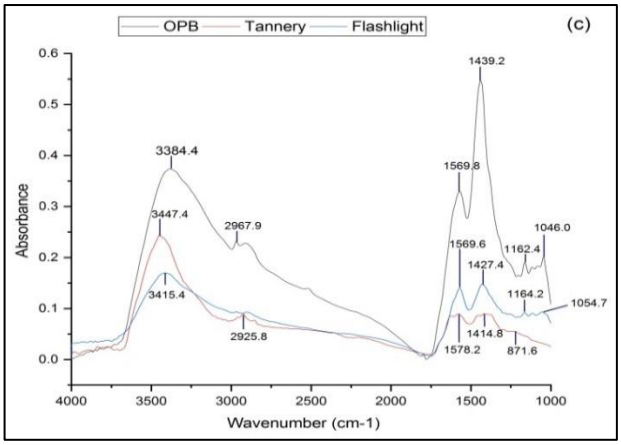

Figure 4.9 FTIR spectra of orange peel and its biochar (a), OPB after adsorption of Cr and Pb (b), OPB after treatment of tannery and flashlight wastewaters (c)

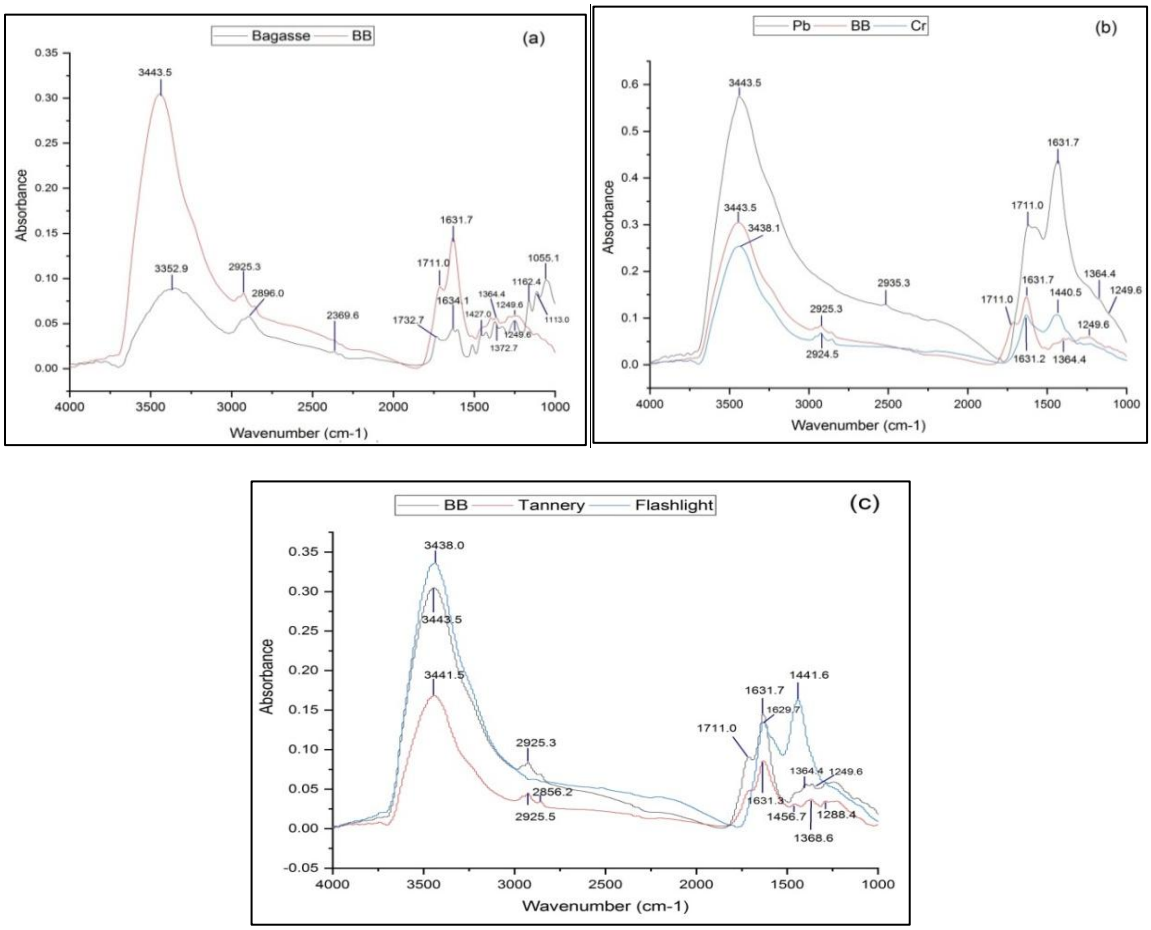

Figure 4.10 FTIR spectra of bagasse and its biochar (a), BB after adsorption of Cr and Pb (b), BB after treatment of tannery and flashlight wastewaters (c)

4.2.2.7 XRD

X-ray diffraction (XRD) patterns of all the four adsorbents before and after adsorption of HMs have been shown in Fig 4.11. It is used to define the crystal structure of adsorbents intended for investigation (Zheng et al. 2017). The sharp diffractogram peaks for all of the adsorbent found to be in the range of 24.35 to 26.41º (2θ). Occurrence of sharp crystalline peak for SLPB at 24.37º (2θ), LPB at 26.59º (2θ), OPB at 24.35º (2θ) and BB at 26.41º (2θ) signified the presence of natural cellulose, lignin and non-crystalline hemicellulose materials (Reddy et al. 2012; Komolwanich et al. 2014; Liu et al. 2014; Ma et al. 2016; Cui et al. 2018; Fallah et al. 2018). After treating both wastewaters, slight change in the position of peaks were recorded for all the four adsorbents, however no change in the crystallinity of biochars was observed (Meng et al. 2018). The sharpest peak of SLPB minutely shifted its position from 24.37º (2θ) to 24.17 and 24.29º (2θ), respectively, after adsorption of Cr and Pb from tannery and flashlight wastewaters. However, change in the intensities can be visualized from Fig 4.11(a), as it was 434 cts for SLPB and 318 and 334 cts for Cr and Pb loaded SLPB. Likewise, the most prominent peak for LPB was recorded at 26.59º (2θ), which minutely changed its position to 26.63 and 24.35º (2θ), respectively, after treating both wastewaters Fig 4.11(b). Some changes in the intensities were also recorded as it was 437 cts before adsorption, which was decreased to 397 and 414 cts, respectively, after adsorption of particular HMs from both wastewaters. The loudest crystalline peak for OPB was recorded at 24.35 º2θ at intensity of 461 cts, which changed its position to 29.49 and 24.37 º(2θ), respectively with decrease in intensities with 343 and 397 cts, correspondingly, after treating tannery and flashlight wastewaters (Fig 4.11c). In the same way, the highest pitched peak for BB was observed at 26.41º (2θ) with an intensity of 427 cts (Fig 4.11d). After adsorption of Cr and Pb from tannery and flashlight wastewaters, a little change in the position of the sharpest peak was recorded at 29.49 and 24.37º (2θ), particularly with noticeable change in the intensities with 343 and 438 cts, respectively. Alternations in the intensities verified the adsorption of HMs, which suppressed the intensities after adsorption of Cr and Pb, respectively, except for BB after treating flashlight wastewater. This increase in the intensity may be caused by presence of alkali (NaOH) in the wastewater or mixture and/or inclusion complex formation after adsorption (Tsiepe et al. 2017; Zhao et al. 2017). However, decrease in the 2θ

positions after adsorption may cause a little decrease in the crystallinity of adsorbents due to presence of different chemicals in wastewaters (Nekouei et al. 2017). According to Devi and Saroha (2014) presence of $CaCO_3$ in the biochar was evident from the occurrence of peaks at 29.21º (2θ). All of the selected biochars exhibited the diffractogram peaks at 29.21º (2θ) with different intensities of 221, 301, 254 and 263 cts for SLPB, LPB, OPB and BB, respectively, confirming the presence of $CaCO_3$ in them. Moreover, results were also in accordance with EDX analysis explained in the section 4.2.2.6. Further, other intermediate peaks were also present in the diffractogram of all the four adsorbents after treating tannery and flashlight wastewaters, which may be attributed to respective bindings of Cr and Pb on to them.

The results of the present study were found to be in good agreement with previous studies done by various workers (Baig et al. 2014; Basu et al. 2017; Slimani et al. 2017; Zhao et al. 2017; Gil et al. 2018; Peng et al. 2018; Qian et al. 2018; Yang et al. 2018). Baig et al. (2014) detected diffraction peak appeared at 16.1 and 22.4 º (2θ) for magnetic Kans grass biochar during adsorption of As (III and V) which could be assigned to natural cellulose. Basu et al. (2017) who observed crystalline peak at 21.49 and at 30.44º (2θ) for cucumber peel before and after adsorption of Pb possessing amorphous nature due to occurrence of hemicellulose and lignin in the biomass. Gil et al. (2018) recorded XRD diffractogram for ostrich bone ash for removal of Hg and Pb at 2θ = 25.87, 29.83, 31.88, 32.99, 34.58, 39.66, 46.51 and 49.47 °. Zhao et al. (2017) found decrease in the diffraction intensity of biochars derived from giant reed (*Arundo donax* L.) prepared at 500 to 800 °C. However, increase in the diffraction intensity was also detected because of small amount of NaOH in the raw material derived from the feedstock. Peng et al. (2018) reported XRD peaks at 14.9, 16.5 and 22.5 º, confirming the crystalline structure of cellulose I in the ramie fiber used for adsorptive removal of Cd ions. Qian et al. (2018) also reported peaks of cellulose centered at 22.5º (2θ) for filter paper modified with sodium alginate composite to treat methylene blue dye from wastewater.

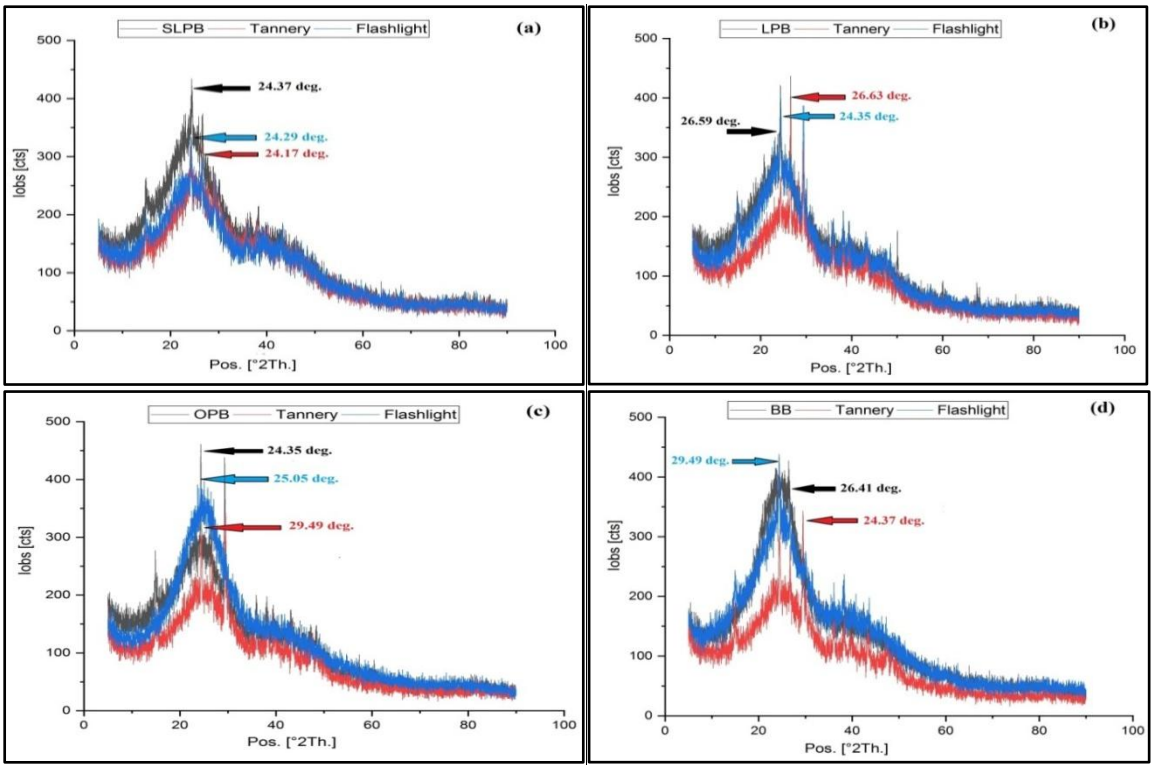

Figure 4.11 X-ray diffractogram of SLPB(a), LPB(b), OPB(c) and BB(d) before and after treatment of tannery and flashlight wastewaters

4.2.3 Different combinations of parameters affecting the adsorption processes

In the present study, SLPB, LPB, OPB and BB were used for removal of Cr and Pb from industrial wastewaters. All of the four adsorbents were provided with different combinations of physicochemical parameters to select the best one for treating wastewaters. Among the various physicochemical parameters i.e. pH, temperature, initial metal concentration, adsorbent dosage and contact time were used for analyzing the performance of biochars selected agricultural wastes. Firstly, the adsorbents were applied on solution of known concentration of 20 ppm each for Cr and Pb before applying it for industrial wastewaters. The influence of these five parameters on removal of HMs from solutions (20 ppm) have been discussed below-

4.2.3.1 Adsorbent Dosage

Biosorption is an effective and promising practice for water and wastewater treatment but sometimes the higher cost is documented as the principal obstacle to its comprehensive applicability. Thus, the optimization of adsorbent dosage is the utmost requirement for scale-up and designing of large scale equipments for industrial and practical approach

(Ahmadi et al. 2016). The dose of the adsorbent is the most important factor, which affects the surface area, availability of binding sites and interaction of HMs with adsorbents (Bansal et al. 2009). It delineates the adsorption capacity of the selected adsorbents at specified initial metal ion concentrations (Bhatti et al. 2016). Different ranges of adsorbent dosage at room temperature (25±3ºC) with initial metal concentration of 20 mg L^{-1} have been tested for the removal of Cr and Pb ions, respectively (Fig 4.12). Further, a detailed description of effect of contact time onto removal percentage and concentration of both HMs have been discussed below-

The effect of SLPB adsorbent dosage was observed in the range of 2.0 to 5.0 and 2.5 to 3.5 g L^{-1}, respectively for Cr and Pb (Fig 4.12a and Table 4.4). The amount of adsorption and removal rate increased with increasing the adsorbent dosage until the equilibrium was attained. The removal rate increased from 72.97 to 83.38 and 72.50 to 93.83 %, respectively by increasing the dosage from 2 to 5.0 and 2.5 to 3.5 g L^{-1} for Cr and Pb. The maximum removal of Cr (83.38%) and Pb (93.83 %) was achieved at 5 and 3.5 g L^{-1} of optimized dosage at 200 and 160 minutes of contact time, respectively. Further increase in adsorbent does not affect removal rate that may be due to aggregation of biomass and HMs at the binding sites causing electrostatic repulsion among them. The amounts of Cr and Pb remained in the solution after saturation points were 3.32 and 1.23 mg L^{-1}, respectively in comparison to initial metal concentration of 20 mg L^{-1}.

The ranges of 2.0 to 4.0 and 3.0 to 6.0 g L^{-1}, respectively of adsorbent dosage at difference of 0.5 g L^{-1} for contact times of 10 to 180 minutes (described in next section 4.2.3.2) with interval of 20 minutes were selected for adsorption of Cr and Pb by LPB (Fig 4.12c and Table 4.4). Likewise, SLPB, amount of adsorption and removal rate also enhanced with increasing adsorbent dosage until the equilibrium point. The removal rate was found to increase from 50.37 to 72.75 and 69.17 to 87.33 %, respectively with increasing dosage of 2 to 4.0 and 3 to 6.0 g L^{-1} for Cr and Pb, respectively. The maximum removal of Cr (72.75%) and Pb (87.33%) was attained with optimized dosage of 4.0 and 6.0 g L^{-1} at 160 minutes of contact time. The amounts of Cr and Pb remained in the solution after saturation point were 5.45 and 2.53 mg L^{-1}, respectively in comparison to initial metal concentration of 20 mg L^{-1}.

OPB was utilized in the 5.0 to 8.0 and 2.5 to 4.5 g L^{-1} dosage at difference of 0.5 g L^{-1}, for contact times of 10 to 180 and 200 minutes with intervals of 20 minutes were

selected for adsorption of Cr and Pb (Fig 4.12e and Table 4.4). Likewise, SLPB and LPB, increase in adsorption amount and removal rate were observed with increasing adsorbent dosage until the equilibrium point. The removal rate increased from 54.93 to 64.87 and 69.67 to 84.15 %, respectively with increasing dosage of 2 to 4.5 and 3 to 6.0 g L^{-1} for Cr and Pb, respectively. The optimum dosage of OPB for removal of Cr and Pb (87.33%) was 8.0 and 4.5 g L^{-1} at 160 and 180 minutes of contact time, respectively. Only 7.03 and 3.17 mg L^{-1} of Cr and Pb, respectively were remained in the solution after saturation point in contrast to initial metal concentration of 20 mg L^{-1}.

The ranges of adsorbent dosages of BB for removal of Cr and Pb were 7 to 10 and 3 to 5 mg L^{-1}, respectively with contact time of 10 to 180 and 160 minutes at intervals of 20 minutes (Fig 4.12g and Table 4.4). As defined for SLPB, LPB and OPB, the adsorption and removal rate were found to increase with increasing adsorbent dosage until the equilibrium. The maximum removal of Cr (59.93%) and Pb (70.42%) was attained with dosages of 10 & 5 g L^{-1} at 160 & 140 minutes, respectively. The amount of Cr and Pb remained in solution after attaining equilibrium 8.02 and 5.92 mg L^{-1}, respectively in contrast to initial metal concentration of 20 mg L^{-1}.

All of four adsorbents showed increase in the adsorption of HMs with increasing dosage. The increase in the adsorbent dosage contributed towards the enhancement of surface area and binding sites that increased the adsorption rate (Attia et al. 2010; Asgari et al. 2013; Sun et al. 2015; Guiza 2017; Temesgen et al. 2018). Thus, instantaneous and equilibrium sorption capacities of different adsorbents are functions of dosage (Ramesh et al. 2013). After attaining equilibrium, further increase in dosage do not affect removal rate at constant initial metal ion concentrations (Lasheen et al. 2012; Bhatti et al. 2016). This may be due to decrease in the quantity adsorbed per unit mass with increasing adsorbent dosage which result in split of flux or concentration gradient between solute (HMs) concentration present in solution and on the surface of the adsorbent (Vadivelan and Kumar 2005). The possible overlap of the binding sites due to aggregation of biomass at higher dosages of adsorbents may also be responsible for the same, which may render the surface area and block the binding spots along with decline in distribution path span (Boveiri Monji et al. 2008; Ahmadi et al. 2016; Manzoor et al. 2017).

The results of the present study were consistent with previous studies of Attia et al. (2010), Soliman et al. (2011), Ramesh et al. (2013), Baig et al. (2014), Ahmadi et al. (2016), Bhatti et al. (2016), Guiza (2017), Tovar et al. (2018) etc. (Table 4.4).

4.2.3.2 Contact time

It is also an important factor that affect adsorption rate of HMs with respect to different adsorbents. A variety of ranges of contact time have been tested for removal of Cr and Pb ions with initial concentration of 20 mg L^{-1} at room temperature (25±3ºC). The time interval was maintained to be 20 minutes from 20 to the maximum range of contact time of selected adsorbents except for initial 10 and 20 minutes as shown in Fig 4.12. The detailed effects of contact time on adsorption rate and initial metal concentrations of Cr and Pb for selected adsorbents have been discussed as following-

The rate of removal increased with increasing the contact time from 10 to 160 and 180 minutes by SLPB for Cr and Pb. During initial 10 minutes, rate of removal 30.32 and 17.88 %, which reached to 83.38 and 93.87 % respectively, for Cr and Pb after attaining equilibrium point (Fig 4.12b). Further increase in contact time do not affected removal process that may be due to exhaustion of active sites. Thus, the optimum contact time required by SLPB for removal of Cr and Pb was 160 and 180 minutes, respectively.

Similarly, removal rate of Cr and Pb by LPB was 17.58 and 26.6 % respectively, during initial 10 minutes. At equilibrium point 72.75 and 87.33 % of Cr and Pb were found to be adsorbed by LPB at 160 minutes of contact time (Fig 4.12d). Thus, the optimum contact time required by LPB for removal of both HMs was 160 minutes.

As described for SLPB and LPB, OPB removed 17.48 and 7.83 % of Cr and Pb during initial 10 minutes of contact time. When contact time was increased from 10 to 160 and 180 for Pb and Cr, removal rate was also increased considerably and reached to 64.87 and 84.15 % at optimum contact times. Further rise in contact time did not affect removal percentage (Fig 4.12f). Therefore, optimum contact time for removal of Cr and Pb was 180 and 160 minutes, respectively.

BB also followed the same trend of removing both HMs ions as that of SLPB, LPB and OPB. During initial 10 minutes 16.30 and 17.88 % of Cr and Pb were removed which attained the equilibrium at 180 and 140 minutes of contact time with removal rate of 59.93 and 93.87 %, respectively. Further enhancement in contact time did not contributed towards the increase in removal percentage (Fig 4.12h). Therefore, the optimum removal rate for both HMs was 180 and 140 minutes, respectively.

The rate of removal in the beginning was found to be higher for both HMs and became slower on later phases. This trend may be exemplified by the accessibility of

active vacant sites and higher electrostatic attraction between the HM ions and ligands present on the surface of adsorbents at initial level (Homagai et al. 2010; Baig et al. 2014; Uçar et al. 2015; Bhatti et al. 2016). At later stages, no. of active sites were reduced and got saturated that decreased the adsorption rate of HMs (Kannan and Karrupasamy 1998; Sliman et al. 2011; Singha and Das, 2012; Vithanage et al. 2015; Guiza, 2017, Temesgen et al. 2018). Further, rise in contact time had no effect on removal rate of HMs and after sometimes it started declining (Feng et al. 2011; Ramesh et al. 2013). This may be due to aggregation of HM ion all around the binding sites of selected biochars causing competition and hindrance in the movement of adsorbate (HMs) for left over sites which delayed the adsorption processes afterwards (Bhatti et al. 2016; Basu et al. 2017; Shehzad et al. 2018). This end up into saturated sites of adsorbents and also resistance due to repulsion of same charges i.e. Cr and Pb molecules in the adsorbents increases. This may also be the possible reason behind the decrease in the removal percentage on increasing the contact time after equilibrium points (Mittal et al. 2010). Thus, mechanism of adsorption is not only governed by physical and chemical characteristics but also on mass transfer process (Lasheen et al. 2012).

The results of the present study were in accordance with prior studies of Attia et al. (2010), Soliman et al. (2011), Ning-chuan and Xue-yi (2012), da Silva et al. (2013), Pan et al. (2013), Ramesh et al. (2013), Baig et al. (2014), Santos et al. (2015), Uçar et al. (2015), Abdelhafez and Li (2016), Ahmadi et al. (2016), Bhatti et al. (2016), Kołodyńska et al. (2017), Basu et al. (2017), Guiza (2017) etc. The details of which have been described in Table 4.4.

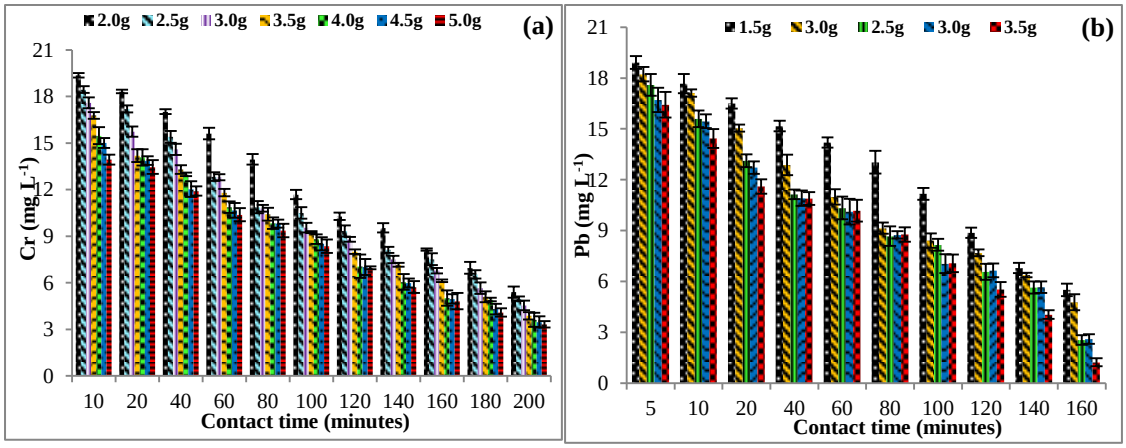

Figure 4.12.1 Effect of adsorbent dosage & contact time on adsorption of Cr (a) and Pb (b) by SLPB at room temperature (25±3ºC) and initial metal ions conc. of 20 mg L^{-1}

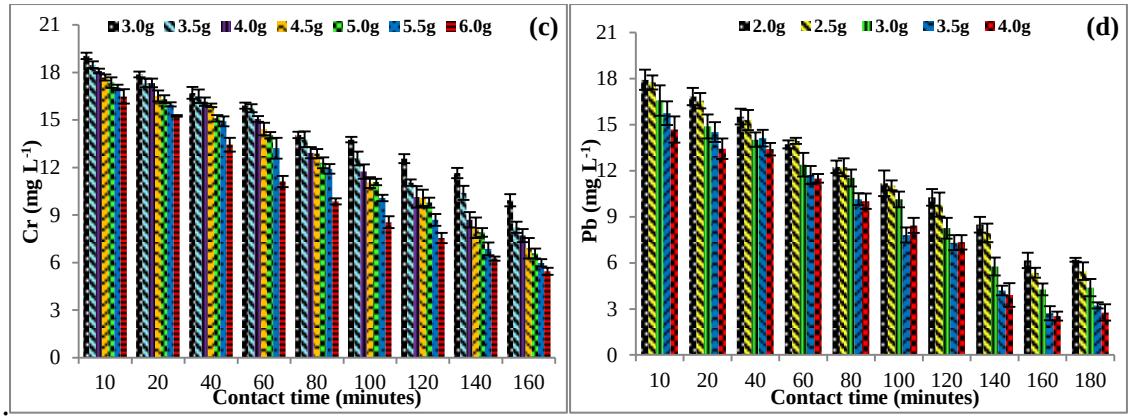

Figure 4.12.2 Effect of adsorbent dosage and contact time on adsorption of Cr (c) and Pb (d) by LPB at room temperature (25±3ºC) and initial metal ions conc. of 20 mg L^{-1}

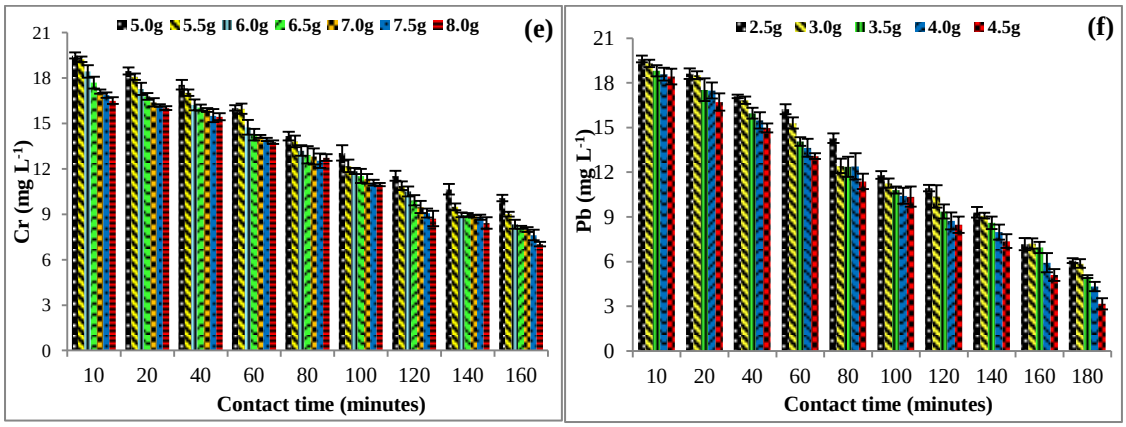

Figure 4.12.3 Effect of adsorbent dosage and contact time on adsorption of Cr (e) and Pb (f) by OPB at room temperature (25±3ºC) and initial metal ions conc. of 20 mg L^{-1}

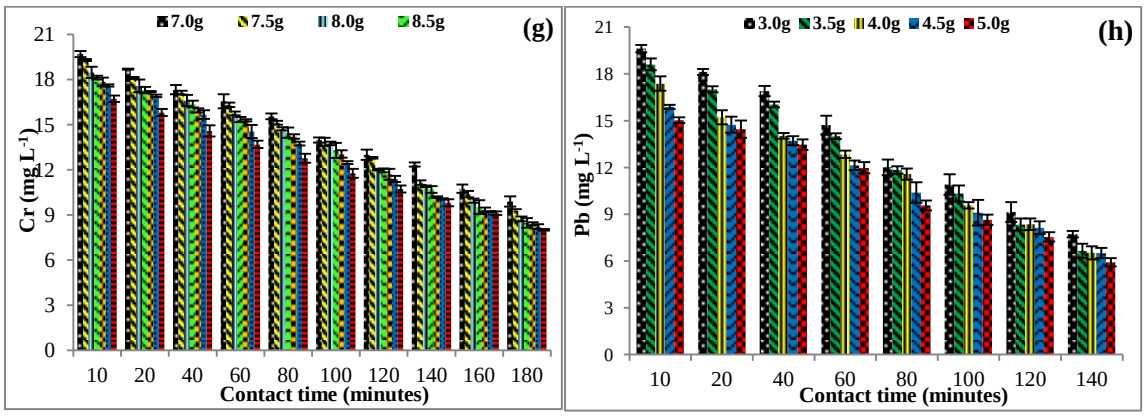

Figure 4.12.4 Effect of adsorbent dosage and contact time on adsorption of Cr (g) and Pb (h) by BB at room temperature (25±3ºC) and initial metal ions conc. of 20 mg L^{-1}, S.D. shown by bars

4.2.3.3 pH

It is a steering factor which administer the adsorption process by influencing surface charges besides controlling other factors like metal speciation, sequestration, mobility & degree of ionization of HMs and competition with co-existing ions of solutions (Nguyen et al. 2013; Ullah et al. 2013; Basu et al. 2017). Metal adsorption is reliant upon kind and ionic state of functional groups existing on surface of adsorbent and their chemistry. These phenomenon are directly connected to pH of medium (Babel and Kurniauan, 2004; Feng et al. 2011).The effect of pH on removal of Cr and Pb have been presented in Fig 4.13, respectively. As previous experiments had shown that formation of metal-hydrolyzed species [$M(OH)^{+}$] might occur with subsequent precipitation of metal-ion hydroxides [$M(OH)_{2(s)}$] pH (>7.0), so, the experiments were not evaluated further on higher pH (Liu and Liu 2003; Ning-chuan and Xue-yi, 2012; Ramesh et al. 2013; Ramos et al. 2015; Hu et al. 2018). The range of pH tested for was 1-4 for SLPB, LPB and OPB, whereas, for BB it was 1-5 for Cr and for Pb 2-6 for SLPB, LPB and OPB; and 2-5 for BB. The experiments were performed for 10, 20-200 and 10, 20-180 minutes of contact time for Cr and Pb respectively, with duration of 20 minutes for 20ppm concentration of both HMs solutions at room temperature considering optimized doses. The trend of removal of HMs by adsorption process was an increase with increasing pH until a certain level, and then decreased. The details of this pattern have been discussed below-

During initial 10 mins, SLPB removed only 7.57 % of Cr at pH 1 and 7.82 % of Pb and 2. In next 10 minutes, the rate of removal was increased to 20.28 and 23.28 %, respectively, for Cr and Pb. Therefore, further test were preceded after 20 minutes of time duration for all of the remaining three adsorbents. Further, no change in removal percentage was noticed after 200 and 180 minutes of contact time for respective metals, which may be due to the exhaustion of the adsorption sites. Moreover, the average removal rate increased from 7.57 to 93.82 % for Cr and 7.82 to 91.2 % for Pb at pH 1 and 2, respectively. As the pH of the solution was increased from 1 to 3, and 2 to 5 for Cr and Pb, the concentration of the metals in the respective solution decreased from 1.24 to 0.91 and 0.11 to 0.03 mg L^{-1} after 200 and 180 minutes of contact time, respectively. The removal rate of Cr was increased from 93.82 to 95.47 % and 91.23 to 97.42 % for Pb with increasing pH from 1 to 3 and 2 to 5. Further, increase in pH, caused the precipitation of Cr and Pb, which increased the concentration of it in the solution. At pH 4 and 6 the

concentration of Cr and Pb increased from 0.91 to 0.92 and 0.52 to 0.55 mg L^{-1} in the solution , respectively. So, further test was not carried out with increasing pH (Fig 4.13a & b). Hence, optimum pH for removal of Cr and Pb from respective solution by SLPB was 3 and 5, respectively.

As explained earlier for SLPB, range of pH for LPB was also same. The pattern of removal of Cr and Pb were also similar to that of SLPB, where removal rate increased with increasing pH from 1 to 3 and 2 to 5 for Cr and Pb, respectively. Further, due to precipitation, the concentration of both metals in their respective solutions increased. The removal rates were found to increase from 91.20 to 94.03 and 91.10 to 96.27 % after increasing pH from 1 to 3 and pH 2 to 5 for Cr and Pb, respectively. The concentrations of both HMs in particular solutions were found to decrease from 1.76 to 1.19 and 1.78 to 0.75 mg L^{-1}, respectively with increasing pH (Fig 4.13a & b). Thus, the optimum pH for removal Cr and Pb from respective solutions by LPB were 3 and 5, respectively as that of SLPB.

As described earlier for OPB, ranges of pH and contact time for OPB were same for removal of Cr and Pb from respective solutions. Increase in removal rate was observed with increase in pH, from 1 to 3 and 2 to 5 for Cr and Pb, respectively. Removal percentage increased from 88.08 to 91.98 & 90.67 to 95.08 % after 180 & 160 minutes of contact time, respectively for removal of Cr and Pb from particular solutions. The concentrations of Cr and Pb remained in solution after foresaid contact times was 1.61 and 0.983 mg L^{-1}, respectively (Fig 4.13). So, optimum pH for removal Cr and Pb from by OPB were found to be 3 and 5, respectively as that of SLPB and LPB.

The pH range was set to be 1-4 and 2-4 for observing the effect of it on removal efficiency of BB with contact time of 20-180 minutes. As explained earlier for other three adsorbents, removal percentage increased with upsurge in pH until equilibrium was achieved at pH 4 for both HMs. The removal percentages were observed to increase from 63.57 to 72.13 and 72.15 to 81.48 %, respectively for Cr and Pb after 180 minutes of equilibrium contact time. Only 5.57 and 3.70 mg L^{-1} of Cr and Pb remained in the solution after adsorption process (Fig 4.13). Thus, the optimum pH for removal Cr and Pb from respective solutions by BB was found to be 4 irrespective of other three adsorbents as explained earlier.

The surfaces of all of adsorbents were found to be acidic in nature, as observed by Boehm titration, which has been explained earlier in section 4.2.2.7. At lower pH (from 1-2) the surface as well as HMs were positively charged generating Coulombic repulsion,

so the adsorption was higher at pH above 2 but lesser overhead pH 5 (Soliman et al. 2011; Guiza, 2017; Poonam et al. 2018). As the pH of the solutions (Cr and Pb) was increased from 1 to 4 (or 5) for different adsorbents, a rise in the removal percentage was observed (Hu et al. 2018). It may be because of increase in the surface negativity of the adsorbents due to presence of more OH^- ions, which allow the deprotonation of functional groups of biochars with release of H^+ and H_3O^+ (Kołodyńska et al. 2017; Chen et al. 2018). Now, these deprotonated functional groups serve as available binding sites, generating strong electrostatic attraction with positively charged adsorbent surface, which increases the adsorption rate (Basu et al. 2017; Shehzad et al. 2018). However, repulsion between positive charged HMs and H^+ & H_3O^+ may also exist, which may be crossed over by strong electrostatic attraction among negative charged OH^- ions present in solution and up-surging surface negativity of adsorbents due to increasing pH and left greater number of ligands with negative charges after deprotonation (Das et al. 2007; Feng et al. 2011; Homagai et al. 2010). Further, as discussed earlier the adsorption of Cr and Pb was favored by acidic medium and above optimum pH (most of the time pH 4 and 5 for respective adsorbents), a sharp decrease in adsorption was observed. The reason behind this may be the increase in electrostatic interactions between adsorbent and the adsorbate, which further, depend upon availability of functional groups (Uçar et al. 2015, Van Vinh et al. 2015). Moreover, basic medium of the solution also contributed towards the dominance of OH^- ions with the negatively charged hydrated ions of Cr and Pb mainly in the form of $Cr_2O_7^{2-}$, $HCrO_4^-$, $Cr_3O_{10}^{2-}$, $Cr_4O_{13}^{2-}$, $HPbO_2^-$ etc. (Pan et al. 2013; Zhang et al. 2013; Bhatti et al. 2016; Rai et al. 2016). These species form complexes with the acidic functional groups, especially with O atoms present on the surfaces of adsorbents, which hindered the adsorption rate. $Cr(OH)_3$, $Cr(OH)_6$, $Pb(OH)_2$, $Pb(NO_3)_2$, $Pb(CH_3COO)_2$, $C_8H_{16}Cr_2O_{10}$ etc. are the main complexes formed which precipitate out in the solution, on increasing pH most of the time above 7 (Leyva-Ramos et al. 1995; Ning-chuan and Xue-yi 2012; Ramesh et al. 2013). These complexes either do not contribute towards adsorption of HMs causing no effect on adsorption rate or decreases it (Iqbal et al. 2009; Ramesh et al. 2013; Guiza 2017). At higher pH, sometimes these metal complexes used to develop positive charges onto their surfaces, which may be in the form oxides (CrO_2^+, $Cr_2O_5^+$, PbO^+), hydrides ($Cr(OH)^{2+}$, $Cr_3(OH)^{+5}$, $Cr_3(OH)_4^{5+}$, $PbOH^+$, $Pb_2(OH)_4^+$) etc. after exhaustion of adsorption sites (Manzoor et al. 2017). This causes repulsion of positive charged metals ions resulting in further decrease in the adsorption of HMs (Leyva-Ramos et al. 1995; Gupta et al. 2011; Uçar et al. 2015). Moreover, as pH

increases, dual competition among the predominating anions of Cr and Pb to be adsorbed and dominating OH^- ions in basic medium are developed (Shin 2017). In addition to this, it may also be justified by the presence of weak covalent coordination bonds formed between the HMs and surface functional groups of biochars (carboxyl, hydroxyl, alkyl etc.) in basic conditions which also decreases the adsorption rate (Attia et al. 2010). Thus, the present study followed these phenomenon as explained above with optimum removal of HMs at pH <5 but >2.

The results of the present study were found to be comparable to Feng et al. (2011); Salam et al. (2011); Soliman et al. (2011); Alfa et al. (2012); Ning-chuan and Xue-yi (2012); Bernard and Jimoh (2013); da Silva et al. (2013); Li et al (2013); Pan et al. (2013); Rezaei (2013); Velazquez-Jimenez et al. (2013); Rajoriya and Kaur (2014); Reddy et al. (2014); Fathima et al. (2015); Uçar et al. (2015); Van Vinh et al. (2015); Abdelhafez and Li (2016); Bhatti et al. (2016); Kołodyńska et al. (2017); Basu et al. (2017); Guiza et al. (2017); Upadhyay et al. (2017); Chen et al. (2018); Tovar et al. (2018); etc. for different adsorbents including biochars of the same agricultural wastes used for removal of Cr^{3+} and Cr^{6+}, Pb^{2+} and other HMs. The details of these previous studies have been tabulated in Table 4.4

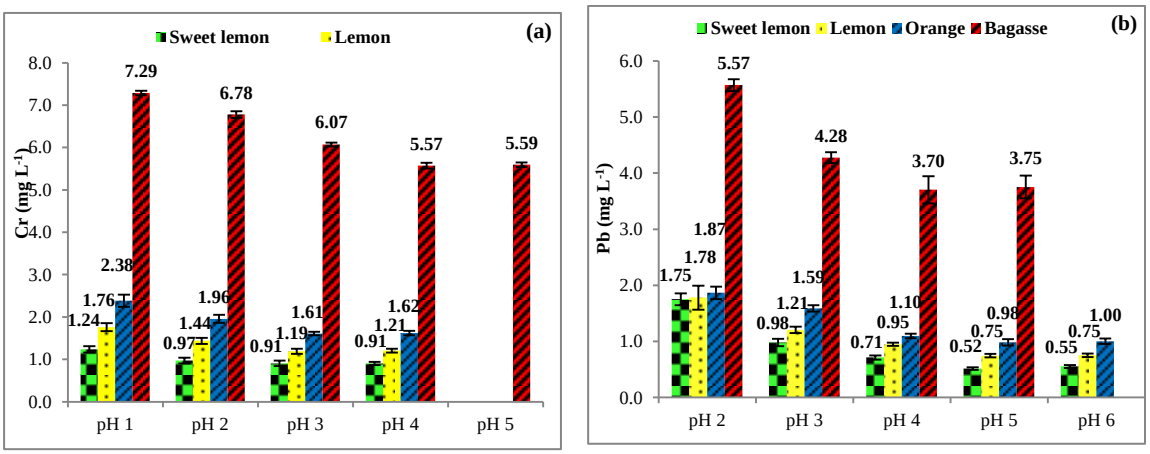

Figure 4.13 Effect of pH on adsorption of Cr (a) and Pb (b) by different adsorbents at room temperature (25±3°C) with optimized dosages and contact time for respective adsorbents and initial metal ions concentration of 20 mg L^{-1}, S.D. shown by bars

4.2.3.4 Temperature

Temperature is an important factor that affects mobility of HM ions present in solution. It interferes in chemical reactions and formation & dissociation of chemical bonds during

adsorption (Baig et al. 2014). The effects of temperature on the concentration of HMs present in the solution by all the four biochar adsorbents have been displayed in Fig 4.14. The experiments were performed for 200 and 180 minutes of contact time for Cr and Pb respectively, with duration of 20 minutes for 20 ppm concentration of both HMs solutions at different temperatures (25, 35, 45, 65 and 75ºC) considering optimized doses as discussed in section 4.2.3.1.

The range of temperature selected for SLPB was 25-65 and 75 ºC, respectively, for removal of Pb and Cr from respective solutions. The rate of removal increased from 72.67 to 84.77 and 89.70 to 94.30 % with increasing temperature from 25 to 65 and 55 ºC for Cr and Pb, respectively. After this, the removal rate decreased to 0.57 and 0.37 % after further increase of 10ºC in temperature for Cr and Pb. At saturation point, only 3.04 and 1.14 mg L^{-1} of Cr and Pb were remained in the solution, respectively in comparison to initial HM concentration of 20 mg L^{-1} (Fig 4.14 a & b). So, the optimum temperature for removal of Cr and Pb was recorded as 65 and 55 ºC, respectively.

Similar to SLPB, LPB was also utilized at 25-65 and 75 ºC, respectively, for removal of Pb and Cr from respective solutions. The rate of removal was found to increase from 65.63 to 79.20 and 84.32 to 91.15 % respectively, with increasing temperature form 25 to 65 and 55 ºC for Cr and Pb. Further increase of 10 ºC, 1.40 and 0.35 % decrease in the removal rate was observed. After maximum adsorption, only 4.16 and 1.77 mg L^{-1} of Cr and Pb remained in the solution (Fig 4.14 a & b). Thus, the maximum removal of Cr and Pb was achieved at optimum temperature of 65 and 55 ºC, respectively.

Likewise SLPB and LPB, OPB was also utilized at 25- 65 and 75 ºC, respectively, for removal of Pb and Cr from respective solutions. The rate of removal was found to increase from 63.62 to 71.85 and 77.57 to 88.98 % respectively, with increasing temperature form 25 to 65 and 55 ºC for Cr and Pb. Further increase in temperature (75 and 65 ºC) caused 0.44 and 1.27 % decrease in removal percentage of Cr and Pb, respectively. Only 5.63 and 2.20 mg L^{-1} of initial concentrations of HMs were remained in the solution after reaching the saturation point (Fig 4.14 Fig 4.14 a & b). Thus, optimum temperature for elimination of Cr and Pb was 65 and 55 º C, respectively.

The temperature range for observing its effect on removal percentage of Cr and Pb was 25-75 ºC. The removal rate was found to increase from 50.83 to 66.05 and 53.20 to 71.30 % respectively, with increasing temperature from 25 to 65 for Cr and Pb. This

was recorded as the maximum removal as further increase in the temperature caused decrease of 0.635 and 0.785 %, respectively, in removal rates of HMs from that of at 65ºC (Fig 4.14 Fig 4.14 a & b). Thus, optimum temperature for removal of Cr and Pb was 65 ºC for both HMs.

All four adsorbents showed rise in adsorption percentage with increase in temperature till 65 and 55 ºC for all of adsorbent for Cr and Pb, respectively, except at 65ºC for BB. The increase in temperature intensified the metal binding tendency and mobility of HM ions tending to be adsorbed, resulting upsurge in removal percentage of HMs (Baig et al. 2014; Fathima et al. 2015). It may also be due to decrease in the boundary layer thickness surroundings adsorbents which in turn decreased mass transfer resistance of adsorbate in boundary layer (Banerjee et al. 2012). This trend proposed that adsorption of both HMs was endothermic and chemisorption was involved in comparison to physisorption (Leyva-Ramos et al. 1995; Mohan et al. 2011; Hu et al. 2018). According to An et al. (2018), synergistic effects of physisorption and chemisorption may cause further decrease in the removal percentage where heat was supposed to be release and utilize, respectfully. These endothermic processes may be controlled by intra particle and pore diffusion as suggested by Wu et al. (2013) and Baig et al. (2014a). The temperature higher than room temperature, boosts adsorption of HMs may also be explained on the basis of enhanced surface activity and kinetic energy of the solute (HMs), nevertheless, physical damage to the adsorbents might reduce adsorption process at much more higher temperatures (Bhatti et al. 2016). Further, lower temperatures also did not favor adsorption processes due to requirement of heat to accelerate the reaction rates (Abdelhafez and Li 2016). The results of the present study was found to be consistent with Liang et al. (2009), Banerjee et al. (2012), Rezaei (2013), Fathima et al. (2015), Abdelhafez and Li (2016); Hu et al. (2018) etc. for different adsorbents including biochars of same agricultural wastes used for Cr^{+3} and Cr^{+6}, Pb^{+2} and other HMs. Details of these previous studies have been presented in Table 4.4.

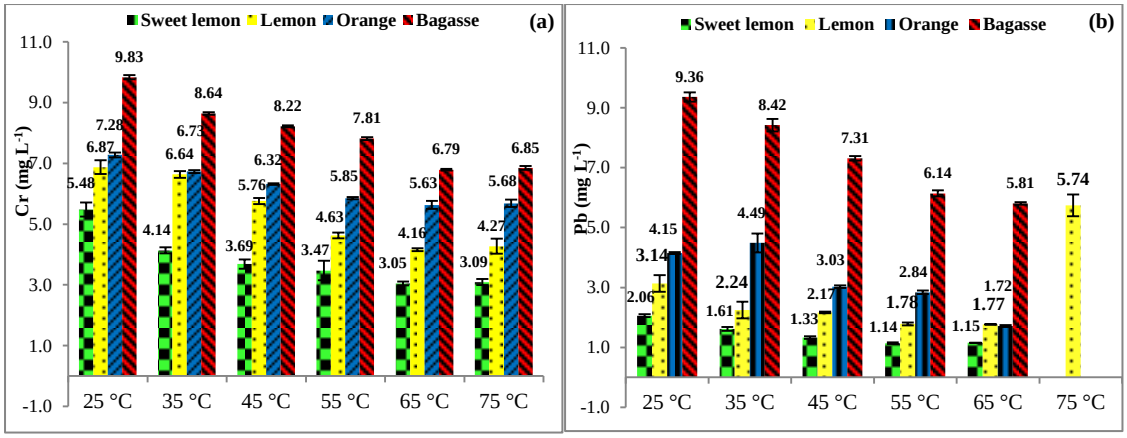

Figure 4.14 Effect of temperature on adsorption of Cr (a) and Pb (b) by different adsorbents with optimized dosages and contact time for respective adsorbents and initial metal ions concentration of 20 mg L^{-1}, S.D. shown by bars

4.2.2.5 Initial metal concentrations

Initial metal concentration is important in describing the capacity of particular adsorbent for extracting different concentrations of HMs onto their surfaces. In addition to this, different industries dispose of different concentrations of HMs into the nearby water bodies (Ahmadi et al. 2016). Therefore, it is pertinent to find out capacity of adsorbent based on different metal ion concentrations so that adsorbents may be utilized practically at industrial levels. Moreover, initial metal ion concentration enforces transport of HMs from solution to surface of adsorbent (Taha et al. 2011). In order to observe effect of initial metal ion concentrations on adsorptive removal of Cr and Pb, different initial metal concentrations (5, 10, 20, 40 mg L^{-1}) were studied with optimized dosages and contact time of respective adsorbent at room temperature (25±3ºC) and shown in Fig 4.15.

SLBP adsorbed about 4.70, 8.53, 15.15 and 29.76 mg L^{-1} of Cr and 4.92, 9.15, 16.19 and 31.32 mg L^{-1} of Pb from initial metal ion concentrations of 5, 10, 20 and 40 mg L^{-1}, respectively. Thus, removal percentage was 94.06, 85.27, 75.74, 74.39 and 95.80, 89.70, 76.05 and 76.875 % for Cr and Pb w.r.t. initial metal ion concentrations. The remaining amount of Cr and Pb for the same initial metal ion concentrations were 0.30, 1.47, 4.85, 10.24 and 0.08, 0.85, 3.81, 8.68 mg L^{-1}, respectively (Fig 4.15 a & b). Thus, results suggested that although the amount of HMs adsorbed onto SLPB was increased with increasing initial metal ion concentration but removal percentage was found to decrease for most of the times with respect to both HMs. The reason behind this

phenomenon might lie in the fact that at lower concentrations more vacant sites were available, which became filled with respective metal ions causing aggregation and repulsion among the charged ions resulting in the decrease in removal rate (Sun et al. 2015; Ahmadi et al. 2016). Hence, based on amount of HM ions adsorbed, the optimum initial metal ion concentration was 40 mg L^{-1} and if the maximum removal rate would be considered then it will be 5 mg L^{-1} for both HMs.

Following the same pattern of SLPB, amount of Cr and Pb adsorbed by LPB were 4.36, 8.11, 13.12, 27.75 and 4.79, 8.97, 15.21, 30.75 mg L^{-1}, respectively for same of the initial metal ion concentrations. The removal rate was decreased mostly with increasing the initial metal ion concentrations as 87.26, 81.07, 65.62, 69.38 and 95.80, 89.70, 76.05, 76.88 %, respectively for Cr and Pb. The remaining concentrations of both the HMs were 0.64, 1.89, 6.88, 12.25 and 0.21, 1.03, 4.79, 9.25 mg L^{-1}, respectively (Fig 4.15 a & b). The same reasons and optimum initial metal ion concentrations as described for SLPB might also be considered for LPB also.

Likewise, SLPB and LPB, the amount of Cr and Pb adsorbed by OPB was 4.08, 7.91, 12.43, 26.71 and 4.41, 8.52, 13.33, 29.61, respectively for same initial metal ion concentrations. The removal rate decreased for most of the times with respect to increasing initial metal ion concentrations for both the HMs and reached to equilibrium point with removal of 81.34, 79.07, 62.17, 66.78 and 88.20, 85.20, 66.65, 74.03 %. The residual amount of both HMs in the solution was 0.93, 2.09, 7.57, 13.29 and 0.59, 1.48, 6.67, 10.39 mg L^{-1}, respectively (Fig 4.15a & b).

The similar pattern of SLPB, LPB and OPB for adsorbed amount and removal percentage for afore said initial metal ion concentrations were established for BB for Cr and Pb. The amount of Cr and Pb adsorbed were 3.73, 5.66, 9.82, 22.52 and 3.87, 6.66, 11.52, 26.30 mg L^{-1} for the similar initial metal ion concentrations. The removal rate was recorded as 74.66, 56.63, 49.09, 56.30 and 77.46, 66.60, 57.62, 65.74 %, respectively for Cr and Pb. The left over amount of the HMs in the solution were 3.73, 5.66, 9.81, 22.52 and 3.87, 6.66, 11.52 and 26.30 mg L^{-1}, respectively (Fig 4.15a & b). The same explanations for the removal pattern and optimum initial metal ion concentrations might also be given for BB as explicated for SLPB and LPB.

The uptake of the HMs increased consistently with escalating concentrations (5 to 40 mg L^{-1}) due to involvement of energetically favorable sites with increasing metal concentration in the aqueous solution (Lasheen et al. 2012), but removal percentage decreased more significantly with further increase in initial metal ion concentrations for

both selected HMs. At lower concentrations, the surface of the adsorbents used to be saturated with the HM ions enhancing removal rate. However, decrease in the rate of removal may be explicated by fact that at higher concentrations formation of more functional groups on the surfaces of adsorbents occurred. However, at the constant adsorbent dosages, the active sites to accommodate HMs were also constant which resulted in decreased removal efficiency (Han et al. 2013; Basu et al. 2017). As elucidated by Nadeem et al. (2016) and Zhao et al. (2017) the steering force for overcoming mass transfer resistance could be served by concentration gradient resisting the mass transfer at elevated concentrations, which may enhance the amount of adsorbed HM ions. Further, increasing initial metal ion concentrations also developed higher competition among the HM ions for limited available active binding sites, which also distressed the removal efficiencies of different adsorbents (Soliman et al. 2011; Sun et al. 2015; Lima et al. 2016). Moreover, the main objective of the study was to get maximum removal rate for both HMs, but removal percentage was reduced with increasing initial metal ion concentrations for the optimized dosage. Therefore, experiments with further higher concentrations were not considered and optimized initial metal ion concentrations for both HMs were reported as 40 mg L^{-1}.

The present study was also supported by earlier studies of Soliman et al. (2011), Ning-chuan and Xue-yi (2012), da Silva et al. (2013), Baig et al. (2014), Uçar et al. (2015), Abdelhafez & Li (2016), Kołodyńska et al. (2017); Bhatti et al. (2016), Baus et al. (2017), Guiza (2017). The details of these studies have been given in the Table 4.4.

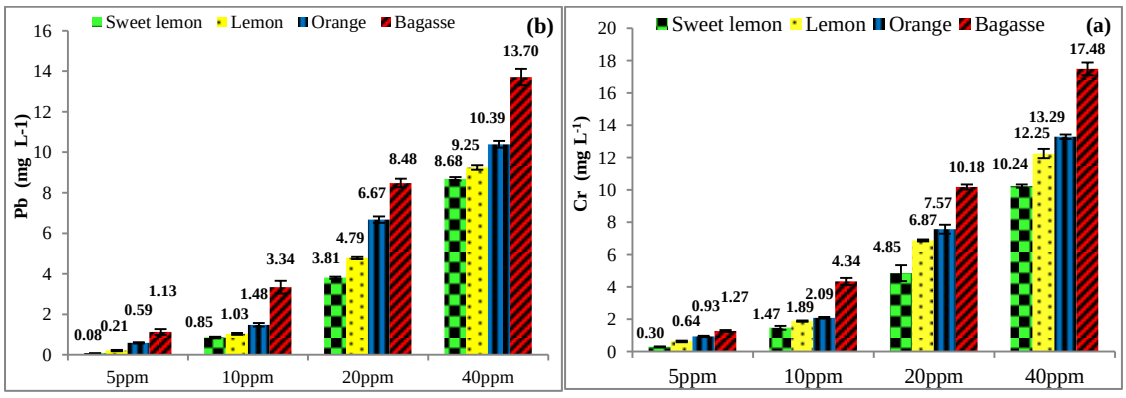

Figure 4.15 Effect of initial concentration on the adsorption of Cr and Pb ions onto by different adsorbents with optimized dose and contact time for respective adsorbents at room temperature (25±3ºC), S.D. shown by bar

Table 4.4 Optimized conditions for removal of heavy metals by different naturally occurring bio-sorbents

S.n.	Metals	Adsorbents	Mode	Parameters	Results(Optimized conditions)	References
1	**Pb^{2+}**	Orange peel xanthate	Batch	1. pH; 2. Contact time; 3. Temperature; 4. Initial metal ion concentration	1. 5; 2. 20 minutes; 3. 30ºC; 4. 100 mg L^{-1}	Liang et al. (2009)
2	**Pb^{2+}, Cd^{2+} & Ni^{2+}**	Orange peel	Batch	1. pH (2 to 5.5); 2. Contact time	1. 5.5; 2. 180 minutes	Feng et al. (2011)
3	**Pb^{2+}**	Sugarcane bagasse	Batch	1. pH (1.0–4.0); 2. Contact time; 3. Dose (25, 50, 75, 100, 125 and 150 mg); 4. Initial metal ion concentration (10–100 µmol)	1. 6; 2. 60 minutes; 3. 100 mg; 4. 100 µL	Soliman et al. (2011)
4	**Cu^{2+} & Zn^{2+}**	Peanut husk charcoal, fly ash and natural zeolite	Electroplating industry & Batch	1. Adsorbent dose; 2. Contact time; 3. pH (4-11); 4. Initial metal ion concentration	1. 5 g L^{-1}; 2. 2hrs and 3hrs respectively; 3. Cu-6, Zn-7 by Peanut husk, Cu-8, Zn-8 by Fly ash, Cu-6, Zn-6 by Natural zeolite; 4. 10 mg L^{-1}	Salam et al. (2011)
5	**Cu^{2+} & Pb^{2+}**	Frond & leaf samples of dump palm	Batch	1. Contact time	1. 90 min	Alfa et al. (2012)
6	**Cd^{2+}, Cu^{2+} & Pb^{2+}**	Orange peel	Batch	1. Adsorbent dose (0.1-1 g L^{-1}); 2. Contact time (5-120 min); 3. Initial metal ion concentration	1. 1 g L^{-1}; 2. 30 min; 3. 20 mg L^{-1}	Lasheen et al. (2012)
7	**Cu^{2+}, Zn^{2+} & Pb^{2+}**	Orange peel	Batch	1. pH (2.5 to 6.0); 2. Contact time; 3. Initial metal ion concentration	1. 5.5 2. 120 minutes, 3. 50 mg L^{-1} (Cu^{2+}& Zn^{2+}) and 200 mg L^{-1} (Pb^{2+})	Ning-chuan and Xue-yi (2012)
8	**Cu^{2+}**	Water melon shells	Batch	1. Adsorbent dose; 2. Contact time; 3. Initial metal ion concentration; 4. Particle size; 5. pH(2-10); 6. Temperature (30, 40 & 50° C)	1. 0.02g L^{-1}; 2. 120 min; 3. 20 ppm 4.150µm & 300 µm; 5. 8; 6. 50 ºC	Banerjee et al. (2012)
9	**Cu^{2+}**	Garden grass	Batch	1. pH; 2. Adsorbent dosage; 3. Initial metal ion concentration; 4. Contact time; 5. Temperature	1. 6; 2. 5 g L^{-1}; 3. 10-100 mg L^{-1}; 4. 400 min (6 hrs); 5. 293–343 °K	Hossain et al. (2012)
10	**Pb^{2+}, Fe^{2+}, Cu^{2+} & Zn^{2+}**	Activated orange peel (Activation by	Electroplating Industry	1. Contact time; 2. Adsorbent dosage; 3. pH	1. 60 min for all except Fe (40min); 2. 1 g/50 ml of effluent; 3. 6 except	Bernard and Jimoh (2013)

S.n.	Metals	Adsorbents	Mode	Parameters	Results(Optimized conditions)	References
		1.0M $ZnCl_2$)			Pb^{2+} (2)	
11	**Co^{2+} & Cr^{3+}**	Sugarcane bagasse	Batch	1. pH (2.4 to 7.1); 2. Contact time; 3. Initial metal conc. 4. Temperature	1. 6.5 and 5.8; 2. 30 minutes; 3. 190 and 180 mg L^{-1} 4. 25 °C.	da Silva et al. (2013)
12	**Ni^{2+} & Co^{2+}**	Biochar of pyrolysis of almond shell	Batch	1. pH; 2. Adsorbent dosage; 3. Contact time	1. 7; 2. Ni- 7 g L^{-1}, Co- 4 g L^{-1}; 3. 15 min for both metals	Kılıç et al. (2013)
13	**Cu^{2+}** and **Cr^{3+}**	Root powder of *Eicchornia crassipes*	Batch	1. pH	1. 5 and 6	Li et al (2013)
14	**Cr^{3+}**	Crop straw derived biochars	Batch	1. pH (2.5 to 5.0); 2. Contact time;	1. 5; 2. 120 minutes;	Pan et al. (2013)
15	**Cd^{2+}, Pb^{2+} & Zn^{2+}**	*Agave salmiana* bagasse	Batch	1. pH; 2. Temperature; 3. Initial conc.	1. 5; 2. 25 ºC; 3. 80 mg L^{-1}	Velazquez-Jimenez et al. (2013)
16	**Cr^{6+}**	*Spirulina* sp.	Batch	1. Contact time; 2. Initial metal conc. and pH; 3.Initial metal conc.; 4. Temperature	1. 120 min; 2. 10 mg L^{-1} and 5; 3. 50 mg L^{-1}; 4. 25 °C	Rezaei (2013)
17	**Ni^{2+}, Cu^{2+}, Zn^{2+}**	Tea waste	Batch	1. Contact time; 2. pH; 3. Adsorbent dosage 4. Initial metal ion concentration	1. 120 min; 2. pH 5; 3. 0.4g /100ml, for Ni, 0.6 g /100ml, for Zn and Cu; 4. 10 ppm.	Thakur and Parmar (2013)
18	**Zn^{2+}**	Lemon and banana peel	Batch	1. Adsorbent dosage; 2. Contact time; 3. pH, 4; Temperature	1. 1g/100ml; 2. 260 minutes; 3. 4; 4. 30^0C	Rajoriya and Kaur (2014)
19	**Cr^{3+}**	Water melon rind	Batch	1. pH; 2. Contact time; 3. Adsorbent dosage; 4. Initial metal ion conc.	1. 3; 2. 30 minutes; 4. 0.5 mg L^{-1}; 5. 50 mg L^{-1}	Reddy et al. (2014)
20	**Cr^{3+}**	Fungal biomass (*Termitomyces clypeatus*)	Batch	1. pH; 2. Temperature (30-70 ºC); 3. Adsorbent dosage.	1. 4; 2. 60 ºC; 3. 5 g L^{-1}	Fathima et al. (2015)
21	**Co^{2+}, Cu^{2+}, & Ni^{2+}**	Sugarcane bagasse	Batch	1. pH (2.0 to 5.75); 2. Adsorbent dose; 3. Contact time; 4. Initial metal ion concentration	1. 5.75 for Co^{2+} and Ni^{2+}, and 5.5 for Cu^{2+}; 2. 0.2 g L^{-1}; 3. 180, 250, and 75 minutes; 4. 25 ° 5. 0.79	Ramos et al. (2015)

S.n.	Metals	Adsorbents	Mode	Parameters	Results(Optimized conditions)	References
					mmol L^{-1}	
22	**Pb^{2+} & Ni^{2+}**	Rapeseed oil cake (activated C)	Batch	1. pH (1-5 and 1-6); 2. Contact time; 3. Initial metal concentration (50-500 ppm)	1. 5 and 6; 2. 360 minutes for both; 3. 250 and 300 ppm	Uçar et al. (2015)
23	**As^{3+}**	Pine cone biochar	Batch	1. pH (2-4)	1. 2	Van Vinh et al. (2015)
24	**Pb^{2+}**	Sugarcane bagasse and orange peel biochar	Batch	1. pH (2-6); 2. Contact time (5 to 360 minutes); 3. Initial concentration (5.64 to 223.34 mg L^{-1}); 4. Temperature (15-45 ºC); 5. Adsorbent dose	1. 5; 2. 30 and 15 minutes; 3. 57 mg L^{-1}; 4. 25º C; 5. 1 g L^{-1}	Abdelhafez and Li (2016)
25	**Zr^{4+}**	Citrus peel	Batch	1. pH (2.0 to 5.0); 2.Adsorbent dosage; 3. Contact time; 4. Temperature; 5. Initial metal conc.	1. 3.5, 2. 0.05 g, 3. 40 minutes, 4. 30°C; 5. 90 mg L^{-1}	Bhatti et al. (2016)
26	**Cu^{2+}, Zn^{2+}, Cd^{2+}, Co^{2+} & Pb^{2+}**	Artificial biochar	Batch	1. pH (2.5 to 5.0); 2. Contact time; 3. Initial metal ion conc.	1. 5, 2. 360, 3. 200 mg L^{-1}	Kołodyńska et al. (2017)
27	**Cd^{2+}**	Husk of lentil	Batch	1. pH; 2. Temperature	1. 5; 2. No significant effect	Basu et al. (2016)
28	**Pb^{2+}**	Cucumber peel	Batch	1. pH; 2. Contact time	1. 5; 2. 60 minutes	Basu et al. (2017)
29	**Cu^{2+}**	Orange peel	Batch	1. pH, 2. Temperature; 3. Contact time; 4. Initial metal ion concentration	1. 5; 2. 20 ºC; 3. 60 minutes; 4. Increased adsorption	Guiza (2017)
30	**Hg^{2+}**	Biomass of *Bacillus licheniformis*	Batch	1. Metal concentration; 2. Adsorbent dosage; 3. pH; 4. Contact time	1. 5-1000 µg ml^{-1}; 2. 25 mg; 3. 7; 4. 1 hr	Upadhyay et al. (2017)
31	**Cd^{2+}**	Litchi peel, orange peel, pomegranate peel and banana peel	Batch	1. pH (1 to 7); 2. Initial concentration; 3. Adsorbent dose 4. contact time; 5. Temperature	1. 5; 2. 300 mg L^{-1}; 3. 0.1 g 4. 10 hrs; 5. 25 °C	Chen et al. (2018)
32	**Ni^{2+}**	Na_2S-modified biochar	Batch	1. pH (1.8-7.0); 2. Temperature (10-50ºC);	1. 6; 2. 50 ºC	Hu et al (2018)
33	**Cr**	Sweet lemon peel	Tannery wastewater	1. Adsorbent dose; 2. Contact time	1. 5.0 g L^{-1}; 2. 200 minutes	Poonam and Kumar (2018)

S.n.	Metals	Adsorbents	Mode	Parameters	Results(Optimized conditions)	References
34	**Pb**	Sugarcane bagasse	Flashlight wastewater	1. Adsorbent dose; 2. Contact time; 3. pH (2-5)	1. 5 g L^{-1}; 2. 140 minutes; 3. 5	Poonam et al. (2018)
35	**Pb**	Lemon peel	Batch	1. pH; 2. Adsorbent dose	1. 6; 2. 0.5 g	Tovar et al. (2018)
36	**Cr**	Sweet lemon peel biochar	**Batch**	1. Adsorbent dosage (2-5 g L^{-1}); 2. Contact time (10-220 minutes); 3. pH (1-4); 4. Temperature (25-75 ºC); 5. Initial metal ion concentration (5-40 mg L^{-1})	1. 5 g L^{-1}; 2. 200 minutes; 3. 3; 4. 65 ºC; 5. 40	**Present study**
37	**Pb**	Sweet lemon peel biochar		1. Adsorbent dosage (2- 3.5 g L^{-1}); 2. Contact time (10-180 minutes); 3. pH (2-6); 4. Temperature (25-65 ºC); 5. Initial metal ion concentration (5-40 mg L^{-1})	1. 3.5 g L^{-1}; 2. 160 minutes; 3. 5; 4. 55 ºC; 5. 40	
38	**Cr**	Lemon peel biochar		1. Adsorbent dosage (2-4 g L^{-1}); 2. Contact time (10-180 minutes); 3. pH (1-4); 4. Temperature (25-75 ºC); 5. Initial metal ion concentration (5-40 mg L^{-1})	1. 4 g L^{-1}; 2. 160 minutes; 3. 3; 4. 65 ºC; 5. 40	
39	**Pb**	Lemon peel biochar		1. Adsorbent dosage (3-6 g L^{-1}); 2. Contact time (10-220 minutes); 3. pH (2-6); 4. Temperature (25-65 ºC); 5. Initial metal ion concentration (5-40 mg L^{-1})	1. 6 g L^{-1}; 2. 200 minutes; 3. 5; 4. 55 ºC; 5. 40	
40	**Cr**	Orange peel biochar		1. Adsorbent dosage (5-8 g L^{-1}); 2. Contact time (10-180 minutes); 3. pH (1-4); 4. Temperature (25-75 ºC); 5. Initial metal ion concentration (5-40 mg L^{-1})	1. 8 g L^{-1}; 2. 160 minutes; 3. 3; 4. 65 ºC; 5. 40	
41	**Pb**	Orange peel biochar		1. Adsorbent dosage (2.5-4.5 g L^{-1}); 2. Contact time (10-200 minutes); 3. pH (2-6); 4. Temperature (25-65 ºC); 5. Initial metal ion concentration (5-40 mg L^{-1})	1. 4.5 g L^{-1}; 2. 180 minutes; 3. 5; 4. 55 ºC; 5. 40	
42	**Cr**	Bagasse biochar		1. Adsorbent dosage (7-10 g L^{-1}); 2. Contact time (10-180 minutes); 3. pH (1-5); 4. Temperature (25-75 ºC); 5. Initial metal ion concentration (5-40 mg L^{-1})	1. 10 g L^{-1}; 2. 160 minutes; 3. 4; 4. 65 ºC; 5. 40	
43	**Pb**	Bagasse biochar		1. Adsorbent dosage (3-5 g L^{-1}); 2. Contact time (10-160 minutes); 3. pH (2-5); 4. Temperature (25-75 ºC); 5. Initial metal ion concentration (5-40 mg L^{-1})	1. 5 g L^{-1}; 2. 140 minutes; 3. 4; 4. 65 ºC; 5. 40	

4.3. Optimization of control techniques for removal of heavy metals from industrial wastewaters using agricultural wastes/by-products.

In the present section, optimization process for removal of HMs by the selected adsorbents from industrial wastewater (tannery and flashlight) has been described. Further, the best suited adsorption isotherms (Langmuir and Freundlich), kinetics (pseudo first and second order) and thermodynamic parameters were discussed for adsorptive removal of HMs from industrial wastewaters. In addition the maximum adsorption capacity and removal efficiency with desorption ability of all the four adsorbents were also discussed. The detailed accounts of the process has been given below-

4.3.1. Optimized conditions for removal of heavy metals (Cr and Pb)

Details of the optimized conditions for maximum removal of both HMs have been summarized in Table 4.5

Comparative study of the all four adsorbents suggested that SLPB was the best for removal of Cr and Pb. The optimized dose and contact time was found to be in range of 5.0 to 10 g and 160 to 180 minutes for Cr and 3.5 to 5.0 g and 140 to 180 minutes for Pb, respectively. The maximum removal efficiencies followed the trends of BB<OBB<LPB<SLPB for dosage and contact time, pH, temperature and initial metal concentrations. pH was found to be the most important factor impelling removal of both HMs from wastewaters. The maximum removal of Cr and Pb was found to be 95.47 and 97.42 %, respectively at pH 3 and 5 by SLPB, respectively. pH and temperature affect the surface charges and mobility of ions which are important aspects of adsorption (Baig et al. 2014; Guiza 2017). Further, alteration in adsorbent dosage and contact time also affected adsorption but their removal percentage was a bit low. Further, effect of initial metal concentration on the removal efficiencies of all four adsorbents was lowest. The reason may be dependence of this factor onto the adsorbent dosage and contact time (Basu et al. 2017). Findings related that, the most important parameter that affected the removal process was pH and the best-suited adsorbent was SLPB.

Table 4.5 Optimized conditions of different parameters for removal of Cr and Pb by selected adsorbents

S.n.	Adsorbent	Heavy metal	Dose (g L^{-1}) and Contact time (minutes)		pH		Temperature (°C)		Initial metal ion conc. (mg L^{-1})	
			Value	Removal (%)	Value	Removal (%)	Value	Removal (%)	Value	Removal (%)
1	SLPB	Cr	5.0 & 200	83.38	3	95.47	65	84.77	40	74.39
2	SLPB	Pb	3.5 & 160	93.87	5	97.42	55	94.30	40	78.30
3	LPB	Cr	6.0 & 160	72.75	3	94.03	65	79.20	40	69.38
4	LPB	Pb	4.0 & 160	87.33	5	96.27	55	91.15	40	76.88
5	OPB	Cr	8.0 & 160	64.87	3	91.97	65	71.85	40	66.78
6	OPB	Pb	4.5 & 180	84.15	5	95.08	55	88.98	40	74.03
7	BB	Cr	10.0 & 180	59.93	4	72.13	65	66.05	40	56.30
8	BB	Pb	5.0 & 140	70.42	4	81.23	65	71.30	40	65.74

4.3.2. Optimization of control technique for improving physicochemical properties of industrial wastewaters

The best-optimized conditions as described in Table 4.5 were used to improve the physicochemical properties and to remove the HMs present in wastewaters of tannery and flashlight manufacturing industries. The main characteristics that affect the quality of the wastewater are of BOD, COD, EC and pH. Therefore, the selected adsorbents were applied in its best-optimized conditions to enhance the quality of industrial wastewaters before its possible discharge into the near-by water bodies. The details of all of the optimized control techniques have been given below-

4.3.2.1. Effect of optimized adsorbent dosage and contact time on BOD of industrial wastewaters

The optimized adsorbent dosage and contact time used for all four adsorbents for improving the quality of tannery and flashlight industrial wastewaters. The concentration of BOD has been found to reduce for both wastewaters on treating it

with all of the four adsorbents (Fig 4.16a & b). The initial concentration of BOD was found to be 3742.80 and 2968.02 mg L^{-1} for tannery and flashlight wastewaters, respectively. On treating these with SLPB, LPB, OPB and BB, the concentration of BOD was reduced to 1727.23, 2189.59, 2346.28, 2682.01 and 1966.77, 2080.38, 2230.42 and 2315.08 mg L^{-1}, respectively, at room temperature (25±3ºC). The removal percentages of BOD for tannery wastewater for SLPB, LPB, OPB and BB were increased from 12.12, 12.12, 11.13 and 10.39 % to 53.85, 41.50, 37.31 and 28.34 % respectively, until the optimum dosage and contact time. In the same manner, for flashlight wastewater the BOD removal percentage was also increased from 18.23, 16.71, 12.05 and 11.29 to 33.74, 29.91, 24.85 and 22.00 %, respectively. The trend of improvement in BOD of both wastewaters was observed as BB<OPB<LPB<SLPB. The main reason behind this may be the surface area of the adsorbents as, the maximum removal of BOD was reported with the SLPB possessed maximum surface areas, followed by LPB, OPB and BB. Thus, the best adsorbent for improving the BOD of wastewaters was SLPB.

Lowering of organic masses present in the wastewaters might cause drop in the concentration of BOD. The organic mass might adhere to the adsorbents, which were filtered out from wastewater lowering the organic masses as well as the BOD of the wastewater (Tahir and Naseem 2007). The study of Ayoub et al. (2011) supported the present study for reduction in BOD concentration of tannery wastewater after post treatment of wastewater by lime/bittern coagulation and activated carbon adsorption.

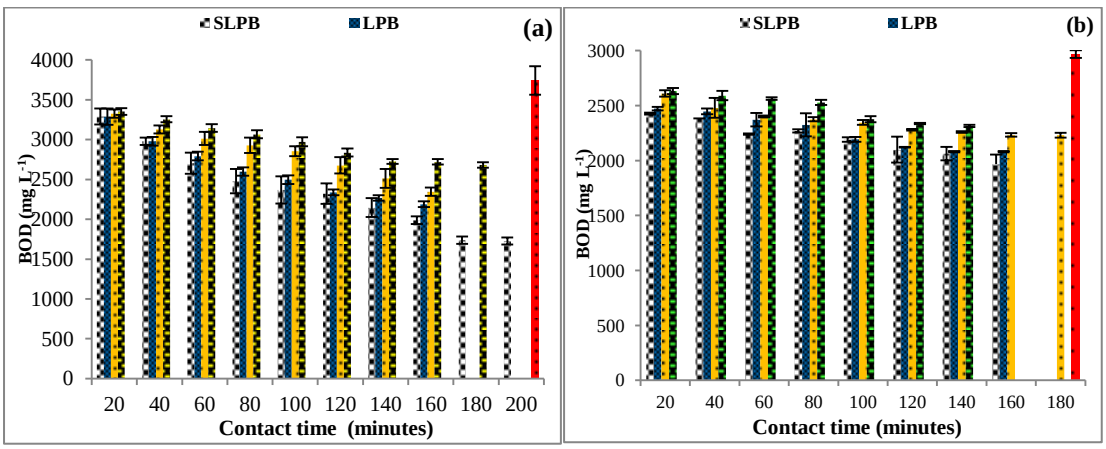

Figure 4.16 Effect of different adsorbents on BOD of tannery (a) and flashlight (b) wastewaters at optimized dosages, contact time and room temperature (25±3ºC), ±S.D.

4.3.2.2. Effect of optimized adsorbent dosage and contact time on COD of industrial wastewater

Optimized dosage and contact time were applied to bring the reduction in COD of both wastewaters. The reduction in COD was observed with increasing dosage and contact time until the saturation point (Fig 4.17 a & b). The initial COD of tannery and flashlight wastewaters was observed as 23780.0 and 12000.5 mg L^{-1}, respectively. At the saturation point of all of SLPB, LPB, OPB and BB, COD was reduced to 7666.67, 8200.0, 16726.67, and 22706.67 mg L^{-1}, respectively for tannery wastewater and 6883.33, 9917.83, 9667.33 and 10338.83 mg L^{-1}, respectively for flashlight wastewater. The application of SLPB, LPB, OPB and BB reduced COD concentration of tannery wastewater from 22.75, 24.31, 5.94 and 3.59 % to 67.76, 65.52, 29.66 and 4.51 % by respectively, until optimum dosage and contact time. Likewise, the COD of flashlight wastewater was reduced from 29.63, 10.97, 6.02 and 6.15 to 42.64, 17.35, 19.44 and 13.85 % respectively, by the application of SLPB, LPB, OPB and BB. Similar to BOD, the trend of reduction in COD of wastewaters caused by various biosorbents followed the pattern BB<OPB<LPB<SLPB.

Improvement in water quality due to the adsorption process was quite apparent which may be due to the reduction of organic matter form the wastewaters as that of BOD (Tahir and Naseem 2007). The results of present study was supported by Ayoub et al. (2011) who reported reduction in the COD of tannery wastewater after post treatment of the wastewater by lime/bittern coagulation and activated carbon adsorption process.

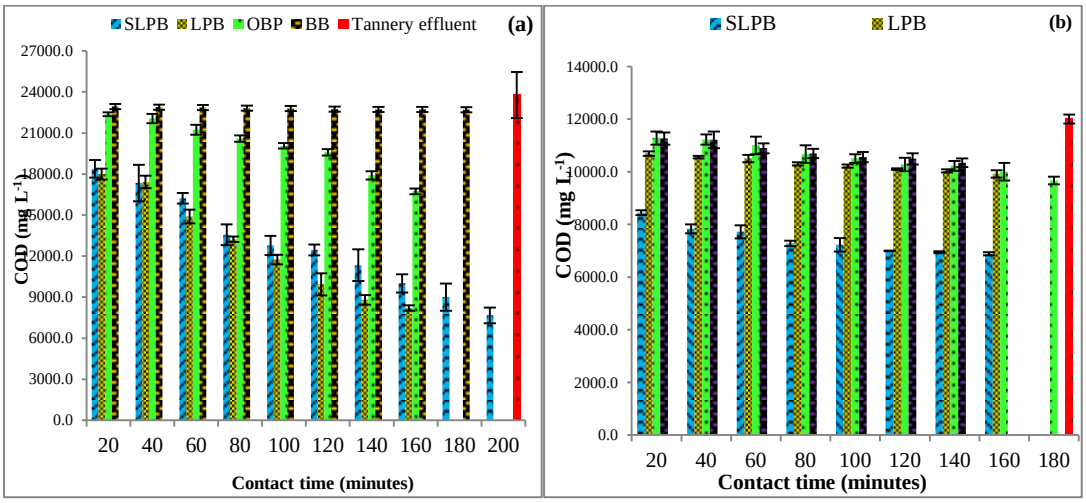

Figure 4.17 Effect of different adsorbents on COD of tannery (a) and flashlight (b) wastewaters at optimized dosages, contact time and room temperature (25±3ºC), ±S.D.

4.3.2.3. Effect of optimized adsorbent dosage and contact time on pH of industrial wastewaters

Optimized dosage and contact time for all of the four adsorbents, also affected pH of the wastewater generated from tannery and flashlight manufacturing units. However, the influence on the pH was very low as compared to BOD and COD. The pH of tannery and flashlight wastewaters were 8.67 and 4.70, which was reduced by 6.15, 6.15, 2.69, 5.0 and 13.53, 13.53, 3.53 and 11.76 %, respectively by treatments of SLPB, LPB, OPB and BB. After attaining the saturation points, the pH of tannery and flashlight wastewaters treated by four adsorbents was found to be 8.133, 8.133, 8.433, 8.233 and 4.07, 4.07, 4.07, 4.15, respectively (Fig 4.15 a & b).

The reduction in pH of both wastewaters might be caused by the effect of adsorbent's pH as the surface of SLPB, LPB, OPB and BB were enriched with surface acidic groups (Fig 4.6) as explained in section 4.2.2.7. These acidic groups might release H^+ ions in the wastewaters after addition of the adsorbents, which might be the possible reason for reduction in the pH of both industrial wastewaters.

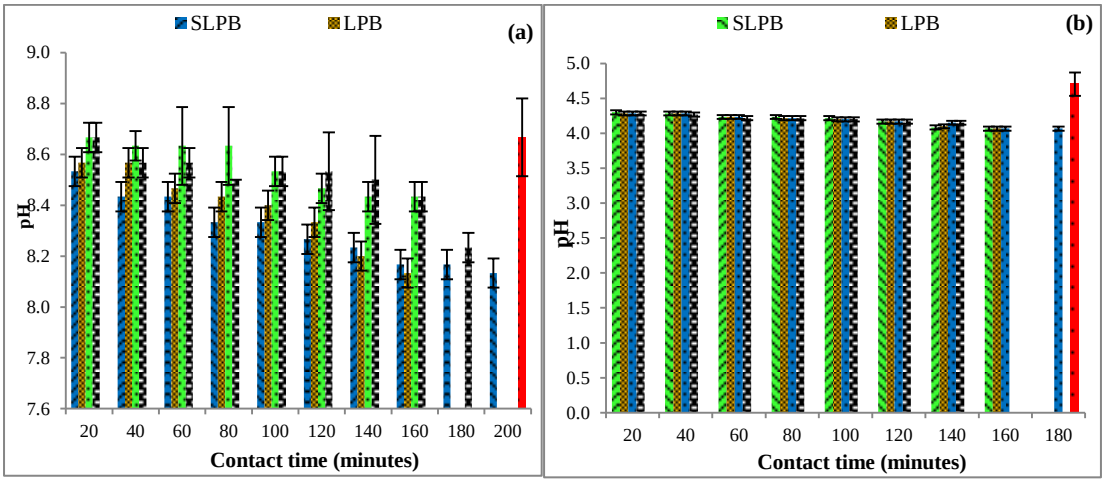

Figure 4.18 Effect of different adsorbents on pH of tannery (a) and flashlight (b) wastewaters at optimized dosages, contact time, pH and room temperature (25±3ºC), ±S.D.

4.3.2.4. Effect of optimized adsorbent dosage and contact time on improving electrical conductivity (EC) of industrial wastewaters

The optimized dosage and contact time were applied to observe its effect on EC of tannery and flashlight industrial wastewaters. Likewise pH, EC of both wastewaters was also not affected significantly. EC of tannery and flashlight wastewaters was

recorded as 16.39 and 24.17 mS cm^{-1}, respectively. After treating both wastewaters with optimizes dosage of SLPB, LPB, OPB and BB, EC was reduced to 13.93, 14.0, 13.92, 14.55 and 21.24, 21.74, 22.19, 23.28 mS cm^{-1}, respectively (Fig 4.19). The reduction (%) was observed to be 15.0, 14.58, 15.09, 11.22 and 12.13, 10.04, 8.19, 3.67 %, respectively. Change in EC was not so much pronounced, however, it might be caused due to decrease in pH and availability of excess of surface acidic groups.

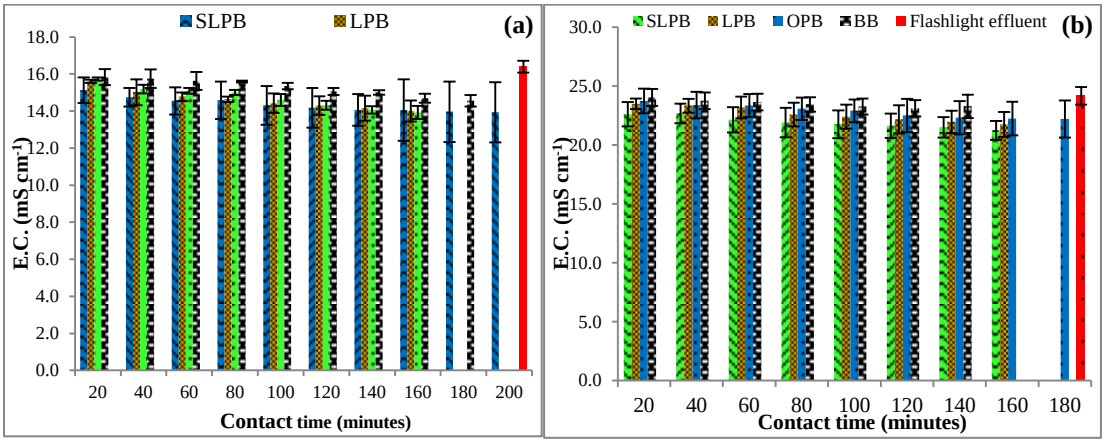

Figure 4.19 Effect of different adsorbents on EC of tannery (a) and flashlight (b) wastewaters at optimized dosages, contact time and room temperature (25±3ºC), ±S.D.

4.3.3 Optimization of different techniques for removal of heavy metals (HMs) from industrial wastewaters

The main objective of the study was to remove HMs present in wastewaters discharged by tannery and flashlight manufacturing industries. Foremost HM present in tannery wastewater was found to be chromium (Cr), whereas, in flashlight wastewater Pb was prominent 3.842 and 2.39 mg L^{-1}, respectively. Among different parameter, three parameters *viz.* adsorbent dosage, contact time and pH were considered for removal of HMs from tannery and flashlight wastewaters. The reason was high removal percentage during optimization process which did not require any special supervision or technical acquaintance during operation. The details of these optimized parameters on the removal of HMs present in tannery and flashlight wastewaters have been given below-

4.3.3.1 Effect of optimized adsorbent dosage and contact time on removal of heavy metals from industrial wastewaters

The effect of optimized dosage and contact time on removal of Cr and Pb from tannery and flashlight wastewaters was the same as that of solutions of known concentration. The removal percentage improved with increasing adsorbent dosage & contact time and became stagnant after achieving the saturation point (Fig 4.20). The optimized dosage and contact time of four adsorbent were same as descried in above section 4.3.1. The concentration of Cr in tannery wastewater and Pb in flashlight wastewater were 3.842 and 2.393 mg L^{-1}, respectively. After attaining the saturation point with SLPB, LPB, OPB and BB, the concentration of Cr and Pb remained in the tannery and flashlight wastewaters were 0.084, 0.327, 0.513, 0.990 and 0.069, 0.292, 0.333, 0.589 mg L^{-1}, respectively. These residual concentrations of both HMs fall under the recommended standards of Inland Surface Water-Bangladesh Standard (Chowdhury et al. 2013). The residual concentration of Pb after treating it with SLPB fell under the recommended concentration of CPCB (Table 4.1). During initial 20 minutes about 77.60, 70.68, 65.21 and 52.02 % of Cr from tannery wastewater 73.78, 66.07, 57.88 and 64.79 % of Pb from flashlight wastewater were removed. The maximum removal of Cr and Pb were accomplished by SLPB (97.82 & 97.11 %) followed by LPB (91.50 & 87.80 %), OPB (86.64 & 86.07%) and BB (74.23 & 75.38 %) at the end.

The reason behind increase in removal rate with increasing dose and contact time was the availability of free vacant sites at initial level. Later on the adsorption of both HMs were slowed down which might be due to difficulty in occupying the remaining vacant binding sites (Tahir et al. 2016). Further, intraparticle diffusion process might also be responsible at later stage caused by the exhaustion of binding sites and aggregation of remaining HMs (Manzoor et al. 2017). This phenomenon generated alterations in the concentration gradients among HMs and adsorbent causing decrease in the removal percentage (Kanchana et al. 2011). Similar trends of chromium and lead adsorption by various biomasses has been reported in previous work as a function of contact time and adsorbent dosage e.g. orange (*Citrus cinensis*) waste (Pérez Marín et al. 2009); sugarcane bagasse (Ullah et al. 2013); Polymer-based hybrid (Vetriselvi and Santhi 2015), peanut hull waste (Tahir et al. 2016a); corn cob waste (Manzoor et al. (2017) etc. Ullah et al. (2013) reported equilibrium time of 240 minutes for removal of Cr (II and VI) from tannery wastewater by sugarcane bagasse waste. Mohammed and Sahu (2015) reported removal of 99% of Cr by adsorption at pH 4, contact time 240 min and adsorbent dosage of 3.5 g L^{-1} by eucalyptus bark.

Dinh et al. (2017) reported about 92.35% adsorption of Pb at equilibrium time of 120 mins by MnO_2 loaded chitosan. Lee et al. (2017) testified optimum contact time 90 minutes for removal of Pb by biochar from palm oil sludge. Vergili et al. (2017) reported 2 g L^{-1} and 360 minutes of contact time with high Pb elimination as 83% by weak acid cation resin from battery (flashlight) industry wastewater. Likewise, Ravulapalli and Kuntha (2018) reported adsorbent dosage of 2g L^{-1} and agitation time 30 minutes for removal of 96.8 % of Pb from battery manufacturing industrial wastewater by carbon prepared from the seeds of *Caryota urens* plant. Zhang et al. (2018) described contact time of 60 minutes for maximum removal of Pb by oxidized mesoporous carbon (OMC).

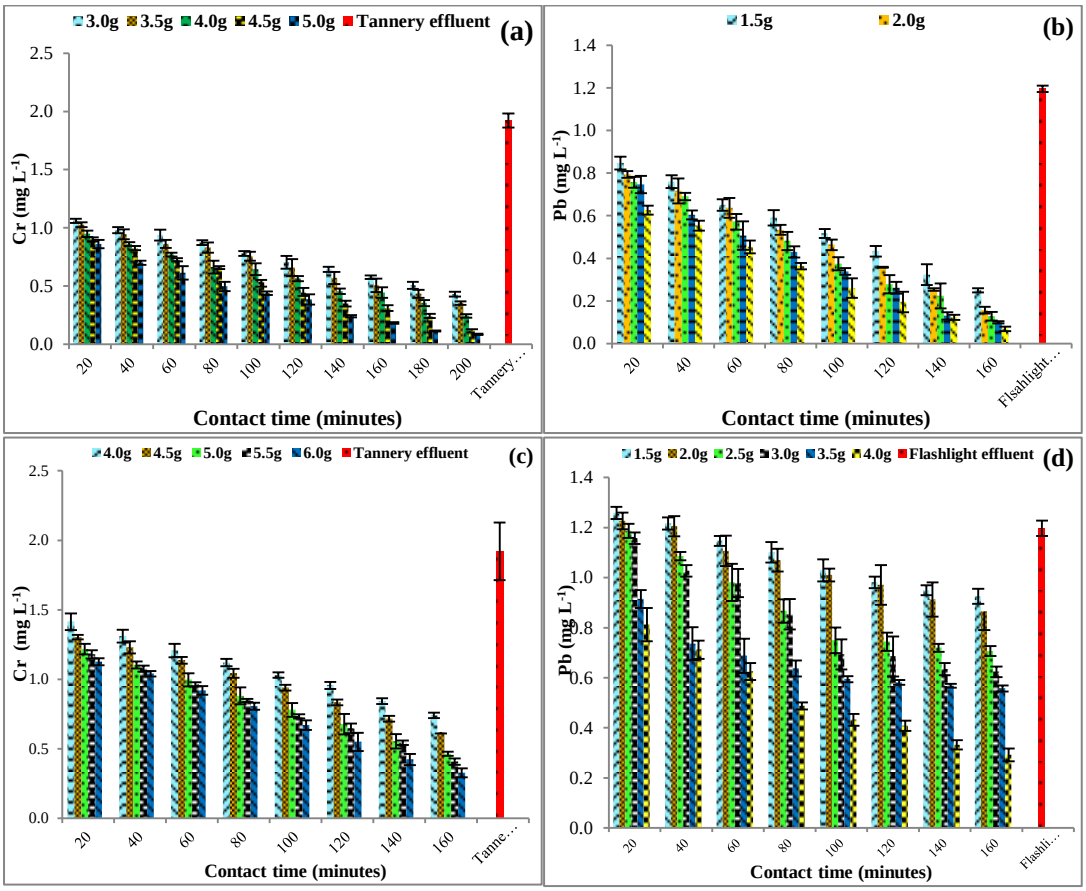

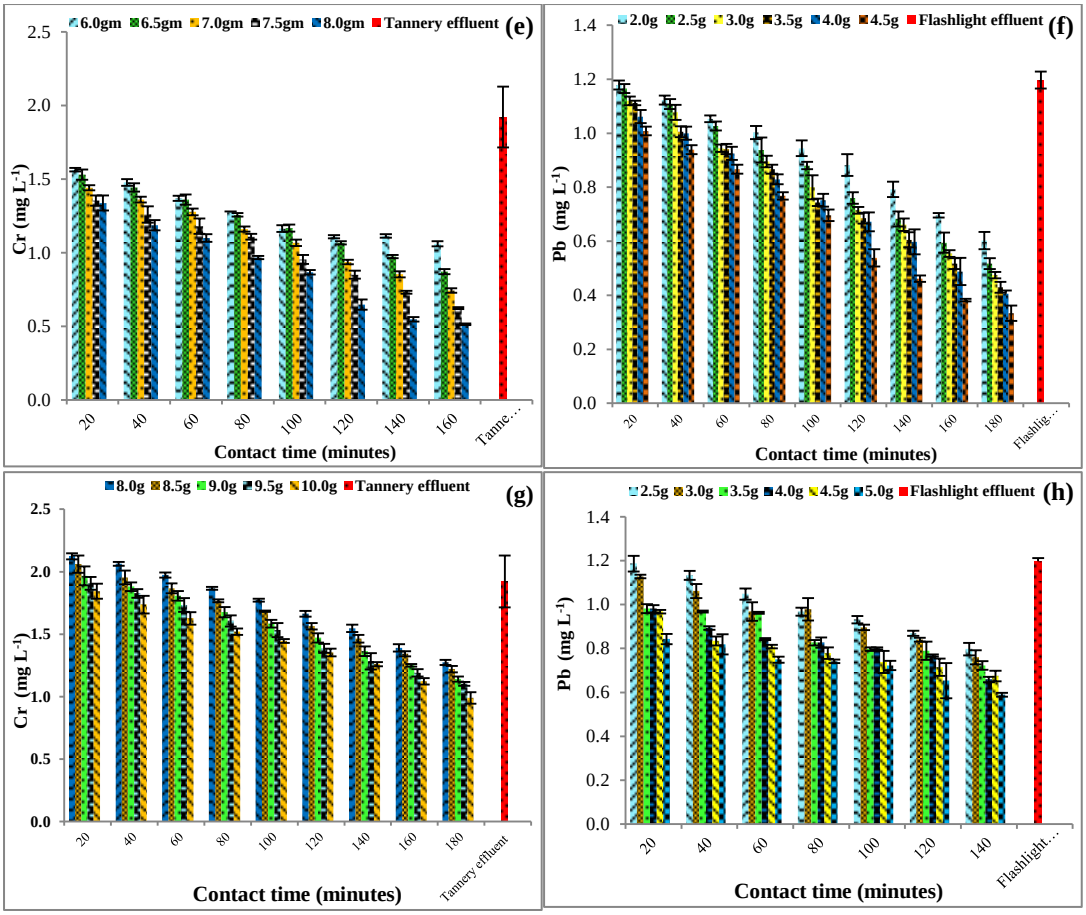

Figure 4.20 Effect of adsorbent dosage and contact time on the concentration of Cr and Pb, present in tannery and flashlight wastewaters by SLPB(a, b), LPB(c, d), OPB (e, f) and BB(g, h) at room temperature (25±3ºC), ±S.D. *For clear visibility concentrations of Cr and Pb have been divided by 2

4.3.3.2 Optimization of pH for removal of heavy metals from industrial wastewaters

Effect of the optimized pH was also the same as that of solutions of known concentration (20ppm), described in the section 4.2.3.3., except for BB. The removal rate increased with increasing pH until the equilibrium was attained at particular pH of less acidic in nature (Fig 4.21). The maximum removal of Cr by all selected adsorbent was attained at relatively less acidic pH i.e. between 4-5. Further, the maximum removal of Pb from flashlight wastewater was recorded at pH 5 in place of pH 4 by BB. This might be due to presence of extra OH^- ions in the form of alkaline salts, which could attract the positively charged metal ions, contributing towards extra removal (11.76%) at pH5 in comparison to pH 4. At saturation point only 0.08, 0.33,

0.51 and 0.99 mg L^{-1} of Cr and 0.07, 0.29, 0.33 and 0.59 mg L^{-1} of Pb were left in tannery and flashlight wastewater, respectively. These residual concentrations of both HMs fall under the recommended standards of Inland Surface Water-Bangladesh Standard (Chowdhury et al. 2013).Moreover, the maximum removal of Cr and Pb was accomplished by SLPB (97.4 & 96.80 %) followed by LPB (91.32 & 88.16 %), OPB (86.03 & 85.66 %) and BB (84.12 & 77.02 %). In comparison to adsorbent dosage and contact time, HMs removal percentages were high, but the differences were not marked.

The flexible behavior of Cr and Pb adsorption at different pH values might be due to surface charges. In the range of pH 2–3, $HCrO_4^-$, $HPbO_2^-$ ions dominated and with increasing pH, it was converted into CrO_4^- and PbO_2^- (Liu and Liu 2003; Wang et al. 2009). Further, the surface used to be bear positive charges at lower pH, which resulted in higher adsorption of both HMs due to higher electrostatic interactions (Ullah et al. 2013). Results of present study were in agreement with previous literatures available on the usage of different adsorbents for removal of HMs from industrial wastewaters including tannery and flashlight e.g. Bahadir et al. (2007) reported optimum pH; 4.5 for removal of Pb from battery manufacturing wastewater by *Rhizopus arrhizus* biomass. Similarly, Bairagi et al. (2011) reported 86% removal of Pb at optimum pH; 5 for by *Aspergillus versicolor* from battery manufacturing industrial wastewater. Ullah et al. (2013) reported pH 2 for maximum removal of Cr present in tannery wastewater using sugarcane bagasse as adsorbent. Mohammed and Sahu (2015) and Dinh et al. (2017) reported optimum pH 4 for removal of 81% of Cr and 92.35% of Pb from eucalyptus bark and manganese dioxide nanoparticles loaded chitosan, respectively. Bhatti et al. (2017), who have reported 79.6% removal of Cr present in tannery wastewater by using tire as adsorbent with dose 1.3 g, pH 3 and contact time 910 min. Manzoor et al. (2017) also reported the removal of Cr(III) from tannery wastewater at pH 5, contact time 400 min and adsorbent dose 0.1 g, whereas for Cr(VI), pH 2.0 with average removal of 64.52 and 55.88 %, respectively by corn cob biomasses. Anandkumar and Mandal (2011) and Zhao et al. (2017a) reported pH 2 for successful elimination of Cr from tannery wastewater by using TiO_2 hollow spheres and tannery residual biomass as adsorbent. Yan et al. (2016) also reported pH 5 as optimum pH for removal of Pb by porous leather particles. Although, the removal percentages of these studies were quite low in comparison to present study but pH

used for the process was same as that of present study. Zhang et al. (2018) reported optimum pH 5 for adsorption of Pb onto oxidized mesoporous carbon (OMC). Ravulapall and Kuntha (2018) observed 89.0% removal of Pb at optimum pH 7 by carbon derived from seeds of *Caryota urens* plant.

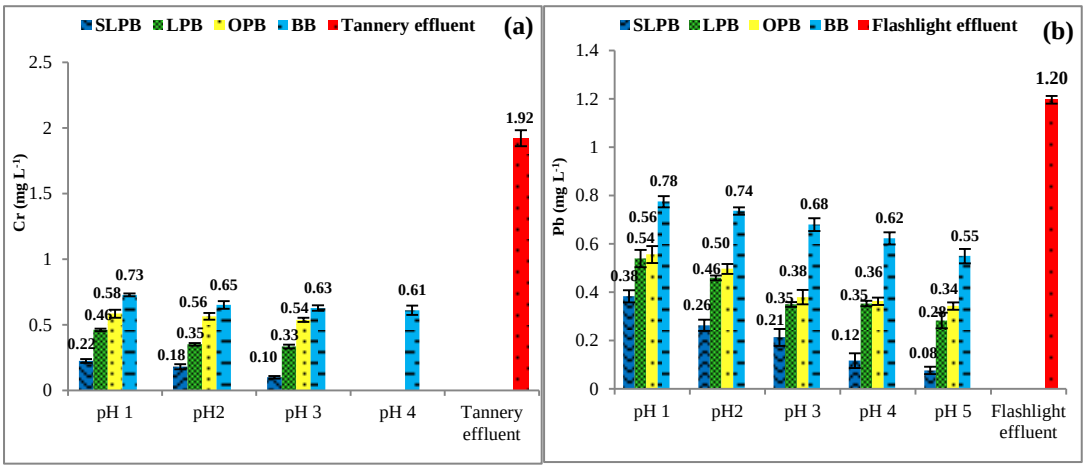

Figure 4.21 Effect of pH on the concentration of Cr (a) and Pb (b) present in tannery and flashlight wastewaters after treating it by SLPB, LPB, OPB and BB with optimized dosage and contact time at room temperature (25±3ºC), S.D. shown by bar

4.3.3. Kinetic studies for removal of heavy metals (Cr and Pb) from industrial wastewaters

In comparison to the effect of adsorbent dosage and contact time on removal of Cr and Pb, from tannery and flashlight wastewaters, the effect of pH was also the same. Only insignificant difference of about 1-2% were recorded for all of the adsorbent and about 10 % less removal was observed by BB for Cr. As the concentration of the HMs in wastewaters was constant, the kinetic study of HMs was focused concerning the optimized adsorbent dosage and contact time in the place of concentration. The optimized conditions used for applying the kinetic modeling have already been described in the section 4.2.3.

The kinetic studies are an important parameter to define basic behaviors of adsorbent and provide information regarding the adsorption mechanism and speed of the process (Wang et al. 2012; Uçar et al. 2015; Bhatti et al. 2017; Mella et al. 2017; Farooghi et al. 2018). Usually, pseudo-first order model assumes that the adsorption

rate is controlled by only one process or a mechanism involving a sole class of adsorbing sites, whereas, the impression of pseudo-second order model is that the adsorption procedure is a chemically mediated involving valence forces by the exchange or sharing of electrons between adsorbate and adsorbent (Guan et al. 2016). It is applied when rate of capturing of sites is proportional to square of no. of unoccupied sites on adsorbent (Ho and McKay 2000). Thus, the kinetics involved in the adsorption of Cr and Pb present in tannery and flashlight wastewaters, were studied following pseudo first and pseudo second order models given by Lagergren et al. (1898) and Ho et al. (2000), respectively.

The plots of pseudo-first-order and pseudo-second order for the adsorption of Cr and Pb onto different adsorbents have been presented in Fig 4.22.

The results of the kinetic models for Cr and Pb are depicted in Table 4.6-4.13

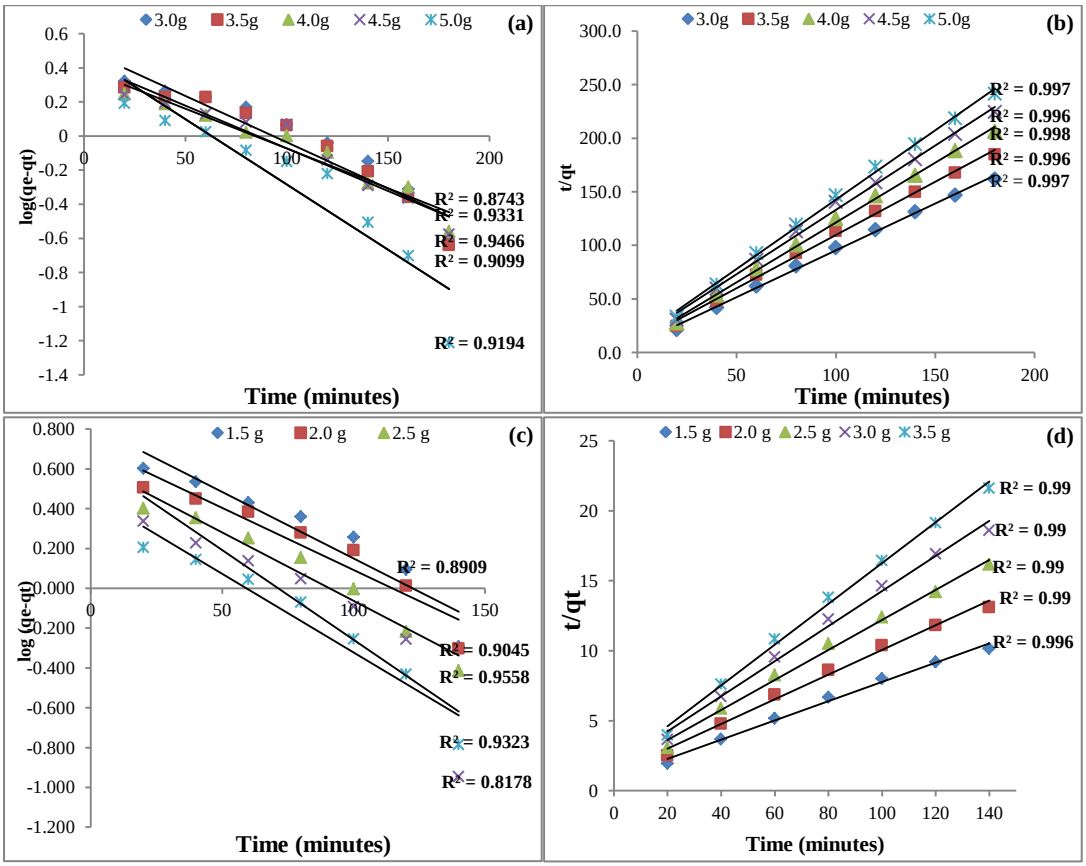

Figure 4.22.1 Role of time pseudo first order kinetic plots and pseudo second order kinetic plots for removal of Cr (a, b) and Pb (c, d) from industrial wastewaters by SLPB

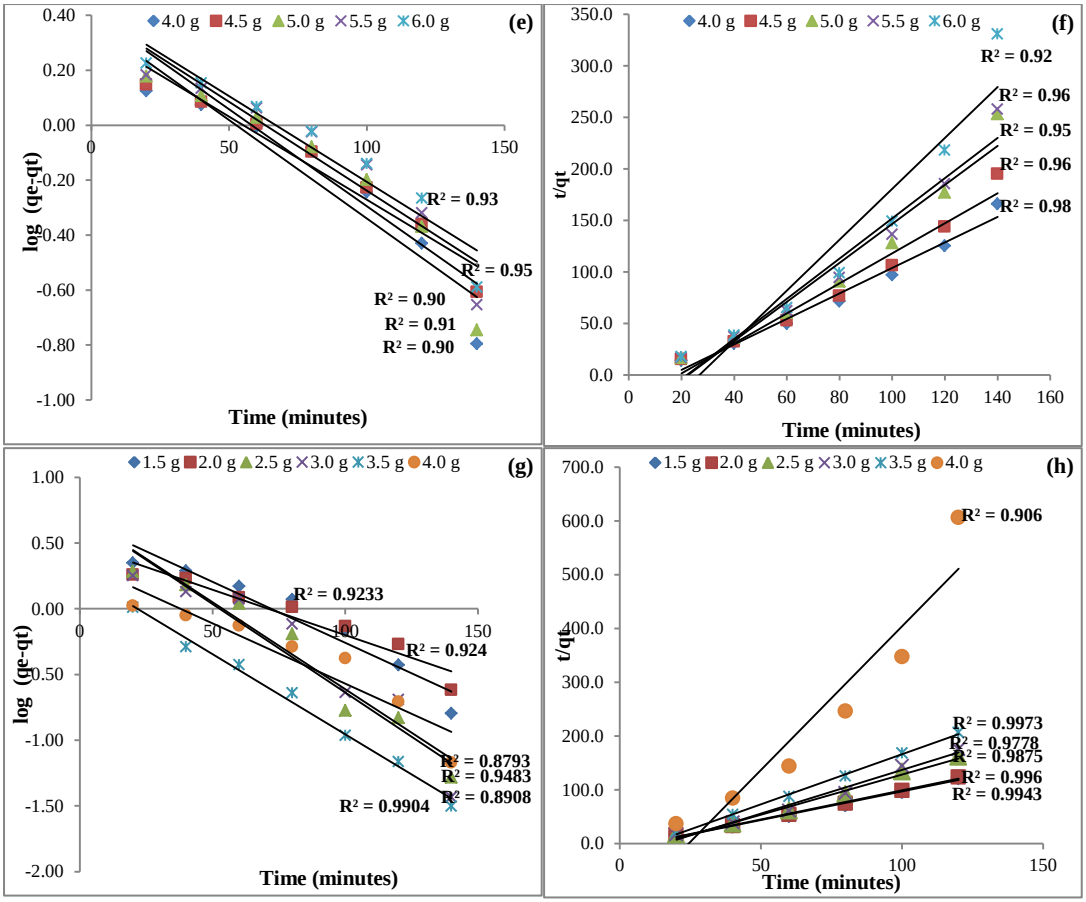

Figure 4.22.2 Role of time pseudo first order kinetic plots and pseudo second order kinetic plots for removal of Cr (e, f) and Pb (g, h) from industrial wastewaters by LPB

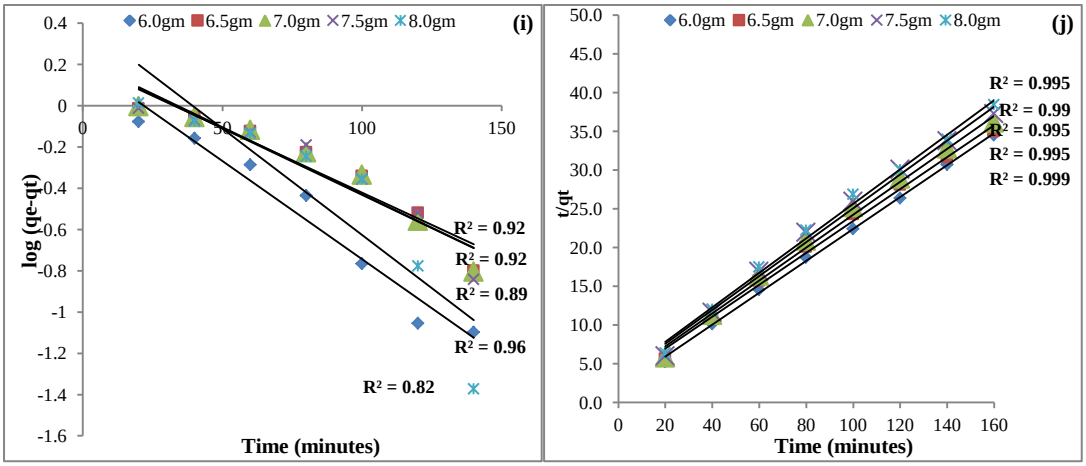

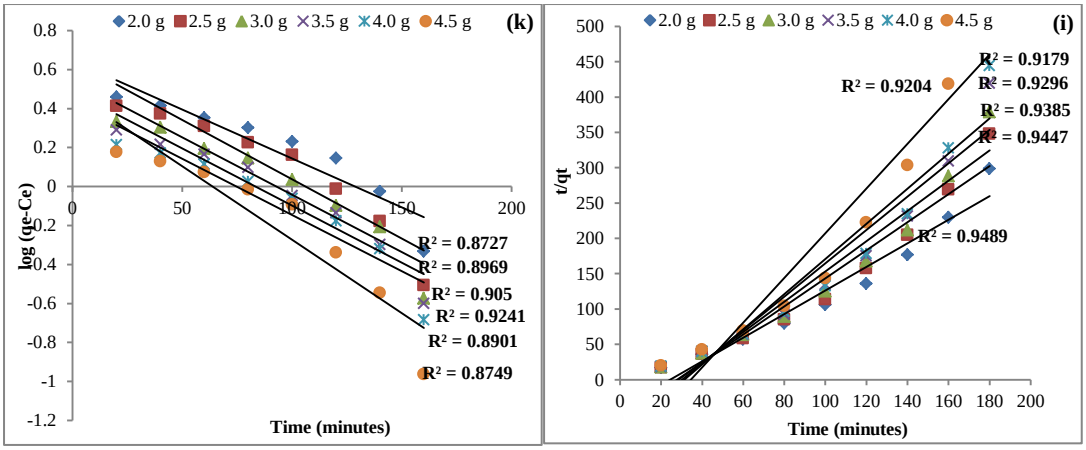

Figure 4.22.3 Role of time pseudo first order kinetic plots and pseudo second order kinetic plots for removal of Cr (i, j) and Pb (k, l) from industrial wastewaters by OPB

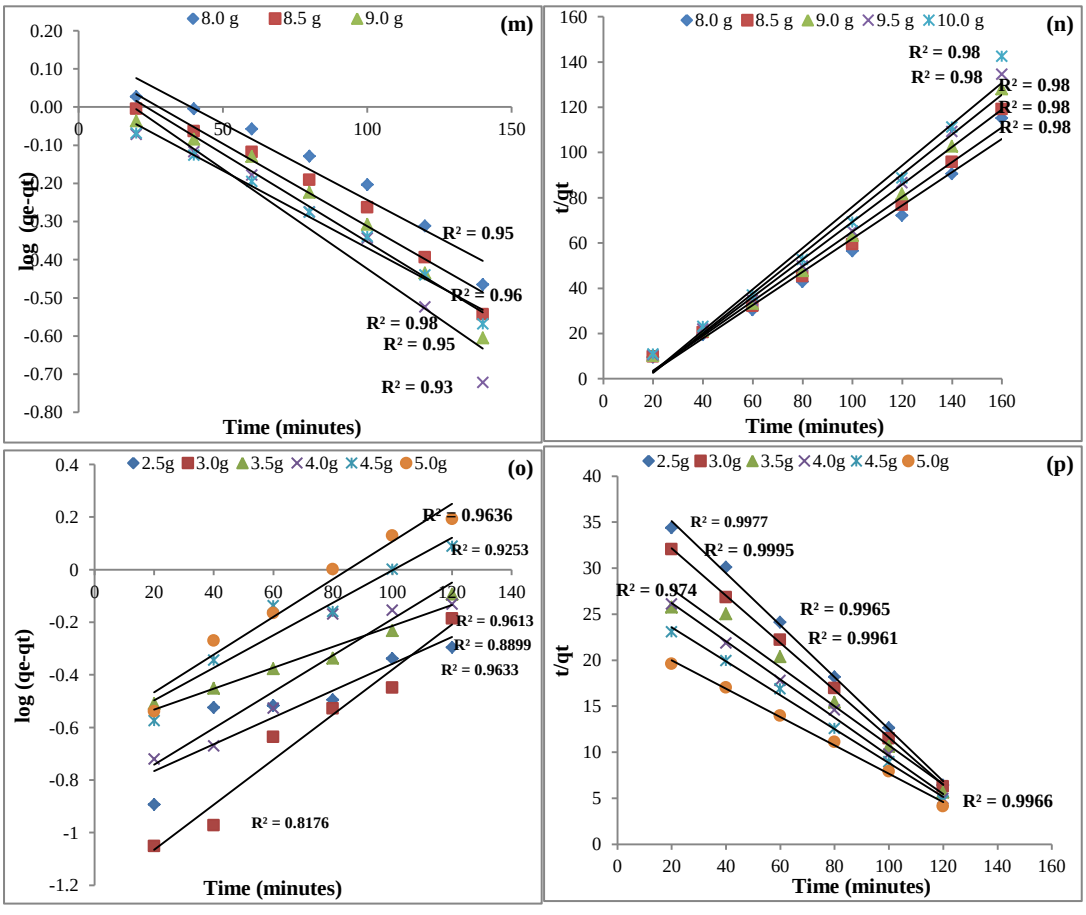

Figure 4.22.4 Role of time pseudo first order kinetic plots and pseudo second order kinetic plots for removal of Cr (m, n) and Pb (o, p) from industrial wastewaters by BB

Table 4.6 Pseudo first order and pseudo second order kinetic constants for sorption of Cr onto SLPB

Parameters	**Dosage (g)**				
	3.0	**3.5**	**4.0**	**4.5**	**5.0**
q_e (exp.) (mg g^{-1})	11.38	9.97	9.00	8.28	7.52
Pseudo First order model constants					
q_1 (mg g^{-1})	3.34	3.21	2.48	2.68	3.02
K_1 (min^{-1})	0.24	0.25	0.22	0.23	0.35
R^2	0.92	0.90	0.95	0.93	0.87
Pseudo Second order model constants					
q_2 (mg g^{-1})*	10.78	9.40	8.52	7.77	7.30
K_2 (g^{-1} $mg^{-1}min^{-1}$)	73.84	106.08	84.32	139.89	135.89
R^2	0.997	0.996	0.998	0.996	0.997
h (mg $g^{-1}min^{-1}$)	1.14	1.01	0.90	0.83	0.77

* Calculated from graph q_e/t vs 1/t

Table 4.7 Pseudo first order and pseudo second order kinetic constants for sorption of Pb onto SLPB

Parameters	**Dosage (g)**				
	1.5	**2.0**	**2.5**	**3.0**	**3.5**
q_e (exp.) (mg g^{-1})	14.29	11.18	9.05	7.65	6.64
Pseudo First order model constants					
q_1 (mg g^{-1})	7.76	5.19	4.20	4.39	2.93
K_1 (min^{-1})	0.01	0.01	0.01	0.02	0.02
R^2	0.89	0.91	0.96	0.82	0.93
Pseudo Second order model constants					
q_2 (mg g^{-1})*	13.51	10.42	8.62	7.41	6.41
K_2 (g^{-1} $mg^{-1}min^{-1}$)	11.97	17.36	20.50	23.61	19.84
R^2	0.99	0.99	0.99	0.99	0.996
h (mg $g^{-1}min^{-1}$)	14.71	11.36	9.35	8.00	6.90

* Calculated from graph q_e/t vs 1/t

Table 4.8 Pseudo first order and pseudo second order kinetic constants for sorption of Cr onto LPB

Parameters	**Dosage (g)**				
	4.0	**4.5**	**5.0**	**5.5**	**6.0**
q_e (exp.) (mg g^{-1})	7.75	7.16	6.03	6.24	5.85
Pseudo First order model constants					
q_1 (mg g^{-1})	2.62	2.56	2.57	2.16	2.38

K_1 (min^{-1})	0.01	0.01	0.01	0.01	0.02
R^2	0.93	0.90	0.91	0.95	0.90
Pseudo Second order model constants					
q_2 (mg g^{-1})*	8.64	7.51	5.87	5.48	4.57
K_2 (g^{-1} $mg^{-1}min^{-1}$)	31.63	52.35	95.59	95.87	178.04
R^2	0.98	0.96	0.95	0.96	0.92
h (mg $g^{-1}min^{-1}$)	0.81	069	0.53	0.51	0.41

* Calculated from graph q_e/t vs 1/t

Table 4.9 Pseudo first order and pseudo second order kinetic constants for sorption of Pb onto LPB

Parameters	**Dosage (g)**					
	1.5	**2.0**	**2.5**	**3.0**	**3.5**	**4.0**
q_e (exp.) (mg g^{-1})	9.83	7.68	6.77	5.92	5.27	5.70
Pseudo First order model constants						
q_1 (mg g^{-1})	5.14	5.10	4.67	3.08	2.23	1.83
K_1 (min^{-1})	0.02	0.01	0.03	0.03	0.03	0.02
R^2	0.92	0.92	0.95	0.89	0.99	0.88
Pseudo Second order model constants						
q_2 (mg g^{-1})*	0.96	0.92	0.71	0.65	0.55	0.17
K_2 (g^{-1} $mg^{-1}min^{-1}$)	76.02	68.37	286.56	102.63	208.35	314.59
R^2	0.997	0.98	0.99	0.99	0.99	0.91
h (mg $g^{-1}min^{-1}$)	0.94	0.93	0.67	1.60	0.54	0.19

* Calculated from graph q_e/t vs 1/t

Table 4.10 Pseudo first order and pseudo second order kinetic constants for sorption of Cr onto OPB

Parameters	**Dosage (g)**				
	6.0	**6.5**	**7.0**	**7.5**	**8.0**
q_e (exp.) (mg g^{-1})	4.63	4.57	4.42	4.29	4.16
Pseudo First order model constants					
q_1 (mg g^{-1})	1.62	1.60	1.66	1.635	2.29
K_1 (min^{-1})	0.02	0.01	0.01	0.01	0.02
R^2	0.96	0.93	0.92	0.89	0.82
Pseudo Second order model constants					
q_2 (mg g^{-1})*	0.56	0.36	0.33	0.31	0.30

K_2 (g^{-1} $mg^{-1}min^{-1}$)	15.55	38.09	42.56	46.49	50.84
R^2	0.999	0.995	0.995	0.99	0.995
h (mg $g^{-1}min^{-1}$)	4.85	4.85	4.71	4.57	4.48

* Calculated from graph q_e/t vs 1/t

Table 4.11 Pseudo first order and pseudo second order kinetic constants for sorption of Pb onto OPB

Parameters	**Dosage (g)**					
	2.0	**2.5**	**3.0**	**3.5**	**4.0**	**4.5**
q_e (exp.) (mg g^{-1})	8.98	7.53	6.42	5.63	4.99	4.59
Pseudo First order model constants						
q_1 (mg g^{-1})	4.42	4.43	3.51	3.08	2.70	3.03
K_1 (min^{-1})	0.01	0.01	0.01	0.01	0.01	0.02
R^2	0.87	0.90	0.91	0.92	0.89	0.88
Pseudo Second order model constants						
q_2 (mg g^{-1})*	8.01	6.85	5.88	5.19	4.56	4.27
K_2 (g^{-1} $mg^{-1}min^{-1}$)	0.02	0.02	0.02	0.02	0.03	0.03
R^2	0.95	0.95	0.92	0.93	0.92	0.92
h (mg $g^{-1}min^{-1}$)	1.10	0.75	0.6	0.56	0.54	0.47

* Calculated from graph q_e/t vs 1/t

Table 4.12 Pseudo first order and pseudo second order kinetic constants for sorption of Cr onto BB

Parameters	**Dosage (g)**				
	8.0	**8.5**	**9.0**	**9.5**	**10.0**
q_e (exp.) (mg g^{-1})	3.21	3.08	3.00	2.88	2.85
Pseudo First order model constants					
q_1 (mg g^{-1})	1.43	1.32	1.28	1.26	1.09
K_1 (min^{-1})	0.01	0.01	0.01	0.01	0.01
R^2	0.95	0.96	0.95	0.93	0.98
Pseudo Second order model constants					
q_2 (mg g^{-1})*	2.97	2.82	2.64	2.52	2.37
K_2 (g^{-1} $mg^{-1}min^{-1}$)	18.27	18.09	22.41	25.65	25.69
R^2	0.96	0.98	0.98	0.98	0.99
h (mg $g^{-1}min^{-1}$)	1.36	1.30	1.21	1.14	1.10

* Calculated from graph q_e/t vs 1/t

Table 4.13 Pseudo first order and pseudo second order kinetic constants for sorption of Pb onto BB

Parameters	**Dosage (g)**					
	2.5	**3.0**	**3.5**	**4.0**	**4.5**	**5.0**
q_e (exp.) (mg g^{-1})	6.41	5.47	4.79	4.35	3.83	3.62
Pseudo First order model constants						
q_1 (mg g^{-1})	2.47	0.93	0.89	0.96	0.96	0.82
K_1 (min^{-1})	0.02	0.01	0.01	0.01	0.02	0.01
R^2	0.82	0.96	0.89	0.96	0.93	0.96
Pseudo Second order model constants						
q_2 (mg g^{-1})*	3.436	3.846	4.348	4.587	5.181	6.135
K_2 (g^{-1} $mg^{-1}$$min^{-1}$)	4.888	6.586	24.263	8.456	11.474	15.061
R^2	0.998	0.999	0.974	0.997	0.996	0.997
h (mg $g^{-1}$$min^{-1}$)	3.546	3.891	4.717	4.831	5.435	6.536

* Calculated from graph q_e/t vs $1/t$

The interpretation and conformity of experimental data and model predicted were based on the values of correlation coefficients (R^2) (Bhatti et al. 2017). R^2 values of pseudo-second-order kinetic model were higher than pseudo-first-order model for all four adsorbents treating Cr and Pb from tannery and flashlight wastewaters (Table 4.6-4.13). Adsorption by SLPB possessed R^2 values as 0.92, 0.90, 0.95, 0.93 and 0.87 for pseudo first order and 0.997, 0.996, 0.998, 0.996 and 0.997 for pseudo second order rate kinetic for removal of Cr from tannery wastewater at optimized conditions, respectively. Likewise, R^2 values for pseudo first and second order rate kinetics acquired by SLPB for treating flashlight wastewater were .89, 0.91, 0.82, 0.93 and 0.99, 0.99, 0.99, 0.996, respectively. Same trend was also followed by LPB for treating tannery and flashlight wastewaters as it showed R^2 values for pseudo first and second order rate kinetics as 0.93, 0.896, 0.91, 0.95, 0.90 and 0.93, 0.90, 0.91, 0.95, 0.90; and 0.92, 0.92, 0.95, 0.89, 0.99, 0.88 and 0.997, 0.98, 0.99, 0.99, 0.99, 0.91, respectively. Treatment of both industrial wastewaters by OBP possessed R^2 values as 0.96, 0.93, 0.92, 0.89, 0.81 & 0.999, 0.995, 0.99, 0.995 in regards of tannery wastewater and 0.97, 0.90, 0.91, 0.92, 0.89, 0.88 & 0.95, 0.95, 0.94, 0.93, 0.92, 0.92 for flashlight wastewater, respectively for pseudo first and second order rate kinetics. Likewise, BB also showed R^2 values closer to 1 for pseudo first and second order rate

kinetics for adsorption of Cr and Pb from industrial wastewaters. The values were 0.95, 0.96, 0.95, 0.93, 0.98 & 0.95, 0.96, 0.95, 0.93, 0.98, respectively for Cr and 0.82, 0.96, 0.89, 0.96, 0.93 & 0.998, 0.999, 0.974, 0.997, 0.996, respectively for Pb.

Although the adsorption process partially followed rate equations at different times as the differences in R^2 values were very rare for adsorption of both HMs by the selected adsorbents but the best agreement was seen between the experimental data and those obtained within the pseudo-second order (Dinh et al. 2017). Further, higher values of R^2 in comparison to pseudo first order kinetics also supported this interpretation. In addition to this, determination coefficients for pseudo-first order were also good and obtained straight-line for intercepts plotted for log ($q_e - q_t$) against t. However, values of these intercepts were neither close to nor nearby the values of q_e. Further, the determination coefficients for the pseudo-second order were the maximum and the q_e values acquired from plots of t/q_t against t were also very close to those obtained from the experimental data (Table 4.6-4.13) for both HMs by all the selected adsorbents. Therefore, adsorption reactions were likely to be pseudo second order, assuming that rate of adsorption is directly proportional to no. of active surface sites (Ho and McKay 1999; Marsal et al. 2012). It is usually affected by amount of HMs present on surfaces of adsorbents and amount of metal adsorbed at equilibrium time (Vergili et al. 2017). Thus, it could be concluded that the adsorption mechanism of both metals followed chemisorption more appropriately than physisorption as pseudo second order kinetic model fitted well with adsorption of both HMs (Bairagi et al. 2011; Yan et al. 2016; Bai et al. 2017; Panda et al. 2017; Poonam et al. 2018; Zhang et al. 2018). The results of the present study is in good agreement with previous studies conducted on adsorption of Cr(II and VI) and Pb(II) *viz.* Bairagi et al. (2011); Marsal et al. (2012); Fabbricino et al. (2013); Martino et al. (2013); Yan et al. (2016); Bai et al. (2017); Dinh et al. (2017); Manzoor et al. (2017); Panda et al. (2017); Ravulapalli and Kuntha (2018); and Zhang et al. (2018).

4.3.4. Adsorption isotherm for removal of heavy metals (Cr and Pb) from industrial wastewaters

Adsorption isotherms are applied to define the adsorption equilibrium for wastewater treatment by providing valuable information about adsorbent surface (Naiya et al. 2014). It is an important aspect of adsorption studies to optimize the design of the process and adsorption capacity with behavior of the adsorbents (Anandkumar and

Mandal 2011; Bai et al. 2017; Farooghi et al. 2018). At equilibrium, tannery and flashlight wastewaters were allowed with varying dosages of adsorbent to treat these wastewaters to examine the maximum loading capacities until the optimum removal was achieved at room temperature (25±3ºC). Because of their simplicity, Freundlich and Langmuir equations are the most widely used models to describe relationship between equilibrium metal biosorption q_e (mg L^{-1}) and final concentrations C_e (mg L^{-1}) at equilibrium (Azza et al. 2013; Yan et al. 2016; Panda et al. 2017). Therefore, adsorption processes were justified by linear forms of Langmuir and Freundlich isotherms (Langmuir 1918; Freundlich 1906).

Plots of $1/q_e$ versus $1/C_e$ for the adsorption of Cr and Pb have been presented in Fig 4.23. The interpretation of the isothermic model was based on the values of R^2 for both HMs. The R^2 values of Langmuir & Freundlich isothermic model for adsorption of Cr and Pb onto the surface of SLPB were 0.89 & 0.99 and 0.95 & 0.98, for LPB were 0.97 & 0.99 and 0.96 & 0.94, for OPB were 0.999 & 0.999 and 0.94 & 0.95; and for BB were 0.96 & 0.98 and 0.93 & 0.93, respectively. As the values of R^2 for both the isotherms were nearby 1, and there were a little variation between both isotherms, results implied that in comparison to Langmuir, Freundlich isothermic model better fitted for adsorption of Cr and Pb from tannery and battery wastewaters (Mella et al. 2017). However, both isothermic models may be considered to fit with adsorptive removal of Cr and Pb experimental data (Tahir and Naseem 2007; Marsal et al. 2012; Baccar et al. 2013; Manzoor et al. 2017; Farooghi et al. 2018). From the perspective of reliability coefficients and graphs, it was observed that Freundlich isotherm showed better prophesy of Cr and Pb adsorption by SLPB, LPB, OPB and BB. Therefore, it could be concluded that adsorbent surfaces were heterogeneous and availed multi-layer adsorption with interactions between adsorbate and absorbent (Dinh et al. 2017). Whereas, assumption of Langmuir model was that there were no interactions between solute particles and adsorbent surfaces with monolayer adsorption of HMs (Uçar et al. 2015). Further, results of present study were in good agreement with Azza et al. (2013), Martino et al. (2013), Guan et al. (2016), Yan et al. (2016); Karunanayake et al. (2017), Lee et al. (2017), Manzoor et al. (2017), Farooghi et al. (2018); Ravulapalli and Kuntha (2018); Zhang et al. (2018) etc. These studies reported the good fit of Langmuir and Freundlich isothermic models for adsorption of

various HMs including Cr(III & VI) and Pb(II), favoring more appropriately to Freundlich (based of R^2 values), similar to present study.

The value of R_L is equal to 1 show linear and 0 means irreversible adsorption. In present study, R_L value was less than 0 for all four selected adsorbents for treating tannery and flashlight wastewaters which represented favourable adsorption of Cr and Pb (Anandkumar and Mandal 2011, Sönmezay et al. 2012, Martino et al. 2013, Lee et al. 2017, Ravulapalli and Kuntha 2018). The parameters of Langmuir and Freundlich isotherms are presented in Table 4.14 and separation factor (R_L) in Table 4.15.

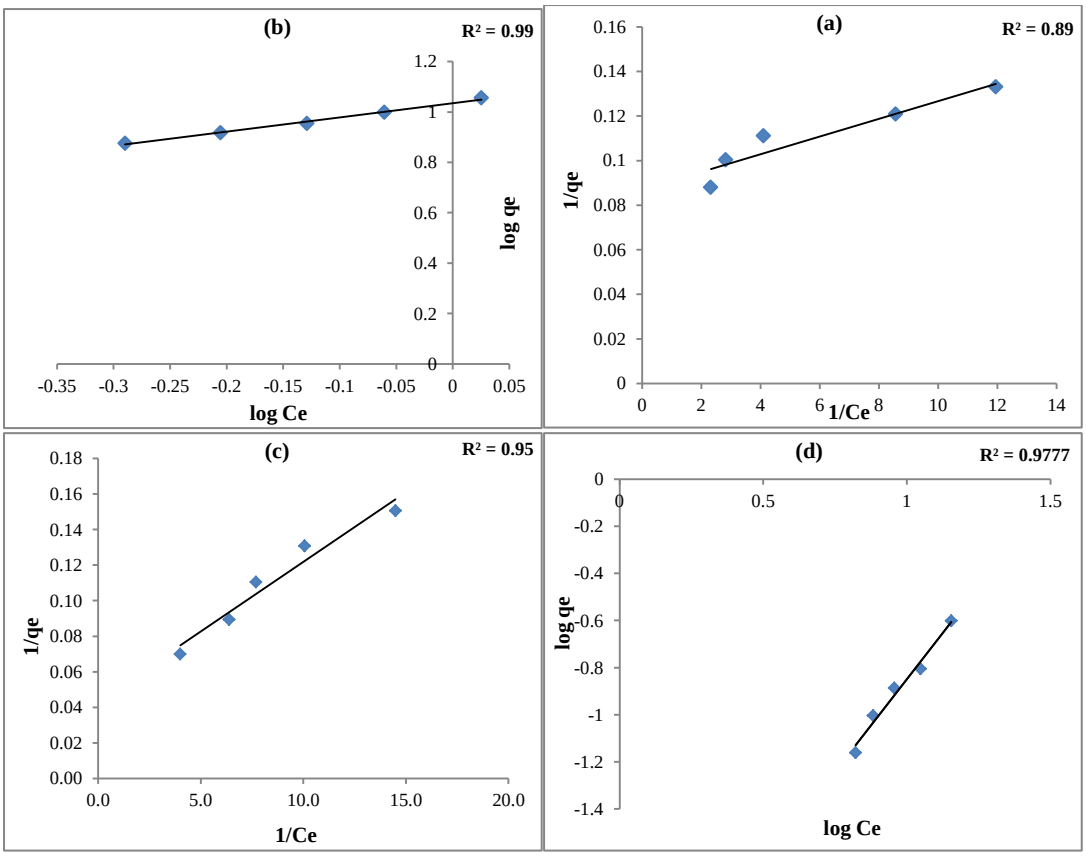

Figure 4.23.1 Langmuir and Freundlich isotherm models for adsorption of Cr (a, b) and Pb (c, d) on SLPB

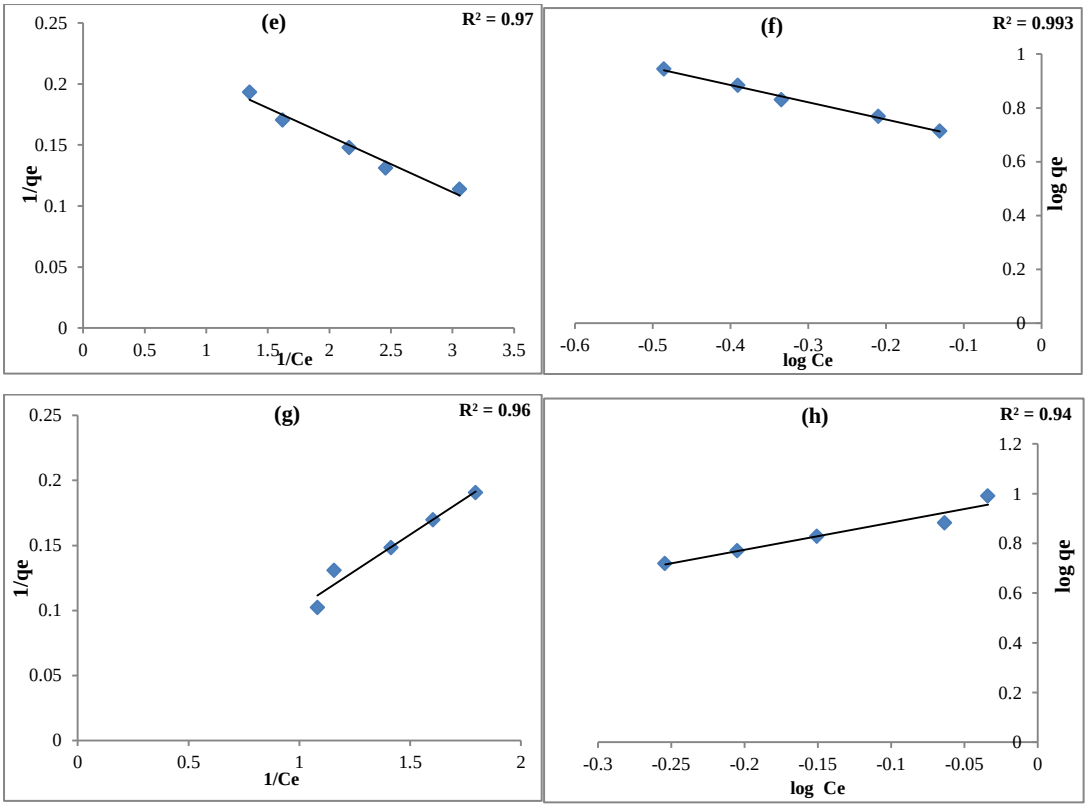

Figure 4.23.2 Langmuir and Freundlich isotherm models for adsorption of Cr (e, f) and Pb (g, h) on LPB

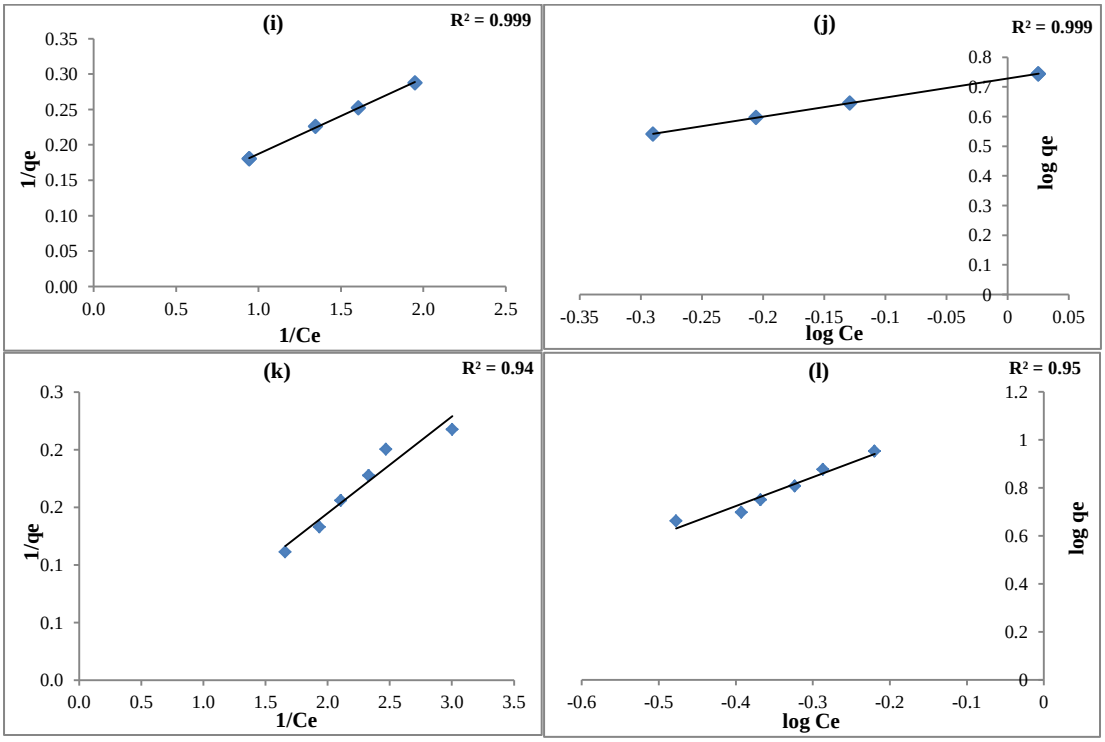

Figure 4.23.3 Langmuir and Freundlich isotherm models for adsorption of Cr (i, j) and Pb (k, l) on OPB

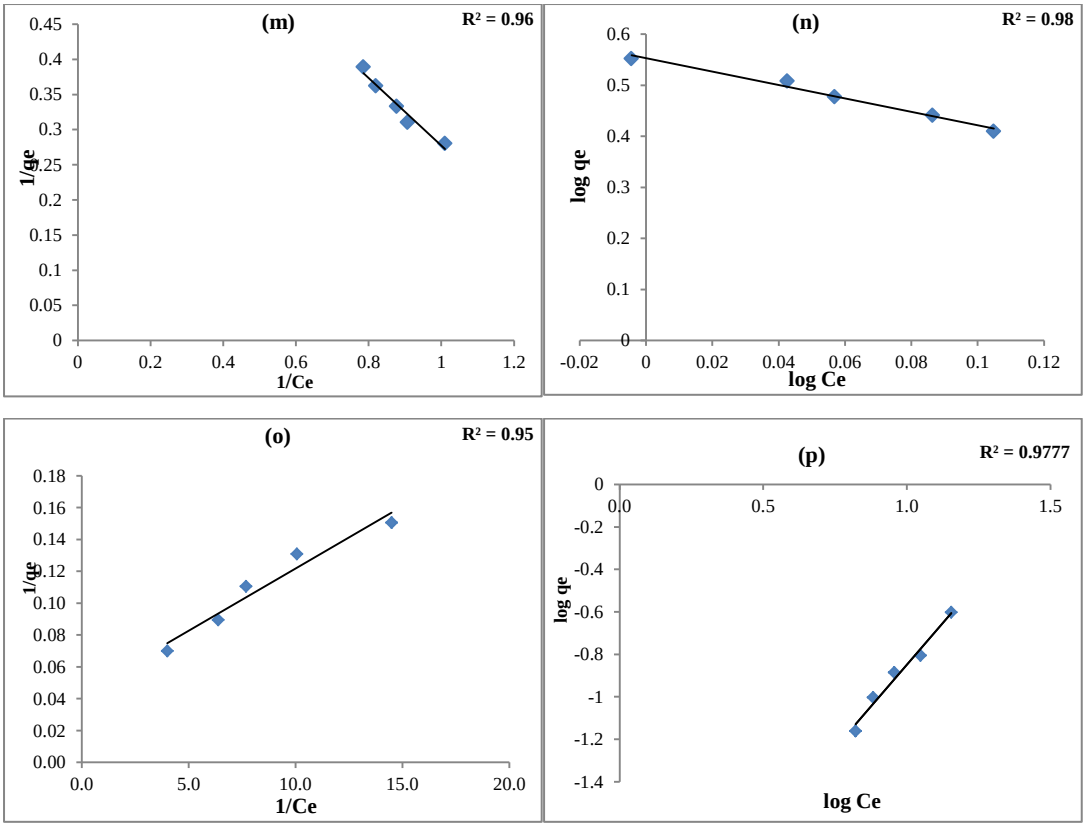

Figure 4.23.4 Langmuir and Freundlich isotherm models for adsorption of Cr (m, n) and Pb (o, p) on BB

Table 4.14 Langmuir along with Freundlich isotherm constants for the adsorption of Cr and Pb by different adsorbents

Adsorbents	Heavy metals	Langmuir constants			Freundlich constants		
		q_{max} (mg g^{-1})	**b (L mg^{-1})**	**R^2**	**K_F (mg g^{-1})**	**n**	**R^2**
SLPB	Cr	**2872.50**	11.50	**0.89**	3.70	0.97	**0.99**
	Pb	**2840.91**	22.73	**0.95**	0.004	0.64	**0.98**
LPB	Cr	**874.96**	40.16	**0.97**	4.25	0.64	**0.99**
	Pb	**940.69**	105.26	**0.96**	9.84	0.9	**0.94**
OPB	Cr	**116.75**	12.52	**0.999**	5.35	1.56	**0.999**
	Pb	**512.53**	43.10	**0.94**	16.11	0.83	**0.95**
BB	Cr	**2.745**	1.32	**0.96**	1.31	3.57	**0.98**
	Pb	**12.74**	4.12	**0.93**	0.36	2.29	**0.93**

*Values are given for optimum dosages for treating tannery wastewater (3.842 mg L^{-1}) and flashlight wastewater (2.39 mg L^{-1})

Table 4.15 Separation factor (R_L) form Langmuir isotherm for Cr and Pb of tannery and flashlight wastewaters

SLPB	Dose (g)	3.0	3.5	4.0	4.5	5.0	-	-
Cr	R_L	0.18	0.16	0.14	0.13	0.12	-	-
SLPB	Dose (g)	1.5	2.0	2.5	3.0	3.5	-	-
Pb	R_L	0.22	0.18	0.15	0.13	0.11	-	-
LPB	Dose (g)	4.0	4.5	5.0	5.5	6.0	4.0	-
Cr	R_L	0.20	0.18	0.16	0.20	0.14	0.20	-
LPB	Dose (g)	1.5	2.0	2.5	3.0	3.5	4.0	1.5
Pb	R_L	0.998	0.998	0.998	0.997	0.997	0.996	0.998
OPB	Dose (g)	6.0	6.5	7.0	7.5	8.0	-	-
Cr	R_L	0.12	0.1	0.10	0.10	0.09	-	-
OPB	Dose (g)	2.0	2.5	3.0	3.5	4.0	4.5	-
Pb	R_L	0.66	0.61	0.57	0.53	0.50	0.47	-
BB	Dose (g)	8.0	8.5	9.0	9.5	10.0	-	-
Cr	R_L	0.69	0.67	0.68	0.66	0.64	-	-
BB	Dose (g)	2.5	3.0	3.5	4.0	4.5	5.0	-
Pb	R_L	0.75	0.72	0.69	0.66	0.63	0.60	

4.3.4.1. Adsorption capacities of different adsorbent and removal efficiency of adsorption

The amount of adsorbents in grams required to adsorb maximum amount of HMs or pollutants in milligrams onto their surface is known as its maximum or monolayer adsorption capacity. It is usually calculated with the help of Langmuir isotherm and is denoted as q_{max}. The adsorption capacity of Cr and Pb on different agricultural wastes have been summarized in the Table 4.16.

The monolayer adsorption capacity (q_{max}) of SLPB, LPB, OPB and BB for removal of Cr and Pb were found to be 2872.5 and 2840.91, 874.96 and 940.69, 116.75 and 512.53, 2.75 and 12.74 mg g^{-1}, respectively (Table 4.16). The value of q_{max} for BB was found to be less than previous reported literatures; the reason may lie in fact that treatment of wastewaters with constant concentration was performed in comparison to solutions of metals containing higher concentrations (Naiya et al. 2014; Wang et al. 2012). In addition to this, previous studies of Feng and Guo (2012); Doke and Khan (2012); Isaac and Shivakumar (2013); Reddy et al. (2014); Fathima et al. (2015); Vetriselvi and Santhi (2015); Elabbas et al. (2016); Wu et al. (2016); Basu et al. (2017); Esteves et al. (2017); Gaur et al. (2018) etc. many others supported the findings of present study, details of which have been given in Table 4.16.

Table 4.16 Comparative account of metal adsorption capacities of various waste materials

S. No.	Adsorbent	Heavy metals	Adsorption capacity(mg g^{-1})	References
1	Oak wood charcoal and wood charcoal ash	Cr^{6+}	30.1 and 46.17	Pehlivan et al. (2011)
2	Walnut shell and citric acid modified walnut shell	Cr^{6+}	0.154 and 0.596 mmol g^{-1}	Altun and Pehlivan (2012)
3	Orange peel NaOH and $CaCl_2$ treated	Pb^{2+}	209.8	Feng and Guo (2012)
4	Activated carbon of wood ash shell	Cr^{6+}	151.51	Doke and Khan (2012)
5	*Eichhornia crassipes* root activated	Cr^{6+}	36.34	Giri et al. (2012)
6	Biomass of *Eicchornia*	Pb^{2+}	90%	Ibrahim et al. (2012)
7	Coir pith (chemically modified)	Cr^{6+}	196.00	Suksabye and Thiravetyan (2012)
8	Corn cob (physically and chemically modified)	Cr^{3+}	84.546	Fonseca-Correa et al. (2013)
9	*Annona squamosa* shell (Custard apple)	Pb^{2+}	90.93	Isaac and Shivakumar (2013)
10	Root powder of *Eicchornia crassipes*	Cr^{3+}	33.98	Li et al. (2013)
11	Rose petals waste	Pb^{2+}	119.92	Manzoor et al. (2013)
12	Biomass of *Spirulina* sp	Total Cr	90.91	Rezaei (2013)
13	Marigold (biocarban)	Pb^{2+}, Cr^{3+}	94.8% & 95.4%	Singanan and Peters (2013)
14	Avage bagasse	Pb^{2+}	22.64	Velazquez-Jimenez et al. (2013)
15	Tea residue	Pb^{2+}	64.10	Yang and Cui (2013)
16	Watermelon rind	Cr^{3+}	172.6	Reddy et al. (2014)
17	Biomass of *Termitomyces clypeatus*	Cr^{3+}	24.84	Fathima et al. (2015)
18	Black rice husk ash	Cr^{6+}	98.46%	Georgieva et al. (2015)
19	Forest bio-waste	Pb^{2+}	74.35	Kim et al. (2015)
20	Banana peel	Pb^{2+}	15.1 μmol g^{-1}	Šabanović et al. (2015)
21	Polymer based hybrid	Cr^{6+}	81.4	Vetriselvi and Santhi (2015)
22	Egg shell and powdered marble	Cr^{3+}	~99%	Elabbas et al. (2016)
23	Pineapple waste	Pb^{2+}	77.16	Mopoung and Kengkhetkit (2016)
24	Rice straw (modified with rice straw)	Cr^{6+}	15.82	Wu et al. (2016)
25	Cucumber peel	Pb^{2+}	133.60	Basu et al. (2017)
26	Heat-treated wood of *Pinus*	Cr	19.4	Esteves et al. (2017)

	pinaster			
27	Corncob (modified)	Cr^{6+}	131.6	Lin et al. (2017)
28	*Hizikia fusiformis* sea weed	Pb^{2+}	2.89	Shin (2017)
29	**Sweet lemon peel**	Cr	**2872.50**	Poonam and Kumar (2017) **(Present study)**
30	**Sweet lemon peel**	**Pb^{2+}**	**2840.91**	**Present study**
31	**Lemon peel (present study)**	**Cr**	**874.96**	**Present study**
32	**Lemon peel (present study)**	**Pb^{2+}**	**940.69**	**Present study**
33	**Orange peel (present study)**	**Cr**	**116.75**	**Present study**
34	**Orange peel (present study)**	**Pb^{2+}**	**512.53**	**Present study**
35	**Bagasse (present study)**	**Cr**	**2.75**	**Present study**
36	Soya bean seeds	Pb^{2+}	0.72	Gaur et al. (2018)
37	**Bagasse (present study)**	**Pb^{2+}**	**12.74**	Poonam et al. (2018) **(Present study)**

4.3.5. Thermodynamic studies for removal of heavy metals (Cr and Pb) from industrial wastewaters

The effect of temperature onto the adsorption of 5, 10, 20 and 40 ppm aqueous solution of Cr and Pb was studied at optimum dosage and contact time for estimation of thermodynamic parameters. The temperature range for Cr and Pb were in between 298 to 338K as discussed in section 4.2.3.4. Two real wastewaters were not selected due to difficulty in maintaining the temperature in comparison to contact dosage and contact time. Since, temperature influences the adsorption process, so the thermodynamic studies were concentrated upon the solutions of known concentrations.

The negative value of ΔG^o indicates the spontaneous nature of the adsorption process, whereas positive values reflect non-spontaneous adsorption. Further, the values of ΔH^o gave an idea about the type interactions between the adsorbent and adsorbate (Mella et al. 2017; Fontoura et al. 2017). The positive and values ΔH^o indicates endothermic and exothermic adsorption, respectively. Whereas, positive value of ΔS^o represents increased randomness and negative value shows decrease in randomness at solid–solution interface during adsorption (Erentürk and Malkoç 2007; Anandkumar and Mandal 2011; Marsal et al. 2012; Sönmezay et al. 2012; Baccar et al. 2013; Dinh et al. 2017; Khan et al. 2017). The Van't Hoff plots for the determination of the thermodynamic parameters have been shown in Fig 4.24 and values given in Table 4.17. Besides above, results were found to be in good agreement with previous studies of Altun and Pehlivan (2012); Hossain et al. (2012); Wang et al. (2012); Yadav et al. (2012); Kılıç et al. (2013); Reddy et al. (2014);

Elabbas et al. (2016); Wu et al. (2016); Deniz and Karabulut (2017), the details of which have been given in Table 4.18

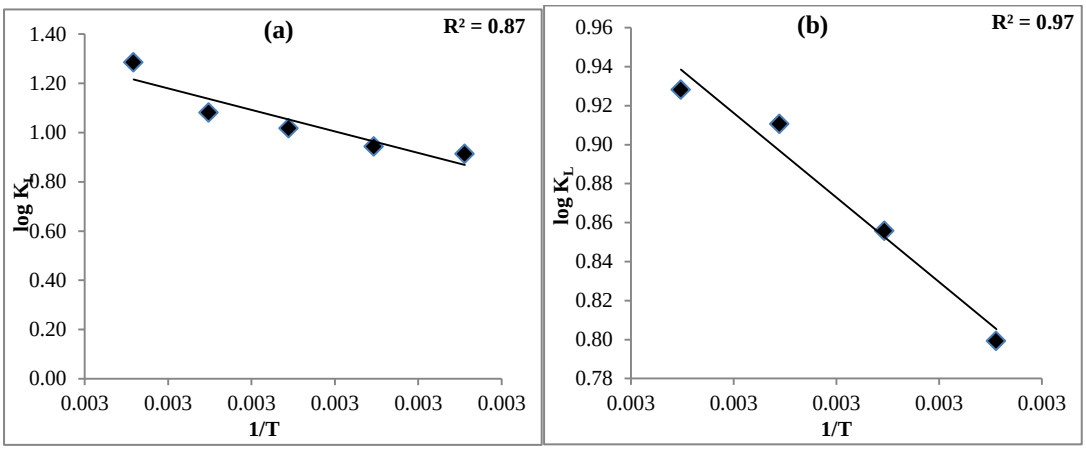

Figure 4.24.1 Van't Hoff plots for adsorption of Cr (a) and Pb (b) from aqueous solutions (5, 10, 20 and 40 mg L^{-1}) by SLPB with optimized conditions

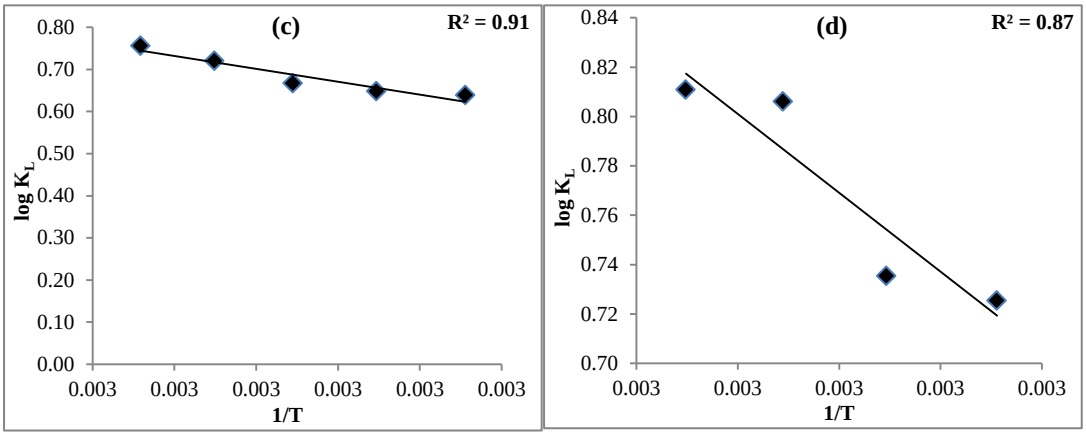

Figure 4.24.2 Van't Hoff plots for the adsorption of Cr (c) and Pb (d) from aqueous solutions (5, 10, 20 and 40 mg L^{-1}) by LPB with optimized conditions

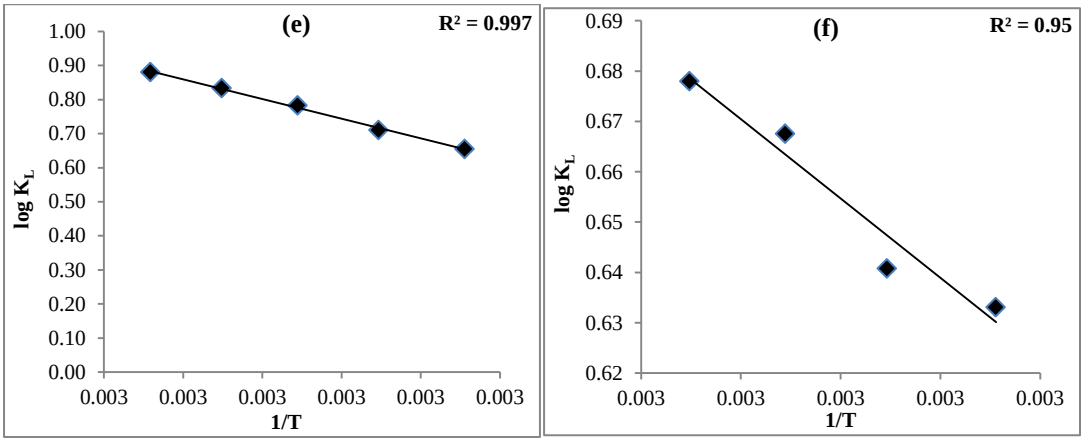

Figure 4.24.3 Van't Hoff plots for the adsorption of Cr (e) and Pb (f) from aqueous solutions (5, 10, 20 and 40 mg L^{-1}) by OPB with optimized conditions

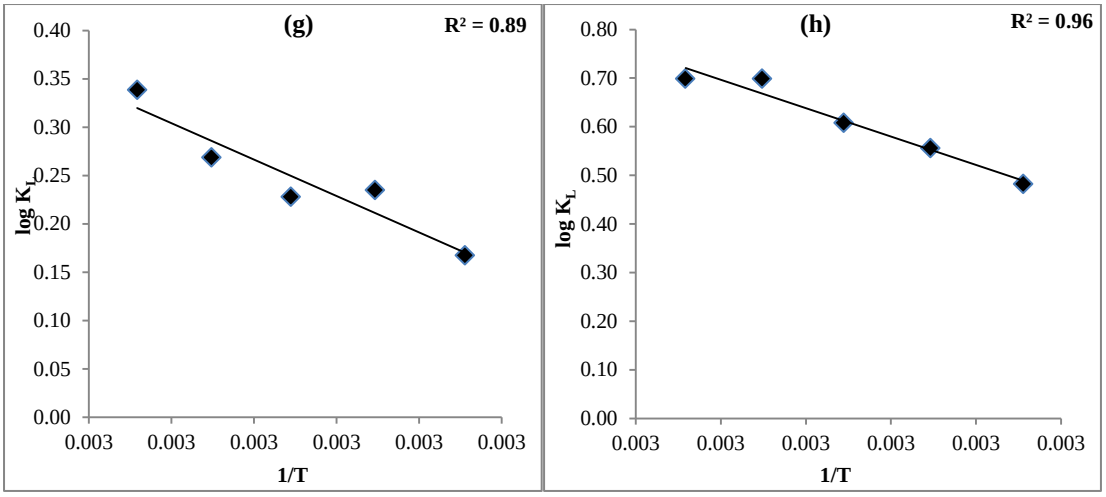

Figure 4.24 Van't Hoff plots for the adsorption of Cr (g) and Pb (h) from aqueous solutions (5, 10, 20 and 40 mg L^{-1}) by BB with optimized conditions

Table 4.17 Thermodynamic parameters for adsorption of Cr and Pb onto different adsorbents

SN	Adsorbent and Heavy metal	ΔH° (kJ mol^{-1})	ΔS° (kJ mol^{-1})	ΔG^0 (kJ mol^{-1})				
				T= 298K	T= 308K	T= 318K	T= 328K	T= 338K
1	**SLPB Cr**	7258.85	31.57	-2259.80	-2412.88	-2686.19	-2942.70	-3604.47
2	**SLPB Pb**	3600.54	18.35	-1976.62	-2187.61	-2403.04	-2526.71	-
3	**LBB Cr**	2541.79	13.70	-1579.17	-1656.08	-1759.83	-1961.04	-2120.11
4	**LPB Pb**	2651.44	14.87	-1794.16	-1880.02	-2127.25	-2207.30	-
5	**OPB Cr**	4796.49	21.52	-1619.64	-1815.53	-2065.37	-2266.90	-2468.99
6	**OPB Pb**	1308.25	9.62	-1565.82	-1638.09	-1761.96	-1845.75	-
7	**BB Cr**	3130.10	11.92	-413.84	-600.81	-601.48	-731.18	-950.07
8	**BB Pb**	4835.25	20.29	-1191.89	-1421.24	-1604.31	-1901.64	-1959.06
Interpretation		Endothermic	Increase in randomness	Spontaneous				

Table 4.18 List of thermodynamic parameters for adsorption isotherm and kinetics for heavy metals adsorbed on different bio-sorbents

S. no.	Adsorbents	Heavy metals	Thermodynamics	References
1	*Viscum album* L.	Pb^{2+}	ΔG = -ve; ΔH, ΔS = +ve	Erentürk and Malkoç (2007)
2	Cashew nut shell	Ni^{2+}	ΔG, ΔH, ΔS = -ve	Kumar et al. (2011)
3	Walnut shell and citric acid modified walnut shell	Cr^{6+}	ΔG = -ve; ΔH, ΔS = +ve	Altun and Pehlivan (2012)

4	Garden grass	Cu^{2+}	ΔG, ΔS = +ve; ΔH = -ve	Hossain et al. (2012)
5	Coir pith (chemically modified)	Cr^{6+}	ΔG, ΔH, ΔS = +ve	Suksabye and Thiravetyan (2012)
6	Bamboo charcoal(modified with cobalt coating)	Cr^{6+}	ΔG, ΔH = -ve; ΔS = +ve	Wang et al. (2012a)
7	Bamboo (modified by $KMnO_4$)	Pb^{2+}	ΔG, ΔH, ΔS = -ve	Wang et al. (2012)
8	Sand (modified)	Cr^{6+}	ΔG, ΔH, ΔS = -ve	Yadav et al. (2012)
9	Almond shell (biochar)	Ni^{2+}, Co^{2+}	ΔG; ΔH; ΔS = +ve	Kılıç et al. (2013)
10	Watermelon rind	Cr^{3+}	ΔG; ΔH; ΔS = -ve	Reddy et al. (2014)
11	Egg shell & powdered marble	Cr^{3+}	ΔG = -ve; ΔH, ΔS = +ve	Elabbas et al. (2016)
12	Rice straw (modified by rice straw)	Cr^{6+}, Ni^{2+}	ΔG = -ve; ΔH, ΔS = +ve	Wu et al. (2016)
13	Composite bio-sorbent of sea weed community	Zn^{2+}	ΔG = -ve	Deniz and Karabulut (2017)
14	Orange peel (Cellulosic waste)	Cu^{2+}	ΔG; ΔH; ΔS = -ve	Guiza (2017)
15	Guar gum–nano zinc oxide	Cr^{6+}	ΔG = -ve; ΔH, ΔS = +ve	Khan et al. (2017)
16	Corncob (modified)	Cr^{6+}	ΔG = -ve; ΔH, ΔS = +ve	Lin et al. (2017)
17	Corn silk	Cu^{2+}, Zn^{2+}	ΔG = -ve; ΔH, ΔS = +ve	Petrović et al. (2017)

*ΔG(-ve)= adsorption process is spontaneous and feasible, ΔG(+ve)= process is non-spontaneous; ΔH(-ve)= endothermic process, ΔH +ve)= exothermic process; ΔS(-ve)= decrease in randomness at solid-liquid interface, ΔS(+ve)= increase in randomness at solid-liquid interface

4.3.6. Desorption and reuse of adsorbents

The HMs loaded adsorbents creates disposal problems due to their hazardous nature (Vetriselvi and Santhi 2015). To overcome these problems desorption of HMs in a suitable eluant is practiced. It is an important process to discover the recuperating capacity and reusability of the adsorbents for applying it commercially (Zhang et al. 2018). Three acids (HNO_3, HCl and H_2SO_4) and one base (NaOH) of 0.1 M were selected as eluants to evaluate desorption of the adsorbed HMs from tannery and flashlight wastewaters. The experiments were performed at optimized conditions of dosage with mixing speed of 150 rpm for 24 hrs at room temperature (25±3ºC). Desorption of Cr and Pb has been presented in Fig 4.25.

About 45.63, 45.75, 55.38 and 54.43 % of Cr desorption was recorded from SLPB, LPB, OPB and BB, respectively. The maximum desorption was attained by 0.1 M HNO_3 for SLPB and 0.1 M HCl for remaining three adsorbents. The order of

desorption for Cr was found be in the order of OPB>BB>LPB>SLPB. Similarly, the maximum desorption of 88.15, 88.98, 86.82 and 90.05 % was achieved by SLPB, LPB, OPB and BB, respectively for Pb. The most suitable eluant for desorption of Pb was 0.1 M HCl for SLPB, LPB and OPB, and 0.1 M HNO_3 for BB. The order of desorption was recorded as BB>LPB>OPB>SLPB. Other eluants used for desorption of Cr were 0.1 M H_2SO_4 and NaOH, which also desorbed Cr and Pb to some extent but low in comparison to HNO_3 and HCl (Fig 4.25). After, first cycle of desorption, further desorption was not found to be satisfactory which may be due to incomplete elution and/or damage of sorption sites (Lam et al. 2016).

The results of present study were in good agreement with previous studies done by Suksabye and Thiravetyan (2012), Rezaei (2013), Velazquez-Jimenez et al. (2013), Vetriselvi and Santhi (2015), Poonam et al. (2018) as these reported maximum desorption of Cr and Pb in single cycle. Furthermore, Mondal (2009), Gupta et al. (2010), Bairagi et al. (2011), Altun and Pehlivan (2012), Li et al. (2013), Reddy et al. (2014), Kariuki e al. (2017), Karunanayake et al. (2017), Lee et al. (2017), Manzoor et al. (2017), Vilardi et al. (2018), Zhang et al. (2018) etc. supported results of present study for desorption of Cr and Pb from different adsorbents using similar eluants. The details of these studies have been summarized in Table 4.19.

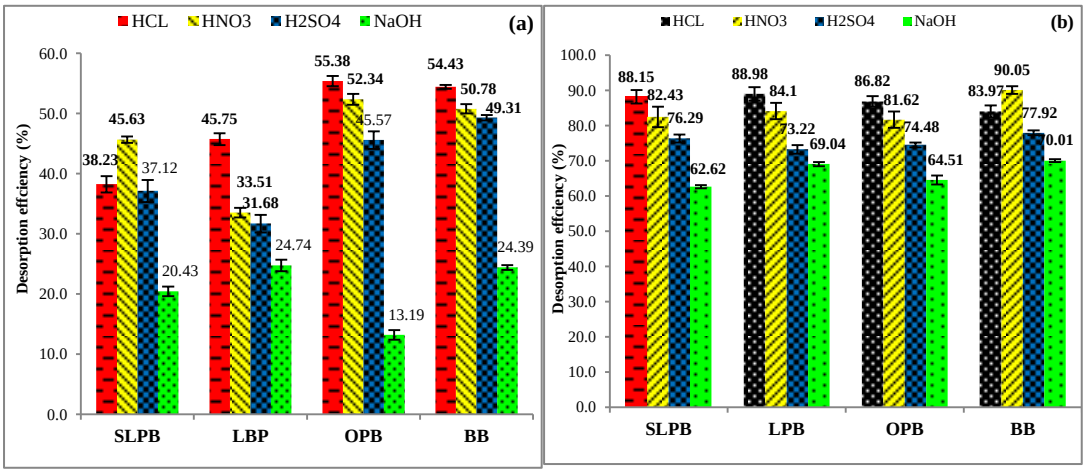

Figure 4.25 Desorption capacity of different eluants for desorption of Cr and Pb from selected adsorbents ±S.D. shown by bar

Table 4.19 Desorption of Cr and Pb from various adsorbents

Heavy metal	Adsorbate	Medium	Eluants	Maximum Efficiency	Cycle	Reference
Pb^{2+}	Tea waste	Aqueous solution	0.1 M HNO_3	99.8 %	4	Mondal (2009)
Cr^{6+}	Carbon slurry	Aqueous solution	1% HNO_3 and HCl, 0.3M NH_4OH and NaCl, deionized water	HNO_3	5	Gupta et al. (2010)
Pb^{2+}	*Aspergillus versicolor*	Battery industrial wastewater	0.1M HCl	85%	5	Bairagi et al. (2011)
Cr^{6+}	Walnut shell	Aqueous solution	0.5 M HCl	25.0%	3	Altun and Pehlivan (2012)
Cr^{3+} & Cr^{6+}	Coir pith	Electroplating industrial wastewater	1 M NaOH and 2M HNO_3	86.68% Cr^{3+} by 2M HNO_3, 11.43% Cr^{6+} by NaOH	-	Suksabye and Thiravetyan (2012)
Cr^{3+}	Root powder of *Eichhornia crassipes*	Aqueous solution	HCl, HNO_3 H_2SO_4, thiourea and EDTA (0.2 M all)	>50% Cr^{3+} by H_2SO_4	3	Li et al. (2013)
Cr	Biomass of *Spirulina* sp.	Aqueous solution	EDTA, HCl, HNO_3 (0.1 M all)	95% by HNO_3	-	Rezaei (2013)
Pb^{2+}	Agave bagasse	Aqueous solution	0.1 N HNO_3	45% at pH 2	-	Velazquez-Jimenez et al. (2013)
Cr^{3+}	Water melon rind	Aqueous solution	HCl, NaOH(0.1 M Both) and water	98.7% by NaCl	4	Reddy et al. (2014)
Cr^{6+} & Pb^{2+}	Polymer-based hybrid	Tannery wastewater	NaOH(1 M)	96%	-	Vetriselvi and Santhi (2015)
Pb^{2+}	Rogers mushroom	Aqueous solution	EDTA and HCl (0.1 M)	~50% Pb^{2+} HCl	3	Kariuki e al. (2017)

Pb^{2+}	Magnetic biochar	Aqueous solution	HCl (0.1 M)	>75%	3	Karunanayake et al. (2017)
Pb^{2+}	Palm oil sludge char	Aqueous solution	HCl (0.05–1.00 mol L^{-1})	0.99 desorption rate	5	Lee et al. (2017)
Cr^{3+} & Cr^{6+}	Corn cob biomass	Tannery wastewater	NaOH (0.1 M)	86 and 79.4 %, respectively	5	Manzoor et al. (2017)
Cr^{6+}	Mixed-iron coated olive stone	Tannery wastewater	NaOH and $C_2H_2O_4$ (1 M)	Not reversible	5	Vilardi et al. (2018)
Pb^{2+}	Oxidized mesoporous carbon	Aqueous solution	Ethanol and diluted NaOH	~ 15.5%	5	Zhang et al. (2018)
Pb^{2+}	Bagasse biochar	Battery industrial wastewater	HNO_3, HCl, H_2SO_4, and NaOH (0.1 M)	~90% by HNO_3	-	Poonam et al. (2018) (**Present study)**

4.3.7 Comparison among different adsorbents based on various optimized parameters to treat industrial wastewaters

A comparative study was conducted to obtain the best adsorbents for treating both industrial wastewaters by selected adsorbents at optimized conditions. Results have been presented in Table 4.20 & 4.21 and Fig 4.26 & 4.27. SLPB was recorded to be the best adsorbents for removal of Cr and Pb from tannery and flashlight wastewater. The removal efficiency and capacity was found to be maximum for SLPB followed by LPB, PB and BB for treating both wastewaters. SLPB followed Freundlich isotherm, whereas, LPB followed Freundlich & Langmuir isotherms for removal of both toxic metals. OPB followed Langmuir and Freundlich for removal of Cr form tannery wastewater, whereas, Freundlich for removal of Pb from flashlight wastewater. Moreover, BB followed Freundlich and Langmuir isotherms for removal of both toxic metals from respective industrial wastewaters. All the selected adsorbents followed pseudo second order kinetics for both HMs from particular industrial wastewaters. In addition to this, the best eluant for extraction of Cr form SLBP was 0.1 M HNO_3**,** whereas, for LBP, OPB and BB was 0.1 M HCl. Likewise, for extraction of Pb form SLBP, LBP, OPB 0.1 M HCl and for BB was 0.1 M HNO_3.

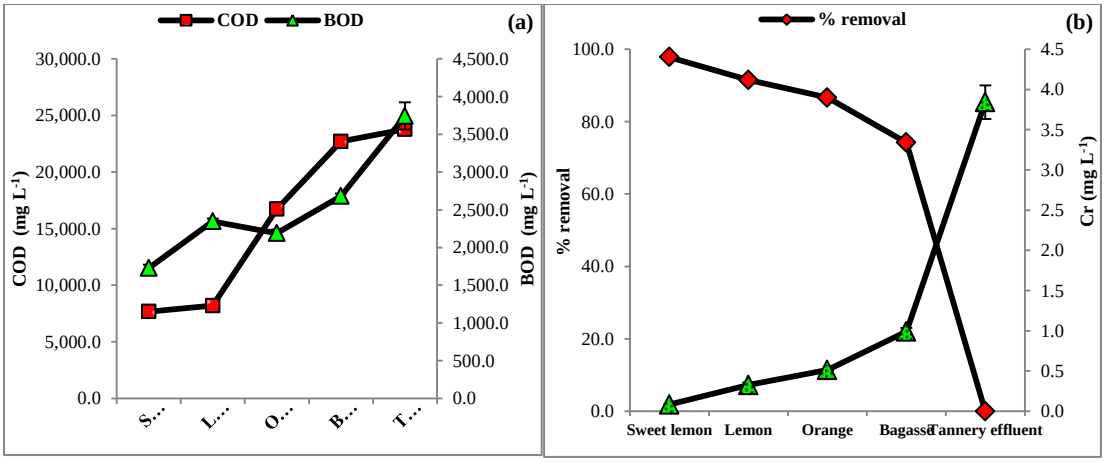

Figure 4.26 Comparative account of different adsorbent for removal of COD, BOD (a) and residual Cr conc. with its removal percentage (b) of tannery wastewater at optimized conditions

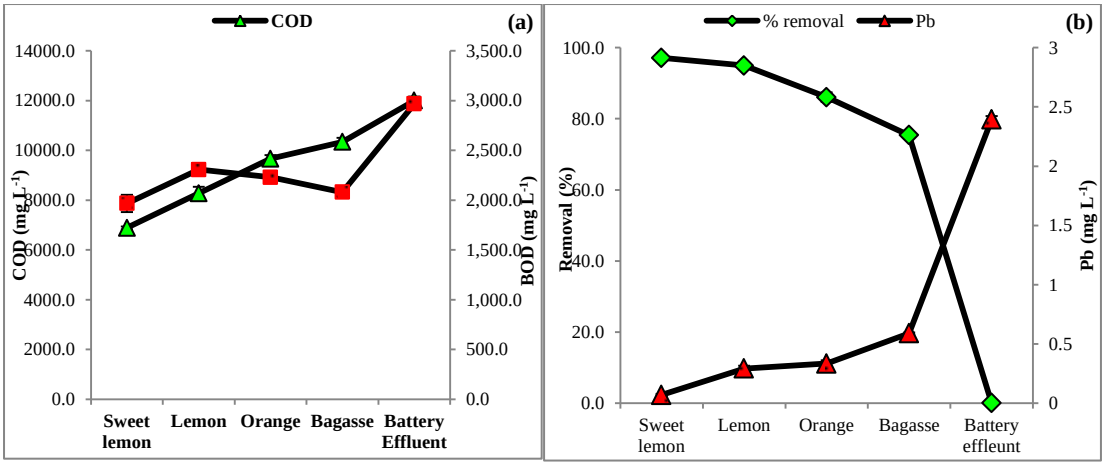

Figure 4.27 Comparison of different adsorbent for removal of COD, BOD (a) and residual Pb conc. with its removal percentage (b) of flashlight wastewater at optimized conditions

Table 4.20 Comparison of optimized conditions of different adsorbents for treatment of tannery wastewater

Adsorbent	**Dose (g)**	**Contact time (min.)**	**q_{max} (mg g^{-1})**	**Isotherm**	**Kinetics**	**Desorption (%) and Eluant (0.1 M)**
Sweet lemon	5.0	200	2872.50	F	PS II	45.63±0.98, HNO_3
Lemon	6.0	160	874.960	F	PS II	45.75±0.54, HCl
Orange	8.0	160	116.750	L and F	PS II	55.38±1.83, HCl
Bagasse	10.0	180	2.745	F	PSII	54.43±0.78, HCl

*L =Langmuir isotherm, F= Freundlich isotherm, PS II = pseudo-order-second rate kinetics

Table 4.21 Comparison of optimized conditions of different adsorbents for treatment of flashlight wastewater

Adsorbent	**Dose (g)**	**Contact time (min.)**	**q_{max} (mg g^{-1})**	**Isotherm**	**Kinetics**	**Desorption (%) and Eluant (0.1M)**
Sweet lemon	3.5	160	**2840.91**	F	PS II	88.15±1.89, HCl
Lemon	4.0	160	**940.69**	L	PS II	88.98±2.94, HCl
Orange	4.5	180	**512.53**	F	PS II	86.82±1.17, HCl
Bagasse	5.0	140	**12.74**	L	PS II	90.05±0.58, HNO_3

*L =Langmuir isotherm, F= Freundlich isotherm, PS II = pseudo-order-second rate kinetic

4.4 Risk assessment of heavy metals to the environment

It is a very important practice to assess the risk involved with wastewaters of different industries as these have a lot of toxic pollutants including heavy metals. These heavy metals have the tendency to be accumulated into living tissues of nearby vegetation, contaminating the food chain, which may harm the health of humans and other living beings (Hossain al. 2015). Therefore, the study of risk assessment became essential part to avoid such hazardous happenings. Risk assessment was observed by irrigating seeds and plants of some economic crops viz. lady's finger, green moong and tomato with treated tannery and flashlight wastewaters. The potential effects of both wastewaters on growth, yield and metal bioaccumulation in the selected economically plants were tested in pot experiments under greenhouse conditions. The details of the results obtained have been discussed as following-

4.4.1 Seed germination test

Economically important plants i.e. vegetables (lady's finger, sponge gourd, bottle gourd, pumpkin, bitter gourd), legumes and oil yielding seeds (green moong, tomato and rapeseed) and fruit (tomato) were selected for seed germination test in tannery and flashlight wastewaters. The germination tests were performed for 3 days with 50 % dilution of treated wastewater. The reason behind this lie in the fact that due to high concentration of pollutants, the seed used to wrought, so, the experiments were performed by diluting wastewaters by 50%. Among these, lady's finger, tomato and green moong were selected for additional tests based on higher seed germination rate. The results of seed germination test have been summarized in Table 4.22 to 4.25.

Table 4.22 Seed germination(%) of legumes, fruit and oil yielding plants treated with tannery wastewater (TO) by different adsorbents

Seeds	**DAY 1**		**DAY 2**		**DAY 3**	
Control						
Green Moong	53.33±5.77		96.67±5.77		100.00±0.00	
Tomato	13.33±11.57		100.0±0.0		100.00±0.00	
Rapeseed	0.00±0.0		60.0±10.0		73.33±5.77	
	TO	**TO (50%)**	**TO**	**TO (50%)**	**TO**	**TO (50%)**
Green Moong	0.00±0.00	93.33±5.77	0.00±0.00	96.67±5.77	0.00±0.00	100.00±0.00
Tomato	0.00±0.00	80.00±0.00	0.00±0.00	90.00±0.0	0.00±0.00	86.67±5.77
Rapeseed	0.00±0.00	10.00±0.00	0.00±0.00	10.00±0.0	0.00±0.00	13.33±5.77
Sweet lemon peel biochar						
Green Moong	0.00±0.00	100.00±0.00	46.667±5.77	100.00±5.77	50.00±10.00	100.00±0.00
Tomato	0.00±0.00	93.33±5.77	40.00±010.00	93.33±5.774	43.33±5.774	86.67±5.77
Rapeseed	0.00±0.00	6.67±5.77	0.00±0.00	13.33±5.77	13.333±5.77	13.33±5.77
Lemon peel biochar						
Green Moong	0.00±0.00	100.00±0.00	56.66±5.77	100.00±5.77	56.67±5.77	56.667±5.77
Tomato	0.00±0.00	93.33±5.77	46.67±5.77	93.33±5.77	50.00±0.00	50.00±0.00
Rapeseed	0.00±0.00	3.33±5.77	0.00±0.00	0.00±0.00	13.33±5.77	0.00±0.00
Orange peel biochar						
Green Moong	0.00±0.00	13.33±5.77	26.67±5.77	100.00±0.00	33.33±5.77	100.00±0.00
Tomato	0.00±0.00	13.33±5.77	26.67±5.77	96.67±5.77	26.67±5.77	96.67±5.77
Rapeseed	0.00±0.00	0.00±0.00	0.00±0.00	20.00±0.00	0.00±0.00	20.00±0.00

Table 4.23 Seed germination (%) of legumes, fruit and oil yielding plants treated with flashlight wastewater by different adsorbents

Seeds	**Day 1**		**Day 2**		**Day 3**	
	FW	**FW (50%)**	**FW**	**FW (50%)**	**FW**	**FW (50%)**
Sweet lemon peel biochar						
Green Moong	0.00±0.00	26.67±5.77	63.33±15.28	100.00±0.00	63.33±5.774	100.00±0.00
Tomato	0.00±0.00	13.33±5.77	66.67±5.77	93.33±5.77	66.67±5.774	93.33±5.77
Rapeseed	0.00±0.00	0.00±0.00	20.00±5.77	56.67±5.77	20.00±0.00	56.67±5.77
Lemon peel biochar						
Green Moong	0.00±0.00	13.333±5.774	56.67±5.77	100.00±0.00	56.667±5.774	100.00±0.00
Tomato	0.00±0.00	6.67±5.774	43.33±5.77	93.33±5.77	53.333±5.774	93.33±5.77
Rapeseed	0.00±0.00	6.67±5.774	10.00±0.00	53.33±5.77	13.333±5.774	56.67±5.77
Orange peel biochar						
Green Moong	0.00±0.00	23.33±5.774	40.00±0.00	100.00±0.00	56.67±5.77	100.00±0.00
Tomato	0.00±0.00	20.00±0.00	43.33±5.77	93.333±5.77	43.33±5.77	93.33±5.77
Rapeseed	0.00±0.00	0.00±5.774	3.33±5.77	50.00±0.00	6.67±5.77	46.67±5.77

Table 4.24 Seed germination (%) of vegetables treated with tannery wastewater by different adsorbents

Seeds	Day 1	Day 2	Day 3
Control			
lady's finger	43.33±5.774	63.33±5.77	96.67±5.77
sponge gourd	16.67±5.774	46.67±5.77	96.67±5.77
bottle gourd	13.33±5.774	30.00±0.00	96.67±5.77
pumpkin	20.00±0.00	46.67±5.77	93.33±5.77
bitter gourd	13.33±5.774	26.67±5.77	90.00±0.00
Sweet lemon peel biochar			
lady's finger	0.00±0.00	16.67±5.77	76.67±5.77
sponge gourd	0.00±0.00	66.67±5.77	43.33±5.77
bottle gourd	0.00±0.00	0.00±0.00	0.00±0.00
pumpkin	0.00±0.00	0.00±0.00	23.33±5.77
bitter gourd	0.00±0.00	66.667±11.55	13.33±5.77
Lemon peel biochar			
lady's finger	0.00±0.00	83.33±5.774	73.33±20.82
sponge gourd	0.00±0.00	20.00±10.00	53.33±5.77
bottle gourd	0.00±0.00	10.00±0.00	10.00±10.00
pumpkin	0.00±0.00	16.67±11.55	36.67±5.77
bitter gourd	0.00±0.00	13.33±5.77	20.00±10.00
Orange peel biochar			
lady's finger	0.00±0.00	66.67±11.55	93.33±5.77
sponge gourd	0.00±0.00	16.67±5.77	43.33±5.77
bottle gourd	0.00±0.00	0.00±0.00	3.33±5.77
pumpkin	0.00±0.00	66.667±5.77	20.00±5.77
bitter gourd	0.00±0.00	0.00±0.00	3.333±5.77
Tannery wastewater (50% dilution)			
lady's finger	0.00±0.00	66.67±11.55	90.00±5.77
sponge gourd	0.00±0.00	16.67±5.77	16.67±5.77
bottle gourd	0.00±0.00	0.00±0.00	3.33±5.77
pumpkin	0.00±0.00	66.67±5.77	16.67±5.77
bitter gourd	0.00±0.00	0.00±0.00	6.67±5.77

Table 4.25 Seed germination (%) of vegetables treated with flashlight wastewater by different adsorbents

Seeds	Day 1	Day 2	Day 3
Sweet lemon peel biochar			
lady's finger	16.667±5.774	66.667±5.77	76.67±5.77
sponge gourd	13.333±5.774	53.333±5.77	43.33±5.77
bottle gourd	13.333±5.774	56.667±5.77	0.00±0.00
pumpkin	3.333±5.774	26.667±5.77	23.33±5.77
bitter gourd	16.667±5.774	16.667±5.77	10.00±10.00
Lemon peel biochar			
lady's finger	86.67±23.09	96.67±5.77	100.0±0.00
sponge gourd	0.00±0.00	6.67±5.77	53.33±5.77
bottle gourd	0.00±0.00	13.33±5.77	26.67±20.82
pumpkin	0.00±0.00	6.67±5.77	33.33±15.28
bitter gourd	0.00±0.00	6.67±5.77	23.33±15.28
Orange peel biochar			
lady's finger	0.00±0.00	53.33±5.77	90.00±5.77
sponge gourd	0.00±0.00	16.67±5.77	16.67±5.77
bottle gourd	0.00±0.00	10.00±10.0	3.33±5.77
pumpkin	0.00±0.00	13.33±5.77	16.67±5.77
bitter gourd	0.00±0.00	10.00±10.00	6.67±5.77
Flashlight wastewater (50% dilution)			
lady's finger	13.33±5.77	53.33±5.77	93.33±5.77
sponge gourd	0.00±0.00	6.67±5.77	43.33±5.77
bottle gourd	0.00±0.00	0.00±0.00	3.33±5.77
pumpkin	0.00±0.00	13.33±5.77	20.00±0.00
bitter gourd	0.00±0.00	0.00±0.00	3.33±5.77

As seen from Table 4.22 to 4.25, green moong and tomato among legumes, fruit and oil yielding plants, and lady's finger among vegetables exhibited maximum germination index at day 3. In initial two days, the germination rates of all seeds were found to be in the range of 0.00 to 66.67 %. Green moong, tomato and lady's finger represented 100 & 100, 86.67 & 93.33 and 96.67 & 76.67 % seed germination by SLPB treated wastewater at day 3. Similarly, seeds of green moong, tomato and lady's finger irrigated with LPB treated the wastewater of tannery and flashlight

wastewaters represented 76.67 & 100, 56.67 & 50 % and 100 & 53.33 % of germination index. Similar results were also obtained for OPB treated wastewater with 100 & 96.67, 100 & 93.33 and 90 % of germination index for seeds of green moong, tomato and lady's finger, respectively. Furthermore, seeds were found to wrought in the treated wastewater of both industries due to higher concentrations salts and other pollutants which affected the germination index adversely. None of seeds were germinated in such conditions, therefore, experiments were performed with 50 % of dilution of treated wastewater afterwards. About 90 and 93.33% of germination index was observed with 50% diluted tannery and flashlight wastewaters as compared to 0 % for lady's finger seeds for both wastewaters without dilution. Moreover, tap water was used as control for conducting seed germination experiments, which demonstrated 100 % germination rate at day 3. Other seeds i.e. sponge gourd, bottle gourd, pumpkin, bitter gourd and rap seeds were not able to tolerate the concentrations of both wastewaters. Thus, lady's finger, tomato and green moong were selected for pot experiments in greenhouse effect to explore the effect of residue Cr and Pb onto the growth parameters and its bioaccumulation into the plants. Results of the present study were in good agreement with Asfaw et al. (2012) who reported maximum seed germination of tomato plants in the tannery wastewater dilute up to 25% and least in undiluted wastewater.

4.4.2 Effect of treated wastewaters on growth parameters of lady's finger, tomato and green moong

The growth parameters (root length, no. of roots, shoot length, no. of leaves, fresh and dry weight) of the selected plants and bioaccumulation of heavy metals in the plants were observed on 15, 30, 60, 90 and 120 days after seed sowing (DAS). The tap water was used as control. Details of the effect of treated wastewaters on the bioaccumulation of HMs and plant growth parameter have been given below-

4.4.2.1 Effect on lady's finger *(Abelmoschus esculentus)*

Lady's finger is an important economic crop, which are grown in a larger number all over the world. The effect of treated tannery and flashlight wastewaters irrigation on the growth parameters and bioaccumulation of Cr and Pb 15, 30, 60, 90 and 120 DAS have been presented in Table 4.26 & 4.27. All of the growth parameters including

root length, no. of roots, shoot length, number of leaves, fresh and dry weight showed significant decrease in comparison to control after 15, 30, 60, 90 and 120 DAS. At fruiting time (120 DAS), decrease in the root length was 57.77, 88.85, 85.92 & 89.44 % , in number of roots 39.39, 52.52, 40.40 & 40.40 %, in shoot length 9.93, 11.50, 14.51 & 29.41 %, in number of leaves 20.22 % (no change for LPB), in fresh weight 53.46, 4998, 54.33 & 66.49 %, in dry weight 48.58, 47.37, 50.20 & 10.93 % and no. of fruits 42.79 (SLPB, OPB and BB) & 49.795 (LPB) %, respectively recorded in comparison to control for SLPB, LPB, OPB and BB treated tannery wastewater irrigation. In the same way, flashlight treated wastewaters irrigation also recorded retardation in the growth parameters. Decrease in root length was 39.58, 50.73, 46.93 & 53.66 % , in number of roots 40.40, 47.48, 41.42 & 56.58 %, in shoot length 6.93, 0, 10.46 & 16.86 %, in number of leaves 0, 0, 20.22 & 20.22 %, in fresh weight 20.25, 49.65, 47.44 & 58.90 %, in dry weight 10.93, 40.49, 47.37 & 24.29 % and in no. of fruits 57.08, 57.08, 42.79 & 85.71 %, respectively in comparison to control for SLPB, LPB, OPB and BB treated flashlight wastewater irrigation.

Further, the concentration of Cr and Pb in SLPB, LPB, OPB and BB treated wastewaters were found to be very low as 0.08, 0.33, 0.51 & 0.99, and 0.07, 0.29, 0.33 & 0.59 mg L^{-1} respectively. When these treated wastewaters were used to irrigate lady's finger plants, only 0.005, 0.004, 0.013 & 0.035 mg L^{-1} and 0.003, 0.006, 0.009 & 0.009 mg L^{-1}, respectively of Cr and Pb were found to be bio-accumulated. Among these, only BB treated tannery wastewater transferred maximum amount of Cr into the plant followed by OPB, LPB and minimum by SLPB. Similar trend was also reported for flashlight irrigated wastewater. The bio-accumulated amount in lady's finger was found to be very low except for plants of BB treated tannery wastewater.

Table 4.26 Effect of tannery wastewater treated by different biochars on growth parameters of lady's finger *(Abelmoschus esculentus)*

SN	Days	Parameters	Control	Sweet Lemon	Lemon	Orange	Bagasse
1	15	**Root length (cm)**	4.63±0.85	3.17±0.35	3.47±0.35	3.40±0.56	2.77±0.15
	30		4.23±0.25	3.87±0.21	4.07±0.32	4.00±0.20	3.33±0.31
	60		11.37±1.03	8.00±0.46	8.07±0.15	7.97±0.47	6.20±0.30
	90		13.83±1.53	5.70±0.44	2.27±0.21	1.50±0.30	1.43±0.42
	120		11.37±1.03	4.80±0.36	1.27±0.21	1.60±0.17	1.20±0.27
2	15		11.33±1.16	8.33±1.16	10.33±0.58	10.00±2.65	8.33±1.53

	30	**No. of roots**	22.00±2.00	17.00±1.732	15.67±0.58	13.67±1.53	14.67±1.16
	60		34.33±4.04	31.33±1.16	31.67±1.53	31.33±3.22	27.33±2.08
	90		34.33±1.16	24.33±2.08	19.67±1.54	19.67±2.08	22.33±3.07
	120		33.00±2.646	20.00±2.00	15.67±1.53	19.67±2.08	19.667±5.69
3	15		13.57±1.36	14.70±0.62	12.83±1.19	14.57±0.65	12.27±2.57
	30	**Shoot**	21.13±0.85	18.33±1.11	18.13±0.21	17.43±2.90	22.53±3.47
	60	**length(cm)**	24.93±1.36	22.17±1.53	22.50±2.36	20.58±1.22	19.40±2.03
	90		27.93±2.50	23.07±2.53	21.60±2.54	21.30±1.71	18.30±3.69
	120		25.50±1.18	22.97±3.12	22.57±1.50	21.80±0.82	18.00±1.87
4	15		4.33±0.58	3.33±0.58	4.00±1.00	4.33±0.58	3.33±0.58
	30	**No. of leaves**	4.67±0.58	6.67±0.58	5.33±0.58	5.333±0.58	5.67±1.16
	60		2.33±1.16	2.33±0.58	2.33±0.58	1.67±0.58	1.333±0.58
	90		2.33±0.58	1.67±0.58	2.67±0.58	2.33±0.58	1.67±0.58
	120		1.667±0.58	1.33±0.58	1.67±0.58	1.33±0.58	1.33±0.58
5	15		1.60±0.07	0.98±0.07	1.16±0.08	1.25±0.23	0.91±0.06
	30	**Fresh weight**	3.12±0.52	2.56±0.34	2.45±0.12	1.48±0.27	2.76±0.42
	60	**(g)**	2.11±0.35	2.52±0.23	2.14±0.08	1.52±0.08	1.41±0.02
	90		2.84±0.35	1.17±0.07	1.34±0.11	1.22±0.11	0.80±0.13
	120		2.99±0.86	1.39±0.22	1.50±0.26	1.37±0.40	1.00±0.13
6	15		0.18±0.04	0.09±0.01	0.09±0.01	0.13±0.02	0.08±0.01
	30	**Dry weight**	0.31±0.06	0.25±0.05	0.28±0.04	0.15±0.03	0.20±0.07
	60	**(g)**	0.27±0.03	0.24±0.02	0.19±0.01	0.13±0.01	0.13±0.01
	90		0.19±0.03	0.12±0.03	0.13±0.02	0.12±0.01	0.32±0.18
	120		0.25±0.06	0.13±0.02	0.13±0.02	0.12±0.03	0.22±0.04
7	15		0.00±0.00	0.00±0.00	0.00±0.00	0.00±0.00	0.00±0.00
	30	**Buds/fruits**	0.00±0.00	0.00±0.00	0.00±0.00	0.00±0.00	0.00±0.00
	60		2.33±0.58	1.67±0.58	1.67±0.58	1.667±0.577	1.33±0.58
	90		3.00±1.00	1.67±0.58	1.33±0.58	2.00±1.00	1.33±0.58
	120		2.33±0.58	1.33±0.58	1.67±1.53	1.333±0.577	1.33±1.16
Cr (mg L^{-1}) in treated wastewater			0.00±0.00	0.08±0.01	0.33±0.03	0.51±0.01	0.99±0.05
Cr (mg kg^{-1})) in plant biomass			0.00±0.00	0.01±0.00	0.004±0.00	0.01±0.00	0.04±0.01

Table 4.27 Effect of flashlight wastewater treated by different biochars on growth parameters of lady's finger (*Abelmoschus esculentus*)

S. No.	Days	Parameters	Control	Sweet Lemon	Lemon	Orange	Bagasse
1	15		4.63±0.85	3.63±0.15	2.80±0.53	2.80±0.30	2.43±0.21
	30	**Root**	4.23±0.25	4.93±0.47	3.40±0.27	3.47±0.25	3.83±0.35
	60	**length**	11.37±1.03	8.27±0.21	9.40±0.85	7.97±0.68	8.00±0.56
	90	**(cm)**	13.83±1.53	9.43±0.97	7.50±0.89	6.50±0.61	5.53±0.25
	120		11.37±1.03	6.87±0.31	5.60±0.56	6.03±0.80	5.267±0.416
2	15		11.33±1.16	10.33±2.08	8.33±0.58	8.33±0.58	7.67±0.58
	30	**No. of**	22.00±2.00	21.33±1.16	18.67±1.16	17.67±2.31	16.33±1.53
	60	**roots**	34.33±4.04	30.67±1.16	29.33±1.16	27.67±1.53	26.33±2.31
	90		34.33±1.16	22.67±2.31	21.33±3.06	23.33±1.53	17.33±2.08
	120		33.00±2.65	19.67±1.53	17.33±2.08	19.33±3.06	14.33±4.04
3	15		11.93±1.53	15.33±2.52	66.00±5.74	18.00±2.00	17.67±1.16
	30	**Shoot**	21.13±0.85	24.07±1.38	21.50±0.89	21.33±1.66	20.37±0.81
	60	**length(cm)**	24.60±1.90	22.83±0.95	25.40±2.38	23.53±1.74	22.13±1.95

	90		25.93±4.12	22.70±2.26	25.90±2.43	22.93±3.12	21.67±0.97
	120		25.50±1.18	23.73±1.97	25.50±0.91	22.83±2.52	21.20±3.01
4	15	**No. of leaves**	4.33±0.58	3.33±0.58	3.33±0.58	3.67±0.58	4.33±0.58
	30		4.67±0.58	6.33±0.58	5.00±1.00	4.67±0.58	4.33±0.58
	60		2.33±1.16	2.33±1.16	1.67±1.53	2.33±1.16	2.00±1.73
	90		2.67±0.58	2.33±1.16	1.33±0.58	1.33±0.58	1.33±0.58
	120		1.67±0.58	1.67±0.58	1.67±0.58	1.33±0.58	1.33±0.58
5	15	**Fresh weight (g)**	1.60±0.07	0.92±0.20	1.40±0.30	1.28±0.04	1.23±0.03
	30		3.12±0.52	4.91±0.85	2.43±0.61	1.36±0.10	1.31±0.03
	60		2.10±0.35	3.18±0.25	3.09±0.39	2.78±0.21	2.66±0.27
	90		3.18±0.25	3.09±0.39	2.78±0.21	2.66±0.27	1.19±0.05
	120		2.99±0.86	2.39±0.34	1.51±0.26	1.57±0.26	1.23±0.18
6	15	**Dry weight (g)**	0.18±0.04	0.07±0.02	0.12±0.05	0.14±0.01	0.10±0.02
	30		0.31±0.06	0.32±0.06	0.24±0.07	0.11±0.01	0.13±0.02
	60		0.19±0.03	0.19±0.01	0.13±0.01	0.13±0.02	0.11±0.01
	90		0.26±0.05	0.26±0.06	0.27±0.02	0.25±0.03	0.11±0.01
	120		0.25±0.06	0.22±0.02	0.15±0.01	0.13±0.02	0.19±0.06
7	15	**Buds/fruits**	0.00±0.00	0.00±0.00	0.00±0.00	0.00±0.00	0.00±0.00
	30		0.00±0.00	0.33±0.58	0.33±0.58	0.67±0.58	0.00±0.00
	60		2.67±0.58	2.33±1.16	1.67±0.58	1.67±0.58	1.67±0.58
	90		3.00±1.00	1.33±0.58	1.33±0.58	1.00±1.00	0.00±0.00
	120		2.33±0.58	1.00±1.00	1.00±1.00	1.33±0.58	0.33±0.58
Pb (mg L^{-1}) in treated wastewater			0.00±0.00	0.07±0.01	0.29±0.03	0.33±0.03	0.59±0.01
Pb (mg kg^{-1})) in plant biomass			0.00±0.00	0.00±0.00	0.01±0.00	0.01±0.00	0.01±0.00

Figure 4.28 Comparison of effect of tannery wastewater treated by different adsorbents on lady's finger (*Abelmoschus esculentus*) by control (TO = tannery wastewater; SL= sweet lemon; L= lemon and O= orange)

Figure 4.29 Comparison of effect of flashlight wastewater treated by different adsorbents on lady's finger (*Abelmoschus esculentus*) by control (BO= flashlight wastewater; SL= Sweet lemon; L= lemon and O= orange)

4.4.2.2 Effect on tomato *(Solanum lycopersicum)*

Similar trend of significant decrease in growth parameters like that of lady's finger was also observed on tomato also after 15, 30, 60, 90 and 120 DAS in comparison to control (Table 4.28 & 4.29). At fruiting time, decrease in the root length was 27.08, 30.95, 33.98 & 46.54 %, in number of roots 7.23, 2.67, 3.04 & 16.0 %, in shoot length 33.74, 30.21, 29.76 & 33.70 %, in number of leaves 42.87, 35.69, 32.15 & 21.44 %, in fresh weight 19.86, 21.14, 22.57 & 5370 %, in dry weight 32.24, 40.58, 45.16 & 63.59 % and in no. of fruits 30.44, 39.13, 52.17 & 52.17 %, respectively for SLPB, LPB, OPB and BB treated tannery wastewater irrigation in comparison to the control. Similarly, flashlight treated wastewater irrigation also resulted in poor growth and development of tomato plants. Decrease in root length was 12.77, 23.16, 30.30 & 36.58 %, in number of roots 18.25, 11.03, 18.25 & 18.25 %, in shoot length 17.6, 13.90, 27.69 & 27.24 %, in number of leaves 42.87, 14.26, 24.97 & 21.44 %, in fresh weight 19.86 (for all) %, in dry weight 37.30, 9.99, 13.38 & 12.49 % and in no. of fruits 78.26, 56.53, 73.91 & 73.91 %, respectively in comparison to control for SLPB, LPB, OPB and BB treated flashlight wastewater irrigation.

Further, the concentration of Cr and Pb in biosorbent treated wastewater were found to be very low same as that of irrigation wastewater utilized for lady's finger. After irrigation to tomato plants, only 0.00, 0.01, 0.01 & 0.04 mg L^{-1} and 0.00, 0.01, 0.01 & 0.01 mg L^{-1}, respectively of Cr and Pb were found to be present in the plant biomass. Among these, BB and OPB treated tannery wastewater transferred higher amount of Cr into the plant whereas, LPB and SLPB treated tannery wastewater irrigation transferred a very low concentration into the plant biomass. The bio-accumulated amount of Cr and Pb in tomato plants was very little except for plants irrigated with BB and OPB treated tannery wastewater.

Table 4.28 Effect of tannery wastewater treated by different biochars on growth parameters of tomato (*Solanum lycopersicum*)

SNo.	Days	Parameters	Control	Sweet Lemon	Lemon	Orange	Bagasse
1	15	**Root length (cm)**	2.63±0.15	1.43±0.12	1.13±0.06	2.37±0.32	2.150±0.09
	30		5.17±0.40	3.53±1.00	3.93±0.38	4.17±0.35	4.033±0.21
	60		16.83±1.7	11.13±1.74	11.07±0.51	12.13±2.12	10.633±0.85
	90		16.60±0.72	14.60±3.58	12.60±1.85	11.67±1.68	10.767±0.46
	120		15.40±1.31	11.23±1.06	10.63±0.91	10.17±1.60	8.233±1.03
2	15	**No. of roots**	11.67±0.58	10.33±0.58	9.67±0.58	8.00±1.73	8.33±1.16
	30		25.67±2.08	20.33±2.52	22.00±3.00	22.67±4.62	23.00±4.58
	60		51.67±3.51	43.00±2.65	50.00±2.65	52.00±2.65	44.67±3.51
	90		63.67±3.79	55.00±3.61	56.67±2.08	53.33±4.16	45.33±4.51
	120		57.67±2.52	51.333±3.51	55.33±3.06	55.00±4.36	43.67±4.73
3	15	**Shoot length (cm)**	12.13±0.55	8.53±0.45	9.37±0.32	10.43±0.40	10.23±0.25
	30		30.03±4.10	28.40±4.19	24.33±1.94	27.23±3.73	23.57±1.27
	60		39.17±3.11	29.97±2.25	32.83±2.52	35.03±4.38	33.57±1.50
	90		60.57±1.95	37.53±1.95	36.77±3.98	41.73±3.27	38.20±3.16
	120		59.47±3.66	39.40±3.01	41.50±3.32	41.77±2.97	39.43±0.75
	15	**No. of leaves**	9.67±0.58	10.67±0.58	9.33±0.58	7.33±0.58	8.33±0.58
	30		8.33±1.53	7.33±0.58	6.33±0.58	7.33±1.16	6.33±0.58
	60		10.33±1.53	8.33±1.53	9.67±1.53	8.67±1.16	8.33±0.58
	90		10.67±1.53	6.68±1.16	7.67±1.16	8.33±0.58	7.33±1.53
	120		9.33±2.31	5.33±0.56	6.00±0.00	9.33±0.58	7.33±1.16
5	15	**Fresh weight(g)**	0.85±0.16	0.78±0.12	0.32±0.06	0.46±0.08	0.53±0.03
	30		6.78±1.85	3.69±0.55	4.43±0.19	4.69±0.47	4.3±0.97
	60		20.59±1.07	10.50±1.92	17.31±1.87	12.24±1.26	11.43±0.77
	90		26.33±0.86	13.93±1.32	12.47±1.00	12.57±1.90	8.10±0.85
	120		23.47±1.42	16.73±1.21	16.47±2.63	16.17±2.16	9.67±0.80
6	15	**Dry weight (g)**	0.07±0.03	0.08±0.0	0.04±0.01	0.05±0.01	0.04±0.01
	30		0.62±0.16	0.35±0.11	0.29±0.04	0.49±0.18	0.50±0.13
	60		1.77±0.20	0.97±0.18	1.64±0.24	1.14±0.08	1.05±0.07
	90		2.03±0.21	1.30±0.12	1.19±0.05	1.15±0.10	0.78±0.10
	120		2.56±0.40	1.61±0.23	1.52±0.25	1.41±0.09	0.93±0.12
7	15	**Buds/Flowers**	0.00±0.00	0.00±0.00	0.00±0.00	0.00±0.00	0.00±0.00
	30		0.667±0.577	0.00±0.00	0.00±0.00	0.00±0.00	0.00±0.00

	60		4.667±1.155	3.67±0.58	3.67±1.16	2.33±0.58	3.33±1.16
	90		7.667±0.577	5.33±0.58	5.33±0.58	4.33±0.58	3.33±1.53
	120		7.667±1.528	5.33±0.58	4.67±0.58	3.67±1.16	3.67±0.58
Cr (mg L^{-1}) in treated wastewater			0.00±0.00	0.08±0.0	0.00±0.00	0.51±0.01	0.99±0.05
Cr (mg kg^{-1}) in plant biomass			0.000±0.00	0.00±0.00	0.01±0.01	0.01±0.00	0.04±0.01

Table 4.29 Effect of flashlight wastewater treated by different biochars on growth parameters of tomato (*Solanum lycopersicum*)

S.No.	**Days**	**Parameters**	**Control**	**Sweet Lemon**	**Lemon**	**Orange**	**Bagasse**
1	15	**Root length (cm)**	2.53±0.25	2.77±0.38	2.33±0.23	2.60±0.17	2.23±0.15
	30		5.17±0.40	5.00±0.36	5.00±0.8	4.27±0.21	3.67±0.38
	60		16.83±1.65	15.73±0.68	16.60±0.46	15.63±0.76	14.40±0.82
	90		16.60±0.72	15.60±1.06	16.40±1.06	11.63±0.91	12.23±0.81
	120		15.40±1.31	13.43±1.16	11.83±0.67	10.73±1.01	9.77±0.67
2	15	**No. of roots**	11.67±0.58	8.33±0.58	8.33±0.58	8.00±1.732	7.33±0.58
	30		25.67±2.08	21.67±1.53	18.67±0.58	21.00±1.00	18.33±0.58
	60		51.67±3.51	48.67±3.22	51.00±3.61	50.00±4.36	51.33±4.04
	90		63.67±3.79	57.33±3.06	58.00±6.08	52.00±3.61	47.33±5.03
	120		57.67±2.52	41.67±3.51	48.00±3.00	41.67±4.04	41.67±6.51
3	15	**Shoot length(cm)**	12.13±0.55	12.03±0.38	12.03±0.74	12.63±0.15	10.83±0.35
	30		30.03±4.10	27.63±2.08	19.97±3.14	24.07±1.91	23.43±0.86
	60		39.17±3.11	26.40±0.58	32.90±0.72	32.37±0.23	29.40±0.62
	90		60.57±1.95	48.60±0.58	53.97±1.46	47.67±1.56	44.30±3.35
	120		59.47±3.66	49.00±3.15	51.20±2.46	43.00±2.88	43.27±4.29
4	15	**No. of leaves**	9.67±0.56	8.33±0.58	8.33±0.58	9.33±0.58	8.67±0.58
	30		8.33±1.53	6.67±0.58	5.33±0.58	6.00±1.00	5.33±0.58
	60		10.33±1.53	8.67±0.58	9.33±0.58	9.00±1.73	7.33±1.53
	90		10.67±1.53	10.33±1.53	9.67±2.08	8.33±0.58	9.67±2.08
	120		9.33±2.31	8.00±2.00	7.00±1.00	5.67±0.58	7.33±1.53
5	15	**Fresh weight(g)**	0.85±0.16	0.92±0.03	0.87±0.02	1.02±0.03	0.84±0.03
	30		6.78±1.85	5.26±1.12	5.38±0.28	2.95±0.34	1.48±0.30
	60		20.59±1.07	7.34±0.34	9.10±0.54	7.41±0.57	8.81±0.43
	90		26.33±0.86	20.73±2.25	18.82±1.89	15.83±1.16	15.500±1.00
	120		23.47±1.42	22.89±1.46	20.88±1.58	17.87±0.93	23.300±3.21
6	15	**Dry weight (g)**	0.07±0.03	0.06±0.01	0.07±0.01	0.06±0.01	0.05±0.01
	30		0.62±0.16	0.46±0.08	0.50±0.03	0.28±0.04	0.13±0.03
	60		1.77±0.20	0.72±0.03	0.87±0.04	0.74±0.04	0.84±0.02
	90		2.03±0.21	1.86±0.12	1.69±0.16	1.46±0.18	1.37±0.17
	120		2.56±0.40	2.31±0.18	2.22±0.11	1.59±0.21	2.24±0.33
7	15	**Buds/fruits**	0.00±0.00	0.00±0.00	0.00±0.00	0.00±0.00	0.00±0.00
	30		0.67±0.58	0.00±0.00	0.00±0.00	0.00±0.00	0.00±0.00
	60		4.67±1.16	2.67±1.16	1.33±0.58	4.00±1.73	1.67±0.58
	90		7.67±0.58	3.67±1.53	3.67±1.53	2.67±1.16	2.67±0.58
	120		7.67±1.53	1.67±0.58	3.33±0.58	2.00±1.00	2.00±1.00
Pb (mg L^{-1}) in treated wastewater			0.00±0.00	0.07±0.01	0.29±0.03	0.33±0.03	0.59±0.01
Pb (mg kg^{-1})) in plant biomass			0.00±0.00	0.00±0.00	0.01±0.00	0.01±0.00	0.01±0.00

Figure 4.30 Comparison of effect of tannery wastewater treated by different adsorbents on tomato (*Solanum lycopersicum*) by control (Details are same as Fig. 5.28)

Figure 4.31 Comparison of effect of flashlight wastewater treated by different adsorbents on tomato (*Solanum lycopersicum*) by control (Details are same as Fig. 5.29)

4.4.2.3 Effect on green moong (*Vigna radiata*)

Decrease in growth parameters similar to lady's finger and tomato was also observed on green moong after 15, 30, 60, 90 and 120 DAS in comparison to control (Table 4.30 & 4.31). At fruiting time, decrease in the root length was 37.34, 22.79, 39.55 %, in number of roots 30.51, 15.25 & 11.88 %, in shoot length 19.14, 21.76 & 24.93 %,

in number of leaves 40.01, 20.22 & 40.01 %, in fresh weight 25.77, 55.27 & 52.96 %, in dry weight 48.64, 54.09 & 53.18 % and in no. of fruits 20.22, no change & 20.21 %, respectively for SLPB, LPB and OPB treated tannery wastewater irrigation in comparison to the control. Similarly, flashlight treated wastewater irrigation also reported decrease in growth and development of green moong plants. Decrease in root length was 35.13, 18.04 & 34.49 %, in number of roots 15.25, 15.25 & 13.56 %, in shoot length 4.55, 11.57 & 1.93 %, no change in number of leaves, in fresh weight 26.65, 26.92 & 61.42%, in dry weight 28.63, 27.27 & 58.18 % and in no. of fruits 20.22, 20.22 & 40.01 %, respectively in comparison to control for SLPB, LPB, OPB and BB treated flashlight wastewater irrigation. Whereas, the plants irrigated with BB treated tannery and flashlight wastewater died within 90 DAS.

Further, the concentration of Cr and Pb in biosorbent treated wastewater swere found to be very low same as that of irrigation wastewaters used for lady's finger and tomato. Only 0.004, 0.005 & 0.008 mg L^{-1} and 0.001, 0.001 & 0.002 mg L^{-1}, respectively of Cr and Pb were found to be present in the green moong plants, after irrigation of SLPB, LPB and OPB treated tannery and flashlight wastewaters. Although, plants irrigated with BB treated wastewaters died within 90 DAS, but OPB, LPB and SLPB treated tannery and flashlight wastewaters irrigation transferred a very low concentration into the plant biomass. Thus, the bio-accumulated amount of both HMs in green moong plants was very low except for plants irrigated with BB. The results were in good agreement with Javaid et al. (2000) who reported retardation in growth and pod yield of green moong grown in soil contaminated by tannery wastewater.

Table 4.30 Effect of tannery wastewater treated by different biochars on growth parameters of green moong (*Vigna radiata*)

S. No.	Days	Parameters	Control	Sweet Lemon	Lemon	Orange	Bagasse
1	15	**Root length (cm)**	2.80±0.30	2.63±0.38	2.70±0.35	2.17±0.31	2.40±0.46
	30		4.70±0.35	2.27±0.21	4.30±1.15	4.40±1.15	3.83±0.25
	60		9.27±0.68	7.57±0.50	7.93±.67	9.07±0.45	8.63±0.51
	90		12.40±1.15	7.23±0.81	8.20±0.30	6.80±0.87	dead
	120		10.53±0.70	6.60±1.25	8.13±2.20	6.37±2.04	dead
2	15	**No. of roots**	10.33±1.16	8.667±1.53	7.33±0.58	9.67±0.58	9.67±2.08
	30		18.00±3.00	17.33±1.16	14.67±1.53	19.00±1.00	19.33±1.16
	60		23.67±1.53	22.33±2.52	22.00±2.65	21.00±1.00	20.33±1.53

	90		20.33±1.53	13.67±2.52	20.67±3.06	20.00±2.00	dead
	120		19.67±4.51	13.67±3.22	16.67±3.22	17.33±4.16	dead
3	15	**Shoot length (cm)**	21.10±0.56	18.40±1.87	13.70±1.23	20.13±0.35	18.27±0.42
	30		22.60±0.56	17.60±0.95	23.60±1.412	21.00±0.78	18.67±1.39
	60		25.40±0.27	21.50±4.58	23.07±2.30	27.70±1.04	26.67±0.93
	90		25.70±0.44	20.87±2.10	18.73±2.03	18.10±1.35	dead
	120		24.20±1.57	19.57±0.95	18.93±1.38	18.17±1.53	dead
	15	**No. of leaves**	6.33±0.58	6.33±0.58	5.00±1.00	6.67±0.58	5.33±1.16
	30		7.67±2.08	6.00±1.00	6.00±1.00	5.00±1.00	4.67±1.16
	60		4.33±0.58	4.33±0.58	4.00±1.00	3.33±0.58	3.67±0.58
	90		2.33±0.58	1.67±0.58	1.33±0.58	1.333±0.578	dead
	120		1.67±0.58	1.00±1.00	1.33±0.58	1.00±1.00	dead
5	15	**Fresh weight(g)**	0.85±0.18	1.06±0.06	0.47±0.09	1.22±0.15	0.960±0.08
	30		1.98±0.19	1.42±0.07	3.03±0.14	2.59±0.50	1.803±0.04
	60		3.29±0.75	2.39±0.17	2.60±0.20	2.68±0.18	2.760±0.24
	90		2.50±0.30	0.95±0.13	1.03±0.13	1.15±0.13	dead
	120		2.60±0.27	1.19±0.20	1.16±0.09	1.23±0.27	dead
6	15	**Dry weight (g)**	0.12±0.03	0.13±0.02	0.04±0.02	0.17±0.02	0.11±0.09
	30		0.38±0.03	0.22±0.05	0.49±0.04	0.48±0.11	0.30±0.05
	60		0.27±0.06	0.23±0.02	0.24±0.03	0.26±0.01	0.26±0.02
	90		0.22±0.03	0.09±0.01	0.123±0.05	0.11±0.01	dead
	120		0.22±0.03	0.11±0.02	0.10±0.01	0.10±0.01	dead
7	15	**Buds/fruits**	0.00±0.00	0.00±0.00	0.00±0.00	0.00±0.00	0.00±0.00
	30		2.00±1.73	0.67±0.58	0.33±0.58	1.00±1.00	1.67±0.58
	60		3.67±0.58	3.33±0.58	3.00±1.00	3.67±0.58	3.33±0.58
	90		2.33±0.58	1.67±0.58	2.00±1.00	1.67±0.58	dead
	120		1.67±0.58	1.33±0.58	1.67±0.58	1.33±0.58	dead
Cr (mg L^{-1}) in treated wastewater			0.00±0.00	0.084±0.01	0.33±0.03	0.51±0.01	0.99±0.05
Cr (mg kg^{-1}) in plant biomass			0.00±0.00	0.00±0.00	0.01±0.00	0.01±0.00	dead

Table 4.31 Effect of flashlight wastewater treated by different biochars on growth parameters of green moong (*Vigna radiata*)

S. No.	Days	Parameters	Control	Sweet Lemon	Lemon	Orange	Bagasse
1	15	**Root length (cm)**	2.80±0.30	3.43±0.21	3.50±0.30	2.73±0.21	2.167±0.31
	30		4.70±0.35	2.70±0.27	3.43±0.21	3.37±0.38	3.167±0.35
	60		9.267±0.681	6.40±0.17	8.97±1.10	8.63±0.42	8.100±0.70
	90		12.40±1.15	7.30±0.78	10.33±0.91	7.30±0.56	dead
	120		10.53±0.70	6.83±1.46	8.63±2.14	6.90±1.70	dead
2	15	**No. of roots**	10.33±1.16	10.33±0.58	7.33±0.58	7.33±1.16	7.67±1.16
	30		18.00±3.00	15.00±2.65	14.00±1.732	16.33±1.53	13.00±1.73
	60		23.67±1.53	17.33±2.08	17.667±2.082	18.67±3.22	16.67±1.53
	90		20.33±1.53	16.33±1.53	22.00±3.00	17.33±2.08	dead
	120		19.67±4.51	16.67±2.89	16.67±5.03	17.00±2.65	dead
3	15	**Shoot length(cm)**	21.10±0.56	15.57±1.86	20.97±0.42	22.07±0.61	21.40±0.92
	30		22.60±0.56	26.60±1.55	22.37±0.71	24.13±2.12	21.40±0.76
	60		25.40±0.27	21.80±0.30	23.03±0.50	26.733±1.55	23.87±2.28
	90		25.70±0.44	21.10±1.87	24.43±2.16	22.200±2.04	dead
	120		24.20±1.57	23.10±2.55	21.40±0.92	23.733±0.68	dead

4	15	**No. of leaves**	6.33±0.58	5.67±0.58	5.67±0.58	5.67±0.58	5.67±0.58
	30		7.667±2.08	6.33±0.58	5.67±0.58	5.33±0.58	4.33±0.58
	60		4.33±0.58	3.33±0.58	4.33±0.58	3.33±1.53	3.67±1.53
	90		2.33±0.58	1.67±0.58	1.67±0.58	1.67±0.58	dead
	120		1.67±0.58	1.67±0.58	1.67±0.58	1.00±1.00	dead
5	15	**Fresh weight (g)**	0.85±0.18	0.90±0.19	0.71±0.18	0.75±0.11	0.82±0.15
	30		1.98±0.19	2.42±0.24	2.03±0.41	2.06±0.07	1.73±0.40
	60		3.29±0.75	2.40±0.23	2.22±0.13	2.89±0.29	2.46±0.18
	90		2.50±0.30	2.27±0.21	1.78±0.20	0.83±0.23	dead
	120		2.60±0.27	1.91±0.17	1.90±0.61	1.00±0.09	dead
6	15	**Dry weight (g)**	0.120±0.030	0.119±0.045	0.097±0.015	0.110±0.020	0.120±0.036
	30		0.377±0.032	0.393±0.067	0.367±0.197	0.230±0.104	0.270±0.036
	60		0.270±0.061	0.227±0.021	0.210±0.010	0.270±0.026	0.233±0.015
	90		0.217±0.031	0.203±0.015	0.150±0.030	0.080±0.030	dead
	120		0.220±0.026	0.157±0.015	0.160±0.056	0.092±0.008	dead
7	15	**Buds/fruits**	0.00±0.00	0.00±0.00	0.00±0.00	0.00±0.00	0.00±0.00
	30		2.00±1.73	1.00±1.00	1.00±1.00	1.00±1.00	0.67±0.58
	60		3.67±0.58	2.67±0.58	3.667±0.58	3.33±0.58	3.33±0.58
	90		2.33±0.58	1.33±0.58	1.667±0.58	1.00±1.00	dead
	120		1.67±0.58	1.33±0.58	1.333±0.58	1.00±0.00	dead
Pb (mg L^{-1}) in treated wastewater			0.00±0.00	0.07±0.01	0.29±0.03	0.33±0.03	0.59±0.01
Pb (mg kg^{-1})) in plant biomass			0.00±0.00	0.001±0.001	0.001±0.001	0.002±0.001	dead

Figure 4.32 Comparison of effect of tannery wastewater treated by different adsorbents on green moong (*Vigna radiate*) by control (Details are same as Fig. 5.28)

Figure 4.33 Comparison of effect of flashlight wastewater treated by different adsorbents on green moong (*Vigna radiate*) by control (Details are same as Fig. 5.29)

The maximum growth parameters were recorded with tannery and flashlight wastewater treated with sweet lemon followed by lemon and orange biochars in all of the plants. Whereas, concentrations of Cr and Pb were found to be lowest with treatment of SLPB, followed by LPB and OPB for all three selected plants. The concentrations of HMs bio-accumulated in the selected plant species were very low for almost all of the selected adsorbents but the best one was reported by SLPB and the concentrations were under the limit prescribed by CPCB i.e. 0.05 mg L^{-1} for both HMs, and also under the limit given by WHO i.e. 0.1-0.2 mg kg^{-1} for Cr & 0.1 mg kg^{-1} for Pb (Jhamaria et al. 2015). Auda et al. (2011) reported normal range of Pb in edible plants as 0.02 to 20 mg kg^{-1}, which was very high as compared to bioaccumulation of Pb in all of the selected plants in the present study. Such concentrations may be considered as negligible, but the development of fruits were also found to be very low in comparison to control like that of growth parameters. This might be due to higher concentrations of salts present in the treated wastewaters, which may be removed by following various other eco-friendly techniques e.g. coagulation where alum is utilized as potential coagulant, electro dialysis that involve the application of electric field for removal of ionic contaminants etc. (Teh et al. 2014). This may increase the growth and development of plants as well as also reduce the concentrations of HMs with combination of adsorption technique. Moreover, the bioaccumulation of HMs in the selected plants irrigated with biosorbent treated wastewaters will not cause any severe effect onto the health of human and other animals feeding on it. The main reason for such impression is that the conc. of HMs in

the plant system was very low and translocation of such a little concentration into the fruits will hardly be noticeable. Therefore, it may be concluded that irrigation of these plants with the biosorbent treated wastewater will not cause any threat or risk to the lives of humans.

The results of the present study were in good agreement with Thapliyal et al. (2011) who found conc. of Cr in lady's finger biomass to be 18 μ g^{-1} after irrigating the plants with domestic wastewater. Jhamaria et al. (2015) observed retarded growth and 15.26 and 4.25 mg kg^{-1} of Cr and 11.39 and 5.21 mg kg^{-1} of Pb accumulated into tomato and lady's finger, respectfully, after irrigation with untreated industrial wastewater (dye). Hossain et al. (2015) reported concentrations of Cr(< 0:05) and Pb(< 0:01) below the detection limit in the fruits of cherry tomato, after treatment of wastewater sludge and sludge biochar. In the same way, Ali et al. (2017) reported bioaccumulation of 0.26 & 0.33 mg kg^{-1} of Cr and 0.96 & 0.51 mg kg^{-1} of Pb in lady's finger and tomato after irrigation with industrial wastewater. Alghobar and Suresha (2017) reported the conc. of Cr and Pb to be 15 and 12 mg kg^{-1} in tomato after irrigation of treated sewage wastewater. Likewise, Cheshmazar et al. (2018) found that 0.44 and 1.71 mg kg^{-1} of Cr and Pb bioaccumulation in tomato plants after irrigation with industrial and municipal wastewater.

Chapter 5

Conclusion

Conclusion

With rising competition for water and deteriorating freshwater resources, consumption of marginal quality water for different domestic and agricultural purposes has posed new challenges for environmental management during past few decades, especially in developing countries including India. Although, industrial usage of water is very low when compared to agricultural usage, dumping of industrial wastewaters on land and/or on surface water bodies make water resources unsuitable for other usages. Industries discharge various inorganic, organic and biological pollutants into receiving water bodies with inappropriate or even without treatment of wastewaters. Such contaminated water possesses different toxic pollutants among which heavy metals (HMs) are the primary ones that have the potential to get bio-accumulated with contamination of the food chain. Agricultural practices often use these contaminated water for irrigation that may result in the food chain contamination with hazardous effects onto the health of human beings.

Heavy metals are the most troublesome pollutants in respect to their toxicity, bioaccumulation properties as precursor of many bio-chemical reactions in the environment. Although, many conventional and non-conventional techniques have been developed for removal and treatment of the contaminated wastewater, but none of them have proved to be the best one in all the aspects (like cost effectiveness, energy consumption, secondary pollutants etc.). In present scenario, biosorption has emerged as an innovative, eco-friendly, cost effective and probable alternative to prevailing conventional technologies for elimination and/or recovery of contaminants and metal ions from aqueous solutions. Among different bio-sorbents available, naturally occurring agricultural wastes with excess carbon substances have shown excellent potential for adsorption of heavy metals. Furthermore, most of the heavy metals adsorbed can also be recycled and reused by the process of desorption.

Among various industries, tannery and flashlight manufacturing industries are very common and hold important place in the economy of our country; India. However, often these industries discharge wastewater on the land or into nearby water bodies without proper treatment. The wastewaters possess different inorganic and

organic pollutants, especially heavy metals i.e. Cr and Pb. The objective of the present study was to treat both of these two wastewaters by adsorption process with the help of biochar of the some fruit and industrial wastes *viz.* peels of sweet lemon (*Citrus limetta*), lemon (*Citrus limon*) & orange peel (*Citrus sinensis*) and bagasse after physicochemical characterization of the selected adsorbents. The potential of naturally occurring bio-wastes to work as suitable adsorbent for Cr and Pb present in both of the industrial wastewater had been examined. Different parameters that influence the adsorption process like pH, temperature, surface area, dosage etc., related isotherms and kinetics, desorption potential of different adsorbents were also analyzed.

The physicochemical characterizations were based on the observations of proximate and ultimate studies, CHNS, surface properties, SEM & EDX, FTIR and XRD eruditions. The proximate and ultimate studies revealed that the highest surface area was of SLPB (30.62 m^2 g^{-1}) followed by LPB (24.89 m^2 g^{-1}), OPB (15.21 m^2 g^{-1}) and BB (12.628 m^2 g^{-1}). Whereas average pore volume was 0.053, 0.037, 0.025 and 0.039 cc g^{-1} and average pore diameter was 1.612, 2.145, 2.371 and 1.579, for SLPB, LPB, OPB and BB, respectively. The maximum biochar yield was obtained by SLPB (86.67%) followed by lemon peel (84.47%), orange peel (79.20%) and bagasse (73.33%). Further, the total concentration of surface acidic groups in SLPB, LPB, OPB and BB was 7.382, 7.480, 7.408 and 7.033 mol gm^{-1}, respectively with maximum carboxylic acids with values of 5.30, 4.925, 4.483 and 5.15 mol gm^{-1}, respectively. The concentration of lactonic and phenolic groups in the selected adsorbents was 0.508, 1.90, 2.108, 1.283 and 1.573, 0.655, 0.817, 0.601 mol gm^{-1}, respectively. It reflected that all of the adsorbents had the important acid functional groups i.e. carboxylic groups, phenolic groups, lactonic (esters) groups that shall help in the adsorption of HMs by different ion-exchange, complexion, addition and substitution chemical reactions. Moreover, CHNS study reported that among all four adsorbents SLPB and LPB showed higher C and H content with lower H/C ratio which suggest it to be more efficient adsorbents than OPB and LPB which possessed comparatively lesser C and H content with higher H/C ratio. This suggested that all of the selected adsorbents had significant surface properties to bind HMs onto their surfaces.

The alterations in the surface morphology before and after adsorption of HMs were ascertained by the study of SEM and EDX. The selected biosorbents possessed

flattened, walls smooth and homogenous surface their natural form whereas, temperature treatments increased the surface area and converted it into biochar that had amorphous, uniformly porous and heterogeneous surfaces holding irregular cavities and pore of different shape and sizes. After adsorption of HMs from both of the wastewater, the irregular cavities became filled with some white, crystalline structure which may be caused by the formation of different complexes of the respective metals. Thus, SEM studies supported the successful adsorption of HMs. Whereas, EDX analysis of all of the four adsorbents also confirmed the adsorption of HMs as changes in peaks of natural agricultural wastes and as biochar before adsorption and after adsorption of HMs were established by the absence and presence of peaks of HMs in the spectrums, respectively. Initially, peaks of all of the selected biosorbents displayed existence of some common elements (C, O and Ca). After conversion into biochar all of them retained peaks of C, O, Ca etc. as major element which may be due to the removal of lignin, cellulose, volatiles etc. during thermal strokes. Further, EDX spectrums of treated wastewaters i.e. tannery and flashlight also showed the presence of respective HMs (Cr and Pb) with the existence of other elements like Na, K, Cl, Mg, Bi, Zr, Pt etc. These extra elements were found to be present in both of the wastewater. Thus, EDX study suggested that HMs present in wastewater and other pollution causing elements may also be eliminated successfully by the application of selected adsorbents.

The chemical configuration and chief surface functional groups responsible for effective adsorption of HMs were determined by FTIR study. FTIR spectroscopy illustrated that selected adsorbents were found to be rich in gathering of different functional and chemical groups. The strong peaks between 3846.8 and 3352.9 cm^{-1} were attributed to -OH stretching vibrations of biopolymers and poly saccharides (lignin, pectin, cellulose etc.) that symbolized the composition of agricultural wastes. Further, shift in the position of peaks among biochars before and after adsorption of HMs proposes that process was smoothed by chemisorption as a resultant of binding of HMs by the nucleophilic functional groups. Further, some of the functional groups were lost after adsorption of HMs which implied that these groups were consumed in the uptake of the respective HMs. The alteration of secondary amide into primary amide and -CH to C=C were marked of formation and dissociation of bonds and groups through ion exchange or some other mechanisms that favored adsorption of

HMs onto surfaces of all selected adsorbents. In addition to this, the breakdown of polysaccharides components present in the adsorbents pointed towards the breaking and rearrangement of stronger bonds of carboxyl groups and involvement of P, S and N were evident from the different related groups present in all of the four adsorbents in the form of sulfonic groups, amides, organo-phosphorus compounds etc. Moreover, phenolic, carboxylic and alkyl groups also played significant role in the adsorption of HMs by providing adsorption sites. The results of EDX analysis and surface acidic groups also supported the FTIR analysis for all of selected adsorbents.

The changes in the structural crystallites of selected adsorbents before and after adsorption of HMs were studies on the basis of XRD. The sharpest diffractogram peaks for all of the adsorbents were found to be in the range of 24.35 to 26.41º (2θ). The existence of sharp crystalline peak for SLPB at 24.37º (2θ), LPB at 26.59º (2θ), OPB at 24.35º (2θ) and BB at 26.41º (2θ) signified the presence of natural cellulose, lignin and non-crystalline hemicellulosic materials. After treating both wastewaters, slight changes in the position of peaks were recorded that demonstrated no change in the crystallinity of biochars. The minute alternations in the intensities verified the adsorption of HMs that suppressed the intensities after adsorption of Cr and Pb, respectively, except for BB after treating flashlight wastewater. This increase in the intensity may be caused by presence of alkali (NaOH) in the wastewater or mixture and/or inclusion complex formation after adsorption. Whereas, decrease in 2θ positions after adsorption might cause little decrease in the crystallinity of adsorbents due to presence of different chemicals in the wastewater. Further, all selected biochars exhibited diffractogram peaks at 29.21º (2θ) with different intensities of 221, 301, 254 and 263 cts for SLPB, LPB, OPB and BB, respectively, confirming the presence of $CaCO_3$ in them. These results were also in agreement with the surface Boehm titration and EDX analysis. In addition to this, the intermediate peaks present in the diffractogram of all the four adsorbents after treating tannery and flashlight wastewater might be attributed to respective bindings of Cr and Pb on to them.

Comparative study of all four adsorbents was based on the parameters *viz.* adsorbent dosage, contact time, pH, temperature and initial metal ion concentration. The optimized dose and contact time were found to be in range of 5.0 to 10 g L^{-1} and 160 to 180 minutes for Cr and 3.5 to 5.0 g L^{-1} and 140 to 180 minutes for Pb,

respectively. The increasing order of removal efficiencies was BB<OBB<LPB<SLPB for all of the selected parameters. pH and temperature affect the surface charges and mobility of the ions which are important aspects of adsorption. The maximum removal of Cr and Pb was found to be 95.47 and 97.42 %, at pH 3 and 5 and temperature of 65 and 55 ºC, respectively by SLPB. Further, the effect of initial metal concentration on removal efficiencies of all selected adsorbents was lowest that may be due to dependence of this factor onto adsorbent dosage and contact time. Besides, the most important parameter that affected the removal process was pH and the best-suited adsorbent was SLPB.

Further, concentration of BOD was reduced for both wastewaters on treating it with selected adsorbents. The removal percentages of BOD for tannery wastewater by SLPB, LPB, OPB and BB increased from 12.12, 12.12, 11.13 and 10.39 % to 53.85, 41.50, 37.31 and 28.34 % respectively, until the optimum dosage and contact time. Likewise, BOD removal percentage was also increased from 18.23, 16.71, 12.05 and 11.29 to 33.74, 29.91, 24.85 and 22.00 %, respectively for flashlight wastewater. The increasing order of improvement in BOD of both wastewaters was observed as BB<OPB<LPB<SLPB. In addition to this, application of selected adsorbents also reduced COD concentration of tannery wastewater from 22.75, 24.31, 5.94 and 3.59 % to 67.76, 65.52, 29.66 and 4.51 %, respectively at optimum dosage and contact time. The pH of tannery and flashlight wastewaters were 8.67 and 4.70, which was reduced by 6.15, 6.15, 2.69, 5.0 and 13.53, 13.53, 3.53 and 11.76 %, respectively by treatments of SLPB, LPB, OPB and BB. After attaining saturation, pH of tannery and flashlight wastewaters treated by four adsorbents was found to be 8.133, 8.133, 8.433, 8.233 and 4.07, 4.07, 4.07, 4.15, respectively. The reduction in pH of both wastewaters might be caused by the effect of adsorbent's pH as the surface of adsorbents was enriched with acidic groups. Likewise pH, EC of both wastewaters was also not affected significantly. EC of tannery and flashlight wastewater was 16.39 and 24.17 mS cm^{-1}, respectively. After treating it with optimizes dosage of SLPB, LPB, OPB and BB, EC was reduced to 13.93, 14.0, 13.92, 14.55 and 21.24, 21.74, 22.19, 23.28 mS cm^{-1}, respectively. The reduction (%) was observed to be 15.0, 14.58, 15.09, 11.22 and 12.13, 10.04, 8.19, 3.67 %, respectively. Further, alteration in EC was not much distinct, however, it might be caused due to reduction in pH and availability of excess of surface acidic groups.

The main objective of the study was to remove HMs present in wastewaters discharged by tannery and flashlight manufacturing industries. Chromium (Cr) and lead (Pb) were chief HMs present in tannery and flashlight industrial wastewaters. Among different parameters, three *viz.* dosage, contact time and pH were considered for removal of HMs both wastewaters. These parameters showed high removal percentage during optimization process and also did not require any special supervision or technical acquaintance during operation. The concentration of Cr in tannery wastewater and Pb in flashlight wastewater were 3.842 and 2.393 mg L^{-1}, respectively. After treatment with SLPB, LPB, OPB and BB, the residual concentration of Cr and Pb wastewaters were 0.084, 0.327, 0.513, 0.990 and 0.069, 0.292, 0.333, 0.589 mg L^{-1}, respectively. The maximum removal of Cr and Pb were attained by SLPB (97.82 & 97.11 %) followed by LPB (91.50 & 87.80 %), OPB (86.64 & 86.07%) and BB (74.23 & 75.38 %) at the end. The best results were obtained at relatively less acidic pH (between 3-5). However, treatment with BB recorded maximum removal of Pb at pH 5. At saturation point only 0.08, 0.33, 0.51 and 0.99 mg L^{-1} of Cr and 0.07, 0.29, 0.333 and 0.59 mg L^{-1} of Pb were left in tannery and flashlight wastewater, respectively which fell under recommended limits of Inland Surface Water-Bangladesh Standards. Moreover, the maximum removal of Cr and Pb was accomplished by SLPB (97.4 & 96.80 %) followed by LPB (91.32 & 88.16 %), OPB (86.03 & 85.66 %) and BB (84.12 & 77.02 %).

The kinetic studies describe elementary conducts of adsorbent and deliver information about adsorption mechanism. The pseudo-first order model follows that adsorption rate was controlled by the mechanism involving a sole class of adsorbing sites, whereas, the imprint of pseudo-second order model is that adsorption procedure is a chemically mediated involving valence forces by exchange or sharing of electrons between adsorbate and adsorbent. Thus, the kinetics involved in the adsorption of Cr and Pb present in tannery and flashlight wastewater, were studied following pseudo first and pseudo second order models. The higher values of R^2 were recorded for pseudo second order kinetic model in comparison to pseudo first order. Therefore, the adsorption reactions were likely to be pseudo second order, which assumes that rate of adsorption was directly proportional to the number of active surface sites. Thus, it could be concluded that the adsorption mechanism of both metals followed

chemisorption more appropriately than physisorption as pseudo second order kinetic model fitted well with adsorption of both HMs.

Further, due to their simplicity, the Freundlich and Langmuir equations were used to describe the relationship between equilibrium metal biosorption q_e (mg L^{-1}) and final concentrations C_e (mg L^{-1}) at equilibrium. The interpretations of isothermic model were based on values of R^2 for both HMs. The R^2 values of Langmuir & Freundlich isothermic model for adsorption of Cr and Pb onto the surface of SLPB were 0.889 & 0.993 and 0.952 & 0.978, for LPB were 0.971 & 0.991 and 0.957 & 0.936, for OPB were 0.999 & 0.999 and 0.94 & 0.953; and for BB were 0.959 & 0.984 and 0.93 & 0.927, respectively. As the values of R^2 for both of the isotherms were nearby 1, and were higher for Freundlich isothermic model, so it better fitted for adsorption of Cr and Pb from tannery and battery wastewater in comparison to Langmuir. Thus, it could be concluded that adsorbent surfaces were heterogeneous and availed multi-layer adsorption with interactions between adsorbate and absorbent. In addition to this, the monolayer adsorption capacity (q_{max}) of SLPB, LPB, OPB and BB for the removal of Cr and Pb were found to be 2872.5 and 2840.91, 874.96 and 940.69, 116.75 and 512.53, 2.745 and 12.741 mg g^{-1}, respectively.

Further, thermodynamic parameters (ΔG°, ΔH^{o} and ΔS^{o}) were estimated to observe the effect of temperature onto the adsorption of 5, 10, 20 and 40 ppm aqueous solution of Cr and Pb at optimum dosage and contact time. The negative value of ΔG° indicates the spontaneous nature of the adsorption process, whereas positive values reflect non-spontaneous adsorption. Further, the values of ΔH^{o} gave an idea about the type interactions between the adsorbent and adsorbate. The positive and negative values ΔH^{o} indicates endothermic and exothermic adsorption, respectively. Whereas, positive value of ΔS^{o} represents the increased randomness and negative value shows decrease in randomness at the solid–solution interface during adsorption. The results indicated that the adsorptive removal of Cr and Pb were endothermic, spontaneous and increase in randomness with increased temperature was recorded as values of ΔH^{o}, ΔG° & ΔS^{o} were positive, negative and positive.

The desorption study revealed that about 45.63, 45.75, 55.38 and 54.43 % of Cr desorption was recorded by SLPB, LPB, OPB and BB, respectively. The maximum desorption was attained by 0.1 M HNO_3 for SLPB and 0.1 M HCl for

remaining three adsorbents. The order of desorption for Cr was found be in the order of OPB>BB>LPB>SLPB. Similarly, the maximum desorption of 88.15, 88.98, 86.82 and 90.05 % was achieved by SLPB, LPB, OPB and BB, respectively for Pb. The most suitable eluant for desorption of Pb were 0.1 M HCl for SLPB, LPB and OPB, and 0.1 M HNO_3 for BB. The order of desorption was recorded as BB>LPB>OPB>SLPB.

The best adsorbents for treating both industrial wastewater by selected adsorbents at optimized conditions was found to be SLPB based on the comparison with other three adsorbents as removal efficiency and capacity was found to be maximum for SLPB followed by LPB, PB and BB for treating both of the wastewater. SLPB followed Freundlich isotherm, whereas, LPB followed Freundlich & Langmuir isotherms for removal of both of the toxic metals. OPB followed Langmuir and Freundlich for removal of Cr form tannery wastewater, whereas, Freundlich for removal of Pb from flashlight wastewater. Moreover, BB followed Freundlich and Langmuir isotherms for removal of both of the toxic metals from respective industrial wastewater. All of the selected adsorbents followed pseudo second order kinetics for both of the HMs from respective industrial wastewater. In addition to this, the best eluant for extraction of Cr from SLBP was 0.1 M HNO_3**,** whereas, for LBP, OPB and BB was 0.1 M HCl. Likewise, for extraction of Pb form SLBP, LBP, OPB 0.1 M HCl and for BB was 0.1 M HNO_3.

Further, phyto-toxicity of treated wastewaters was tested on some of the economic plants i.e. vegetables (lady's finger, sponge gourd, bottle gourd, pumpkin, bitter gourd), legumes and oil yielding seeds (green moong, tomato and rapeseed) and fruit (tomato) by performing seed germination test. Green moong and tomato among legumes, fruit and oil yielding plants, and lady's finger among vegetables exhibited maximum germination index at day 3. Green moong, tomato and lady's finger represented 100 & 100, 86.667 & 93.33 and 96.667 & 76.667 % seed germination by SLPB treated wastewater at day 3. Similarly, seeds of green moong, tomato and lady's finger irrigated with LPB treated the wastewater of tannery and flashlight wastewater represented 76.667 & 100, 56.667 & 50 % and 100 & 53.33 % of germination index. Similar results were also obtained for OPB treated wastewaters with 100 & 96.667, 100 & 93.33 and 90 % of germination index for seeds of green

moong, tomato and lady's finger, respectively. Furthermore, seeds were used to wrought in the treated wastewater of both of the industries due to higher concentrations salts and other pollutants which affected the germination index adversely. Therefore, experiments were performed with 50 % of dilution of treated wastewater afterwards. About 90 and 93.33 % of germination index was observed with 50% diluted tannery and flashlight wastewater as compared to 0 % for lady's finger seeds for both wastewaters without dilution. Moreover, tap water was used as control for conducting seed germination experiments, which established 100% germination rate at day 3. Other seeds i.e. sponge gourd, bottle gourd, pumpkin, bitter gourd and rap seeds were not able to tolerate the concentrations of both of the wastewater. Thus, lady's finger, tomato and green moong were selected for pot experiments in the greenhouse conditions to explore the effect of residue Cr and Pb onto the growth parameters and its bioaccumulation into the plants. Further, the maximum growth parameters were recorded with tannery and flashlight wastewaters treated with sweet lemon followed by lemon and orange biochars in all of the plants. The concentrations of Cr and Pb were found to be lowest by treatment of SLPB, followed by LPB and OPB for all three selected plants. Whereas, the amount of HMs bio-accumulated in selected plant species were very low after treatment with all of selected adsorbents but the best one was observed with SLPB and amounts were under prescribed limits of CPCB i.e. 0.05 mg L^{-1} for both HMs, and also under the limit of WHO i.e. 0.1-0.2 mg kg^{-1} for Cr & 0.1 mg kg^{-1} for Pb. Such concentrations may be considered as negligible, however, development of fruits was found to be very low in comparison to control like that of growth parameters. This might be due to higher concentrations of salts present in the treated wastewater, which may be removed by following various other eco-friendly techniques e.g. coagulation where alum is utilized as potential coagulant, electro dialysis that involve the application of electric field for removal of ionic contaminants etc. This might increase growth and development of plants as well as might reduce concentrations of HMs with combination of adsorption technique. Moreover, the bioaccumulation of HMs in selected plants irrigated with biosorbent treated wastewater will not cause any severe effect onto the health of human and other animals feeding on it as the conc. of HMs in the plant system was very low and translocation of such a little concentration into fruits will hardly be noticeable. Therefore, it may be concluded that irrigation of these plants with the biosorbent treated wastewater will not cause any threat or risk to the lives of humans.

Most of the previous studies done so far, have utilized either chemical or modified adsorbents for treating industrial wastewater. These chemical may generate hazardous toxic secondary pollutant, which may harm the quality of water bodies. In present study, usage of biochars of different agricultural wastes did not cause any harm to the quality of water body and made the process of removal of HMs from wastewater eco-friendly and cost efficient. Thus, it can be concluded that, 1) All of the selected naturally occurring bio-wastes showed excellent heavy metal adsorption ability at optimized conditions. 2) Different functional groups associated with adsorbents, their surface areas and smaller pore size facilitate the adsorption process. 3) The adsorption conditions such as temperature and pH of the medium also influenced the adsorption process. 4) Adsorption was an exothermic process, spontaneous process with increasing randomness with increasing temperature until the optimized temperature was obtained. 5) The best-fitted kinetic model for adsorption of Cr and Pb from tannery and flashlight wastewater by all of the four selected bio-sorbents was pseudo-second-order rate kinetics. It depicted that the mechanism involved in removal of both of the HMs followed chemisorption in comparison to physisorption. 6) The mechanism was multilayered and heterogeneous as all of the adsorbents were in accordance with the Freundlich isotherm.

Regardless of enough progress made in the field of adsorptive removal of heavy metals and other pollutants, there are still some knowledge gaps to be filled. Additional studies related to- 1) improve the adsorption capacity by mixing up two or more adsorbents of different characteristics; 2) the studies should be formed for medium polluted with multiple contaminants with one or mixture of different adsorbents; 3) reusability of different adsorbents after adsorption by the process of desorption; 4) generation and collection of different precious metals after adsorption; and, 5) lowering the cost associated with the use, reuse and regeneration of the adsorbent and precious metals.

References

References

Abas SNA, Ismail MHS, Kamal L, Izhar S (2013) Adsorption Process of Heavy Metals by Low-Cost Adsorbent: A Review. World Applied Sciences Journal 28:1518-1530

Abdel-Fattah TM, Mahmoud ME, Ahmed SB, Huff MD, Lee JW, Kumar S (2015) Biochar from woody biomass for removing metal contaminants and carbon sequestration, Journal of Industrial and Engineering Chemistry 22:103-109

Abdelhafez AA, Li J (2016) Removal of Pb(II) from aqueous solution by using biochars derived from sugarcane bagasse and orange peel. Journal of the Taiwan Institute of Chemical Engineers 61:367-375

Abdellah AM, Abdel-Magid H, Shommo EI (2013) Assessment of Groundwater Quality in Southern Suburb of the Omdurman City of Sudan, Greener Journal of Environmental Management and Public Safety 2(2):083-090

Adeogun AI, Kareeem SO, Adebayo OS, Samson O, Balogun SA (2017) Comparative adsorption of amylase, protease and lipase on $ZnFe_2O_4$: kinetics, isothermal and thermodynamics studies. Biotech 7:198

Agbalagba OE, Agbalagba OH, Ononugbo CP, Alao AA (2011) Investigation into the physico-chemical properties and hydrochemical processes of groundwater from commercial boreholes In Yenagoa, Bayelsa State, Nigeria. African Journal of Environmental Science and Technology 5(7):473-481

Aharoni C, Ungarish M (1977) Kinetics of activated chemisorption. Part 2. Theoretical models. Journal of the Chemical Society, Faraday Transactions 73:456-464

Ahmad M, Rajapaksh AU, Lim JE, Zhang M, Bolan N, Mohan D, Vithanage M, Lee SS, Ok YS (2014) Biochar as a sorbent for contaminant management in soil and water: a review. Chemosphere 99:19-33

Ahmadi M, Kouhgardi E, Ramavandi B (2016) Physico-chemical study of dew melon peel biochar for chromium attenuation from simulated and actual wastewaters. Korean J Chem Eng 33(9):2589-2601

Ahmady-Asbchin S, Andrés Y, Gérente C, Cloirec P L (2008) Biosorption of Cu(II) from aqueous solution by *Fucus serratus*: Surface characterization and sorption mechanisms. Bioresource Technology 99:6150-6155

Ahmed MK, Das M, Islam MM, Akter MS, Islam S, Al-Mansur MA (2011) Physico-Chemical Properties of Tannery and Textile Effluents and Surface Water of River Buriganga and Karnatoli, Bangladesh. World Appl Sci J 12(2):152-159

Ahmed TF, Sushil M, Krishna M (2012) Impact of dye industrial effluent on physicochemical characteristics of Kshipa River, Ujjain City, India. Int Res J Environ Sci 1:41-45

Akan JC, Moses EA, Ogugbuaja VO (2007) Assessment of tannery industrial effluent from Kano metropolis, Nigeria Asian network for Scientific information. J Appl Sci 7(19):2788-2793

Akpomie KG, Dawodua FA (2015) Physicochemical analysis of automobile effluent before and after treatment with an alkaline-activated montmorillonite. Journal of Taibah University for Science 9(4):465-476

Alfa YM, Hassan H, Nda-Umar UI (2012) Agricultural waste materials as potential adsorbent for removal of heavy metals from aqueous solutions. International Journal of Chemical Research 2249-0329

Alghobar MA, Suresha S (2017) Evaluation of metal accumulation in soil and tomatoes irrigated with sewage water from Mysore city, Karnataka, India. Journal of the Saudi Society of Agricultural Sciences 16:49-59

Ali F, Ullah H, Khan I (2017) Heavy metals accumulation in vegetables irrigated with industrial influents and possible impact of such vegetables on human health. Sarhad Journal of Agriculture, 33(3):489-500

Alluri HK, Ronda SR, Settalluri VS, Bondili VS, Suryanarayana V, Venkateshwar P (2007) Biosorption: An eco-friendly alternative for heavy metal removal. African Journal of Biotechnology 6(11):2924-2931

Altun T and Pehlivan E (2012) Removal of Cr(VI) from aqueous solutions by modified walnut shells. Food Chemistry 132:693-700

An Y, Zhang X, Wang X, Chen Z, Wu X (2018) Nano@lignocellulose intercalated montmorillonite as adsorbent for effective Mn(II) removal from aqueous solution. Scientific Reports 8:10863

Anandkumar J and Mandal B (2011) Adsorption of chromium (VI) and Rhodamine B by surface modified tannery waste: Kinetic, mechanistic and thermodynamic studies. Journal of Hazardous Materials 186:1088-1096

Anastopoulos I, Bhatnagar A, Lima, EC (2016) Adsorption of rare earth metals: A review of recent literature. Journal of Molecular Liquids 221:954-962

Anastopoulos I, Kyzas GZ (2014) Agricultural peels for dye adsorption: A review of recent literature. Journal of Molecular Liquids 200:381-389

APHA (2005) Standard methods for the examination of water and waste water, 21st edn. American Public Health Association, Washington, DC

Argun ME, Dursum S (2008) A new approach to modification of natural adsorbent for heavy metal adsorption. Bioresour Technol 99:2516-2527

Arulkumar M, Thirumalai K, Sathishkumar P, Palvannan, T (2012) Rapid removal of chromium from aqueous solution using novel prawn shell activated carbon. Chemical Engineering Journal 185–186:178-186

Asfaw A, Sime M, Itanna F (2012) Determining the Effect of Tannery Effluent on Seeds Germination of SomeVegetables in Ejersa Area of East Shoa, Ethiopia. International Journal of Scientific and Research Publications 2(12):1-10

Asgari G, Ramavandi B, Rasuli L, Ahmadi M (2013) Cr (VI) adsorption from aqueous solution using a surfactant-modified Iranian zeolite: characterization, optimization, and kinetic approach. Desal Water Treat 51:6009

Attia AA, Khedr SA, Elkholy SA (2010) Adsorption of chromium ion (VI) by acid activated carbon. Brazilian Journal of Chemical Engineering 27(1):183-193

Auda MA, Zinada IA, Ali EES (2011) Accumulation of heavy metals in crop plants from Gaza Strip, Palestine and study of the physiological parameters of spinach plants. Journal of the Association of Arab Universities for Basic and Applied Sciences 10:21-27

Ayoub GM, Hamzeh A, Semerjian L (2011) Post treatment of tannery wastewater using lime/bittern coagulation and activated carbon adsorption. Desalination 273:359-365

Azza MAA, Nabila SA, Hany HAG, Rizka KA (2013) Biosorption of cadmium and lead from aqueous solution by fresh water alga *Anabaena sphaerica* biomass. J Adv Res 4:367-374

Babel S, Kumiawan T A (2004) Cr(VI) removal from synthetic waste water using coconut shell charcoal and commercial activated carbon modified with oxidizing a gents and/or chitosan. Chemosphere 54:951

Babel S, Kurniawan TA (2003) Low-cost adsorbents for heavy metals uptake from contaminated water: a review. Journal of Hazardous Materials 97:219-243

Baccar R, Blánquez P, Bouzid J, Feki M, Attiya H, Sarrà M (2013) Modeling of adsorption isotherms and kinetics of a tannery dye onto an activated carbon

prepared from an agricultural by-product. Fuel Processing Technology 106:408-415

Bahadir T, Bakan G, Altas L, Buyukgungor H (2007) The investigation of lead removal by biosorption: An application at storage battery industry wastewaters. Enzyme and Microbial Technology 41:98-102

Bai R, Zhang Y, Zhao Z, Liao Q, Chen P, Zhao P, Guo W, Yang F, Li L (2017) Rapid and highly selective removal of lead in simulated wastewater of rare-earth industry using diglycolamic-acid functionalized magnetic chitosan adsorbents, Journal of Industrial and Engineering Chemistry DOI 10.1016/j.jiec. 2017.10.053

Baig SA, Sheng T, Sun C, Xue X, Tan L, Xu X (2014a) Arsenic removal from aqueous solutions using Fe_3O_4-HBC composite: effect of calcination on adsorbents performance. PloS one 9(6)- PloS one 9(6) DOI 10.1371/journal.pone.0100704

Baig SA, Zhu J, Muhammad N, Sheng T, Xu X (2014) Effect of synthesis methods on magnetic Kans grass biochar for enhanced As(III, V) adsorption from aqueous solutions. Biomass and bioenergy 71:299-310

Bairagi H, Md. Khan MMR, Ray L, Guha AK (2011) Adsorption profile of lead on *Aspergillus versicolor*: A mechanistic probing. Journal of Hazardous Materials 186:756-764

Banerjee K, Ramesh ST, Nidheesh PV, Bharathi K S (2012) A novel agricultural waste adsorbent, watermelon shell for the removal of copper from aqueous solutions. Iranica Journal of Energy and Environment 3:143-156

Bansal M, Singh D, Garg VK (2009) A comparative study for the removal of hexavalent chromium from aqueous solution by agriculture wastes' carbons. J Hazard Mater 15(171):83-92

Basu M, Guha AK, Ray L (2017) Adsorption of lead on Cucumber Peel. Journal of Cleaner Production 151:603-615

Basu M, Guha AK, Raya L (2016) Adsorption Behavior of Cadmium on Husk of Lentil. Process Safety and Environment Protection DOI 10.1016/j.psep.2016.11.025

Batista EMCC, Shultz J, Matos TSS, Fornari MR, Ferreira TM, Szpoganicz B, de Freitas RA, Mangrich AS (2018) Effect of surface and porosity of biochar on

water holding capacity aiming indirectly at preservation of the Amazon biome. Scientific Reports 8:10677

Bernard E, Jimoh A (2013) Adsorption of Pb, Fe, Cu, and Zn from industrial electroplating wastewater by orange peel activated carbon. International Journal of Engineering and Applied Sciences 4(2):60-80

Bharagava RN and Mishra S (2018) Hexavalent chromium reduction potential of *Cellulosimicrobium* sp. Isolated from common effluent treatment plant of tannery industries. Ecotoxicology and Environmental Safety 147:102-109

Bharathi K, Ramesh S (2013) Removal of dyes using agricultural waste as low-cost adsorbents: a review, Appl Water Sci 3:773-790

Bhatia D, Sharma NR, Kanwar R, Singh J (2018) Physicochemical assessment of industrial textile effluents of Punjab (India). Applied Water Science 8:83

Bhatnagar A, Minocha AK, Sillanpää M (2010) Adsorptive removal of cobalt from aqueous solution by utilizing lemon peel as biosorbent. Biochemical Engineering Journal 48:181-186

Bhatti HN, Zaman Q, Kausar A, Noreen S, Iqbal M, (2016) Efficient remediation of Zr(IV) using citrus peel waste biomass: Kinetic, equilibrium and thermodynamic studies. Ecological Engineering 95:216-228

Bhatti JA, Ahmad N, Iqbal N, Zahid M, Iqbal M (2017) Chromium adsorption using waste tire and conditions optimization by response surface methodology. Journal of Environmental Chemical Engineering http://dx.doi.org/10.1016/j. jece.2017.04.051

BIS (2012) Indian standards specifications for drinking water, IS:10500, Bureau of Indian Standards, New Delhi, http://cgwb.gov.in/Documents/WQ-standards.pdf

Boehm HP (1994) Some aspects of the surface chemistry of carbon blacks and other carbons. Carbon 32, 759-769

Boehm HP (2002) Surface oxides on carbon and their analysis: a critical assessment. Carbon 40:145-149

Boehm HP, Diehl E, Heck W, Sappok R (1964) Surface oxides of carbon. Angewandte Chem Int Ed 3:669-77

Božić D, Gorgievski M, Stanković V, Štrbacb N, Šerbula S, Petrović N (2013) Adsorption of heavy metal ions by beech sawdust - Kinetics, mechanism and equilibrium of the process. Ecological Engineering 58:202-206

Brunauer S, Emmett PH, Teller E (1938) Adsorption of gases in multimolecular layers. Journal of the American Chemical Society 60:309-319

Cataldo DA, Haroon M, Schrader LE, Youngs VL (1975) Rapid colorimetric determination of nitrate in plant tissue by nitration of salicylic acid. Commun Soil Sci Plant Anal 6:71-86

Carmo Ramos SNdC, Xavier ALP, Teodoro FS, Elias MMC, Gonçalves FJ, Gil LF, Freitas RPd, Gurgel LVA (2015) Modeling mono- and multi-component adsorption of cobalt(II), copper(II), and nickel(II) metal ions from aqueous solution onto a new carboxylated sugarcane bagasse. Part I: Batch adsorption study. Industrial Crops and Products 74:357-371

Cely P, Tarquis A, Paz-Ferreiro J, Mendez A, Gasco G (2014) Factors driving the carbon mineralization priming effect in a sandy loam soil amended with different types of biochar. Solid Earth 5:585-594

Central pollution control board (CPCB) (2013) Pollution Assessment: River Ganga. Status of Grossly Polluting Industries (GPI) http://cpcb.nic.in/industry-effluent-standards/

Chen K, He J, Li Y, Cai X, Zhang K, Liu T, Hu Y, Lin D, Kong L, Liu J (2017) Removal of cadmium and lead ions from water by sulfonated magnetic nanoparticle adsorbents. Journal of Colloid and Interface Science DOI 10.1016/j.jcis.2017.01.082

Chen Y, Wang H, Zhao W, Huang S (2018) Four different kinds of peels as adsorbents for the removal of Cd (II) from aqueous solution: Kinetics, isotherm and mechanism. Journal of the Taiwan Institute of Chemical Engineers 000:1-6

Cheshmazar E, Arfaeinia H, Karimyan K, Sharafi H, Hashemi SE (2018) Dataset for effect comparison of irrigation by wastewater and ground water amount of heavy metals in soil and vegetables: Accumulation, transfer factor and health risk assessment. Data in Brief 18:1702-1710

Chia, CH, Gong B, Joseph SD, Marjo CE, Munroe P, Rich AM (2012) Imaging of mineral-enriched biochar by FTIR, Raman and SEM–EDX. Vib Spectrosc 62:248-257

Chowdhury M, Mostafa MG, Biswas, TK, Saha, AK (2013) Treatment of leather industrial effluents by filtration and coagulation processes. Water Resources and Industry 3:11-22

Coates J (2000) Interpretation of infrared spectra, a practical approach. In: Meyers,R.A. (Ed.) Encyclopaedia of Analytical Chemistry. John Wiley & Sons Ltd., Chichester pp10815-10837

Cui S, Wang X, Zhang X, Xia W, Tang X, Lin B, Wu Q, Zhang X, Shen X (2018) Preparation of magnetic $MnFe_2O_4$-Cellulose aerogel composite and its kinetics and thermodynamics of Cu(II) adsorption. Cellulose 25:735-751

da Silva AGM, Rodrigues TS, de Assis LVAG, Aparecida P, Gil LF, Robles-Dutenhefner PA (2013) A new use for modified sugarcane bagasse containing adsorbed Co^{2+} and Cr^{3+}: Catalytic oxidation of terpenes. Industrial Crops and Products 50:288-296

Das S, Das A, Guha A (2007) A Study on the Adsorption Mechanism of Mercury on *Aspergillus versicolor* biomass. Environ Sci Technol 41:8281-8287

Deniz F, Karabulut, A (2017) Biosorption of heavy metal ions by chemically modified biomass of coastal seaweed community: Studies on phycoremediation system modeling and design. Ecological Engineering 106:101-108

Derivation of the BET and Langmuir Isotherms, October 5, 2011. http://chem.colorado.edu/chem4581_91/images/stories/IsothermDerv.pdf. Assessed 02 October 2018

Dermentzis K, Valsamidou E, Marmanis D (2012) Simultaneous removal of acidity and lead from acid lead battery wastewater by aluminum and iron electrocoagulation. Journal of Engineering Science and Technology Review 5(2):1-5

Devi P and Saroha AK (2014) Synthesis of the magnetic biochar composites for use as an adsorbent for the removal of pentachlorophenol from the effluent. Bioresource Technology 169:525-531

Dinh V-P, Le N-C, Tuyen LA, Hung NQ, Nguyen VD, Nguyen N-T (2018) Insight into adsorption mechanism of lead(II) from aqueous solution by chitosan loaded MnO_2 nanoparticles. Materials Chemistry and Physics doi: 10.1016/j.matchemphys.2017.12.071

Dirilgen N (2011) Mercury and lead: assessing the toxic effects on growth and metal accumulation by *Lemna minor*. Ecotoxicology and Environmental Safety 74:48-54

Doke KM, Khan EM (2012) Equilibrium, kinetic and diffusion mechanism of Cr(VI) adsorption onto activated carbon derived from wood apple shell. Arabian Journal of Chemistry DOI 10.1016/j.arabjc.2012.07.031

Dubinin MM, Radushkevich LV (1947) Equation of the characteristic curve of activated charcoal. Proc Acad Sci Phy. Chem Sec USSR 55:331-333

Elabbas S, Mandi L, Berrekhis F, Pons MN, Leclerc JP, Ouazzan N (2016) Removal of Cr(III) from chrome tanning wastewater by adsorption using two natural carbonaceous materials: Eggshell and powdered marble. Journal of Environmental Management 166:589-595

El-Sheikh AH, Newman AP (2004) Characterization of activated carbon and physiochemical techniques. Journal of Analytical and Applied Pyrolysis 71:151-164

Erentürk S, Malkoç E (2007) Removal of lead(II) by adsorption onto *Viscum album* L.: Effect of temperature and equilibrium isotherm analyses. Applied Surface Science 253:4727-4733

Esteves B, Cruz‐Lopes L, Ferreira J, Pereira H, Domingos I (2017) Heat-treated wood as chromium adsorption material. Eur J Wood Prod 75:903-909

Fabbricino M, Naviglio B, Tortora G, d'Antonio L (2013) An environmental friendly cycle for Cr(III) removal and recovery from tannery wastewater. Journal of Environmental Management 117:1-6

Fallah Z, Isfahani HN, Tajbakhsh M, Tashakkorian H, Ammouei A (2018) TiO_2-grafted cellulose via click reaction: an efficient heavy metal ions bioadsorbent from aqueous solutions. Cellulose 25:639-660

FAO (2018) 3 Tanneries, Management of Waste from Animal Product Processing. http://www.fao.org/wairdocs/lead/x6114e/x6114e05.htm Accessed 17 July 2018

Farooghi A, Sayadi MH, Rezaei MR, Allahresani A (2018) An efficient removal of lead from aqueous solutions using $FeNi_3@SiO_2$ magnetic nanocomposite. Surfaces and Interfaces 10:58-64

Fathima A, Aravindhan R, Rao JR, Nair BU (2015) Biomass of *Termitomyces clypeatus* for chromium(III) removal from chrome tanning wastewater. Clean Technologies and Environmental Policy 17:541-547

Faust SD, Aly OM (1987) Burterworth publishers, Stoneham, M.A, USA

Febrianto J, Kosasih AN, Sunarso J, Ju Y, Indraswati N, Ismadji S (2009) Equilibrium and kinetic studies in adsorption of heavy metals using biosorbent: A summary of recent studies. Journal of Hazardous Materials162:616-645

Feng N, Guo X (2012) Characterization of adsorptive capacity and mechanisms on adsorption of copper, lead and zinc by modified orange peel. Trans Nonferrous Met Soc China 22:1224-1231

Feng N, Guo X, Liang S, Zhu Y, Liu J (2011) Biosorption of heavy metals from aqueous solutions by chemically modified orange peel. Journal of Hazardous Materials 185:49-54

Fernandez ME, Nunell GV, Bonelli PR, Cukiermen AL (2014) Activated carbon developed from orange peels: batch and dynamic competitive adsorption of basic dyes. Ind Crops Prod 62:437-445

Fonseca-Correa R, Giraldo L, Moreno-Pirajᾶn JC (2013) Trivalent chromium removal from aqueous solution with physically and chemically modified corncob waste. Journal of Analytical and Applied Pyrolysis 101:132-141

Fontoura JTD, Rolim GS, Mella B, Farenzen M, Gutterres M (2017) Defatted microalgal biomass as biosorbent for the removal of Acid Blue 161 dye from tannery effluent. Journal of Environmental Chemical Engineering 5:5076-5084

Freundlich H (1906) Adsorption in solutions (57) Z Phys Chem, Germany, pp 385-470

Fu F, Wang Q (2011) Removal of heavy metal ions from wastewaters: A review. Journal of Environment Management 9:407-418

Gani A, Naruse I (2007) Effect of cellulose and lignin content on pyrolysis and combustion characteristics for several types of biomass. Renew Energy 32:649-61

Gaur N, Kukreja A, Yadav M, Tiwari A (2018) Adsorptive removal of lead and arsenic from aqueous solution using soya bean as a novel biosorbent: equilibrium isotherm and thermal stability studies. Applied Water Science 8:98

Georgieva VG, Tavlieva MP, Genieva SD Vlaev LT (2015) Adsorption kinetics of Cr(VI) ions from aqueous solutions onto black rice husk ash. Journal of Molecular Liquids 208:219-226

Ghaedi M, Ghezelbash GR, Marahel F, Ehsanipour S, Najibi A, Soylak M (2010) Equilibrium, thermodynamic, and kinetic studies on lead(II) biosorption from aqueous solution by Saccharomyces cerevisiae biomass. Clean - Soil, Air, Water 38:877-885

Gharabaghi M, Irannajad M, Azadmehr AR (2012) Selective sulphide precipitation of heavy metals from acidic polymetallic aqueous solution by thioacetamide. Industrial & Engineering Chemistry Research 51:959-968

Gil A, Amiri MJ, Abedi-Koupai J, Eslamian S (2018) Adsorption/reduction of Hg(II) and Pb(II) from aqueous solutions by using bone ash/nZVI composite: effects of aging time, Fe loading quantity and co-existing ions. Environ Sci Pollut Res 25:2814-2829

Giri AK, Patel R, Mandal S (2012) Removal of Cr(VI) from aqueous solution by *Eichhornia crassipes* root biomass-derived activated carbon. Chem Eng J 185-186:71-81

Gleick PH (1993) Water in Crisis: A Guide to the World's Freshwater Resources Oxford University Press Table 2.1 Water reserves on the earth pp 13

Gomez-Serrano V, Pastor-Villegas J, Duran-Valle CJ, Valenzuela Calahorro C (1996) Heat treatment of rockrose char in air. Effect on surface chemistry and porous texture. Carbon 34(4):533-8

Goutam SP, Saxena G, Singh V, Yadav AK, Bharagava RN, Thapa KB (2017) Green synthesis of TiO_2 nanoparticles using leaf extracts of *Jatropha curcas* L. for photocatalytic degradation of tannery wastewater. Chemical Engineering Journal DOI 10.1016/j.cej.2017.12.029

Grassi M, Kaykioglu G, Belgiorno V, Lofrano G (2012) Chapter 2 Removal of Emerging Contaminants from Water and Wastewater by Adsorption Process. G. Lofrano (ed.), Emerging Compounds Removal from Wastewater, SpringerBriefs in Green Chemistry for Sustainability DOI 10.1007/978-94-007-3916-1_2

Guan X, Yan S, Xu Z, Fan H (2016) Gallic acid-conjugated iron oxide nanocomposite: an efficient, separable, and reusable adsorbent for remediation of Al (III)-contaminated tannery wastewater. Journal of Environmental Chemical Engineering DOI 10.1016/j.jece.2016.12.010

Guiza S (2017) Biosorption of heavy metal from aqueous solution using cellulosic waste orange peel. Ecological Engineering 99:134-140

Guo X, Zhang S, Shan X (2008) Adsorption of metal ions on lignin. J Hazard Mater 151:134-142

Gupta VK, Agarwal S, Saleh TA (2011) Synthesis and characterization of alumina-coated carbon nanotubes and their application for lead removal. J Hazard Mater 185:17-23

Gupta V, Rastogi A, Nayak A (2010) Adsorption studies on the removal of hexavalent chromium from aqueous solution using a low cost fertilizer industry waste material. Journal of Colloid and Interface Science 342:135-141

Hall KR, Eagleton LC, Acrivos A, Vermeulen T (1966) Pore- and solid-diffusion kinetics in fixed-bed adsorption under constant pattern conditions. Ind Eng Chem Fundam 5:212-223

Han Y, Boateng AA, Qi PX, Lima IM, Chang J (2013) Heavy metal and phenol adsorptive properties of biochars from pyrolyzed switchgrass and woody biomass in correlation with surface properties. Journal of Environmental Management 118:196-204

Hassan AF, Abdel-Mohsen AM, Fouda MMG (2014) Comparative study of calcium alginate, activated carbon, and their composite beads on methylene blue adsorption. Carbohydr Polym 102:192-198

Hernández-Montoya V, Pérez-Cruz MA, Mendoza-Castillo DI, Moreno-Virgen MR, Bonilla-Petriciolet A (2013) Competitive adsorption of dyes and heavy metals on zeolitic structures. Journal of Environmental Management 116:213-221

Ho Y, McKay G (1999) Pseudo-second order model for adsorption system. Process Biochem. 34:451-465

Ho YS, Mckay G (2000) The kinetics of sorption of divalent metal ions onto sphagnum moss peat, Water Resources 34(3):735-742

Ho YS, Mckay G, Wase DJ, Foster CF (2000) Study of the sorption of divalent metal ions on to peat. Advances in Science and Technology 18:639-650

Homagai PL, Ghimire KN, Inoue K (2010) Adsorption behavior of heavy metals onto chemically modified sugarcane bagasse. Bioresource Technology 101:2067-2069

Hossain MA, Ngo HH, Guo WS, Setiadi T (2012) Adsorption and desorption of copper(II) ions onto garden grass. Bioresource Technology 121:386-395

Hossain MK, Strezov V, Nelson PF (2015) Comparative Assessment of the Effect of Wastewater Sludge Biochar on Growth, Yield and Metal Bioaccumulation of Cherry Tomato. Pedosphere 25(5):680-685

Hu X, Xue Y, Liu L, Zeng Y, Long L (2018) Preparation and characterization of Na2S-modified biochar for nickel removal. Environmental Science and Pollution Research DOI 10.1007/s11356-018-1298-6

Huang L, Kong J, Wang W, Zhang C, Niu S, Gao B (2012) Study on Fe(III) and Mn(II) modified activated carbons derived from *Zizania latifolia* to removal basic fuchsin. Desalination 286:268-276

Ibrahim HS, Ammar, NS, Soylak, M, Ibrahim, M (2012) Removal of Cd(II) and Pb(II) from aqueous solution using dried water hyacinth as a biosorbent. Spectrochimica Acta Part A: Molecular and Biomolecular Spectroscopy 96:413-420

Indian Standards (1993) The Environment (Protection) Third Amendment Rules, General Standards For Discharge of Environmental Pollutants Part-A: Effluents 545-560

Iqbal M, Saeed A, Zafar SI (2009) FTIR spectrophotometry, kinetics and adsorption isotherms modeling, ion exchange, and EDX analysis for understanding the mechanism of Cd^{2+} and Pb^{2+} removal by mango peel waste. J Hazard Mater 164:161-171

Isaac CPJ and Sivakumar A (2013) Removal of lead and cadmium ions from water using *Annona squamosa* shell: kinetic and equilibrium studies, Desalination and Water Treatment 51:40-42

Islam BI, Musa AE, Ibrahim EH, Sharafa SAA, Elfaki BM (2014) Evaluation and Characterization of Tannery. Journal of Forest Products & Industries 3(3):141-150

ISW-BDS (1997) GOB, Report on Bangladesh Census of Manufacturing Industries (CMI), Bangladesh Bureau of Statistics, Dhaka

Jadhav SB, Chougle AS, Dhawal PS, Pereira CS, Jadhav JP (2015) Application of response surface methodology for the optimization of textile effluent biodecolorization and its toxicity perspectives using plant toxicity, plasmid nicking assays. Clean Technol Enviro 17:709-720

Javaid A, Ashraf S, Bajwa R (2000). Effect of Tannery Industrial Effluents on Crop Growth and VAM Colonization in *Vigna radiata* (L) Wilczek and *Zea mays* L. Pakistan Journal of Biological Sciences 3:1292-1295

Jhamaria C, Bhatnagar, Naga JP (2015) Accumulation of heavy metals in soil and vegetables due to wastewater irrigation in a semiarid region of Rajasthan, India. International Journal of Environment, Ecology, Family and Urban Studies 5(5):1-10

Jindo K, Mizumoto H, Sawasa Y, Sanchez-Monedero A, Sonoki T (2014) Physical and chemical characterization of biochars derived from different agricultural residues. Biogeosciences 11:6613-6621

Kanchana S, Jeyanthi J, Dinesh Kumar R (2011) Equilibrium and kinetic studies on biosorption of chromium(VI) on to *Chlorella* species. Eur J Sci Res 63:255-62

Kannan N, Karrupasamy K (1998) Low cost adsorbents for the removal of phenyl acetic acid from aqueous solution. Indian J Environ Protect 18(9):683-690

Karim AA, Kumar M, Mohapatra S, Panda CR, Singh A (2015) Banana peduncle biochar: Characteristics and adsorption of hexavalent chromium from aqueous solution. Int Res J Pure Appl Chem7(1):1-10

Kariuki Z, Kiptoo J, Onyancha D (2017) Biosorption studies of lead and copper using rogers mushroom biomass '*Lepiota hystrix'*. South African Journal of Chemical Engineering 23:62-70

Karunanayake AG, Todd OA, Crowley M, Ricchetti L, Jr CUP, Anderson R, Mohan D, Mlsna T (2017) Lead and cadmium remediation using magnetized and nonmagnetized biochar from Douglas fir. Chemical Engineering Journal DOI 10.1016/j.cej.2017.08.124

Kelly-Vargas K, Cerro-Lopez M, Reyna-Tellez S, Bandala ER, Sanchez-Salas JL (2012) Biosorption of heavy metals in polluted water, using different waste fruit cortex. Physics and Chemistry of the Earth 37-39:26-29

Khan AA, Paquiza L (2011) Characterization and ion-exchange behavior of thermally stable nano-composite polyaniline zirconium titanium phosphate: its analytical application in separation of toxic metals. Desalination 265:242-254

Khan TA, Nazir M, Ali I, Kumar A (2017) Removal of Chromium(VI) from aqueous solution using guar gum–nano zinc oxide biocomposite adsorbent. Arabian Journal of Chemistry, 10:S2388-S2398

Kılıç M, Kırbıyık Ç, Çepelioğullar Ö, Pütün AE (2013) Adsorption of heavy metal ions from aqueous solutions by bio-char, aby-product of pyrolysis. Applied Surface Science 283:856- 862

Kim N, Park, M, Park D (2015) A new efficient forest biowaste as biosorbent for removal of cationic heavy metals. Bioresource Technology 175:629-632

Kim WK, Shim T, Kim YS, Hyun S, Ryu C, Park YK, Jung J (2013) Characterization of cadmium removal from aqueous solution by biochar produced from a giant *Miscanthus* at different pyrolytic temperatures. Bioresource Technology 138:266-270

Kisliuk P (1957) The sticking probabilities of gases chemisorbed on the surfaces of solids. Journal of Physics and Chemistry of Solids 3(1-2):95-101

Kołodyńska D, Krukowska J, Thomas P (2017) Comparison of Sorption and Desorption Studies Comparison of sorption and desorption studies of heavy metal ions from biochar and commercial active carbon. Chemical Engineering Journal 307:353-363

Komolwanich T, Tatijarern P, Prasertwasu S, Khumsupan D, Chaisuwan T, Luengnaruemitchai A, Wongkasemjit S (2014) Comparative potentiality of Kans grass (*Saccharum spontaneum*) and Giant reed (*Arundo donax*) as lignocellulosic feedstocks for the release of monomeric sugars by microwave/chemical pretreatment. Cellulose 21(3):1-14.

Korrapati N, Saroj P, Gaur N (2017) Morphological and Elemental analysis of the effluent of Lead-acid battery manufacturing. Journal of Applied Biology & Biotechnology 5(03):052-056

Kumar N, Bauddh K, Dwivedi N, Barman SC, Singh DP (2012) Accumulation of metals in selected macrophytes grown in mixture of drain water and tannery effluent and their phytoremediation potential. J Environ Biol 33:923-927

Kumar N, Bauddh K, Singh R, Anand K, Barman SC, Singh DP (2009) Phytotoxicity of trace metals (Cu & Cd) to Gram (*Cicer arientinum*) and Mung (*Phaseoilus mungo*). J Ecophysiol Occup Hlth 9:59-65

Kumar N, Poonam, Kumar S, Singh D (2015) Ground water quality evaluation at suburban areas of Lucknow, U.P., India. International Journal of Environmental Sciences 6(3):376-387

Kumar PS, Ramalingam S, Kirupha, SD, Murugesan A, Vidhyadevi T, Sivanesan S (2011) Adsorption behavior of nickel(II) onto cashew nut shell: Equilibrium,

thermodynamics, kinetics, mechanism and process design. Chemical Engineering Journal 167:122-131

Kurniawan A, Sisnandy VCA, Trilestari K, Sunarso J, Indraswati N, Ismadji S (2011) Performance of durian shell waste as high capacity biosorbent for Cr(VI) removal from synthetic wastewater. Ecological Engineering 37:940-947

Kyzas GZ, Matis KA (2014) New biosorbent materials: selectivity and bioengineering insights, Processes 2:419-440

Lagergren S (1898) Kungl. Svenska Vetenskapasakad, Handl 24:1-39

Lakherwal D (2014) Adsorption of heavy metals: A review. International Journal of Environmental Research and Development 2249-3131(4):41-48

Lam SS, Liew RK, Wong YM, Yek NYP, Ma NL, Lee CL, Chase HA (2017) Microwave-assisted pyrolysis with chemical activation, an innovative method to convert orange peel into activated carbon with improved properties as dye adsorbent. Journal of Cleaner Production DOI 10.1016/j.jclepro.2017.06.131

Lam YF, Lee LY, Chua SJ, Lim SS, Gan S (2016) Insights into the equilibrium, kinetic and thermodynamics of nickel removal by environmental friendly *Lansium domesticum* peel biosorbent. Ecotoxicol Environ Saf 127:61-70

Lambert JB et al. (1987) Introduction to organic spectroscopy, Macmillon Publication, New york

Lammers K, Arbuckle-Keil G, Dighton J (2009). FT-IR study of the changes in carbohydrate chemistry of three New Jersey pine barrens leaf litters during simulated control burning. Soil Biology and Biochemistry 41(2):340-347

Langmuir I (1916) The constitution and fundamental properties of solids and liquids, part I solids J Am Chem Soc 38:2221-2295

Langmuir I (1918)The adsorption of gases on plane surfaces of glass, mica and platinum. Journal of the American Chemical Society 4(9):1361-1403

Lasheen MR, Ammar NS, Ibrahi HS (2012) Adsorption/desorption of Cd(II), Cu(II) and Pb(II) using chemically modified orange peel: Equilibrium and kinetic studies. Solid State Sciences 14:202-210

Lee XJ, Lee LY, Hiew BYZ, Gan S, Gopakumar ST, Ng HK (2017) Multistage optimizations of slow pyrolysis synthesis of biochar from palm oil sludge for adsorption of lead. Bioresource Technology 245:944-953

Lee Y, Park J, Ryu C, Gang KS, Yang W, Park YK, Jung J, Hyun S (2013) Comparison of biochar properties from biomass residues produced by slow pyrolysis at 500°C. Biores Technol 148:196-201

Lehmann J and Joseph S (2015) Biochar for Environmental Management: Science, Technology and Implementation: Routledge, New York, USA, http://www.biochar-international.org/projects/book

Li J, Zheng L, Liu H (2017) A novel carbon aerogel prepared for adsorption of copper(II) ion in water. J Porous Mater 24:1575-1580

Li K, Wang X (2009) Adsorptive removal of Pb(II) by activated carbon prepared from *Spartina alterniflora*: equilibrium, kinetics and thermodynamics. Biores Technol 100:2810-2815

Li X, Liu S, Na Z, Lua D, Liu Z (2013) Adsorption, concentration, and recovery of aqueous heavy metal ions with the root powder of *Eichhornia crassipes*. Ecological Engineering 60:160-166

Liang S, Guo X, Feng N, Tian Q (2009) Application of orange peel xanthate for the adsorption of Pb^{2+} from aqueous solutions. Journal of Hazardous Materials 170:425-429

Liang S, Guo X, Feng N, Tian Q (2010) Isotherms, kinetics and thermodynamic studies of adsorption of Cu^{2+} from aqueous solutions by Mg^{2+}/K^{+} type orange peel adsorbents. Journal of Hazardous Materials 174:75-762

Lim SF, Zheng YM, Chen JP (2009) Organic arsenic adsorption onto a magnetic sorbent. Langmuir 25(9):4973-4978

Lima LKS, Silva MGC, Vieira MGA (2016) Study of binary and single biosorption by the floating aquatic macrophyte *Salvinia natans*. Brazilian Journal of Chemical Engineering 33(03):649-660

Lin H, Han S, Donga Y, He Y (2017) The surface characteristics of hyperbranched polyamide modified corncob and its adsorption property for Cr(VI). Applied Surface Science 412:152-159

Liu A and Liu Q (2003) Distribution of Pb(II) species in aqueous solutions. Journal of Colloid and Interface Science 268:266-269

Liu DY, Sui G, Bhattacharyya D (2014) Synthesis and characterisation of nanocellulose-based polyaniline conducting films. Compos Sci Technol 99:31-36

Liu FN, Zhang G, Meng Q, Zhang H (2008) Performance of nanofiltration and reverse osmosis membranes in metal effluent treatment, Chinese Journal of Chemical Engineering.16:441-445

Lu HL, Zhang WH, Yang YX, Huang XF, Wang SZ, Qiu RL (2012) Relative distribution of Pb^{2+}sorption mechanisms by sludge-derived biochar. Water Research 46(3):854-862

Luo X, Wang C, Luo S, Dong R, Tu X, Zeng G (2012). Adsorption of As (III) and As(V) from water using magnetite Fe_3O_4-reduced graphite oxideeMnO_2 nanocomposites. Chem Eng J 187:45-52

Ma X, Liu C, Anderson DP et al (2016) Porous cellulose spheres: preparation, modification and adsorption properties. Chemosphere 165:399-408

Machado FM, Bergmann CP, Fernandes THM, Lima EC, Royer B, Calvete T (2011) Adsorption of reactive red M-2BE dye from water solutions by multi-walled carbon nanotubes and activated carbon. J Hazard Mater 192:1122-1231

Mahamad MN, Zaini MAA, Zakaria ZA (2015) Preparation and characterization of activated carbon from pineapple waste biomass for dye removal. Int. Biodeter Biodeg 102:274-280

Maiti SK (2004) Handbook of Methods in Environmental Studies, Vol 1, Water and Wastewater Analysis. ABD Publishers, Jaipur, India

Malwade K, Lataye D, Mhaisalkar V, Kurwadkar S, Ramirez D (2016) Adsorption of hexavalent chromium onto activated carbon derived from *Leucaena leucocephala* waste sawdust: kinetics, equilibrium and thermodynamics. International Journal of Environmental Science and Technology 13:2107-21164

Mandal T, Dasgupta D, Mandal S, Datta S (2010) Treatment of leather industry wastewater by aerobic biological and Fenton oxidation process. Journal of Hazardous Materials 180:204-211

Mansoorian HJ, Mahvi AH, Jafari AJ (2014) Removal of lead and zinc from battery industry wastewater using electrocoagulation process: Influence of direct and alternating current by using iron and stainless steel rod electrodes. Separation and Purification Technology 135:165-175

Manzoor Q, Nadeem R, Iqbal M, Saeed R, Ansari TM (2013) Organic acids pretreatment effect on *Rosa bourbonia* phyto-biomass for removal of Pb(II) and Cu(II) from aqueous media. Bioresour Technol 132:446-452

Manzoor Q, Sajid A, Hussain T, Iqbal M, Abbas M, Nisar J (2017) Efficiency of immobilized *Zea mays* biomass for the adsorption of chromium from simulated media and tannery wastewater. Journal of Materials Research and Technology DOI 10.1016/j.jmrt.2017.05.016

Marín ABP, Aguilar M, Meseguer V, Ortuño J, Sáez J, Lloréns M (2009) Biosorption of chromium (III) by orange (*Citrus cinensis*) waste: batch and continuous studies. Chem Eng J 155:199-206

Marin-Rangel VM, Cortes-Martines R, Villanueva RAC, Garnica-Romo MG, Martinez-Flores HE (2012) As(V) biosorption in an aqueous solution using chemically treated lemon (*Citrus aurantifolia swingle*) residues. Journal of Food Science 71:10-14

Marsal A, Maldonado F, Cuadros S, Bautista ME, Manich AM (2012) Adsorption isotherm, thermodynamic and kinetics studies of polyphenols onto tannery shavings. Chemical Engineering Journal 183:21-29

Martino AD, Iorio M, Capasso R (2013) Sustainable sorption strategies for removing Cr^{3+} from tannery process wastewater. Chemosphere 92:1436-1441

Martins LR, Rodrigues JAV, Adarme OFH, Melo TMS, Gurgel LVA, Gil LF (2017) Optimization of cellulose and sugarcane bagasse oxidation: Application for adsorptive removal of crystal violet and auramine-O from aqueous solution. Journal of Colloid and Interface Science 494:223-241

Mary GS, Sugumaran P, Ramalakshmi B, Ravichandran P, Seshadri S (2016) Production, characterization and evaluation of biochar from pod (*Pisum sativum*), leaf (*Brassica oleracea*) and peel (*Citrus sinensis*) wastes. Int J Recycl Org Waste Agricult 5:43-53

Mckay G and Ho YS (1999) Pseudo-second-order model for sorption processes. Process Biochemistry 34:451

Mehmood S, Rizwan M, Bashir S, Ditta A, Aziz O, Yong LZ, Dai Z, Akmal M, Ahmed W, Adeel M, Imtiaz M, Tu S (2017) Comparative effects of biochar, slag and ferrous–Mn ore on lead and cadmium immobilization in soil. Bulletin of Environmental Contamination and Toxicology DOI 10.1007/s00128-017-2222-3

Mella B, Rosero MJP, Costa DES, Gutterres M (2017) Utilization of tannery solid waste as an alternative biosorbent for acid dyes in wastewater treatment, Journal of Molecular Liquids DOI 10.1016/j.molliq.2017.06.131

Mendez A, Paz-Ferreiro J, Araujo F, Gasco B (2014) Biochar from pyrolysis of deinking paper sludge and its use in the treatment of a nickel polluted soil. J Anal Appl Pyrolysis 107:46-52

Meng J, Cui J, Yu J, Huang W, Wang P, Wang K, Liu M, Song C, Chen P (2018) Preparation of green chelating fibers and adsorption properties for Cd(II) in aqueous solution. J Mater Sci 53:2277-2289

Mittal A, Mittal J, Malviya A, Gupta VK (2010) Removal and recovery of Chrysoidine Y from aqueous solutions by waste materials. J Colloid Interf Sci 344:497-507

Mohammed K and Sahu O (2015). Bioadsorption and membrane technology for reduction and recovery of chromium from tannery industry wastewater. Environmental Technology & Innovation 4:150-158

Mohan D, Sharma R, Singh VK, Steele P, Jr, CUP (2012) Fluoride removal from water using bio-char, a green waste, low-cost adsorbent: equilibrium uptake and sorption dynamics modeling. Ind Eng Chem Res 51:900-914

Mohan D, Rajput S, Singh VK, Steel PH, Jr HUP (2011) Modeling and evaluation of chromium remediation from water using low cost bio-char, a green adsorbent. Journal of Hazardous Materials 188:319-333

Momcilovic M, Purenovic M, Bojic A, Zarubica A, Randelovic M (2011) Removal of lead(II) ions from aqueous solutions by adsorption onto pine cone activated carbon. Desalination 276:53-59

Mondal MK (2009) Removal of Pb(II) ions from aqueous solution using activated tea waste: Adsorption on a fixed-bed column. Journal of Environmental Management 90:3266-3271

Monji AB, Ahmadi SJ, Zolfonoun E (2008) Selective biosorption of zirconium and hafnium from acidic aqueous solutions by rice bran: wheat bran and *Platanus orientalis* tree leaves. Separat Sci Technol 43:597-608

Mopoung R, Kengkhetkit N (2016) Lead and cadmium removal efficiency from aqueous solution by NaOH treated pineapple waste. Int J Appl Chem 12:23-35

Nadeem R, Manzoor Q, Iqbal M, Nisar J (2016) Biosorption of Pb(II) onto immobilized and native Mangifera indica waste biomass. J Ind Eng Chem 35:185-194

Naeem A, Westerhoff P, Mustafa S (2007) Vanadium removal by metal (hydr)oxide adsorbents. Water Research 41:1596-1602

Naiya TK, Bhattacharya AK, Das SK (2009) Adsorption of Cd(II) and Pb(II) from aqueous solutions on activated alumina. Journal of Colloid and Interface Science 333:14-26

Nekouei F, Nekouei S, Keshtpour F, Noorizadeh, Wang S (2017) $Cr(OH)_3$-NPs-CNC hybrid nanocomposite: a sorbent for adsorptive removal of methylene blue and malachite green from solutions. Environ Sci Pollut Res 24:25291-25308

Netzahuatl-Muñoz AR, Guillén-Jiménez FDM, Chávez-Gómez B, Villegas-Garrido TL, Cristiani-Urbina E (2012) Kinetic study of the effect of pH on hexavalent and trivalent chromium removal from aqueous solution by *Cupressus lusitanica* bark. Water Air Soil Pollut 223:625-641

Ngulube T, Gumbo JR, Masindi V, Maity A (2017) An update on synthetic dyes adsorption onto clay based minerals: A state-of-art review. Journal of Environmental Management 191:35-57

Nguyen TAH, Ngo HH, Guo WS, Zhang J, Liang S, Yue QY, Li Q, Nguyen TV (2013) Applicability of agricultural waste and by-products for adsorptive removal of heavy metals from wastewater: Review. Bioresource Technology 148:574-585

Ning-chuan F and Xue-yi G (2012) Characterization of adsorptive capacity and mechanisms on adsorption of copper, lead and zinc by modified orange peel. Trans. Nonferrous Met Soc China 22:1224-1231

Novotny EH, Maia CMBdF, Carvalho MTdM, Madari BE (2015) Biochar: pyrogenic carbon for agricultural use - a critical review. R Bras Ci Solo 39:321-344

Oickle AM, Goertzen SL, Hopper KR, Abdalla YO, Andreas HA (2010) Standardization of the Boehm titration: Part II. Method of agitation, effect of filtering and dilute titrant. Carbon 48:3313-3322

Ouaissa YA, Chabani M, Amrane A, Bensmaili A (2012) Integration of electro coagulation and adsorption for the treatment of tannery wastewater -The case of an Algerian factory, Rouiba. Procedia Engineering 33:98-101

Özçimen D, Ersoy-Meriçboyu A (2010) Characterization of biochar and bio-oil samples obtained from carbonization of various biomass materials. Renewable Energy 35(6):1319-1324

Pakula M, Walczyk M, Biniak S, Światkowski A (2007) Electrochemical and FTIR studies of the mutual influence of lead (II) or iron (III) and phenol on their

adsorption from aqueous acid solution by modified activated carbons. Chemosphere 69:209-219

Pan J, Jiang J, Xu R (2013) Adsorption of Cr(III) from acidic solutions by crop straw derived biochars. Journal of Environmental Sciences 25(10):1957-1965

Panda H, Tiadi N, Mohanty M, Mohanty CR (2017) Studies on adsorption behavior of an industrial waste for removal of chromium from aqueous solution. South African Journal of Chemical Engineering 23:132-138

Park D, Yun Y, Park JM (2010) The past, present, and future trends of biosorption. Biotechnol. Bioprocess Eng 15:86-102

Park JH, Sik Y, Kim SH, Cho JS, Heo JS, Delaune RD, Sea DC (2015) Competitive adsorption of heavy metals onto sesame straw biochar in aqueous solutions. Chemosphere, ption of heavy metals onto sesame straw biochar in aqueous solutions. Chemosphere DOI 10.1016/j.chemosphere.2015.05.093

Pehlivan E, Pehlivan E, Kahraman (2012) Hexavalent chromium removal by Osage Orange. Food Chemistry 133:1478-1484

Peng W, Li H, Liu Y, Song S (2017) A review on heavy metal ions adsorption from water by graphene oxide and its composites. Journal of Molecular Liquids 230:496-504

Peng X, Su, S, Xia M, Lou K, Yang F, Peng S, Cai Y (2018) Fabrication of carboxymethyl-functionalized porous ramie microspheres as effective adsorbents for the removal of cadmium ions. Cellulose DOI 10.1007/s10570-018-1656-z

Petrović M, Šoštarić T, Stojanović M, Petrović J, Mihajlović M, Ćosović A, Stanković S (2017) Mechanism of adsorption of $Cu^{2+}$and Zn^{2+} on the corn silk (*Zea mays* L.). Ecological Engineering 99:83-90

Piccin JS, Gomes CS, Feris LA, Gutterres M (2012) Kinetics and isotherms of leather dye adsorption by tannery solid waste. Chemical Engineering Journal 183:30-38

Pintor AMA, Vilar VJP, Botelho CMS, Boaventura RAR (2014) Optimization of a primary gravity separation treatment for vegetable oil refinery wastewaters. Clean Techn Environ Policy 16:1725-1734

Poonam and Kumar N (2018) Efficiency of sweet lemon (*Citrus limetta*) biochar adsorbent for removal of chromium from tannery effluent. Indian Journal of Environmental protection 38(3):246-256

Poonam, Bharti SK, Kumar N (2018) Kinetic study of lead (Pb^{2+}) removal from battery manufacturing wastewater using bagasse biochar as biosorbent. Applied Water Science 8:119

Prakash KL and Somashekar RK (2006) Groundwater quality - Assessment on Anekal Taluk, Bangalore Urban district, India, Journal of Environmental Biology 27(4):633-637

Qian L-W, Yang M-X, Zhang S-F, Hou C, Song W-q, Yanf J-F, Tang R-H (2018) Preparation of a sustainable bioadsorbent by modifying filter paper with sodium alginate, with enhanced mechanical properties and good adsorption of methylene blue from wastewaters. Cellulose DOI 10.1007/s10570-018-1674-x

Qiao Y, Wu J, Xu Y, Fang Z, Zheng L, Cheng W, Tsang EP, Fang J, Zhaod D (2017) Remediation of cadmium in soil by biochar-supported iron phosphate nano particles. Ecological Engineering 106:515-522

Rai MK, Shahi G, Meena V, Meena R, Chakraborty S, Singh RS, Rai BN (2016) Removal of hexavalent chromium Cr (VI) using activated carbon prepared from mango kernel activated with H_3PO_4. Resource-Efficient Technologies 2:S63-S70

Rajoriya S, Kaur B (2014) Adsorptive Removal of Zinc from Waste Water by Natural Biosorbents. International Journal of Engineering Science Invention 3(6):60-80

Ramesh ST, Rameshbabu N, Gandhimathi R, Kumar MS, Nidheesh PV (2013) Adsorptive removal of Pb(II) from aqueous solution using nano-sized hydroxyapatite. Appl Water Sci 3:105-113

Ramos RL, Rubio LF, Coronado RMG, Barron JM (1995) Adsorption of Trivalent Chromium from Aqueous Solutions onto Activated Carbon. J Chem Tech Biotechnol 62:64-67

Ramos SNdC, Xavier ALP, Teodoro FS, Elias MMC, Gonçalves FJ, Gil LF, de Freitas RP, Gurgel LVA (2015) Modeling mono- and multi-component adsorption of cobalt(II), copper(II), and nickel(II) metal ions from aqueous solution onto a new carboxylated sugarcane bagasse. Part I: Batch adsorption study. Industrial Crops and Products 74:357-371

Ravulapalli S and Kunta R (2018) Removal of lead (II) from wastewater using active carbon of *Caryota urens* seeds and its embedded calcium alginate beads as adsorbents. Journal of Environmental Chemical Engineering 6:4298-4309

Reddy DHK, Lee S, Seshaiah K (2012) Biosorption of toxic heavy metal ions from water environment using honeycomb biomass - an industrial waste material. Water Air Soil Pollut 223:5967-5982

Reddy NA, Lakshmipathy R, Sarada NC (2014) Application of *Citrullus lanatus* rind as biosorbent for removal of trivalent chromium from aqueous solution. Alexandria Engineering Journal 53:969-975

Redlich O, Peterson DL (1959) A useful adsorption isotherm. The Journal of Physical Chemistry 63:1024

Rezaei H (2013) Biosorption of chromium by using *Spirulina* sp. Arabian Journal of Chemistry DOI 10.1016/j.arabjc.2013.11.008

Roberts DA, Paul NA, Dworjanyn SA, Bird MI, Nys Rd (2015) Biochar from commercially cultivated seaweed for soil amelioration. Scientific Reports 5:9665 DOI 10.1038/srep09665

Rocha GJdM, Nascimento VM, Gonçalves AR, Silva VFN, Martín C (2015) Influence of mixed sugarcane bagasse samples evaluated by elemental and physical–chemical composition. Ind Crops Prod 64:52-58

Ruthven DM (1984) Physical adsorption and the characterisation of porous adsorbents. Principles of Adsorption and the Adsoprtion Process. John Wiley and Sons Inc 29-61

Šabanović E, Memić M, Sulejmanović J, Huremović J (2015) Pulverized banana peel as an economical sorbent for the preconcentration of metals. Anal Lett 48(3):442–452

Sadaka S, Sharara MA, Ashworth A, Keyser P, Allen F, Wright A (2014) Characterization of Biochar from Switchgrass Carbonization. Energies 7(2):548-567

Salam OEA, Reiad NA, ElShafei MM (2011) A study of the removal characteristics of heavy metals from wastewater by low-cost adsorbents. Journal of Advanced Research 2:297-303

Samsuri AW, Sadegh-Zadeh F, Seh-Bardan BJ (2013) Characterization of biochars produced from oil palm and rice husks and their adsorption capacitiesfor heavy metals. Int J Environ Sci Technol 11:967-976

Santos CM, Dweck J, Vitto RS, Rosa AH, de Morais LC (2015) Application of orange peel waste in the production of solid biofuels and biosorbents. Bioresource Technology 196: 469-479

Sarkar TC, Azam SMGG, Abd El‐Gawad AM, Gaglione SA, Bonanomi G (2017) Sugarcane bagasse: a potential low‐cost biosorbent for the removal of hazardous materials. Clean Techn Environ Policy 19:2343-2362

Seredych M, Bandosz TJ (2011) Removal of dibenzothiophenes from model diesel fuel on sulfur rich activated carbons. Appl Catal B Environ 106:133-141

Shakoor S and Nasar A (2016) Removal of methylene blue dye from artificially contaminated water using *citrus limetta* peel waste as a very low cost adsorbent. Journal of the Taiwan Institute of Chemical Engineers DOI 10.1016/j.jtice.2016.06.009

Sharma S, Malaviya P (2016) Bioremediation of tannery wastewater by chromium resistant novel fungal consortium. Ecological Engineering 91:419-425

Shehzad K, Xie C, He J, Cai X, Xu W, Liu J (2018) Facile synthesis of novel calcined magnetic orange peel composites for efficient removal of arsenite through simultaneous oxidation and adsorption Journal of Colloid and Interface Science 511:155-164

Shin WS (2017) Adsorption characteristics of phenol and heavy metals on biochar from *Hizikia fusiformis*. Environmental Earth Sciences 76:782

Singanan M and Peters E (2013) Removal of toxic heavy metals from synthetic wastewater using a novel biocarbon technology. Journal of Environmental Chemical Engineering 1:884–890

Singh B, Das SK (2012) Removal of Pb(II) ions from aqueous solution and industrial effluent using natural biosorbents. Environ Sci Pollut Res 19:2212-2226

Sips R (1948) On the structure of a catalyst surface. J Chem Phys 16:490-495

Slimani R, Ouahabi IE, Elmchaouri A, Cagnon B, Antri SE, Lazar S (2017) Adsorption of copper (II) and zinc (II) onto calcined Animal Bone Meal. Part I: Kinetic and thermodynamic parameters. Chemical Data Collections DOI 10.1016/j.cdc.2017.06.006

Soliman EM, Ahmed SA, Fadl AA (2011) Reactivity of sugar cane bagasse as a natural solid phase extractor for selective removal of Fe(III) and heavy-metal ions from natural water samples. Arabian Journal of Chemistry 4:63-70

Solum MS, Pugmire RJ, Jagtoyen M, Derbyshire F (1995) Evolution of carbon structure in chemically activated wood. Carbon 33:1247-54

Song J, Kong H, Jang J (2011) Adsorption of heavy metal ions from aqueous solution by polyrhodanine-encapsulated magnetic nanoparticles. Journal of Colloid and Interface Science 359:505–511

Sönmezay A, Öncel MS, Bektaş N (2012) Adsorption of lead and cadmium ions from aqueous solutions using manganoxide minerals. Trans Nonferrous Me Soc China 22:3131−3139

SPC Water, Sanitation Program: Water Distribution http://www.pacificwater.org/pages.cfm/water-services/water-demand-management/water-distribution/?printerfriendly=true Accessed 24 October 2018

Srinivasan SK, Ganguly S (1991) FT-IR spectroscopic studies of metal nitrates supported on a modified montmorillonite clay. Catal Lett 10:279-288

Štefelová J, Zelenka T, Slovák V (2017) Biosorption (removing) of Cd(II), Cu(II) and methylene blue using biochar produced by different pyrolysis conditions of beech and spruce sawdust. Wood Sci Technol 51:1321-1338

Sud D, Mahajan G, Kaur MP (2008) Agricultural waste material as potential adsorbent for sequestering heavy metal ions from aqueous solutions-A review. Bioresource Technology 99:6017-6027

Suksabye P and Thiravetyan P (2012) Cr(VI) adsorption from electroplating plating wastewater by chemically modified coir pith. Journal of Environmental Management 102:1-8

Sun L, Chen D, Wan S, Yu Z (2015) Performance, kinetics, and equilibrium of methylene blue adsorption on biochar derived from eucalyptus saw dust modified with citric, tartaric, and acetic acids. Bioresource Technology 198:300-308

Swathi M, Singh AS, Aravind S, Sudhakar PKA, Gobinath R, Saranya D (2014) Adsorption studies on tannery wastewater using rice husk. Scholars Journal of Engineering and Technology 2(2B):253-257

Taha GM, Arifien AE, El-Nahas S (2011) Removal efficiency of potato peels as a new biosorbent material for uptake of Pb(II), Cd(II) and Zn(II) from the aqueous solutions. Journal of Solid Waste Technology and Management 37:128-140

Tahir H, Sultan M, Akhtar N, Hameed U, Abid T (2016) Application of natural and modified sugar cane bagasse for the removal of dye from aqueous solution. Journal of Saudi Chemical Society 20:S115-S121

Tahir N, Bhatti HN, Iqbal M, Noreen S (2016a) Biopolymerscomposites with peanut hull waste biomass and applicationfor crystal violet adsorption. Int J Biol Macromol 94:210-20

Tahir SS ans Naseem R (2007) Removal of Cr(III) from tannery wastewater by adsorption onto bentonite clay. Separation and Purification Technology 53:312-321

Tan X, Fang M, Cheng C, Yu S, Wang X (2008) Counterion effects of nickel and sodium dodecylbenzene sulfonate adsorption to multiwalled carbon nanotubes in aqueous solution. Carbon 46:1741-1750

Temesgen F, Gabbiye N, Sahu O (2018) Biosorption of Reactive Red Dye (RRD) on Activated Surface of Banana and Orange Peels: Economical Alternative for Textile Effluent, Surfaces and Interfaces DOI 10.1016/j.surÞn.2018.04.007

Tempkin MI, Pyzhev V (1940) Kinetics of ammonia synthesis on promoted iron catalyst. Chemical Research in the USSR, 12:327-356

Thakur LS, Parmar M (2013) Adsorption of heavy metal (Cu^{2+}, Ni^{2+} and Zn^{2+}) from synthetic waste water by tea waste adsorbent. International Journal of Chemical and Physical Sciences 2(6):6-19

Thapliyal A, Vasudevan P, Dastidar MG, Tandon M, Mishra S (2011) Irrigation with domestic wastewater: Responses on growth and yield of ladyfinger *Abelmoschus esculentus* and on soil nutrients. J. Environ. Biol. 32:645-651

The CY, Wu TY, Juan JC (2014) Potential use of rice starch in coagulation–flocculation process of agro-industrial wastewater: Treatment performance and flocs characterization. Ecological Engineering 71:509-519

Tomar V, Prasad S, Kumar D (2013) Adsorptive removal of fluoride from water samples using Zr–Mn composite material. Microchemical Journal 111:116-124

Tovar CT, Ortiz AV, Correa DA, Gómez NP, Amor MO (2018) Lead (II) remotion in solution using lemon peel (*Citrus limonum*) modified with citric acid. International Journal of Engineering and Technology 10(1):117-122

Trakal L, Veselská V, Šafařík I, Číhalová S, Komárek M (2016) Lead and cadmium sorption mechanisms on magnetically modified biochars. Bioresource Technology 203:318–324

Tsiepe JT, Mamba BB, Abd-El-Aziz IAS, Mishra AK (2017) Fe_3O_4-β-cyclodextrin-Chitosan Bionanocomposite for arsenic removal from aqueous

solution. Journal of Inorganic and Organometallic Polymers and Materials DOI 10.1007/s10904-017-0741-3

Uçar S, Erdem M, Tay T, Karagö z S (2015) Removal of lead (II) and nickel (II) ions from aqueous solution using activated carbon prepared from rapeseed oil cake by Na_2CO_3 activation. Clean Techn Environ Policy17:747-756

Ullah I, Nadeem R, Iqbal M, Manzoor Q (2013) Biosorption of chromium onto native and immobilized sugarcane bagasse waste biomass. Ecol Eng 60:99-107

Ungureanu G, Santos S, Boaventura R, Botelho C (2015) Arsenic and antimony in water and wastewater: Overview of removal techniques with special reference to latest advances in adsorption. Journal of Environmental Management 151:326-342

UNIDO (2011) "Introduction to treatment of tannery effluents", Vienna, pp. 7-11, 18-21, 31-32.

Upadhyay KH, Vaishnav AM, Tipre DR, Patel BC, Dave SR (2017) Kinetics and mechanisms of mercury biosorption by an exopolysaccharide producing marine isolate *Bacillus licheniformis*. 3 Biotech 7:313

Vadivelan V, Kumar KV (2005) Equilibrium, kinetics, mechanism, and process design for the sorption of methylene blue onto rice husk. J Colloid Interf Sci 286:90-100

Vajihabanu H, Kannahi M, Mary DA (2015) Analysis of Physico-Chemical Parameter, Heavy Metal Content and microbial load in Battery Industry Effluent. Int J Pure App Biosci 3(6):81-86

Van Vinh N, Zafar M, Behera SK, Park H-S (2015) Arsenic(III) removal from aqçeous solution by raw and zinc-loaded pine cone biochar: equilibrium, kinetics, and thermodynamics studies. Int J Environ Sci Technol 12:1283-1294

Velazquez-Jimenez LH, Pavlick A, Rangel-Mendez JR (2013) Chemical characterization of raw and treated agave bagasse and its potential as adsorbent of metal cations from water. Industrial Crops and Products 43:200-206

Venkatesha NJ, Bhat YS, Prakash BSJ (2016) Volume accessibility of acid sites in modified montmorillonite and triacetin selectivity in acetylation of glycerol. Appl Catal A: Gen 496:51-57

Vergili I, Gönder ZB, Kaya Y, Gülten G, Selva C (2017) Sorption of Pb (II) From Battery Industry Wastewater Using a Weak Acid Cation Exchange Resin. Process Safety and Environment Protection DOI 10.1016/j.psep.2017.03.018

Verma, T, Ramteke PW, Grag SK (2008) Quality assessment of treated tannery wastewater with special emphasis on Pathogenic *E. coli* detection through serotyping, Environmental Monitoring and Assessment 145:243-249.

Vetriselvi V and Santhi RJ (2015) Redox polymer as an adsorbent for the removal of chromium(VI) and lead(II) from the tannery effluents. Water Resources and Industry 10:39-52

Vilardi G, Pulido JMO, Stoller M, Verdone N, Palma LD (2018) Fenton oxidation and Chromium recovery from Tannery wastewater by means of iron-based coated biomass as heterogeneous catalyst in fixed-bed columns, Chemical Engineering Journal DOI 10.1016/j.cej.2018.06.095

Vithanage M, Mayakaduwa SS, Herath I, Ok YS, Mohan D (2015) Kinetics, thermodynamics and mechanistic studies of carbofuran removal using biochars from tea waste and rice husks. Chemosphere DOI 10.1016/j.chemosphere.2015.11.002

Wang B, Li C, Liang H (2013) Bioleaching of heavy metal from woody biochar using *Acidithiobacillus ferrooxidans* and activation for adsorption. Bioresource Technology 146:803-806

Wang J, Chen B (2015) Adsorption and coadsorption of organic pollutants and a heavy metal by graphene oxide and reduced graphene materials. Chemical Engineering Journal 281:379-388

Wang S, Gao B, Li Y, Mosa A, Zimmerman AR, Ma LQ, Harris WG, Migliaccio KW (2015) Manganese oxide-modified biochars: Preparation, characterization, and sorption of arsenate and lead. Bioresource Technology 181:13-17

Wang XS, Li ZZ, Tao SR (2009) Removal of chromium (VI) fromaqueous solution using walnut hull. J Environ Manag 90:721-9

Wang Y, Wang X, Wang X, Liu M, Yang L, Wu Z, Xia S, Zhao J (2012) Adsorption of Pb(II) in aqueous solutions by bamboo charcoal modified with KMnO4 via microwave irradiation. Colloids and Surfaces A: Physicochem. Eng Aspects 414:1-8

Wang Y, Wang XJ, Liu M, Wu Z, Yang LZ, Xia SQ, Zhao JF (2012a) Cr(VI) removal from water using cobalt-coated bamboo charcoal prepared with microwave heating. Industrial Crops and Products 39:81-88

Wasewar KL (2010) Adsorption of metals onto tea factory waste: a review. International Journal of Recent Research and Applied Studies 3:(3)

Weber TW, Chakraborti RK (1974) Pore and solid diffusion models for fixed bed adsorbers. J Am Inst Chem Eng 20: 228

WHO (2003) Guidelines for drinking-water quality, 2nd ed. Vol. 2. Health criteria and other supporting information. World Health Organization, Geneva http://www.who.int/water_sanitation_health/dwq/chemicals/sodium.pdf

WHO (2009) Potassium in drinking-water, Background document for development of WHO Guidelines for Drinking-water Quality, pp 1-5 http://www.who.int/water_sanitation_health/water-quality/guidelines/chemicals/potassium-background.pdf

WHO (2009a) Calcium and magnesium in drinking-water: public health significance. Geneva, World Health Organization http://whqlibdoc.who.int/publications/2009/9789241563550_eng.pdf

WHO (2011) Hardness in Drinking-water, Background document for development of WHO Guidelines for Drinking-water Quality, pp 1-11 http://www.who.int/water_sanitation_health/dwq/chemicals/hardness.pdf

WHO (2017) Guidelines for drinking-water quality: fourth edition incorporating the first Addendum ISBN 978-92-4-154995-0

Witek-Krowiak A, Harikishore K, Reddy D (2013) Removal of microelemental Cr(III) and Cu(II) by using soybean meal waste: unusual isotherms and insights of binding mechanism. Bioresour Technol 127:350-357

Wu K, Liu R, Li T, Liu H, Peng J, Qu J (2013) Removal of arsenic (III) from aqueous solution using a low-cost by-product in Fe removal plants-Fe-based backwashing sludge. Chem Eng 226 (6):393-401

Wu W, Yang M, Feng Q, McGrouther K, Wang H, Lu H, Chen Y (2012) Chemical characterization of rice straw-derived biochar for soil amendment. Biomass Bioenergy 47:268-76.

Wu Y, Fan Y, Zhang M, Ming Z, Yang S, Arkin A, Fang P (2016) Functionalized agricultural biomass as a low-cost adsorbent: Utilization of rice straw

incorporated with amine groups for the adsorption of Cr(VI) and Ni(II) from single and binary systems. Biochemical Engineering Journal 105:27-35

Yadav S, Srivastava V, Banerjee, S, Weng, C, Sharma YC (2012) Adsorption characteristics of modified sand for the removal of hexavalent chromium ions from aqueous solutions: Kinetic, thermodynamic and equilibrium studies. Catena 100:120-127

Yan T, Luo X, Lin X, Yang J (2016) Preparation, characterization and adsorption properties for lead (II) of alkali-activated porous leather particles, Colloids and Surfaces A: Physicochemical and Engineering Aspects DOI 10.1016/j.colsurfa.2016.10.023

Yang C, Niu D, Zhong Y, Li L, Lv H, Liu Y (2018) Adsorption of uranium by hydrous manganese dioxide from aqueous solution. J Radioanal Nucl Chem 315:533, https://doi.org/10.1007/s10967-018-5705-8

Yang X and Cui X (2013) Adsorption characteristics of Pb (II) on alkali treated tea residue. Water Resources and Industry 3:1-10

Yao Y, Guo B, Inyang M, Zimmerman AR, Cao X, Pullammanappallil P, Yang L (2011) Biochar derived from anaerobically digested sugar beet tailings: characterization and phosphate removal potential. Bioresour Technol 102:6273-6278

Yorgun S, Yıldız D (2015) Preparation and characterization of activated carbons from Paulownia wood by chemical activation with H3PO4. J Taiwan Inst Chem Eng 53:122-131 DOI 10.1016/j.jtice.2015.02.032

Yu Z, Zhou L, Huang Y, Song Z, Qiu W (2015) Effects of a manganese oxide-modified biochar composite on adsorption of arsenic in red soil. Journal of Environmental Management 163:155-162

Zhang S, Niu H, Cai Y, Zhao X, Shi Y (2010) Arsenite and arsenate adsorption on coprecipitated bimetal oxide magnetic nanomaterials: $MnFe_2O_4$ and $CoFe_2O_4$. Chem Eng J 158:599-607

Zhang X, Gao B, Xia H (2014) Effect of cadmium on growth, photosynthesis, mineral nutrition & metal accumulation of bana grass & vetiver grass. Ecotoxicology and Environmental Safety 106:102-108

Zhang X, Lin Q, Luo S, Ruan K, Peng K (2018) Preparation of novel oxidized mesoporous carbon with excellent adsorption performance for removal of malachite green and lead ion. Applied Surface Science 442:322-331

Zhang Z, O'Hara IM, Kent GA, Doherty WOS (2013) Comparative study on adsorption of two cationic dyes by milled sugarcane bagasse. Industrial Crops and Products 42:41-49

Zhao L, Cao X, Mašek O, Zimmerman A (2013) Heterogeneity of biochar properties as a function of feedstock sources and production temperatures. J Hazard Mater 256-57:1-9

Zhao Y, Chang W, Huang Z, Feng X, MaL, Qi X, Lim Z, (2017a) Enhanced removal of toxic Cr(VI) in tannery wastewater by photoelectrocatalysis with synthetic TiO_2 hollow spheres, Applied Surface Science DOI 10.1016/j.apsusc.2017 .01.306

Zhao Y, Huang L, Chen Y (2017) Biochars derived from giant reed (*Arundo donax* L.) with different treatment: characterization and ammonium adsorption potential. Environ Sci Pollut Res 24:25889-25898

Zheng XY, Wang XY, Shen YH, Lu X, Wang TS (2017) Biosorption and biomineralization of uranium(VI) by *Saccharomyces cerevisiae*-Crystal formation of chernikovite. Chemosphere DOI 10.1016/j.chemosphere. 2017.02.035.

Zhu C, Hu T, Tang L, Zeng G, Deng Y, Lu Y, Fang S, Wang J, Liu Y, Yu J (2018) Highly efficient extraction of lead ions from smelting wastewater, slag and contaminated soil by two-dimensional montmorillonite-based surface ion imprinted polymer absorbent. Chemosphere DOI 10.1016/j.chemosphere. 2018.06.105.

Scientific Publications and Achievements

Scientific Publications and Achievements

Research Papers

1. **Poonam** and Kumar N (2018). Efficiency of sweet lemon (*Citrus limetta*) biochar adsorbent for removal of chromium from tannery effluent. Indian Journal of Environmental protection 38 (3):246-256
2. **Poonam**, Bharti SK, Kumar N (2018) Kinetic study of lead (Pb^{2+}) removal from battery manufacturing wastewater using bagasse biochar as biosorbent. Applied Water Science 8:119
3. Bharti SK, Kumar D, Anand S, **Poonam**, Barman SC, Kumar N (2017) Characterization and morphological analysis of individual aerosol of PM_{10} in urban area of Lucknow, India. Micron 103:90-98
4. Bharti SK, Kumar D, Anand S, **Poonam**, Barman SC, Kumar N (2017) Temporal variation and trace metal characterisation of particulate matter in ambient air of rural and urban areas of Lucknow, India. Climate Change and Environmental Sustainability 5(1): 75-82
5. Chandbiwi, **Poonam**, Kumar D, Kumar, N (2017) Ground Water Quality Evaluation in Rural areas of Lucknow, Uttar Pradesh, India. Water and Energy International 60(90):54-59
6. Kumar N, **Poonam**, Kumar S, Singh DP (2015) Ground water quality evaluation at suburban areas of Lucknow, U.P., India. International Journal of Environmental Sciences 6(3):376-387

Book Chapters

1. **Poonam**, Ahmad S, Kumar N, Chakraborty P, Kothari R (2017) Plant Growth Under Stress Conditions: Boon or Bane. In: Shukla V, Kumar S, Kumar N (eds.), Plant Adaptation Strategies in Changing Environment. Springer, Singapore
2. Kumar D, **Poonam**, Bauddh K, Tiwari J, Singh DP, Kumar N (2017) *Ricinus communis*: An Ecological Engineer and a Biofuel Resource. In: Bauddh K,

Singh B, Korstad J (eds.), Phytoremediation Potential of Bioenergy Plants. Springer, Singapore

3. Kumar D, Anand S, **Poonam**, Tiwari J, Kisku GC, Kumar N (2018) Removal of Inorganic and Organic Contaminants from Terrestrial and Aquatic Ecosystems Through Phytoremediation and Biosorption. In: R. C. Sobti et al. (eds.), Environmental Biotechnology: For Sustainable Future. DOI 10.1007/978-981-10-7284-0_3

Newspaper Article

1. **Poonam** and Kumar (2015) Article in Hindi News Paper (Dainik Jargan) entitling "Keetnashak Bigad Rahe Pani ki Sehat" date 27/10/2015.

Conference Papers

1. **Poonam** and Kumar N. (2018). Poster presentation on "ADSORPTIVE REMOVAL HEAVY METALS PRESENT IN WASTEWATER OF DIFFERENT INDUSTRIES BY SWEET LEMON (*Citrus limetta*) BIOCHAR" in 1st North Indian Science Congress-2018 & International Confrence on Science and Technology for sustainable Future, organized by BBA University, Lucknow, from 10th and 11th January, 2018.
2. **Poonam** and Kumar N. (2014). Poster presentation on "Levels of heavy metals in the ground water of suburban areas of Lucknow, U.P., India" in International Conference on Environmental Technology and Sustainable Development: Challenges & Remedies, organized by DES, BBA University, Lucknow, Uttar Pradesh (India), from 21st to 23rd February, 2014.

Accepted Book Chapters

1. **Poonam** and Kumar N (2019) Kinetics, isotherms and cumulative effect of different parameters affecting biosorption of heavy metals present in water or wastewater: A review. In Chowdhary and Raj (eds.), Contaminants and Clean Technologies. CRC Press, Taylor & Francis, USA

Paper communicated

1. P**oonam** and Kumar N (2018) Experimental and kinetic study of removal of Lead (Pb^{2+}) from battery effluent using sweet lemon (*Citrus limetta*) peel biochar adsorbent. Environment Development and Sustainability. (Full length Research paper, **In Minor Revision**)
2. **Poonam**, Bharti SK, Kumar N (2019) Comparative study for sorption and desorption of chromium (Cr) and lead (Pb) and present in two industrial wastewaters by lemon (*Citrus limon*) peel biochar. Ecological Engineering (**Under review**)
3. **Poonam** and Kumar N (2019) An ecofriendly approach for adsorptive removal of Cr by optimized conditions and its application over removal of chromium present in tannery effluent by bagasse biochar. Environmental Sustainability (**With Editor**)

Workshop & Conferences attended

1. Participated in the two days **National Workshop** on Innovative and Technology Transfer to Industries: Role of Universities, on 10th and 11th March, 2014.
2. Participated in the two days **National Workshop** on Innovative and Technology Transfer to Industries: Role of Universities, on 10th and 11th March, 2014
3. Participated in **LUSCON-2014** organized by BBAU, Lucknow.
4. One day **National Seminar**, on ICT in higher Education: Need of the Hour, organized by Information & Guidance Bureau % DLIS, B.B.A.U., Lucknow, on 20th January, 2014, attended.
5. Participated in **LUSCON-2015** held on 31st October, 2015 to 2nd November, 2015 at Babasaheb Bhimrao Ambedkar University
6. Participated in **National Conference** on Climate Change and Sustainable Development: Emerging Issues and Mitigation Strategies (CCSD-2015) held on 23-24 November, 2015, at Department of Environmental Science, Babasaheb Bhimrao Ambedkar University, Lucknow.
7. Participated in **103rd Indian Science Congress-2016**, held on 3rd to 7th January, 2016 at University of Mysuru, Mysuru, Karnataka.

Applied Water Science (2018) 8:119
https://doi.org/10.1007/s13201-018-0765-z

ORIGINAL ARTICLE

Kinetic study of lead (Pb^{2+}) removal from battery manufacturing wastewater using bagasse biochar as biosorbent

Poonam[1] · Sushil Kumar Bharti[1] · Narendra Kumar[1]

Received: 8 March 2018 / Accepted: 2 July 2018

Abstract

Agricultural waste of bagasse was employed for investigating its lead (Pb^{2+}) removal potential from wastewater of battery manufacturing industry. To optimize maximum removal efficacy of the bagasse, it was thermally modified in the form of biochar. Adsorption kinetics and mechanism including various parameters (contact time, dose and pH) were studied employing biochar prepared from bagasse waste. The optimum adsorption occurred at pH 5 with 140 min. of contact time utilizing 5 g of adsorbent dosage at room temperature (25 ± 3 °C). The maximum removal efficiency was recorded as 12.741 mg g^{-1} with 75.376% of removal at optimum pH 5 as compared to the initial concentration in the effluent. The result illustrated the most suitable fit was for Langmuir isotherm with monolayer and homogenous adsorption of Pb^{2+}. The kinetics involved in the process was observed to be pseudo-second-order, which indicates chemisorption as a major phenomenon involved in the process. The characterization of the adsorbent biochar was done by SEM, EDX and FTIR analysis that provided details about ultrastructural and functionality of organic moiety present to have porous and rough surface, favoring the adsorption process. The functional groups identified by the FTIR analysis demonstrated involvement of carboxyl groups in Pb^{2+} binding. Postadsorption elution of metal-loaded bagasse was executed by 0.1 M HNO_3 with about 90% of regeneration.

Keywords Biosorption · Biochar · Isotherms · Kinetics · Desorption · Water pollution · Heavy metals

Introduction

Industrialization and urbanization have all the limits to sustain a healthy and peaceful life on the earth (Li et al. 2017). Among them, aquatic pollution caused by release of various heavy metals (HMs) from different anthropogenic activities is one of the major environmental concerns (Amuda et al. 2007; Ajenifuja et al. 2017). These HMs have the bioaccumulation tendency, non-biodegradable nature and may contaminate the food chain threatening the existence of living beings (Rangabhashiyam and Selvaraju 2015; Poonam and Kumar 2018).

Lead (Pb^{2+}) is one of the most toxic HMs, as lowest concentration in drinking water may cause serious problems to the nervous and reproductive system, kidney, liver, brain and bony tissues (Renner 2010; Andrade et al. 2015). The recommended concentration level of by the Environmental Protection Agency (EPA) is 0.015 and 0.05 mg l^{-1} in drinking and wastewater, respectively (Salmani et al. 2017; Gil et al. 2018). The main sources of the Pb^{2+} pollution are battery manufacturing industry, shooting ranges, paint industries, mining processes, chemical manufacturers, surfactants, preservatives, etc. (Xu et al. 2013; Liu et al. 2016; Laidlaw et al. 2017; Mehmood et al. 2017). The removal of Pb^{2+} from wastewater is accomplished by various conventional techniques like precipitation with hydroxide ion or lime, ion exchange, coagulation, electrochemical process, reverse osmosis and ion flotation (Wang and Chen 2009; Kong et al. 2014; Ehrampoush et al. 2015). But, these methods are expensive as well as produce secondary wastes such as persistent organic pollutants, volatile organic compounds (Salmani et al. 2017; Banerjee et al. 2012). Therefore, one of the most effective and low-cost techniques, adsorption, has attracted researchers for the removal of HMs from

✉ Narendra Kumar
narendrakumar_lko@yahoo.co.in

Poonam
poonam.rgnp@gmail.com

Sushil Kumar Bharti
bhartisushil93@gmail.com

[1] Department of Environmental Science, Babasaheb Bhimrao Ambedkar University, Raebareli Road, Lucknow, UP 226025, India

Published online: 10 July 2018

water bodies (Trans et al. 2010; Uçar et al. 2015). However, modification of adsorbents for better performance may be a restricting factor in view of consumption of energy and chemicals (Gil et al. 2018). Till now available studies suggest the use of readily available and cheaper materials for example agricultural wastes, industrial wastes and household wastes, algae and fungi for the removal of Pb^{2+} from water (Saka et al. 2011; Taha et al. 2011; Ibrahim et al. 2012; Reddy et al. 2014; Cheraghi et al. 2015).

Various researchers have used the by-product of sugarcane, i.e., bagasse adsorption of different pollutants including heavy metals, dyes (Joseph et al. 2009; Saad et al. 2010; Said et al. 2013; Gardare et al. 2015; Abdelhafez and Li 2016; Tahir et al. 2016). It is an easily available waste which can be collected from different sugar mills and juice shops. In the present study bagasse was used as adsorbent for the purpose of removal of Pb^{2+} from battery manufacturing industry effluent. The adsorbent was thermally modified into biochar to enhance the efficiency of adsorbent as thermal treatment increased the surface area and porosity of the adsorbent (Doke and Khan 2017). Adsorption is a surface phenomenon which depends on a number of parameters like pH, contact time, adsorbent dose, initial metal concentration, pore size, temperature, surface area (Buasri et al. 2012; Nguyen et al. 2013; Salmani et al. 2017). The goal of the present study is to assess the effectiveness and performance of bagasse biochar for the removal of Pb^{2+} from wastewater of battery manufacturing industry effluent. Therefore, the effect of contact time and adsorbent dose on room temperature (25 ± 3 °C) and at pH 5 (optimized) was investigated to optimize the kinetics and isotherms involved in the process. The experiments were performed in batch technique, and adsorption capacity was calculated in the each step for the optimization of the parameters.

Materials and methods

Sample collection

Wastewater was collected from the effluent outlet of battery manufacturing industry situated near Aishbagh Park, Lucknow, UP. The samples were collected in sampling gallons of 10 l during winter season (January 2016) to minimize the influence of microbial activity on physicochemical properties of the wastewater which were examined by following methods of APHA (2005).

Adsorbent preparation

Bagasse was collected from sugar juice shops of Rajnikhand, Lucknow. After collection, it was brought to the laboratory and washed out thoroughly first with tap water after that deionized water for removing dust and unwanted objects. Lastly, bagasse was air-dried for 2 weeks to remove the moisture content. Then, it was subjected to pyrolysis at temperature of about 300 ± 10 °C for 2.5 h. After cooling overnight, the biochar was washed thoroughly with deionized water to remove unwanted ash contents. Thereafter, it was dried in the oven and stored in desiccated condition in airtight containers.

Characterization of the adsorbent

All of the chemical reagents used in the present study were of analytical reagent (AR) grade from E. Merck, Darmstadt, Germany. The adsorbent was characterized by atomic adsorption spectrometer (AAS), Fourier transform infrared spectroscopy (FTIR), scanning electron microscope (SEM) and energy-dispersive X-ray analysis (EDX) studies. The concentration of Pb^{2+} was determined by AAS (Varian AA240FS). The functional groups present in the biochar before and after treating the wastewater were determined by FTIR (Nicolet^{TM} 6700). Surface morphology was observed by SEM (JSM-6490LV, manufactured by JEOL, Japan) micrographs. Further, elemental composition was analyzed by EDX (model no. JSM-6490LV, designed by JEOL, Japan) and elemental composition (C, H, N and S %) was analyzed by CHNS analyzer (model no. Flash EA112 Series, manufactured by Thermo Finnegan). Surface area and pore size of bagasse biochar (before and after treatment) were characterized by Quanta Chrome Nova-1000 surface analyzer instrument under liquid N_2 temperature. Further, adsorption–desorption studies were performed in order to determine the evolution of porosity and textural properties and surface are from Brunauer–Emmett–Teller (BET) method. Barrett–Joyner–Halenda (BJH) method was used to evaluate pore diameter and volume and de Boer t-method for the newly generated micropore volume measurement (Venkatesha et al. 2016). The structural integrity of the sample was observed by powder X-ray diffraction (XRD). The data were recorded by step scanning at $2\theta = 0.0200$/s from 30 to 800 on PANalytical X' Pert PRO MPD X-ray diffraction with graphite monochromatized Cu K α radiation ($\lambda = 0.15406$).

Quantitative evaluation of surface acidic functional groups on the adsorbent

The acidic functional groups present on the surface of biochar were determined by the following Boehm titration method (Boehm et al. 1964; Oickle et al. 2010). 0.05 M $NaHCO_3$, Na_2CO_3 and NaOH bases were used in this method. 0.5 g of adsorbent was added in 50 ml of three bases. After that, the samples along with blank were shaken for 24 h at 120 rpm and then filtered it to remove extra particles. Thereafter, 20 ml of filtrate from each one was titrated with 0.05 M HCl

to neutralize the base completely, and then backtitration was done by the blank solution with 0.05 M NaOH. The phenolphthalein indicator was used to determine the end point of the reaction. All titrations were carried out at room temperature (25 ± 3 °C), and the solutions were made up of Millipore water. The difference between molar NaOH and Na_2CO_3 was assumed to be the phenolic group content as described by Oickle (2010) and Abdelhafez and Li (2016).

Following steps were used to calculate different surface acidic groups

1. Calculation of surface acidic groups amount (A_x)

$$A_x = \frac{(V_{bx} - V_x).M_{\mathrm{HCl}}.2.5}{m_x} \text{ mol g m}^{-1}$$

where m_x = mass of biochar (gm), V_{bx} = volume (ml) of HCl used for the titration of blank, V_x = volume (ml) used for sample titration of respective bases solution after biochar addition, M_{HCl} = molarity of HCl concentration in moles/lit., 2.5 is a coefficient for decreasing titration sample volume in comparison with reaction sample volume (50 ml/20 ml),

2. Calculation of the amount of different kinds of surface groups
   a. Amount of phenolic groups, $A_{\mathrm{ph}} = A_3 - A_2 - A_1$
   b. Amount of carboxylic groups, $A_{\mathrm{ca}} = A_1$
   c. Amount of carboxylic from lactones hydrolysis groups $A_{\mathrm{la}} = A_2 - A_1$

   where A_1, A_2 and A_3 are amount of surface acidic groups for $NaHCO_3$, Na_2CO_3 and NaOH, respectively.

Moisture and ash content

Moisture content: 1 g of sample was dried for 24 h in an oven at temperature of 100 ± 5 °C until constant weight was gained. Moisture content was calculated using the following formula

$$\text{Moisture content}(\%) = \frac{w_{\mathrm{i}} - w_{\mathrm{f}}}{W_{\mathrm{i}}} \times 100$$

where w_{i} = initial weight of the adsorbent (gm), w_{f} = final weight of adsorbent after drying (gm).

Ash content: It was determined with the help of muffle furnace by weighing 1 g of the sample and placing it into a porcelain crucible. The crucible was heated up to 500 ± 5 °C for 5 h. The material was allowed to cool down in a desiccator for 15 min. The ash content was calculated by using the following formula

$$\text{Ash content}(\%) = \frac{W_2 - W_0}{W_1 - W_0} \times 100$$

where W_0 = weight of empty crucible (g), W_1 = weight of crucible (g) + weight of adsorbent (gm), W_2 = weight of crucible (g) + weight of ashed sample (g) (Basu et al. 2017; Poonam and Kumar 2018).

Experimental setup

The adsorption experiment was performed by varying adsorbent dosage from 2.0 to 5.0 g L^{-1} at an interval of 0.5 g, for 100 ml in 250-ml Erlenmeyer flasks at rotating speed of 120 rpm. The pH was optimized for maximum adsorption by shifting it from 2 to 5 with 0.1 N NaOH and 0.1 N HCl. The contact time was also optimized by varying it from 20 to 140 min at an interval of 20 min, until the maximum adsorption was achieved.

Adsorption rate kinetics

The adsorption kinetics involved is an important parameter to describe the basic traits of a good adsorbent (Wang et al. 2012). It provides the process which controls the sorbate reactions in the solid–solution interface at different time. The present study pseudo-first- and second-order reactions were utilized to describe the adsorption mechanism involved in the Pb^{2+} removal processes by bagasse biochar (Lagergren 1898; Ho et al. 2000).

The pseudo-first-order kinetic model (Eq. 1) is expressed as

$$In(q_1 - q_t) = Inq_1 - k_1 t \quad (1)$$

where q_1 and q_t are the amount of Pb^{2+} (mg g^{-1}) absorbed at equilibrium and at time t, respectively, and k_1 is the first-order rate constant (min^{-1}).

According to Mckay and Ho (1999), pseudo-second-order kinetic model (Eq. 2) is expressed as

$$\frac{t}{q_t} = \frac{1}{k_2 q_2^2} + \frac{1}{q_2} t \quad (2)$$

$$\frac{1}{q_t} = \frac{1}{K_2 q_2 t} + \frac{1}{q_2} \quad (3)$$

Equation (3), modified Ritchie's second-order kinetic model, is used to calculate the initial sorption rate, h (mg g^{-1} min^{-1}) (Eq. 4).

$$h = K_2 q_2^2 \quad (4)$$

where q_2 is the maximum adsorption capacity (mg g^{-1}) for the pseudo-second-order adsorption, K_2 is the equilibrium rate constant for the pseudo-second-order adsorption (g mg^{-1} min^{-1}), and h is initial sorption rate (mg g^{-1} min^{-1}).

Adsorption isotherm studies

The experimental uptake (q_e) values obtained from batch assay were analyzed using adsorption isotherm models (Langmuir and Freundlich) and separation factor (R_L) at room temperature (25 ± 3 °C) and other optimized conditions, i.e., pH 5, dose 5.0 g and 140 min of contact time.

The linear form of Freundlich adsorption isotherm is given as the following

$$\log q_e = \log K_f + \frac{1}{n} \log C_e$$

where K_f and n are Freundlich constants for distribution coefficient and intensity, respectively.

The Langmuir equation is given as

$$\frac{C_e}{q_e} = \frac{1}{q_{max} K_L} + \frac{C_e}{q_{max}}$$

where q_e is the equilibrium metal ion concentration, C_e is the equilibrium metal ion concentration in the solution (mg l^{-1}), q_{max} is the monolayer adsorption capacity of bagasse biochar (mg g^{-1}), and K_L is the Langmuir adsorption constant (L mg^{-1}).

Analytical method

The amount of Pb^{2+} adsorbed was calculated by the following mass balance relationship

$$q_e = \frac{C_0 - C_e}{w} \times v$$

and percent removal at the equilibrium (q_e) was calculated as the following

$$\text{Removal}(\%) = \frac{(C_0 - C_e)}{C_e} \times 100$$

where C_0 and C_e (mg l^{-1}) are the metal concentrations at initial stage and equilibrium, respectively. v is the volume of the effluent in ml, and w is the weight of the adsorbent in grams(gm).

Desorption study

Desorption experiments were performed with metal-loaded biochar of bagasse to check the reusability of the adsorbent. 0.1 M HCl, HNO_3 and H_2SO_4, and NaOH were used as desorbing eluants. One gram of the Pb^{2+}-loaded adsorbent was added in 100 ml of eluants and incubated for 3 h at 30 °C at 150 rpm.

Results and discussion

Physicochemical properties of battery manufacturing industry effluent

The physicochemical properties of battery manufacturing industry effluent are presented in Table 1. Most of the parameters were found to be beyond the limits prescribed in Bureau of Indian Standards (BIS 10500: 2012) for on land irrigation. pH, temperature and electrical conductivity (EC) affect the ionic concentration of the effluent and influence the chemical reactions in the aquatic environment (Akpomie and Dawodua 2015). Different salts, used in the processes, may be the reason for higher values of pH as well as EC. Chemical oxygen demand (COD), biological oxygen demand (BOD), dissolved oxygen (DO), total dissolved solids (TDS), total suspended solids (TSS) and total solids (TS) define the amount of pollution caused by different organic and inorganic pollutants affecting the water quality. Besides hardness and alkalinity higher concentration of nitrate, phosphate and sulfate may be attributed to the usage of different chemicals and salts during the battery manufacturing processes (Ahmed et al. 2012).

Table 1 Physicochemical properties of battery manufacturing industry effluent

S. no.	Parameters	Average ± SD	BIS (10500:2012) On land for irrigation
1	Color	Transparent white	–
2	Odor	Light vinegar	Non-objectionable
3	Temperature	29.733 ± 0.208	–
4	pH	8.033 ± 0.208	5.5–9
5	EC	24.167 ± 0.751	–
6	BOD	2968.02 ± 29.197	100
7	COD	12,500.50 ± 165.751	–
8	TDS	1455.333 ± 6.429	2100
9	TSS	757.333 ± 74.717	200
10	TS	2217.667 ± 4.028	2300
11	Acidity	583.333 ± 4.578	–
12	Alkalinity	400.00 ± 2.646	–
13	Chloride	140.413 ± 1.859	–
14	Sulfate	43.757 ± 3.174	–
15	Phosphate	67.5033 ± 1.402	–
16	Nitrate	nd	–
17	Total hardness (as $CaCO_3$)	621.00 ± 263.236	–
18	Lead (Pb^{2+})	2.393 ± 0.030	0.1

Results are expressed as mean of five replicates ± SD (i.e., $n = 3$); all the results were expressed in mg l^{-1} except for color, odor, pH, temperature (°C) and EC (Siemen m^{-1})

nd not detected

The concentration of Pb^{2+} in the effluent was found to be 2.393 mg l^{-1} which exceeded the limit of 0.1 mg l^{-1} as prescribed by BIS (10500: 2012). Higher concentration of Pb^{2+} in the water bodies may be harmful for health of flora and fauna (Babel and Kurniawan 2003; Alluri et al. 2007).

Screening of biosorbents

Three thermally modified agrowastes (biochar of bagasse, orange and coir) were observed for their suitability for adsorbing Pb^{2+} (Fig. 1). Among them, bagasse biochar showed maximum adsorptive removal of 75.38% Pb^{2+} in comparison with orange (70.36%) and coir (61.98%) for the same adsorbent dosage of 5.0 g l^{-1}. The variation in the adsorption efficiencies may be attributed to variations in the morphology and binding sites of the adsorbents (Petrović et al. 2017).

Characteristics of adsorbent

The proximate and ultimate study of the adsorbents is summarized in Table 2. The ash content was found to be low with average value of 7.337% because of the biochar-producing processes which eliminate the oxygen content. The moisture content was also found to be very low with average value of 1.968% which facilitated the adsorption process. The bagasse biochar was alkaline in nature as pH was found to be 8.967 which could be recognized by the detachment of alkali metal, i.e., Ca^{2+} as their concentration was found to be moderately high as shown in EDX spectrum of biochar (Fig. 2e). The surface area of the biochar (12.378 m^2 g^{-1}) seems to be rough and irregular which was confirmed by SEM image of bagasse biochar (Fig. 2b). Further, the biochar showed comparatively higher C/H and C/N ratio and less C % (Table 1) which suggests that the charring process was not accomplished well with some decomposed matter.

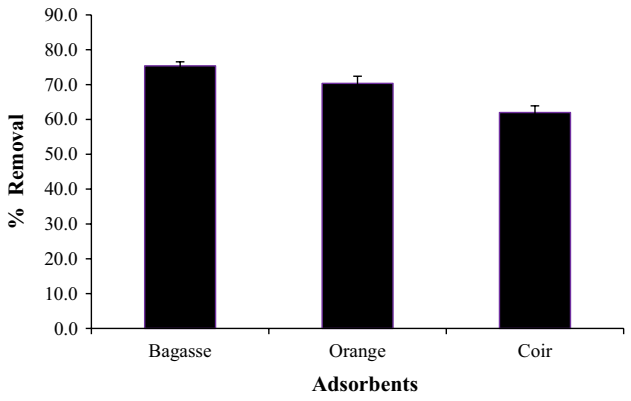

Fig. 1 Adsorption efficiency of different agrowastes at room temperature (25 ± 3 °C), ± SD shown by error bar

Table 2 Characteristics of bagasse biochar

S. no.	Characteristics	Values
1	Moisture content (%)[a]	1.968 ± 0.012
2	Ash content (%)[a]	7.337 ± 0.033
3	pH	9.267 ± 0.208
4	Pore volume (cc/g)[b]	0.039 ± 0.003
5	Pore diameter (nm)[b]	1.579 ± 0.023
6	Surface area (m^2/g)[b]	12.628 ± 0.30
7	C %[c]	38.153 ± 0.531
8	H %[c]	6.076 ± 0.038
9	O %[c]*	50.942 ± 0.215
10	N %[c]	4.557 ± 0.289
11	S %[c]	0.272 ± 0.010
12	C/H ratio[c]	6.314 ± 0.064
13	C/N ratio[c]	8.759 ± 0.002

[a]Data are presented as dry weight percent

[b]Data are retrieved from BET analysis

[c]Data are retrieved from CHNS analyzer

[c]*Determined by difference

This may also be a reason for comparatively lesser specific surface area of the biochar as analyzed by BET. In addition to this, higher values of H and O % indicate availability of binding sites responsible for the successful adsorption of Pb^{2+} (Table 1). The results were found to be in good agreement with Fernandez et al. (2014); Abdelhafez and Li (2016); and Basu et al. (2017).

SEM and EDX

SEM and EDX images showed the change in the morphology of the adsorbent before and after adsorption process (Fig. 2). The differences in SEM image of (a) bagasse, (b) its biochar and (c) Pb^{2+}-loaded biochar could be clearly visualized. Before charring the surface was uniform and very smooth, and after thermal treatment, it became comparatively rough and irregular increasing the surface area. After adsorption, the space became filled with some irregular, crystalline structures which supported the adsorption of Pb^{2+} from the effluent. In addition to this, existence of Pb^{2+} in the EDX spectrum may aslo be considered in the support successful adsorption of the metal (Fig. 2d, e).

FTIR

Adsorption process is affected by the groups and bonds present in the adsorbent. In order to investigate the chemical structure and major functional groups present, which may be responsible for adsorption process, FTIR analysis was carried out (Solum et al. 1995). The spectra of the (a) bagasse, (b) its biochar and (c) Pb^{2+}-loaded biochar are presented

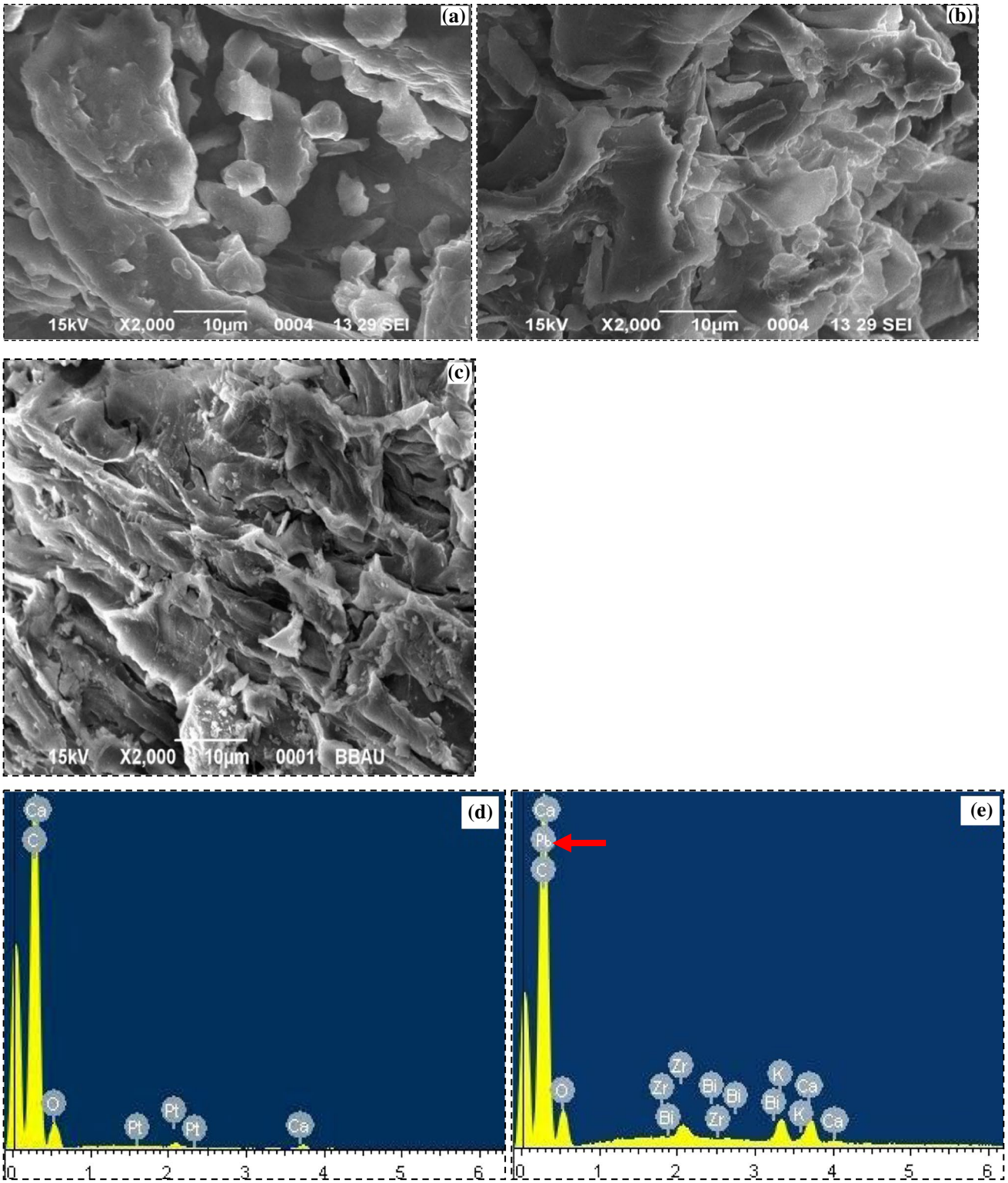

Fig. 2 SEM images of: **a** bagasse, **b** bagasse biochar, **c** lead (Pb^{2+})-loaded bagasse biochar; EDX spectrum of **d** bagasse biochar and **e** lead (Pb^{2+}) adsorbed

in Fig. 3. The broad peaks between 3846 and 3438 cm^{-1} show the presence of –OH stretching vibrations of cellulose, pectin and lignin in all the three spectra (Guo et al. 2008; Reddy et al. 2014). After thermal treatment, most of the major peaks were disappeared except –CH stretching at 2925.3 cm^{-1}, C=O stretch in ketones represented by broad peak at 1711 cm^{-1}, C=C stretch in alkenes and C=O stretch in secondary amides represented by a sharp peak at 1631 cm^{-1}. The stretching of the chemical bonds is marked by the higher carbon content as well as the organic matter (Abdelhafez and Li 2016). After the adsorption of Pb^{2+} the peaks were shifted to 1629.7, 1441.67 and 874.9 7 cm^{-1} representing C=O stretching at C–N stretch in primary amides at C-H and CH_2 deformations, respectively. Conversion of secondary amide to primary amide and –CH to C=C is evident of formation and dissociation of bonds and groups through ion exchange or some other mechanisms (Kim et al. 2015). The shift in the functional groups between non-treated and treated adsorbent suggests that the adsorption of Pb^{2+} might be facilitated by the process of chemisorption resulting in binding of the metal by the nucleophilic functional groups resulting in the formation of metal complex. This process also supported the adsorption of Pb^{2+} onto the bagasse biochar.

Surface acidic groups

The surface acidic group concentrations of bagasse biochar are represented in Fig. 4. The total concentration of surface acidic groups was 7.033 mol g^{-1}. The carboxylic acidic functional groups occupied maximum concentration of 5.15 mol g^{-1} in comparison with other phenolic (1.283 mol g^{-1}) and lactonic (0.601 mol g^{-1}) acidic groups. The results of the Boehm titration indicated majority of carboxylic acidic groups occupying 72.963% of total surface acidic groups, followed by lactonic (18.182%) and phenolic (8.855%) groups. These results were in good agreement with those of FTIR analysis, explained earlier.

Effect of pH

The effect of pH on concentration of Pb^{2+} is presented in Fig. 5. pH is an important controlling parameter in adsorption process as it determines the surface charge of adsorbent, degree of ionization of the adsorbate and extent of dissociation of functional groups present on active sites (Yang and Cui. 2013; Salam et al. 2011). Thus, the effect of H^+ ions concentration in the battery manufacturing industry effluent was studied at different pHs at optimized dosage (5.0 g l^{-1}) and contact time (140 min). Above pH 7, precipitation of oxides of Pb^{2+} was formed; therefore, the study was confined to pH range of 2.0–6.0 (Basu et al. 2017). The optimum pH for the removal of Pb^{2+} was found to be 5. As the pH of the effluent was increased from 2 to 5, the adsorption capacity of the adsorbent also increased from 3.34 to 3.68 mg g^{-1}. In acidic medium, availability of binding sites increases and removal of H^+ ions in the solution facilitates it being replaced by Pb^{2+} which is termed as chelation. Since Pb has +2 charges, two carbon atoms are involved in chelating/binding of the metal resulting in the formation of metal complex. This may also be the probable reason for the shift in the IR spectra too. At lower pH, there was Coulombic repulsion between positively charged binding sites and cations which suppressed the removal rate, further (Liu and Zhang 2009). The result is in agreement with previous studies for the removal of Pb^{2+} by bamboo charcoal (Wang et al. 2012), dried water hyacinth (Ibrahim et al. 2012), rapeseed oil cake (Uçar et al. 2015) and strain of *Alcaligenes* sp. (Jin et al. 2017).

Effect of adsorbent dosage

The effect of adsorbent dosages on the concentration of Pb^{2+} in battery manufacturing industry effluent is presented in Fig. 5. The experiments were carried out at different dosages ranging from 2.5 to 5 g l^{-1}. For convenience in presenting the data, the initial dose was chosen as 2.5 g l^{-1} since the removal rate was found to decrease from 66.696 to 64.345% and so on, when the dosage was reduced from 2.5 to lesser. But, when the amount of adsorbent dosage was increased further from 2.5 to 5.0 g l^{-1}, the removal percentage increased from 66.696 to 75.376%. It can be justified by the fact that increasing dose upsurges the number of binding sites for the metal (Gil et al. 2018). The optimum dose for maximum removal of Pb^{2+} from effluent was recorded 5.0 g l^{-1}. Moreover, when dosage was increased further, removal rate decreased due to overloading and intracellular dissociation phenomenon, which affected the binding capacity of the surface groups (Zhao et al. 2017). These results were in agreement with previous studies performed on many other adsorbents for different metals including Pb^{2+} (Oluyemi et al. 2012; Kılıç et al. 2013; Reddy et al. 2014).

Effect of contact time

The contact time also plays a major role in the adsorption of metals from effluent. The effect of contact time on the concentration of Pb^{2+} in the effluent is shown in Fig. 6. The contact time was varied from 20 to 140 min. In initial 20 min about 64.79% of Pb^{2+} was adsorbed, after which the process slowed down and till 140 min the binding sites of the adsorbents became saturated with 75.376% removal of Pb^{2+}. Thus, the optimum time for the removal of Pb^{2+} was 140 min. No further change in the concentration of Pb^{2+} was observed due to exhaustion of the active binding sites. Similar outcomes were also accomplished when adsorbent

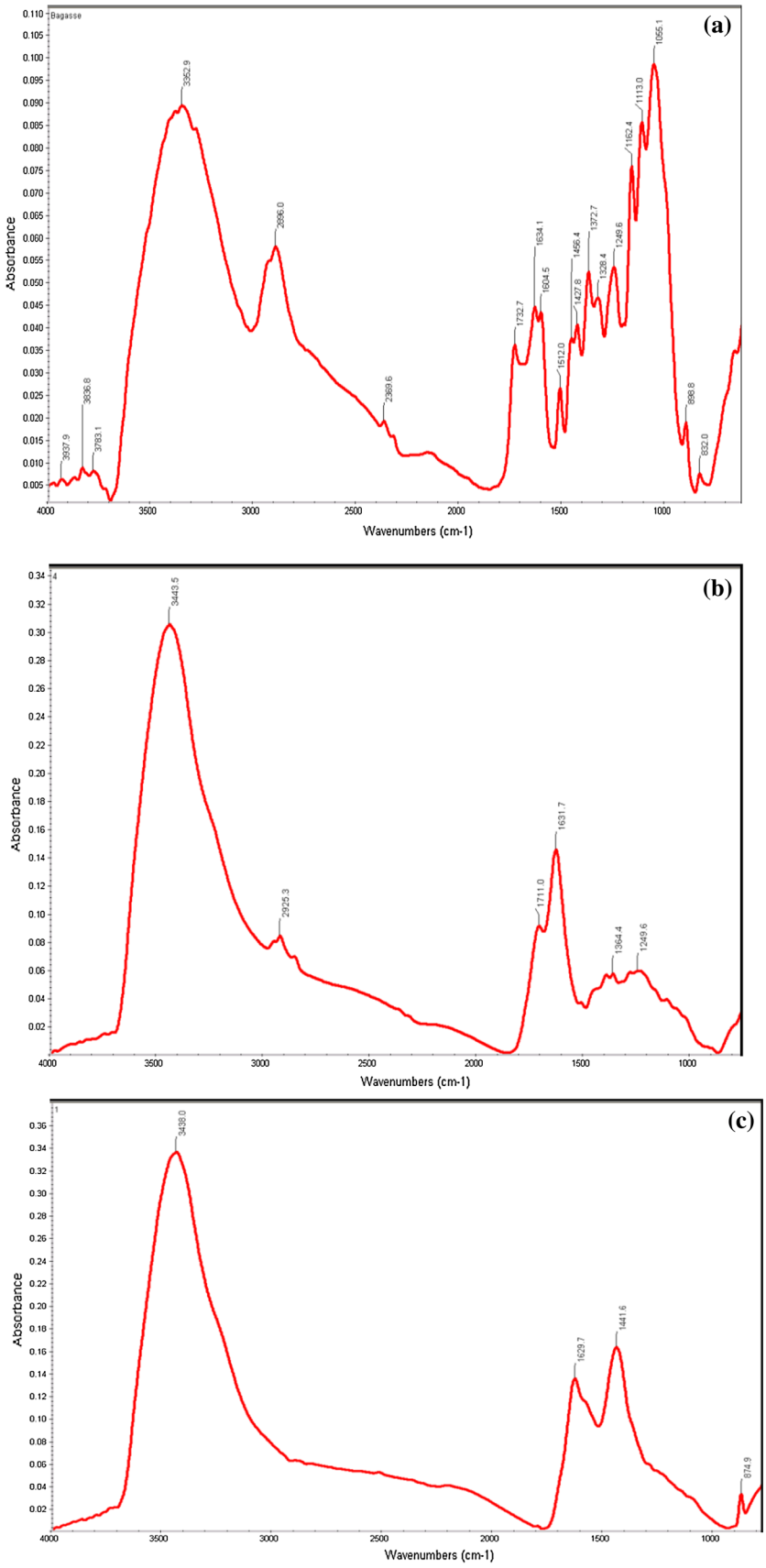

Fig. 3 FTIR spectra of**: a** bagasse, bagasse biochar before **b** and after **c** Pb^{2+} adsorption

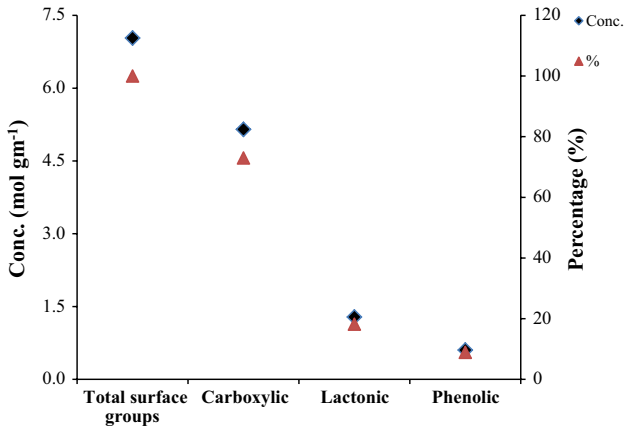

Fig. 4 Surface acidic groups concentration (mol g^{-1}) of bagasse biochar

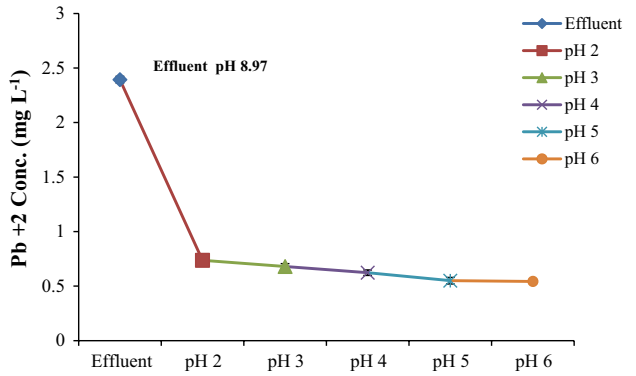

Fig. 5 Effect of different pHs on the concentration of Pb^{2+} in battery manufacturing industry effluent after adsorption at room temperature (25 ± 3 °C) and optimized pH 5, adsorbent dose 5.0 g l^{-1} and contact time of 140 min (SD shown by error bars)

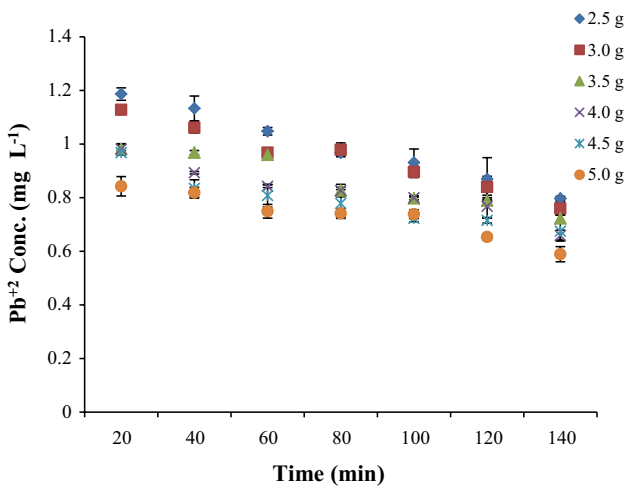

Fig. 6 Effect of time adsorbent dose and contact time lead (Pb^{2+}) concentration, at constant temperature (25 ± 3 °C)

dosage and pH were optimized. Moreover, the results are in agreement with Uçar et al. (2015).

Adsorption kinetics

The plots of pseudo-first order and pseudo-second order for the adsorption of Pb^{2+} onto bagasse are presented in Fig. 7. The linear plots of t versus $\log(q_e - q_t)$ and t versus t/q_t offer the pseudo-first- and second-order rate constants K_1 and K_2, respectively, which are calculated by the slope and intercept. The corresponding values of K_1, K_2, q_e and r^2 are represented in Table 3.

According to correlation coefficients (r^2), the correlation coefficients for pseudo-second-order kinetic model were higher than those of the pseudo-first-order model for Pb^{2+}. This suggests that the adsorption process followed the pseudo-second-order kinetics, indicating adsorption takes place by chemisorptions (Reddy et al. 2014). The results of the present study are in good agreement with previous studies, which also reported that the adsorption process follows the pseudo-second-order kinetics (Uçar et al. 2015; Ibrahim et al. 2012; Wang et al. 2012).

Adsorption isotherm

Adsorption isotherms are used to describe the adsorption equilibrium for wastewater treatments by providing useful information regarding adsorbent surface (Uçar et al. 2015; Naiya et al. 2009). At equilibrium, battery manufacturing industry effluent was allowed to contact with varying dosages of bagasse biochar to examine the maximum loading capacity of the adsorbent used. Adsorption process was justified by applying linear forms of Langmuir and Freundlich isotherms (Langmuir 1918; Freundlich 1906).

The plots of Langmuir isotherm for $1/q_e$ versus $1/C_e$ and Freundlich isotherm for log q_e versus log C_e are presented in Fig. 8. Moreover, values of different parameters for both isotherms and separation factor (R_L) are given in Table 4.

Although there is very less difference between both of the isotherms, the results indicated that in comparison with Freundlich ($r^2 = 0.927$), Langmuir isotherm ($r^2 = 0.9298$) better fitted for the adsorption of Pb^{2+} from battery manufacturing industry effluent. Langmuir model assumes that there were no interactions between solute particles and adsorbent surfaces, and solute particles were distributed in a monolayer carbon surface (Uçar et al. 2015). The monolayer adsorption capacity (q_{max}) of bagasse biochar for the removal of Pb^{2+} from battery manufacturing industry effluent was found to be 12.74 mg g^{-1}. The value of q_{max} was found to be less than previously reported literature; the reason behind this may be the treatment of effluent (with lesser conc. of 2.39 mg l^{-1} Pb^{2+}) than of known solutions of metals (with higher metal

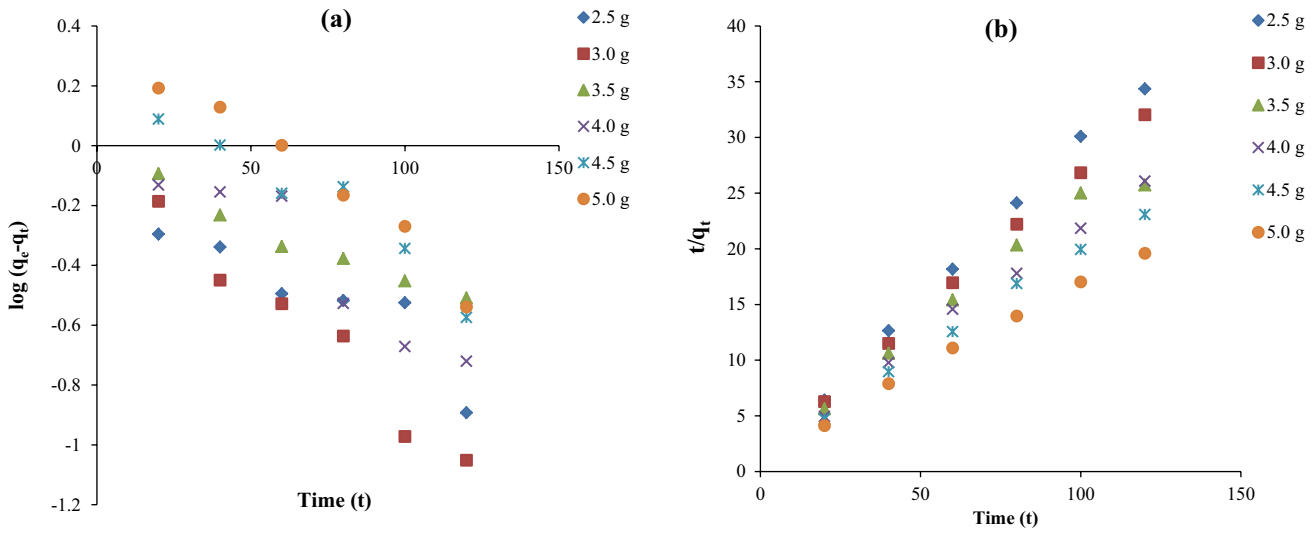

Fig. 7 Role of time **a** pseudo-first-order kinetic plots and **b** pseudo-second-order kinetic plots

Table 3 Pseudo-first-order and pseudo-second-order kinetic constants for sorption of lead (Pb^{2+}) onto bagasse biochar

Parameters	Dosage (g)					
	2.5	3.0	3.5	4.0	4.5	5.0
q_e (exp.) (mg g^{-1})	6.411	5.467	4.792	4.353	3.834	3.621
	Pseudo-first-order model constants					
q_1 (mg g^{-1})	2.471	1.758	1.227	1.135	1.086	1.432
K_1 (min^{-1})	0.016	0.014	0.014	0.009	0.018	0.012
R^2	0.817	0.963	0.961	0.889	0.925	0.963
	Pseudo-second-order model constants					
q_2 (mg g^{-1})*	6.412	5.467	4.792	4.353	3.834	3.621
K_2 (g^{-1} mg^{-1} min^{-1})	15.060	11.474	8.456	24.263	6.586	4.887
r^2	0.997	0.999	0.974	0.996	0.996	0.996
h (mg g^{-1} min^{-1})	6.536	5.435	4.831	4.717	3.891	3.546

*Calculated from graph $1/t$ versus $1/q_t$

conc.) containing higher concentrations of it (Reddy et al. 2014; Naiya et al. 2009; Wang et al. 2012).

Further, the feasibility of Langmuir isotherm can also be proved by a dimensionless constant, viz. separation factor or equilibrium parameter separation factor (R_L) (Hall et al. 1966). It is represented as follows

$$R_L = \frac{1}{1 + K_L C_0}$$

where C_0 is initial metal concentration. If the value of R_L is between 0 and 1, then the adsorption is favorable, and if it is higher than 1, then adsorption is unfavorable. If $R_L = 1$, then adsorption is linear, and the $R_L = 0$ indicates irreversible adsorption. In the present study, R_L value was less than 0, i.e., 0.603, showing favorable adsorption of Pb^{2+} onto bagasse biochar.

Desorption and reuse of adsorbent

Desorption process is a reverse process of adsorption and is important to understand its recovering capacity and reusability for commercial application (Zhang et al. 2018). Three acids (HNO_3, HCl and H_2SO_4) and one base (NaOH) of 0.1 M were used as eluants to assess the desorption process. HNO_3 was found to be the best eluants to desorb about 90.05% of Pb^{2+} from the adsorbent (Fig. 9). The result is in agreement with previous studies done by Naiya et al. (2009) and Mondal (2009).

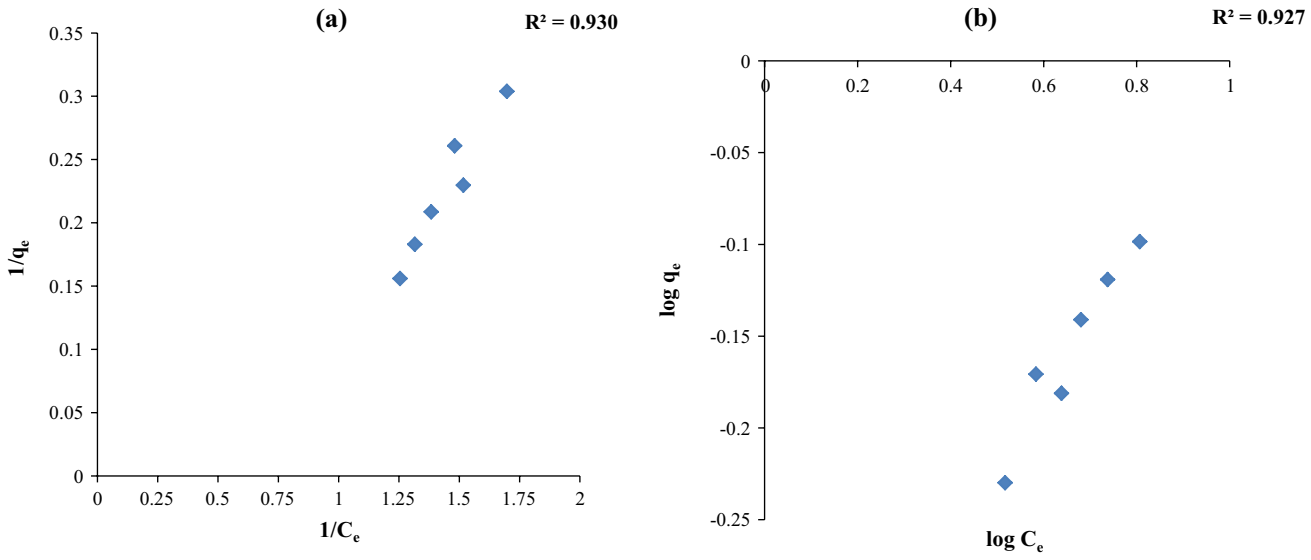

Fig. 8 **a** Langmuir and **b** Freundlich isotherm models for adsorption of Pb^{2+} on bagasse biochar

Table 4 Langmuir along with Freundlich isotherm constants and separation factor for the adsorption of Pb^{2+} on bagasse biochar

Langmuir constants		Freundlich constants			Separation factor	
q_{max} (mg g^{-1})	b (L mg^{-1})	r^2	K_F (mg g^{-1})	n	r^2	R_L*
12.741	4.120	0.930	0.353	2.227	0.927	0.603

*Value is given for optimum dose (5.0 g l^{-1}) and conc. of effluent (2.39 mg l^{-1})

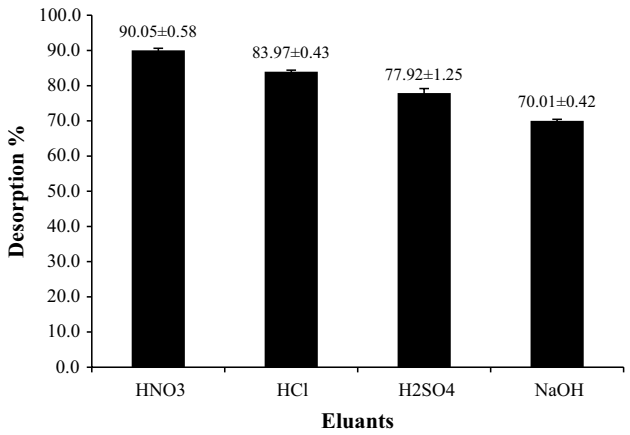

Fig. 9 Desorption efficiency of different eluants for desorption of Pb^{2+} from bagasse biochar ± SD shown by error bar

Conclusions

From different agricultural wastes, bagasse was screened as a potential adsorbent for removing from wastewater of battery manufacturing industry effluent. The adsorption process was found to be dependent upon the pH of the medium as well as the contact time and dosage. The maximum adsorption capacity was recorded as 12.741 mg g^{-1} which is good for removing trace amount of metal from wastewater before disposal to the water bodies. The adsorption capacity of bagasse biochar may be increased by modifying it with various physicochemical methods like charring, addition of chemicals. The results concluded that the bagasse may be used as cost-effective adsorbent for the successful removal of different wastewater generating industries. It may also be utilized in the production of commercial bioadsorbents for removing various heavy metals from industrial effluents.

Acknowledgements The authors would like to thank Mr. Shamshad Ahmad, Department of Environmental Science, and Dr. Vertika Shukla, Department of Applied Geology, BBA University, Lucknow, for their help and support.

References

Abdelhafez AA, Li J (2016) Removal of Pb(II) from aqueous solution by using biochars derived from sugarcane bagasse and orange peel. J Taiwan Inst Chem Eng 61:367–375

Ahmed TF, Sushil M, Krishna M (2012) Impact of dye industrial effluent on physicochemical characteristics of Kshipa River, Ujjain City, India. Int Res J Environ Sci 1:41–45

Ajenifuja E, Ajao JA, Ajayi EOB (2017) Adsorption isotherm studies of Cu(II) and Co(II) in high concentration aqueous solutions on photocatalytically modified diatomaceous ceramic adsorbents. Appl Water Sci 7:3793–3801

Akpomie KG, Dawodua FA (2015) Physicochemical analysis of automobile effluent before and after treatment with an alkaline-activated montmorillonite. J Taibah Univ Sci 9(4):465–476

Alluri HK, Ronda SR, Settalluri VS, Bondili VS, Suryanarayana V, Venkateshwar P (2007) Biosorption: an eco-friendly alternative for heavy metal removal. Afr J Biotechnol 6(11):2924–2931

Amuda OS, Giwa AA, Bello IA (2007) Removal of heavy metal from industrial wastewater using modified activated coconut shell carbon. Biochem Eng J 36:174–181

Andrade V, Mateus M, Batoréu M, Aschner M, dos Santos AM (2015) Lead, arsenic, and manganese metal mixture exposures: focus on biomarkers of effect. Biol Trace Elem Res 166(1):13–23

APHA (2005) Standard methods for the examination of water and waste water, 21st edn. American Public Health Association, Washington, DC

Babel S, Kurniawan TA (2003) Low-cost adsorbents for heavy metals uptake from contaminated water: a review. J Hazard Mater B 97:219–243

Banerjee K, Ramesh ST, Nidheesh PV, Bharathi KS (2012) A novel agricultural waste adsorbent, watermelon shell for the removal of copper from aqueous solutions. Iran J Energy Environ 3:143–156

Basu M, Guha AK, Ray L (2017) Adsorption of lead on Cucumber peel. J Clean Prod 151:603–615

BIS (2012) Indian standards specifications for drinking water. IS:10500, Bureau of Indian Standards, New Delhi. http://cgwb.gov.in/Documents/WQ-standards.pdf

Boehm HP, Diehl E, Heck W, Sappok R (1964) Surface oxides of carbon. Angewandte Chem Int Ed 3:669–677

Buasri A, Nattawut C, Tapang K, Jaroensin S, Panphrom S (2012) Equilibrium and kinetic studies of biosorption of Zn(II) ions from wastewater using modified corn cob. APCBEE Procedia 3:60–64

Cheraghi M, Sobhanardakani S, Zandipak R, Lorestani B, Merrikhpour H (2015) Removal of Pb(II) from aqueous solutions using waste tea leaves. Iran J Toxicol 9(28):1247–1253

Doke KM, Khan EM (2017) Equilibrium, kinetic and diffusion mechanism of Cr(VI) adsorption onto activated carbon derived from wood apple shell. Arab J Chem 10(Supplement 1):S252–S260. https://doi.org/10.1016/j.arabjc.2012.07.031

Ehrampoush MH, Miria M, Salmani MH, Mahvi AH (2015) Cadmium removal from aqueous solution by green synthesis iron oxide nanoparticles with tangerine peel extract. J Environ Health Science Eng 13(1):1

Fernandez ME, Nunell GV, Bonelli PR, Cukiermen AL (2014) Activated carbon developed from orange peels: batch and dynamic competitive adsorption of basic dyes. Ind Crops Prod 62:437–445

Freundlich H (1906) Adsorption in solutions (57). Z Phys Chem Germany 385-470

Gardare VN, Yadav S, Avhad DN, Rathod VK (2015) Preparation of adsorbent using sugarcane bagasse by chemical treatment for the adsorption of methylene blue. Desalin Water Treat. https://doi.org/10.1080/19443994.2014.967727

Gil A, Amiri MJ, Javad M, Abedi-Koupai J (2018) Adsorption/reduction of Hg(II) and Pb(II) from aqueous solutions by using bone ash/nZVI composite: effects of aging time, Fe loading quantity and co-existing ions. Environ Sci Pollut Res 25:2814–2829

Guo X, Zhang S, Shan X (2008) Adsorption of metal ions on lignin. J Hazard Mater 151:134–142

Hall KR, Eagleton LC, Acrivos A, Vermeulen T (1966) Pore- and solid-diffusion kinetics in fixed-bed adsorption under constant pattern conditions. Ind Eng Chem Fundam 5:212–223

Ho YS, Mckay G, Wase DJ, Foster CF (2000) Study of the sorption of divalent metal ions on to peat. Adv Sci Technol 18:639–650

Ibrahim HS, Ammar NS, Ibrahim M (2012) Removal of Cd(II) and Pb(II) from aqueous solution using dried water hyacinth as a biosorbent. Spectrochim Acta A Mol Biomol Spectrosc 96:413–420

Jin Y, Yu S, Teng C, Song T, Dong L, Liang J, Bai X, Xu X, Qu J (2017) Biosorption characteristic of *Alcaligenes* sp. BAPb.1 for removal of lead(II) from aqueous solution. 3. Biotech 7:123

Joseph O, Rouez M, Métivier-Pignon H, Bayard R, Emmaneul E, Gourdon R (2009) Adsorption of heavy metals on to sugar cane bagasse: improvement of adsorption capacities due to anaerobic degradation of the biosorbent. Environ Technol. https://doi.org/10.1080/09593330903139520

Kılıç M, Kırbıyık Ç, Çepelioğullar Ö, Pütün AE (2013) Adsorption of heavy metal ions from aqueous solutions by bio-char, a by-product of pyrolysis. Appl Surf Sci 283:856–862

Kim N, Park M, Park D (2015) A new efficient forest biowaste as biosorbent for removal of cationic heavy metals. Bioresour Technol 175:629–632

Kong Z, Li X, Tian J, Yang J, Sun S (2014) Comparative study on the adsorption capacity of raw and modified litchi pericarp for removing Cu(II) from solutions. J Environ Manag 134:109–116

Lagergren S (1898) Kungl. Svenska Vetenskapasakad Handl 24:1–39

Laidlaw MAS, Filoppelli G, Mielke H, Gulson B, Ball AS (2017) Lead exposure at firing ranges—a review. Environ Law. https://doi.org/10.1186/s12940-017-0246-0

Langmuir I (1918) The adsorption of gases on plane surfaces of glass, mica and platinum. J Am Chem Soc 4(9):1361–1403

Li J, Zheng L, Liu H (2017) A novel carbon aerogel prepared for adsorption of copper(II) ion in water. J Porous Mater 24:1575–1580

Liu Z, Zhang FS (2009) Removal of lead from water using biochars prepared from hydrothermal liquefaction of biomass. J Hazard Mater 167:933–939

Liu B, Chen W, Peng X, Cao Q, Wang Q, Wang D, Meng X, Yu G (2016) Biosorption of lead from aqueous solutions by ion-imprinted tetra ethylene pentamine modified chitosan beads. Int J Biol Macromol 86:562–569

Mckay G, Ho YS (1999) Pseudo-second-order model for sorption processes. Process Biochem 34:451

Mehmood S, Rizwan M, Bashir S, Ditta A, Aziz O, Yong LZ, Dai Z, Akmal M, Ahmed W, Adeel M, Imtiaz M, Tu S (2017) Comparative effects of biochar, slag and Ferrous–Mn ore on lead and cadmium immobilization in soil. Bull Environ Contam Toxicol. https://doi.org/10.1007/s00128-017-2222-3

Mondal MK (2009) Removal of Pb(II) ions from aqueous solution using activated tea waste: adsorption on a fixed-bed column. J Environ Manag 90:3266–3271

Naiya TK, Bhattacharya AK, Das SK (2009) Adsorption of Cd(II) and Pb(II) from aqueous solutions on activated alumina. J Colloid Interface Sci 333:14–26

Nguyen TAH, Ngo HH, Guo WS, Zhang J, Liang S, Yue QY, Li Q, Nguyen TV (2013) Applicability of agricultural waste and by-products for adsorptive removal of heavy metals from wastewater: review. Bioresour Technol 148:574–585

Oickle AM, Goertzen SL, Hopper KR, Abdalla YO, Andreas HA (2010) Standardization of the Boehm titration: part II. Method of agitation, effect of filtering and dilute titrant. Carbon 48:3313–3322

Oluyemi EA, Adeyemi AF, Olabanji IO (2012) Removal of Pb^{2+} and Cd^{2+} ions from wastewaters using palm kernel shell charcoal (pksc). Res J Eng Appl Sci 1(5):308–313

Petrović M, Šoštarić T, Stojanović M, Petrović J, Mihajlović M, Ćosović M, Stanković (2017) Mechanism of adsorption of Cu^{2+} and Zn^{2+} on the corn silk (*Zea mays* L.). Ecol Eng 99:83–90

Poonam, Kumar M (2018) Efficiency of sweet lemon (*Citrus limetta*) biochar adsorbent for removal of chromium from tannery effluent. Indian J Environ Prot 38(3):246–256

Rangabhashiyam S, Selvaraju N (2015) Adsorptive remediation of hexavalent chromium from synthetic wastewater by a natural and $ZnCl_2$ activated Sterculia guttata shell. J Mol Liq 207:39–49

Reddy NA, Lakshmipathy R, Sarada NC (2014) Application of *Citrullus lanatus* rind as biosorbent for removal of trivalent chromium from aqueous solution. Alex Eng J 53:969–975

Renner R (2010) Exposure on tap: drinking water as an overlooked source of lead. Environ Health Perspect 118:A68–A72

Saad SA, Isa KM, Bahari R (2010) Chemically modified sugarcane bagasse as a potentially low-cost biosorbent for dye removal. Desalination 264(1–2):123–128

Said AE-AA, Soliman AS, El-Hafez AAA, Goda MN (2013) Application of modified bagasse as a biosorbent for reactive dyes removal from industrial wastewater. J Water Resoue Prot 5:10–17

Saka C, Şahin Ö, Demir H, Kahyaoğlu M (2011) Removal of lead(II) from aqueous solutions using pre-boiled and formaldehyde-treated onion skins as a new adsorbent. Sep Sci Technol 46(3):507–517

Salam OEA, Reiad NA, ElShafei MM (2011) A study of the removal characteristics of heavy metals from wastewater by low-cost adsorbents. J Adv Res 2:297–303

Salmani MH, Abedi M, Mozaffari SA, Sadeghian HA (2017) Modification of pomegranate waste with iron ions a green composite for removal of Pb from aqueous solution: equilibrium, thermodynamic and kinetic studies. AMB Express 7:225. https://doi.org/10.1186/s13568-017-0520-0

Solum MS, Pugmire RJ, Jagtoyen M, Derbyshire F (1995) Evolution of carbon structure in chemically activated wood. Carbon 33:1247–1254

Taha G, Arifien A, El-Nahas S (2011) Removal efficiency of potato peels as a new biosorbent material for uptake of Pb(II) Cd(II) and Zn(II) from their aqueous solutions. J Solid Waste Technol Manag 37(2):128–140

Tahir H, Sultan M, Akhtar N, Hameed U, Abid T (2016) Application of natural and modified sugar cane bagasse for the removal of dye from aqueous solution. J Saudi Chem Soc 20:S115–S121

Trans VH, Tran LD, Nguyen TN (2010) Preparation of chitosan/magnetite composite beads and their application for removal of Pb(II) and Ni(II) from aqueous solution. Mater Sci Eng C 30:304–310

Uçar S, Erdem M, Tay T, Karagö S (2015) Removal of lead(II) and nickel(II) ions from aqueous solution using activated carbon prepared from rapeseed oil cake by Na_2CO_3 activation. Clean Technol Environ Policy 17:747–756. https://doi.org/10.1007/s10098-014-0830-8

Venkatesha NJ, Bhat YS, Prakash BSJ (2016) Volume accessibility of acid sites in modified montmorillonite and triacetin selectivity in acetylation of glycerol. Appl Catal A Gen 496:51–57

Wang J, Chen C (2009) Biosorbents for heavy metals removal and their future. Biotechnol Adv 27:195–226

Wang Y, Wang X, Wang X, Liu M, Yang L, Wu Z, Xia S, Zhao J (2012) Adsorption of Pb(II) in aqueous solutions by bamboo charcoal modified with $KMnO_4$ via microwave irradiation. Colloids Surf A 414:1–8

Xu X, Cao X, Zhao L, Wang H, Yu H, Gao B (2013) Removal of Cu, Zn, and Cd from aqueous solutions by the dairy manure-derived biochar. Environ Sci Pollut Res 20:358–368

Yang X, Cui X (2013) Adsorption characteristics of Pb(II) on alkali treated tea residue. Water Resourc Ind 3:1–10

Zhang X, Tong J, Hu XB, Wei W (2018) Adsorption and desorption for dynamics transport of hexavalent chromium Cr(VI) in soil column. Environ Sci Pollut Res 25:459–468

Zhao W, Zhou T, Zhu J, Sun X, Xu Y (2017) Adsorption of cadmium ions using the bioadsorbent of *Pichia kudriavzevii* YB5 immobilized by polyurethane foam and alginate gels. Environ Sci Pollut Res. https://doi.org/10.1007/s11356-017-0785-5

IJEP 38 (3) : 246-256 (2018) (Received on December 7, 2017)

Efficiency of Sweet Lemon (*Citrus limetta*) Biochar Adsorbent for Removal of Chromium From Tannery Effluent

Poonam and Narendra Kumar

Babasaheb Bhimrao Ambedkar University, Department of Environmental Science, Lucknow-226 025

The present study investigated the efficiency of biochar prepared from peels of sweet lemon (*C. limetta*) for removing chromium (Cr) from tannery effluent by the process of adsorption. The adsorbent was used in the form of biochar and was characterized by SEM-EDXA and FTIR studies. The study was carried out in batch experiments to investigate the effect of different dosage of adsorbents at different time intervals at constant pH and temperature. The saturation point was found to be 0.5 gm/100 mL of tannery wastewater at 200 min of contact time with maximum removal efficiency of about 98%. The presence of different functional groups and morphological change on biochar enabled the efficient removal of chromium. Further, the adsorption of chromium onto the surface of biochar of the peels of sweet lemon favoured Langmuir adsorption isotherm in comparison to Freundlich adsorption isotherm, which demonstrates that the adsorption process has been monolayer and homogenous.

KEYWORD

Adsorption, Sweet lemon, Chromium, Langmuir adsorption isotherm, Tannery effluent.

INTRODUCTION

Heavy metals are the elements that have specific gravity more than 5, the molecular weight in between 63.5 to 200.6 and density greater than 5.0 gm/cm^3 (Thakur and Parmar, 2013). Toxic heavy metals (Cr, Cd, Ni, As, Pb, etc.), are generated by different industrial processes, like metallurgy, tanning, battery manufacturing, electroplating, fertilizers, pesticides, mining, refining ores, alloy industries, pigment, fuel, etc., (Rajoriya and Kaur, 2014; Jadhav *et al.,* 2015).These toxic metals degrade the environment and cause significant health-related problems to living beings. Further, these also have the tendency of bioaccumulation and thus, contaminate the food chain (Kumar *et al.*, 2012; Marin *et al.*, 2010).The tannery is one of the oldest and fastest growing industries in India and currently accounts for about 2161 tanneries (Kumar, 2006; Swathi *et al.*, 2014). In ancient time, vegetable tannin (extract from plant materials) were used (Fathima *et al.*, 2015) for tanning process, but, now chemical tanning agents are used to convert raw animal hides and skins into leather, consequently making it a potential pollution intensive industry (Golder *et al.*, 2007; Ahmed *et al.*, 2011). Chemical tanning produces dense, highly turbid, coloured and foul-smelling toxic wastewater (Midha and Dey, 2008).When such effluent is disposed off into the nearby water bodies without any or improper treatment, it increases the level of BOD/COD, suspended solids total dissolved solids and heavy metals mainly chromium (Islam *et al.*, 2014; Mert and Kestioglu, 2014).

Chromium is one of the abundant metals in the earth's crust with widespread applications. It exists in many oxidation states among which Cr(III) and Cr(VI) are the most stable (Swathi *et al.,* 2014; Yadav *et al.,* 2012). Further, different chromium salts, for example

chromium sulphate, used during the process of tanning, generate two types of chromium ions, that is Cr^{3+} and Cr^{6+}, which may be present in the form of dichromate ($Cr_2O_7^{2-}$) or as chromate (CrO_4^-) in acidic and alkaline medium, respectively (Makeswari and Santhi, 2014). Comparatively, Cr^{6+} is more toxic than Cr^{3+} due to its carcinogenic, mutagenic and tetragenic effects onto the plants, human and animals (Doke and Khan, 2017). It may cause epigastric pain, haemorrhage, severe diarrhoea, vomiting, nausea, dermatitis, ulcer, lung cancer, etc., (Li *et al.*, 2008; Swathi *et al.*, 2014). The Indian Government's Ministry of Environment and Forests (MoEF), has prescribed limit of 2.0 mg/L of Cr for safe discharge of the tannery effluent into surface water (Yoganarsimhan, 2000). Further, The World Health Organization (WHO) has set the maximum permissible level of 0.05 mg/L for chromium in drinking water (Doke and Khan, 2017).

Nowdays, various conventional and non-conventional technologies are available for water treatment. These include sedimentation, ion- exchange, reverse osmosis, coagulation/ flocculation, filtration and other membrane processes (Swathi *et al.*, 2014; Li *et al.*, 2008). But, due to high capital cost, generation of huge amount of sludge, chemical uses, the focus is diverted towards the use of biological waste materials for removing heavy metals. Further, for accuracy and maximum removal of heavy metals bio-char of the agricultural waste is used as a better and prospective option.

Sweet lemon (*Citrus limetta*) is a native of China, Indonesia, South and Southeast Asia and in the regions of Mediterranean Basin. It is also cultivated in the northeast regions of India, specifically in the hills at high elevations between 1,000 m to 2,700 m. Further, its annual production is very difficult to figure out as it is lumped into 'sweet orange statistics'. According to FAO (Food and Agriculture Organization of United Nations) the production of sweet oranges in India is about 54 million metric tonne among which about 25% comes from sweet lemon (The Earth of India, 2013). It is mainly used for the purpose of juice and the peels are dumped as garbage. These peels can be used for the purpose of biosorption. Biochar of the peels of sweet lemon has been used for the purpose of removing chromium from as charring increases the specific surface area, porosity and superficial surface containing functional groups which in turn increases the adsorption capacity of the bio-waste (Doke and Khan, 2017; Jiang *et al.*, 2003).

In the present study, an attempt was made to assess the physio-chemical characteristics of tannery effluent and biologial oxygen demand, chemical oxygen demand and chromium removal efficiency of biochar prepared from peels of sweet lemon.

MATERIAL AND METHOD

Preparation of sweet lemon (*C. limetta*) biochar for biosorption

Peels of the sweet lemon (*C. limetta*) were collected from local market and were washed thoroughly and air dried. After that the peels were broken down into small pieces and were prepared for the process of bio-charing. Bio-char of the peels were produced into muffle furnace at the temperature of 400 ± 10^0C for 4 hr and was cooled down at room temperature. The biochar was repeatedly washed several times with distilled water and allowed to dry into the oven at a temperature of about 50 ± 10^0C for overnight to remove the moisture. Different dosages of this biochar were used for the purpose of biosorption of total chromium from tannery wastewater (Ranga-bhashiyam and Selvaraju, 2015; Suguihiro *et al.*, 2013).

Adsorption experiment

The experimental uptake (q_e) values obtained from batch assay were analyzed using Langmuir and Freundlich adsorption isotherm for different dosages and times of adsorbents at constant pH and temperature (Fathima *et al.*, 2015). In the process of optimizing the suitable dosage and time for the biosorption of total chromium and COD from the tannery waste- water adsorption experiments were

carried out by batch method using a series of conical flasks containing 100 mL of the wastewater with different dosages of biochar of the peels of sweet lemon, which were shaken on a shaker at a speed of 150 rpm. The exper-iments were run for about 2 and half hour with different dosages (0.3, 0.35, 0.4, 0.45 and 0.5 gm/100 mL) of tannery waste-water at time intervals of 20 min until equilibrium point was reached.

Analytical method

The amount of chromium adsorbed was analyzed on Atomic Adsorption Spectrometer (AAS) (Varian AA240FS). The amount of Cr adsorbed and percent removal in the equilibrium(q_e) were calculated by following mass balance relationship :

$$q_e = \frac{C_0 - C_e}{W} \times V$$

and

$$\text{Removal } (\%) = \frac{C_0}{C_e} x100$$

Where, C_0 and C_e(mg/L) are the metal concentrations at initial stage and equilibrium, respectively. V is the volume of the effluent in mL and W is the weight of the adsorbent in gram (gm).

Moisture content

1 gm of sample was dried for 24 hr in an oven at a temperature of 100 ± 5^0C until constant weight was obtained. After that, the moisture content was determined by using following formula :

$$\text{Moisture content } (\%) = \frac{W_i - W_f}{W_i} x100$$

Where, W_i is initial weight of the adsorbent (gm); W_f is final weight of adsorbent after drying (gm) (Malik and Yadav, 2015).

Ash content

It was determined with the help of muffle furnace by weighing 1gm of the sample and placing it into a porcelain crucible. The crucible was heated upto 500 ± 5^0C for 5 hr. The material was allowed to cool down in a desiccator for 15 min. The ash content was calculated by using following formula :

$$\text{Ash content } (\%) = \frac{W_2 - W_0}{W_1 - W_0} x100$$

Where, W_0 is weight of empty crucible (gm), W_1 is weight of crucible (gm) + weight of adsorbent (gm), W_2 is weight of crucible (gm) + weight of ashed sample (gm) (Malik and Yadav, 2015).

Sorption mechanism

To understand the mechanism of Cr binding with the biochar, spectroscopic study; Fourier transform infrared spectrometer (FTIR) was carried out. Biochar with and without treatment were collected, dried and grounded into fine powder, then was compressed into translucent pellet using potassium bromide with a manual hydraulic pressure. The pellets were then fixed into FTIR (Nicolet™ 6700) and spectrum was recorded over a range of 4,000 to 500/cm and compared with reference standard values (Lambert *et al.,* 1987). Further, the elemental composition of the adsorbent alteration in the surface morphology before and after treatment with different dosages was studied by Scanning Electron Microscope (SEM) and Energy-dispersive X-ray Analysis (EDXA) (JEOL, JSM-6490LV).

RESULT AND DISCUSSION

Characterization of sweet lemon (*C. limetta*)

Scanning electron microscope analysis : SEM micrographs have revealed that surface of maximum dosage (5 g/L) is much more fibrous and have active sites (Figure 1b). It is full of cavities compared to control (Figure 1a). Irregular pores of different sizes are also seen probably as a result of activation of the adsorption sites.

Fourier transform infrared spectrometer analysis : Functional groups present in the adsorbent were detected by Fourier-transform infrared spectroscopy (FTIR) (Figure 2); further, major and minor peaks have been assigned to their respective possible groups

(a) (b)

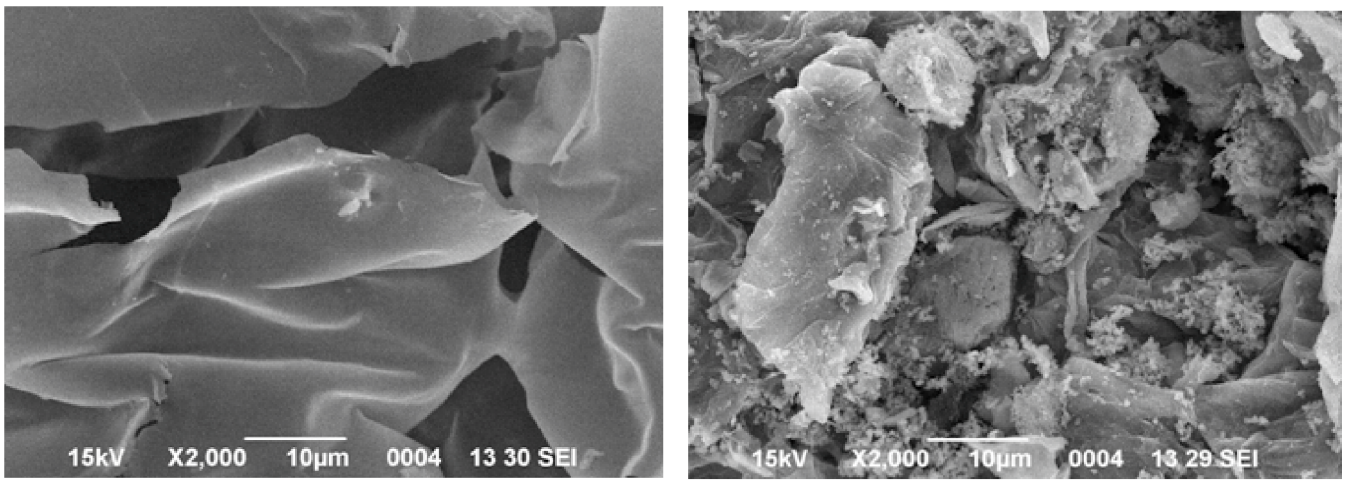

Figure 1. *Scanning electron micrograph of sweet lemon biochar, control (a) and after treatment (b)*

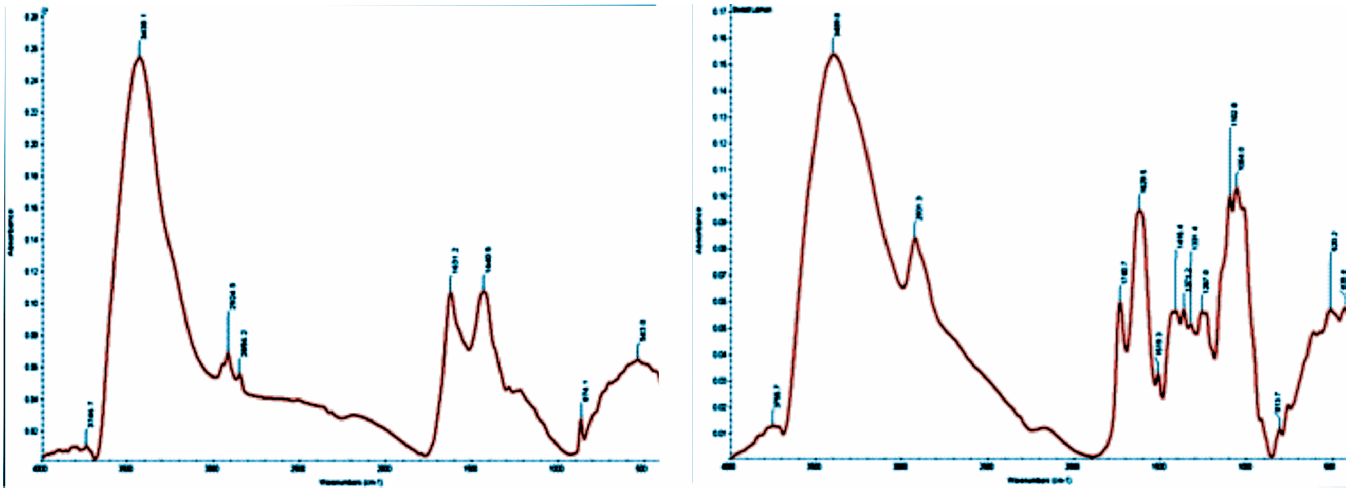

Figure 2. *Fourier trans spectrum of sweet lemon* (Citrus limetta) *before and after treatment*

in table 1. Spectra to 3755.7 to 3746.7/ cm represent the presence of –OH group which may be because of moisture or phenolic compounds. A sharp peak at 2931.3/cm is probably due to hydrogen bonded –OH stretching, wave no. 1629.5 is assigned to the NH_2 in primary amines as a result of - NH_2 deformation or NH^{3+} in amino acids due to -NH_3 deformation. Peak at wave no. 1740/cm is assigned to –C=O find to be present in anhydrides, α keto ester, δ lactones due to C=O stretch.

Physio-chemical characteristics of tannery effluent

Tanneries use organic substances as raw material which is supposed to increase the BOD and COD levels of the effluent (Ahmed *et al.*, 2011). In the present study high concentration of BOD, COD,TDS, TSS and TS were recorded, which may be due to the presence of various inorganic and organic substances that are used for tanning purposes (Table 2). Tannery industries use various kinds of salts and chemicals for the tanning process which in turn the increases EC, alkalinity and hardness. Proteins and other nitrogenous compounds found to be present in animal hides and skins may be the reason for the higher concentration of nitrate. For a good biochar, moisture content should be <1%; the moisture content of sweet lemon peel

Table 1a. *The FTIR spectral characteristics of sweet lemon* (C. limetta) *peel*

IR peak	Frequencies, cm	Assignment
1	3755.7	-OH in alcohol and phenol
2	3409.8	-NH_2 in aromatic amines and amides
3	2931.3	-OH in carboxylic acid, -CH_3 and $-CH_2$ in aliphatic compounds
4	1740.7	C=O in anhydrides, α keto ester, δ-lactones, esters and aldehydes
5	1629.5	C=O and NH_2, in primary amides
6	1519.3	NH in secondary amide, triazine compounds, NO_2 in aromatic nitro compounds
7	1416.4	-OH in carboxylic group, C-N in primary amides
8	1371.2	CH_3 and NO_2 in aliphatic compounds and CH_3isopropyl groups
9	1331.4	NO_2 in aromatic nitro compounds, N=N-O in azoxy compounds, SO_2 in sulphones
10	1267.0	N^+-O^- in pyridine N-oxides, P=O in phosphorous oxy acids and phosphates, C-F in aliphatic floro compounds, Ar-O in alkyl aryl ethers, Si-CH_3 in silanes, C-N in aromatic amines, C-O-C in esters
11	1102.8	C=S in thiocarbonyl compounds, C-O-C aliphatic ether, C-O-H in secondary and tertiary alcohols, C-NH_2 in primary aliphatic amines
12	1064.0	C-NH_2 in primary aliphatic amines, Si-O-Si in siloxanes SO_3H in sulphonic acids, CH-O-H in cyclic alcohols
13	813.7	1,2,4, tribust benzene, R-NH_2 in primary amines, Si-C in organo silicon compounds, Si-CH_3 in silanes, tribust alkenes, C-Cl in chloro compounds, p dibust benzene, triazines
14	520.2	C-Br in bromo compound, NO_2 in aromatic nitro compounds, ring in cyclo alkanes, SO_2 in sulphonyl chlorides, C-C=O in aldehydes and carboxylic acids, C_nH_{2n+1} in alkyl group
15	428.4	C-N-C in amines, Cl-C=O in acid chlorides

Table 1b. *The FTIR spectral characteristics of sweet lemon* (C. limetta) *peel after treatment with maximum dosage (5 gm/L)*

IR peak	Frequencies, cm	Assignment
1	3746.7	-OH in alcohol and phenol
2	3438.1	-NH_2 in aromatic amines, primary amines and amides
3	2924.5	-OH in carboxylic acids, -CH_3 and $-CH_2$ in aliphatic compounds
4	2856.2	CH_3 and $-CH_2$ in aliphatic compounds
5	1631.2	C=O and NH_2 in primary and secondary amides, C=C in alkenes, C=O in tertiary amines and β diketone esters , N-H in primary amides, NH^{3+} in amino acids
6	1440.5	CH_3 in aliphatic compounds, OH in carboxylic acids
7	874.1	Vinylidenes, 1,2,4-tribust benzene
8	543.0	C-C-CN in nitriles, NO_2 in aromatic nitro compounds, C-C=O in aldehydes, ketones and carboxylic acids, O=C=O in amino acids

Table 2. *Physio-chemical properties of tannery effluent*

Parameter	Concentration	BIS (10500:2012) on land for irrigation
Temperature, ^{0}C	18.533 ± 0.058	-
Total dissolved solids (TDS)	13330.000 ±69.541	2100
Total suspended solids (TSS)	4388.667 ±84.672	200
Total solids (TS)	16405.333 ±204.473	2300
pH	7.133 ±0.058	5.5-9
Electrical conductivity (EC), Siemen	16.393 ±0.314	-
Dissolved oxygen (DO)	nd	-
Biological oxygen demand (BOD)	3742.798±179.985	100
Chemical oxygen demand (COD)	23780.00±1680.833	-
Nitrate	88.064 ±1.677	-
Total phosphorus	4.528 ±0.238	-
Chloride	1626.153±155.668	-
Alkalinity	1260.000 ±125.284	-
Hardness	925.240 ±11.555	-
Total chromium	3.842 ±0.4116	-
Ash content,%	7.886 ±1.290	-
Moisture content,%	0.432 ±0.053	-

*Results are expressed as mean of five replicates ± S.D. (that is n=5); nd - Not detected

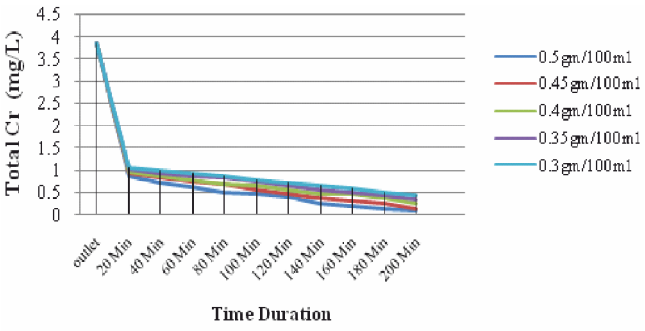

Figure 3. *Effect of different dosage for the adsorption of total chromium on to the biochar of peels of sweet lemon* (Citrus limetta) *biochar*

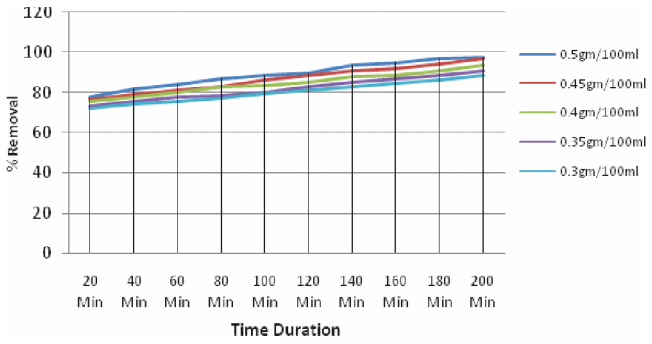

Figure 4. *Removal of chromium from waste-water with different dosage of sweet lemon* (C. limetta) *biochar at different time duration*

biochar was found to be 0.43%; confirms that it was handled and prepared carefully. In addition, lower value of ash content (7.886%) signifies its property to have good charac-teristics of adsorbent.

Effect of different dosage on the adsorption of total chromium

The efficiency of sweet lemon (*C. limetta*) biochar for adsorbing chromium was examined at different adsorbent doses (3, 3.5, 4, 4.5 and 5 gm/L) for tannery wastewater. The influe-nces of adsorbent dosages on adsorption of total chromium at the duration of 20 to 200 min is presented in figures 3 and 4, respectively. Results revealed that the removal of total chromium from wastewater was found to increase with increasing dosage

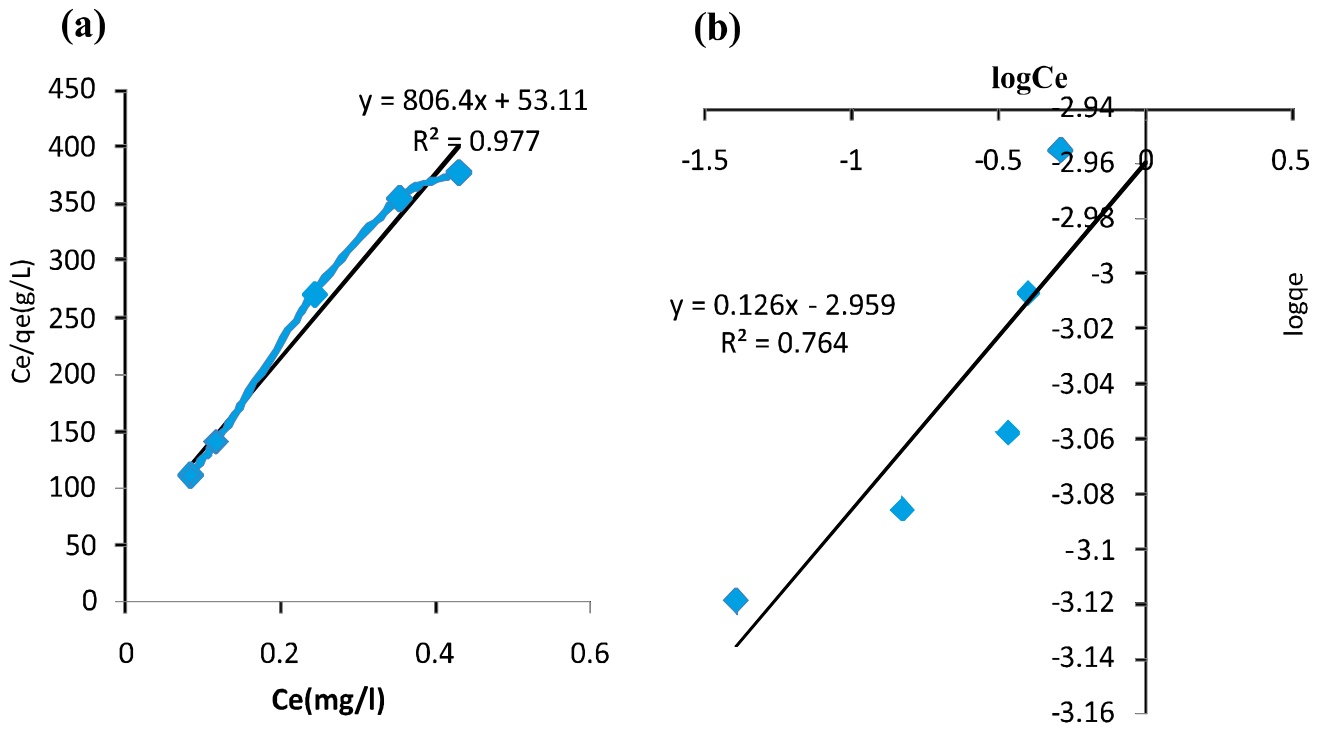

Figure 5. *Langmuir (a) and Freundlich (b) isotherms at different dosages of sweet lemon* (C. limetta) *biochar at constant temperature and pH*

Table 3. *Adsorption isotherm parameters for adsorption of total Cr ions using sweet lemon biochar* (C. limetta)

Isotherm model	Parameter	Value
Langmuir	q_{max}	0.00124 mg/mg
	b	15.184 L/mg
	R^2	0.978
Freundlich	1/n	0.126
	k_F	0.0011 mg/mg
	R^2	0.764

and time interval till adsorbent get saturated. The initial concentration of total chromium in the tannery wastewater was found to be 3.842 mg/L which has been reduced to 0.084 mg/L after treatment with 5 gm/L of adsorbent, which accounts for about 98% removal of total chromium from the wastewater. Thus, equilibrium time for 5 gm of adsorbent per 1000 mL of tannery effluent has been found to be 200 min. Further, with the increase in removal percentage, the active sites became saturated which caused a decrease in adsorption capacity of the adsorbent with time (Garg *et al.,* 2004).

Adsorption isotherm

Equilibrium data has been analyzed with the help of Langmuir adsorption isotherm model and Freundlich adsorption isotherm model (Langmuir 1918; Freundlich 1906). The experiment has been performed for an incubation period of 200 min at 20 min time interval. The Langmuir isotherm is as following :

$$q_e = \frac{bq_{max} C_e}{1 + bC_e}$$

Where, q_e is amount of solute adsorbed onto the biosorbent at equilibrium (mg/g); C_e is residual concentration of solute remaining in the solution after adsorption is complete (mg/g); q_{max} is maximum amount of solute (adsorbate) per unit weight of adsorbent to form a complete monolayer on the surface (mg/g) and b is constant related to the energy of the adsorption. Further, the linearized equation for Langmuir isotherm is :

$$\frac{C_e}{q_e} = \frac{1}{q_{max} b} + \frac{1}{q_{max} C_e}$$

The Langmuir constant q_{max} and b were calculated from the linear plot of C_e/q_e vs C_e, having the slope of $1/q_{max}$ and the intercept of $1/q_{max}$ b (Figure 5a). The data was also subjected to Freundlich isotherm; which is given below :

$$q_e = k_F C_e^{\frac{1}{n}}$$

Where, q_e is the concentration of the solute (adsorbate) adsorbed onto the biosorbent at equilibrium (mg/g), k_F is Freundlich's constant of adsorption capacity, C_e is the concentration of the adsorbate (solute) remained in the solution after completion of the adsorption process (mg/g); and n is Freundlich constant of adsorption intensity. Further, the constant k_F and n were obtained from the linear plot of log q_e vs log C_e. The linearized equation for Freundlich isotherm is :

$$\log q_e = \log k_F + \log C_e$$

The plot log q_e vs log C_e has the slope 1/n and intercept of log k_F (Figure 5b).

According to Langmuir isotherm model, adsorption takes places homogenously at monolayer of the adsorbent's surface, which has a specific number of sites where the solute molecules can be adsorbed and all the sides of the adsorbent will have equal affinity for the metal ion (Fathima *et al.*, 2015). Whereas, Freundlich isotherm assumes that the adsorption takes place heterogeneously on the surface of the adsorbent, which has different types of adsorption sites. The Langmuir and Freundlich constants from the isotherms and their correlation coefficient are also presented in table 3. It is essential to establish the most efficient adsorption model for designing the adsorption system. The correlation factors R for Langmuir and Freundlich isotherms were found to be 0.978 and 0.764, respectively. Suitability of the adsorption isotherms for particular adsorbent is determined with the help of correlation coefficient (R^2) values. The R^2 value for Langmuir isotherm is closer to unity than for the Freundlich isotherm, which suggests that Langmuir isotherm equation is best fitted for the adsorption of Cr ions using sweet lemon (*C. limetta*) biochar.

DISCUSSION

Chromium is one of the most toxic heavy metal released by the chemical tanning industries. The conventional and traditional technologies for removal of heavy metals are very costly and non-ecofriendly. Therefore, there is need of eco-friendly and economically viable technology for removal of heavy metals from wastewater. In the present study a non-conventional technique, that is biosorption, has been used for removal of total chromium from tannery effluent. Biochar prepared from the sweet lemon peels was used as an adsorbent without any kind of pre or post chemical treatment. Few other studies have also reported the application of agricultural wastes for removal of different heavy metals from wastewater, for example rice husk (Dada *et al.*, 2012), peels of orange (Feng *et al.*, 2011), lemon (Rajoriya and Kaur, 2014), water melon shell (Banerjee *et al.*, 2012), banana peel (Achaka *et al.*, 2009), etc.

Li *et al.* (2008) have reported almost complete removal of Cr^{6+} ions from solution when bio-functional magnetic beads and bio-functional beads without magnetic particles were used as an adsorbent for 12 hr. Likewise, Salam *et al.* (2011) used peanut husk charcoal, flyash and natural zeolite as an adsorbent for removal of Cu and Zn coming out of the effluent of electroplating industry. Li *et al.* (2013) have used root powder of *Eicchornia crassipes* for removal of Cu and Cr^{3+} at different pH. Whereas, Fathima *et al.* (2015) examined the effect of pH, temperature and adsorbent dosage on the removal of Cr^{3+} ions with fungal biomass of *Termitomyces clypeatus* as an adsorbent. Optimum dosage was reported to be 5 gm/L with removal percentage of 92.40.

The present study was performed on tannery wastewater using different dosages (0.3, 0.35, 0.4, 0.45 and 0.5 gm/100 mL of wastewater) of biosorbent (biochar of peels of sweet

lemon) at constant pH and temperature at different time duration (20 to 200 min at time intervals of 20 min). Results reported by Fathima *et al.* (2015), 97.825% removal of total chromium than that of Cr^{3+} with an optimum dose of 5 gm/L; was found to be similar to the present study. In comparison to root powder of *Eicchornia crassipes*, biochar of sweet lemon peels can be regarded as better biosorbent for removal of chromium. The results have shown an increase in the removal percentage of the metal with increasing dose and time till the equilibrium point (0.5 gm/100 mL of tannery effluent and 200 min, respectively) and decrease in the adsorption capacity of the adsorbent. This pattern may be attributed to increase in the surface area and availability of functional groups for binding with the metal ions (Wasewar, 2010; Buasri *et al.*, 2012; Kapur and Mondal, 2013). Further, a decrease in the adsorption capacity may be due to the split in the concentration gradient between Cr concentration in the solution and Cr concentration on the surface of the adsorbent (Vasanth and Kumaran, 2005).

Doke and Khan (2017) studied the removal efficiency of activated carbon prepared from wood apple shell for adsorption of Cr(VI) ions. They reported about 95% removal of the metal ion at an optimum dose (125 gm/L) and pH (1.8). Further, the adsorption capacity of the activated carbon prepared from wood apple shell was found to be very high (151.51 mg/mg) in comparison to present findings (2 mg/mg), but the removal percentage of the biochar of sweet lemon was found to be better. Swathi *et al.* (2014) also studied the adsorptive removal of total chromium from tannery wastewater by using rice husk as adsorbent. They reported about 79.94% removal of Cr which was found to be lower with respect to present findings (97.825%). Thus, in comparison to rice husk, biochar of sweet lemon may be regarded as a good adsorbent of chromium. In another study, Fathima *et al.* (2015) used biomass of *Termitomyces clypeatus* as an adsorbent of Cr^{3+} from tannery wastewater with the adsorbent dose of 5 gm/L for maximum 92.4% removal which is again found to be lower in comparison to the present findings (97.825%).

Rangabhashiyam and Selvaraju (2015), have studied the adsorptive removal of Cr(VI) ions by using natural as well as $ZnCl_2$ activated *Sterculia gutta* shell as an adsorbent. They reported an increase from 80.39 to 99.70% and 80.89 to 99.90% removal of Cr(VI) ions by raw and activated *S. gutta* shell, respectively, with an optimum dose of 1.0 gm/L. Whereas, a decrease in adsorption capacity was reported from 40.19 to 9.97 mg/gm and 40.44 to 9.99 mg/gm with raw and $ZnCl_2$ treated *S. gutta* shells, respectively. Similar pattern of increase in the removal percentage with increase in the adsorbent dose and contact time was also reported by Bernard and Jimoh (2013), Benerjee *et al.* (2012), Rajoriya and Kaur (2014), Doke and Khan (2017), Swathi *et al.* (2014), Fathima *et al.* (2015) and Rangabhashiyam and Selvaraju (2015), etc., Bernard and Jimoh (2013) reported increasing removal Pb, Fe, Zn and Cu metal ions till equilibrium point when carbon produced from orange peel was used as an adsorbent. 100% removal of Pb, 70.06% of Fe and 32.53% of Zn, was reported at optimum dose of 1gm/100 mL. Whereas, 0.8 gm/1000 mL an optimum dose was reported for Cu with maximum removal percentage of 61.29. In another study, Banerjee *et al.* (2012) reported 83.5 and 90.5% removal of Zn by peels of lemon and banana, respectively from the artificial medium (10 mg/L) prepared in the lab.

CONCLUSION

Removal efficiency peels of sweet lemon biochar were found to be about 98% at 200 min with a dose of 0.5 gm/100 mL. Further, adsorption process followed Langmuir adsorption isotherm better as compared to Freundlich adsorption which suggests that adsorption is taking place homogenously on the monolayer. Thus, sweet lemon (*C. limetta*) biochar is an effective, mechanically stable and cost-efficient alternative of conventional treatment techniques for the removal of Cr ions from the tannery and other wastewater. However, further research may be explored

with other variables, like temperature, particle size, etc., to further harness the potential of biosorbents.

REFERENCE

Achak, M., *et al*. 2009. Low cost biosorbent 'banana peel' for the removal of phenolic compounds from olive mill wastewater: Kinetic and equilibrium studies. *J. Hazard. Mater.,* 166 (1) : 117-125.

Ahmed, M.K., *et al.* 2011. Physico-chemical properties of tannery and textile effluents and surface water of river Buriganga and Karnatoli, Bangladesh. *World Appl. Sci. J.,* 12 (2) : 152-159.

Banerjee, K., *et al*. 2012. A novel agricultural waste adsorbent, watermelon shell for the removal of copper from aqueous solutions. *Iranica J. Energy and Env.*, 3: 143-156.

Bernard, E. and A. Jimoh. 2013. Adsorption of Pb, Fe, Cu and Zn from industrial electroplating wastewater by orange peel activated carbon. *Int. J. Eng. and Appl. Sci.,* 4 (2) : 95-103.

Buasri, A., *et al.* 2012. Equilibrium and kinetic studies of biosorption of Zn(II) ions from wastewater using modified corn cob. *APCBEE* Procedia. 3 : 60-64.

Dada, A.O., *et al.* 2012. Langmuir, Freundlich, Temkin and Dubinin-Radushkevich isotherms studies of equilibrium sorption of Zn^{2+} unto phosphoric acid modified rice husk. *IOSR J. Appl. Chemistry*. 3 (1) : 38-45.

Doke, K.M. and E.M. Khan. 2017. Equilibrium, kinetic and diffusion mechanism of Cr(VI) adsorption onto activated carbon derived from wood apple shell. *Arabian J. Chemistry.* 10 : S252–S260.

Fathima, A., *et al.* 2015. Biomass of *Termitomyces clypeatus* for chromium (III) removal from chrome tanning wastewater. *Clean Tech. Env. Policy*. 17 : 541–547.

Feng, N., *et al*. 2011. Biosorption of heavy metals from aqueous solutions by chemically modified orange peel. *J. Hazard. Mater.,* 185 : 49–54.

Freundlich, H. 1906. Adsorption in solutions (57). *Z. Phys. Chem. Germany.* pp 385-470.

Garg, V.K., *et al.* 2004. Adsorption of chromium from aqueous solution on treated sawdust. *Bioresour. Tech.,* 92 : 79–81.

Golder, A.K., A.N. Samanta and S. Ray. 2007. Removal of Cr(III) by electrocoagulation with multiple electrodes: Bipolar and monopolar configurations. *J. Hazard. Mater.,* 141: 653–661.

Islam, B.I., *et al*. 2014. Evaluation and characterization of tannery wastewater. *J. Forest Products and Industries.* 3 (3): 141-150.

Jadhav, S.B., *et al.* 2015. Application of response surface methodology for the optimization of textile effluent biodecolourization and its toxicity perspectives using plant toxicity, plasmid nicking assays. *Clean Tech. Env. Policy.* 17 : 709-720.

Jiang, Z., *et al.* 2003. Activated carbon chemically modified by concentrated H_2SO_4 for the adsorption of pollutant from wastewater and the dibenzothiophene from fuel oils. *Langmuir.* 19 : 731-736.

Kapur, M. and M.K. Mondal. 2013. Mass transfer and related phenomena for Cr(VI) adsorption from aqueous solutions onto *Mangifera indica* sawdust. *Chem. Eng. J.,* 218:138–146.

Kumar, U. 2006. Agricultural products and byproducts as a low cost adsorbent for heavy metal removal from water and wastewater : A review. *Sci. Resour. Essays.* 1: 33–37.

Kumar, P.S., *et al*. 2012. Removal of Cd (II) from aqueous solution by agricultural waste cashew nut shell. *Korean J. Chem. Eng.,* 29 : 756–768.

Lambert, J.B., *et al.* 1987. Introduction to organic spectroscopy. **In** Infrared and Raman spectrometries (chapter 10). Macmillan, U.S.A. pp 173-177.

Langmuir, I. 1918. The adsorption of gases on plane surfaces of glass, mica and platinum. *J. American Chemical Society.* 4 (9): 1361-1403.

Li, H., *et al*. 2008. A novel technology for biosorption and recovery hexavalent chromium in wastewater by bio-functional magnetic beads. *Bioresour. Tech.,* 99 : 6271–6279.

Li, X., *et al*. 2013. Adsorption, concentration and recovery of aqueous heavy metal

ions with the root powder of *Eichhornia crassipes*. *Ecological Eng.*, 60 : 160–166.
Makeswari, M. and T. Santhi. 2014. Adsorption of Cr(VI) from aqueous solutions by using activated carbons prepared from *Ricinus communis* leaves: Binary and ternary systems. *Arabian J. Chemistry.* doi.org/10.1016/j.arabjc.2013.10.005.
Malik, D.S. and A. Yadav. 2015. Preparation and characterization of plant based low cost adsorbents. *J. Global Biosci.,* 4 (1) : 1824-1829.
Marin, A.B.P., *et al.* 2010. Biosorption of Zn(II) by orange waste in batch and packed bed systems. *J. Chem. Tech. Biotech.*, 85: 1310-1318.
Mert, B.K. and K. Kestioglu. 2014. Recovery of Cr(III) from tanning process using membrane separation processes. *Clean Tech. Env. Policy.* 16 : 1615–1624.
Midha, V. and A. Dey. 2008. Biological treatment of tannery wastewater for sulphide removal: A review. *Int. J. Chem. Sci.,* 6 (2): 472-486.
Rajoriya, S. and B. Kaur. 2014. Adsorptive removal of zinc from wastewater by natural biosorbents. *Int. J. Eng. Sci. Invention.* 3 (6) : 60-80.
Rangabhashiyam, S. and N. Selvaraju. 2015. Adsorptive remediation of hexavalent chromium from synthetic wastewater by a natural and $ZnCl_2$ activated *Sterculia guttata* shell. *J. Molecular Liquids.* 207: 39–49.
Salam, O.E.A., N.A. Reiad and M.M. ElShafei. 2011. A study of the removal characteristics of heavy metals from wastewater by low-cost adsorbents. *J. Advanced Res.,* 2 : 297-303.
Suguihiro, T.M., *et al.* 2013. An electroanalytical approach for evaluation of biochar adsorption characteristics and its application for lead and cadmium determination. *Bioresour. Tech.,* 143 : 40–45.
Swathi, M., *et al.* 2014. Adsorption studies on tannery wastewater using rice husk. *Scholars J. Eng. Tech.*, 2 (2B) : 253-257.
Thakur, L.S. and M. Parmar. 2013. Adsorption of heavy metal (Cu^{2+}, Ni^{2+} and Zn^{2+}) from synthetic wastewater by tea waste adsorbent. *Int. J. Chemical and Physical Sci.,* 2 (6): 6-19.
The Earth of India. 2017. http://theindianvegan.blogspot.in/2013/03/all-about-sweet-lime-mosambi.html.
Vasanth, K.K. and A. Kumaran. 2005. Removal of methylene blue by mango kernel powder. *Biochem. Eng. J.,* 27: 83–93.
Wasewar, K.L. 2010. Adsorption of metals onto tea factory waste: A review. *I.J.R.R.A.S.,* 3 (3) : 303-322.
Yadav, S., *et al.* 2012. Adsorption characteristics of modified sand for the removal of hexavalent chromium ions from aqueous solutions: Kinetic, thermodynamic and equilibrium studies. *Catena.*, 100: 120–127.
Yoganarsimhan, S.N. 2000. Medicinal plant of India, Tamil Nadu (vol II). Vedams Book (P) Ltd., Bangalore. pp 374.

AUTHOR

1*. Poonam, Research Scholar, Department of Environmental Science, Babasaheb Bhimrao Ambedkar University, Lucknow - 226 025.

2. Narendra Kumar, Assistant Professor, Department of Environmental Science, Babasaheb Bhimrao Ambedkar University, Lucknow - 226 025.